# Development of a Three-dimensional Cell Culture Model for Epidermal Barrier Permeability Testing

by David Lundy

A thesis submitted at Durham University for the degree of Doctor of Philosophy

School of Biological and Biomedical Sciences

Durham University 2012

## Declarations

I declare that experiments described in this thesis were carried out by myself in the School of Biological and Biomedical Sciences, Durham University, under the supervision of Dr Arto Määttä and Professor Stefan Przyborski. This thesis has been composed by myself and is a record of work that has not been submitted previously for a higher degree.

David Lundy

I certify that the work reported in this thesis has been performed by David Lundy, who, during the period of study, has fulfilled the conditions of the Ordinance and Regulations governing the Degree of Doctor of Philosophy.

Dr Arto Määttä Professor Stefan Przyborski

# Abstract

**Development of a Three-dimensional Cell Culture Model for Epidermal Barrier Permeability Testing.**

By David Lundy

In this thesis, a novel 3D polystyrene scaffold was investigated for use as a 3D cell culture material to support keratinocyte culture. Methods of collagen-coating the scaffold were investigated and a keratinocyte model was developed at the air-liquid interface to form an *in vitro* epidermal equivalent. The procedures for culturing keratinocytes were analysed experimentally to promote optimal proliferation and differentiation of the cells.

Keratinocytes cultured in the scaffold showed signs of differentiation, visualised by immunofluorescence staining and ultrastructural analysis by scanning and transmission electron microscopy. The 3D model established is different to other epidermal models as keratinocytes differentiate inside the 3D substrate, rather than forming multiple layers on the air-exposed surface.

Mature cornified envelopes with covalently attached lipids were isolated from the cultures after fourteen days at the air-liquid interface, showing that keratinocytes reached terminal differentiation in the 3D scaffold. Lipid extractions, identification and quantitation showed that the cultures produced a lipid profile similar to native human epidermis, and optimisations to the culture media further improved this similarity.

In the final chapter, the barrier permeability of the 3D model to corticosterone was measured and the model was used to investigate the effect of inhibiting the JNK stress signalling pathway on keratinocyte differentiation and barrier function. This has previously not been investigated using a 3D model, and findings indicated that targeting this pathway may be useful for the treatment of psoriasis, a common skin disorder.

# List of Abbreviations

3T3 - Fibroblast Cell Line

AA - Ascorbic Acid

ABC - ATPase Binding Cassette

AD - Atopic Dermatitis

AP-1 - Activator Protein 1 transcripton factor

AQP - Aquaporin

ASAP-MS - Atmospheric Solids Analysis Probe

ATRA - All-trans Retinoic Acid

BSA - Bovine Serum Albumin

C6S - Chondroitin 6 Sulphate

CaR - Calcium Receptor

CE - Cornified Envelop

CEA - Cultured Epithalial Autograft

CerS - Ceramide Synthase

(c)FBS - (chelexed) Fetal Bovine Serum

CPE - Chemical Penetration Enhancer

$CSO_4$ - Cholesterol Sulphate

DAG - Diacylglycerol

DAPI - 4',6-diamidino-2-phenylindole

DED - De-epidermised Dermis

DKSFM - Define Keratinocyte Serum Free Media

DMEM - Dulbecco's Modified Essential Medium

DMSO - Dimethylsulphoxide

DNA - Deoxyribonucleic Acid

Dsc - Desmocollin

Dsg - Desmoglein

DSP - Desmoplakin

DTT - Dithiothreitol

EBS - Epidermolysis Bullosa Simplex

ECM - Extracellular Matrix

ECVAM - European Centre for the Validation of Alternative Methods

EDC - Epidermal Differentiation Complex

EDTA - Ethylenediaminetetraacetic acid

EGF(-R) - Epidermal Growth Factor (Receptor)

EIA - Enzyme Immunoassay

EPU - Epidermal Proliferation Unit

EURL - European Union Reference Laboratory

FACS - Flow Assisted Cell Sorting

FDA - Food and Drug Administration

FFA - Free Fatty Acids

GluCER - Glucosylceramides

GPHR - Golgi pH Receptor

H&E - Haematoxylin and Eosin

HIPE - High Internal Phase Emulsion

IDP - Inner Dense Plaque

ILK - Integrin Linked Kinase

IP3 - Inositol triphosphate

IV - Ichthyosis Vulgaris

JNK - c-Jun N-terminal Kinase

K1/K10/K5/K14/K6 - Keratin 1/10/5/14/6

KLK - Kallikrein

MEM - Modified Essential Medium

MET - Squamous Cell Carcinoma Cell Line

MMP - Matrix Metalloprotease

MSCs - Mesenchymal Stem Cells

NHDF - Normal Human Dermal Fibroblasts

NH(E)K - Normal Human (Epidermal) Keratinocyte

NLSDI - Neutral Lipid Storage Disease with Ichythosis

NMF - Natural Moisturising Factor

ODP - Outer Dense Plaque

OECD - Organisation for Economic Cooperation and Development

PBS - Phosphate Buffered Saline

PFA - Paraformaldehyde

QC - Quality Control

RAR - Retinoic Acid Receptor

Rf - Retardation factor

RXR - Retinoid X Receptor

SDS - Sodium Dodecyl Sulphate

SEM - Scanning Electron Microscopy/Standard Error of the Mean

SFF - Solid Free Form

SM - Sphingomyelin

SMase - Sphingomyelinase

TEER - Transepithelial Electrical Resistance

TEM - Transmission Electron Microscopy

TEWL - Transepidermal Water Loss

TG - Triglyceride

TGase - Transglutaminase

TLC - Thin Layer Chromatography

TTT - Transient Thermal Transfer

UV - Ultravoilet

WTK - Wild Type Keratinocyte - a mouse keratinocyte cell line

XLI - X-linked Ichythosis

ZO1 - Zonula Occludens 1

# List of Tables

# List of Figures

# 1 Chapter 1

# Introduction

## 1.1 Prologue

The skin is an essential protective organ of the human body. Of particular interest is the epidermis - the upper-most layer of the skin which forms a largely impermeable barrier between the body and the outside world. Disruption to the epidermis by disease, genetic defects or physical damage is implicated in many pathogenic conditions (Uitto et al, 2007, Sandilands et al, 2009). These conditions often reduce the ability of the epidermis to retain water and prevent the entry of foreign substances, resulting in dehydration or infection. The epidermis also represents a barrier to topical delivery of therapeutic agents and so understanding this barrier is essential for successful delivery of transepidermal medications and restoring barrier defects caused by disease (Godin et al, 2007).

In order to study the epidermis, animal and human tissue samples have often been used. However there are clear practical, legal and ethical concerns with using excised samples, cadaver skin or live test subjects. Therefore keratinocytes, the main component of the epidermis, have been cultured *in vitro* in order to study their behaviour. Since the 1980's, keratinocytes have been used to generate tissue equivalents that replicate native epidermis (Prunieras et al, 1983). These equivalents have been primarily used for transplantation (i.e. for burn victims) and for *in vitro* experimentation to increase our understanding of the skin (Pappinen et al, 2007, Sobral et al, 2007). *In vitro* epidermal equivalents can also be used as a tool to further understand keratinocyte behaviour, in particular the complex and highly ordered process of differentiation that results in the formation of the epidermal barrier.

Recently, European Union legislation and changing public perception is reducing the permissibility of testing chemical additives and pharmaceuticals on animals (Hartung, 2010, Wagner et al, 2012). As such, *in vitro* epidermal equivalents are gradually gaining acceptance as alternative methods for testing of pharmaceutical and cosmetic additives and there is a clear and growing demand for models which can accurately predict the permeability of a particular compound through human epidermis (Netzaff et al, 2005).

In this thesis, a novel polystyrene-based 3D scaffold was investigated for its suitability in cell culture as the base for an *in vitro* epidermal model. Once this model

was established, it was characterised in terms of keratinocyte differentiation, then assessed for suitability in epidermal permeability testing.

## 1.2 The Function of Skin

The skin is mainly a protective organ - protecting the body against physical damage, chemical exposure, infectious pathogen entry, radiation and dehydration. The body is protected from impacts and shearing forces by the robust, flexible and self-renewing nature of the skin and a largely impermeable lipid and protein barrier prevents evaporation or absorption of water. Close cell-cell contacts, antibacterial agents and the presence of immune cells prevent pathogen entry through the skin. This thesis will primarily focus on the skin as a barrier to entry of external substances.

The skin is a multi-layered organ composed of two main layers; the dermis and the epidermis which are separated by a basement membrane. The dermis is a supportive, connective tissue formed from collagen, elastic fibres, and extracellular matrix with vasculature that provides nutrition to the epidermis through the basement membrane. The epidermis and dermis interact across this basement membrane through growth factor and cytokine signalling which can regulate keratinocyte behaviour (Werner and Smola, 2001).

The epidermis is a continually renewing tissue, primarily formed by keratinocytes which represent 95% of all epidermal cells. Keratinocytes form this skin barrier through the process of keratinocyte differentiation. Differentiation can be briefly summarised as follows. Basal keratinocytes proliferate while attached to the basement membrane, then detach from the membrane while remaining attached to other keratinocytes. A number of factors then contribute to a co-ordinated process of differentiation during which keratinocytes express insoluble proteins, produce hydrophobic lipids and flatten into insoluble, anucleate corneocytes embedded in a hydrophobic lipid matrix. These corneocytes eventually desquamate from the upper surface of the epidermis, allowing for the constant turnover of the epidermis and maintenance of the renewing epidermal barrier. This process takes approximately 28 days in human skin and disruptions caused by imbalances in proliferation, differentiation or desquamation are implicated in many skin disorders (Baroni et al, 2012, Elias et al, 2012, Sandilands et al, 2009, Uitto et al, 2007).

A diagram showing the structure of the epidermis is shown in Figure 1.1.

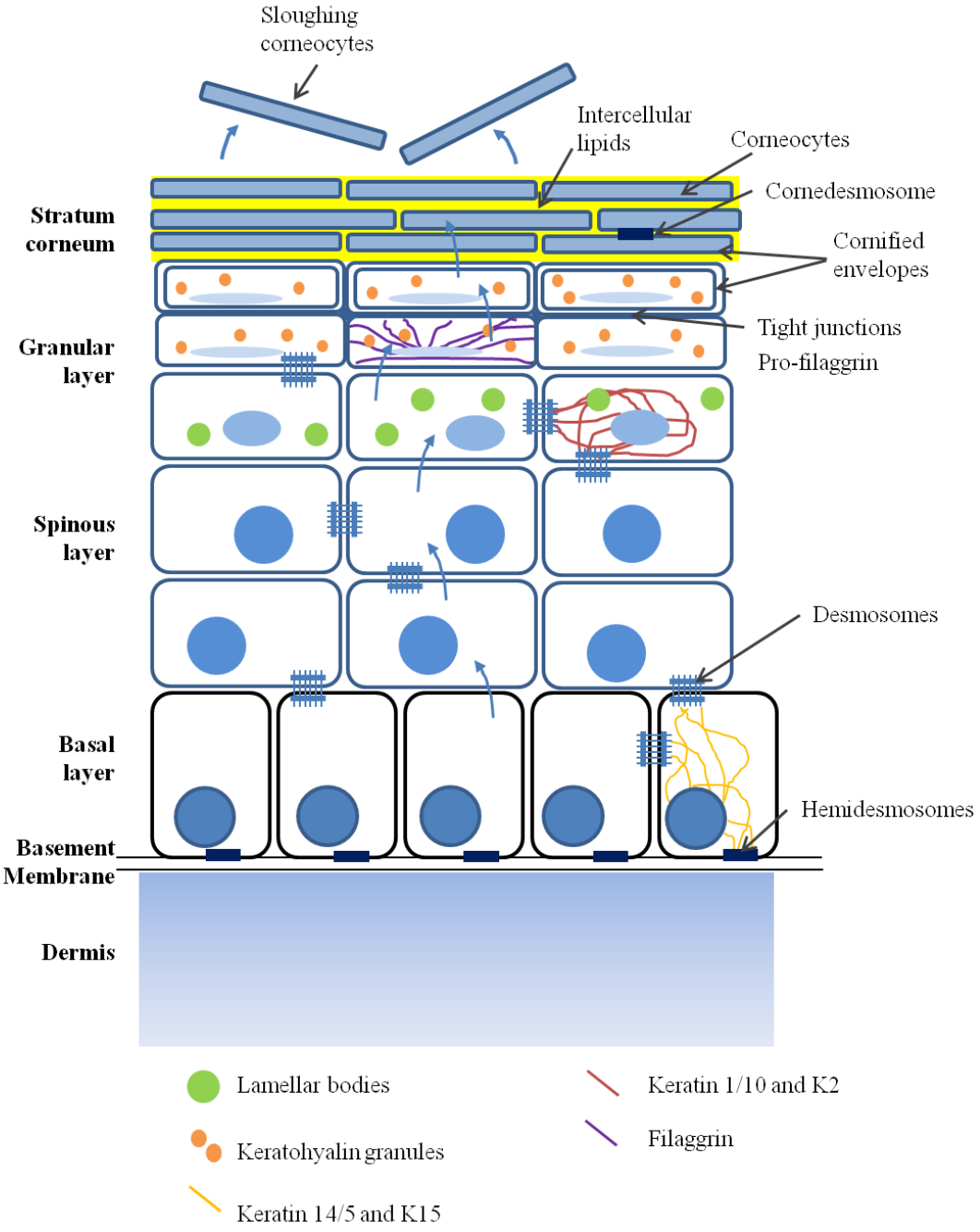


**Figure 1.1. Schematic Overview of Epidermal Differentiation**

Schematic diagram showing keratinocyte transition from the basal layer, through to the stratum corneum and subsequent desquamation. Major features of keratinocyte differentiation such as organelles and changes in keratin expression are noted.

## 1.3 Differentiation of Epidermal Keratinocytes

Epidermal differentiation is a highly organised, multi-stage process during which basal keratinocytes detach from the basement membrane and undergo changes which adapt them for epidermal barrier function. This process is highly complex, involving profound changes in keratinocyte structure, protein expression, enzyme activity, lipid metabolism and multiple signalling pathways. Therefore, a brief overview will be presented containing information necessary for the understanding of material presented in this thesis, although not a complete review of all aspects of epidermal differentiation.

### 1.3.1 The Basal Epidermal Layer

Basal keratinocytes are roughly cuboidal cells attached to the basement membrane which are responsible for the renewal of the epidermis (Wickett and Visscher, 2006). Around 15% of these basal cells are proliferative at any given time under normal conditions, but when the skin is wounded more basal cells are able to enter cell cycle and begin to proliferate (Blanpain and Fuchs, 2006). During routine *in vitro* cell culture, cultured keratinocytes are normally in a state of proliferation which corresponds to approximately this basal state (Micallef et al, 2008).

#### 1.3.1.1 Basal Keratinocyte Integrins

In the skin, basal epidermal keratinocytes are attached to a basement membrane which separates the dermis and epidermis. This basement membrane plays a structural role in the skin and also acts as a semi-permeable barrier to mediate the interaction of the dermis and epidermis through growth factors and cytokines. Keratinocyte keratin filaments attach to hemidesmosomes in the cell membrane which mediate contact with the basement membrane (Breitkreutz et al, 2009).

Integrins are heretodimeric proteins on basal keratinocyte cell surfaces, formed from an alpha and beta subunit which transduce signals between the cell and the extracellular matrix (Watt, 2002). Together, integrins can regulate keratinocyte differentiation, proliferation and adhesion, and are also implicated in aging, wound healing and tumour formation (Watt and Fujiwara, 2011). The first evidence of this was presented by Green, 1977, who showed that keratinocytes held in a liquid suspension begin to terminally differentiate. This is now known to be caused by integrin binding suppressing keratinocyte differentiation. Integrins on basal

keratinocytes bind basement membrane components, the most abundant being integrin α2β1 (binds collagen), α3β1 (laminin 5) and α6β4 (laminin) (Watt, 2002, Cabrijan et al, 2011), suppressing keratinocyte differentiation. Basically, unoccupied integrins send signals to differentiate, while occupied integrins send signals to suppress differentiation (Levy et al, 2000). Intergrin-linked kinase (ILK) is one of the several protein kinases that mediate cellular responses to integrin stimulation and ILK(-/-) mice show reduced transcription of several proteins and enzymes associated with differentiation and barrier function, including transglutaminase 3, small proline rich protein 9 and cornulin (involved in cornified envelope formation) as well as enzymes essential for formation of hydrophobic barrier lipids (Judah et al, 2012). The basement membrane is connected to the dermis by anchoring fibrils (Breitkreutz et al, 2009) and on the dermal side of the basement membrane, spindle-shaped fibroblasts exist in an extracellular matrix of collagen and elastic fibrils embedded in proteoglycans.

#### 1.3.1.2 Basal Keratins

Epidermal keratins are synthesised by keratinocytes in pairs which are classified as either type I (acidic, low molecular weight) or type II (basic/neutral and high molecular weight) (Schweizer et al, 2006). Type I keratins are clustered on chromosome 17 and type II clustered on chromosome 17 (Hesse et al, 2001). As shown in Figure 1.1, basal keratinocytes express the intermediate filaments Keratin 14 (K14) and Keratin 5 (K5) with K14 being type I and K5 being type II. Type I keratins contain a greater proportion of negatively charges amino acid side chains (aspartic or glutamic acid) and type II keratins contain more positively charged side chains (lysine, arginine, histidine), allowing the two keratins to pair together and form insoluble but highly dynamic coiled filaments essential for cell structure and function (Vaidya and Kanojia, 2007). These keratin filaments are organised in an ordered manner inside keratinocytes, appearing to emanate from a nuclear "cage" and extending through the cytoplasm, finally anchoring to junctional desmosomes and hemidesmosomes on the cell membrane (Uitto et al, 2007). Although robust and highly resilient, keratin subunits are not static scaffold. Rather, they participate in a cycle of constant turnover of assembly and disassembly. This begins with formation (nucleation) of keratin subunits at the cell edges, followed by elongation of the filaments and bundling around the cell nucleus. Some filaments form part of a permanent network surrounding the nucleus, while others become soluble and diffuse

through the cytoplasm, ready for integration into new filaments (reviewed by Windoffer et al, 2011).

K5 and K14 are essential for the mechanical and structural integrity of the epidermis, and mutations in either are associated with epidermolysis bullosa simplex (EBS), a condition resulting in severe blister formation (Coulombe et al, 1991 and 2012). This fragility arises partially from weakened individual keratinocytes as well as poor transmittance of force between multiple cells. Lulevich et al, 2010 showed that KEB-7 keratinocytes derived from a Dowling-Meara EBS patient with mutant K14 were 1.6-2.2 times weaker and collapsed more easily when compressed compared to keratinocytes expressing normal K14.

#### 1.3.1.3 Epidermal Desmosomes

Basal keratinocytes are connected to adjacent cells by desmosomes. Desmosomes are intercellular junction structures containing cytoplasmic proteins (plakoglobins, plakophilins and desmoplakin) and transmembrane cadherin proteins (desmocollins and desmogleins). The transmembrane cadherins interact with the cadherins of neighbouring cells in the intercellular space and the cytoplasmic proteins link the cytoplasmic domain of the cadherins to the intracellular keratin networks Cabral et al, 2012). The overall effect of this linkage is to integrate neighbouring cell cytoskeletons, providing tissue cohesion and contributing to the epidermal barrier function (Wickett and Visscher 2006). A schematic diagram of two cells linked by a desmosome is shown in Figure 1.2.

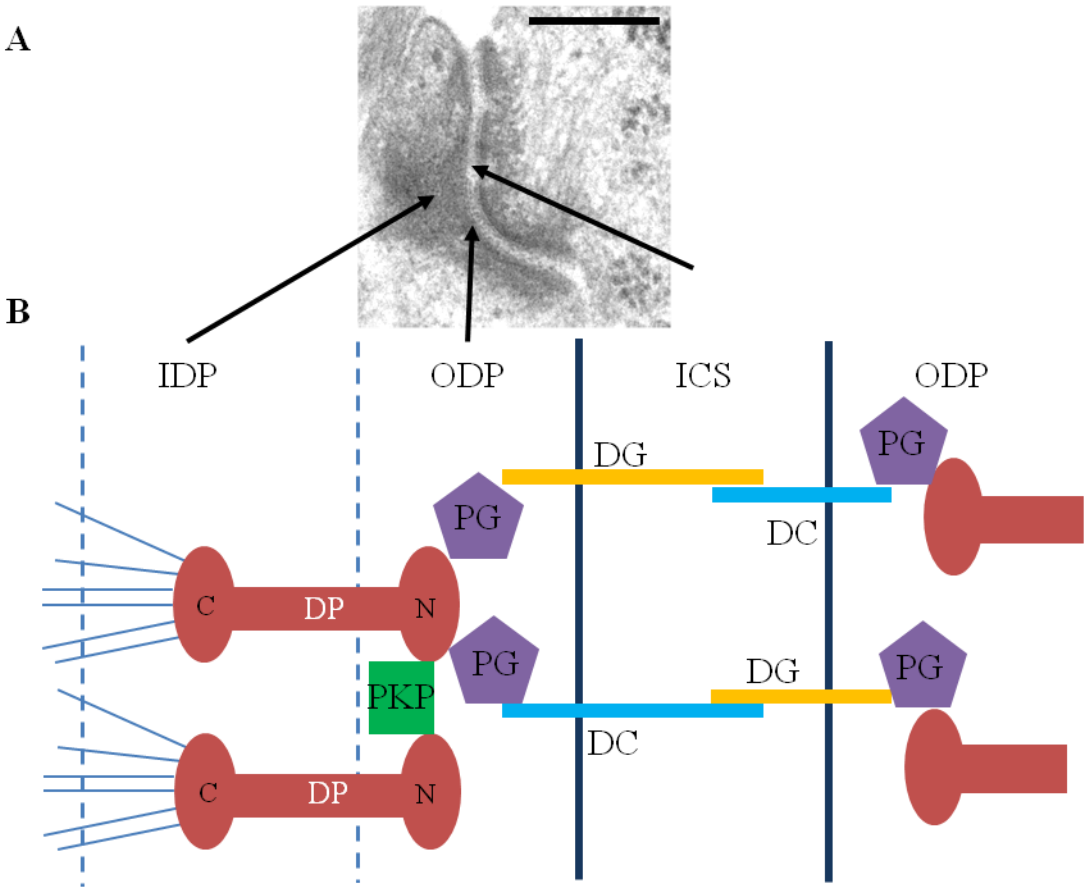


**Figure 1.2. Schematic Structure of Desmosomal Junctions**

A) TEM image of desmosome between two keratinocytes. The inner dense plaque (IDP), outer dense plaque (ODP) and intercellular space (ICS) are clearly visible. Scale bar 250µm. B) Schematic diagram showing keratin intermediate filaments bind C-terminal of desmoplakin in the IDP. The N-terminal of desmoplakin binds plakoglobin (PG) which then binds transmembrane desmoglein (DG) or desmocollin (DC). PG and DG interact in the intercellular space to join neighbouring cells. This shows how desmosomes effectively join adjacent cell keratin cytoskeletons, providing strength to the skin.

Desmoplakin is a rod-shaped protein, constituting the most abundant component of desmosomes. There are two isoforms (DSPI and DSPII) generated by alternate splicing and varying by the length of the central rod domain. Both have an N-terminal domain which binds plakoglobin, which then interacts with the cytoplasmic tail of desmosomal cadherins, and a C-terminal domain which targets to intermediate filaments directly (Sumigray et al, 2011). Both splice variants DSPI and DSPII (and a recently discovered DSPIa variant (Cabral et al, 2010) are expressed in almost identical levels in the epidermis (although DSPI is expressed preferentially in the heart), but the precise function and interplay of each isoform is still not fully understood. It does not appear that the two proteins are redundant to one another in the skin, as siRNA knockout of DSPI or DSPII in cultured keratinocytes shows altered cellular responses to stress induced by stretching (Cabral et al, 2012). It appears that DPSII is more important in intermediate filament stability, but DSPI plays some role in the expression and activity of other plakin proteins (Cabral et al, 2012).

Desmoplakin mutations are associated with a variety of clinical phenotypes including skin fragility, blistering and increased transepidermal water loss, but also cardiomyopathy owing to desmosome importance in contractile heart muscle (Brooke et al, 2012). Desmoplakin also seems important in morphogenesis, as desmoplakin-null embryos die at E6.5 after failing to form blood vessels or heart tissue (Vasioukhin et al, 2001) and skin-targeted ablation of desmoplakin in mice results in post-natal lethality after a few days due to massive water loss caused by blistering (Lai Cheong et al, 2005).

In the intercellular space, desmocollins (Dsc 1-3) and desmogleins (Dsg 1-4) bind to attach neighbouring cells (Naoe et al, 2009). Both desmocollin and desmoglein proteins have an intracellular anchor domain which binds plakoglobin, a transmembrane domain, and varying numbers of extracellular 110 amino acid repeats, each separated by calcium binding motifs. Desmogleins contain an extra intracellular linker protein and terminal domain (Delva et al, 2009). It is not known whether Dsc and Dsg binding is homophilic, heterophilic or a combination of both, but it is known that both proteins are required for optimal cell-cell adhesion (Getsios et al, 2004).

In the epidermis, desmosomes are important for tissue integrity and barrier function as described earlier, and all seven desmocollin and desmoglein cadherins are expressed. Desmoplakin is expressed in all layers of the epidermis but the expression pattern of the desmosomal cadherins changes throughout the process of keratinocyte differentiation, with Dsg2, Dsg3, Dsc2 and Dsc3 preferential in the basal and spinous layers, and upregulation of Dsg1, Dsg4 and Dsc1 in the granular layers (Delva et al, 2009). Peter Elias and colleagues, 2001, expressed basal Dsg3 under an involucrin promoter (i.e. forcing expression in suprabasal differentiating epidermial layers) in mice and showed that the epidermis developed a morphology more closely resembling oral mucosa than stratified epidermis. These mice died within 10 days from severe dehydration even though they showed normal differentiation markers. Whereas Dsg1 and Dsg3 are restricted to stratified epithelia, Dsg2 and Dsg4 are located in most simple epithelia as well (Brennan et al, 2007). In a similar experiment, Brennan et al, 2007 expressed basal Dsg2 under the mouse involucrin promoter and showed a hyperproliferative, hyperplasic morphology with normally basal K14 expression extending into the differentiating granular layer. These experiments show that desmosomes are not only important for tissue integrity, but also play a role in guiding differentiation. These changes will be discussed throughout the relevant stages in this introduction. Merkel cells of the epidermis are also adhered to keratinocytes through desmosomes, although they express plakophilin Pkp2, which is not found in keratinocytes (Rickelt et al, 2012). The importance of this asymmetric connection is not yet understood.

Basal keratinocytes also have an apical centrosome acting as an organiser of microtubules, which is lost as cells detach from the basement membrane and undergo differentiation. Centrosomal proteins Lis1 and Ndel1 are involved in the attachment of microtubules to desmoplakin during differentiation, and loss of either desmoplakin or Lis1 is lethal due to barrier permeability induced dehydration (Sumigray et al, 2011).

#### 1.3.1.4 Keratinocyte Adherens Junctions

Adherens junctions are essential for the structural integrity of the epidermis. The main constituent of epidermal adherens junctions are E-cadherin, a transmembrane protein which links cells by forming homophilic interactions based on calcium ions (Kim et al, 2011). The inner portion of transmembrane E-cadherin couples to actin

via α-catenins and β-catenins and vinculin, thus linking the cytoskeletons of adjacent cells (Young et al, 2003). E-cadherin ablated mice display epidermis with reduced numbers of adherens junctions, and widening of intercellular spaces, leading to stiffness and greater susceptibility to physical damage (Young et al, 2003). These results also showed that E-cadherin plays a role in guiding differentiation, with keratinocytes showing upregulation of K6, a marker of hyperproliferation, and reduced loricrin expression.

Increasing calcium concentration during differentiation induces E-cadherin binding on neighbouring cells and formation of adherens junctions. The E-cadherin-catenin complex at the cell membrane then recruits PLP3-kinase which activates phospholipase C increasing intracellular calcium (Tu et al, 2011). E-cadherin mediated adhesion is regulated by tyrosine kinases such as Fyn, also activated by rising extracellular calcium.

It is becoming clear that cell surface cadherins influence cell signalling, proliferation and differentiation. E-cadherin derived signalling in keratinocytes has been implicating in reducing cellular response to epidermal growth factor (EGF) and inducing growth arrest (Muller et al, 2007). Further evidence for this is provided by *Ctnna1* α-catenin embryonic knockout mice that demonstrated enhanced proliferation of basal epidermal cells, but apoptosis in suprabasal differentiating keratinocytes (possibly due to lack of attachments) and reduced growth factor receptor localisation to the cell membranes. The protection of basal cells against apoptosis was ablated by inhibiting focal adhesion kinase, further supporting the role of adherens junctions in preventing apoptosis and showing the importance of signalling by adherens junctions and focal adhesions (Livshits et al, 2012).

#### 1.3.1.5 Epidermal Stem Cells

The epidermis is an organ which relies on constant renewal, making it the most abundant source of stem cells in the human body (Fuchs, 2012). Cells desquamating from the surface of the stratum corneum are replaced from underneath by cells originating from the proliferating basal layer and these basal proliferative cells also need to be replaced in order to maintain a steady state during turnover of the epidermis. This balance between self-renewal and differentiation is finely regulated, in a complex field of science with implications in cancer, wound healing and skin therapies which is still being revealed (Beck and Blanpain, 2012).

The epidermis can be divided into anatomical structures such as the hair follicle, sebaceous glands, sweat glands and the interfollicular epidermis (IFE). Specific compartments of the epidermis appear to be maintained by stem cells from specific epidermal niches, even though epidermal stem cells are able to differentiate into any epidermal lineage (Blanpain et al, 2007, Ambler and Määttä, 2009). Stem cells, identified as slow-cycling, "label retaining" cells (referring to BrdU DNA labeling, (Bichenbach, 1981)) have been found in several compartments of the epidermis, primarily (~90-95%) in the bulge region of hair follicles, underneath the sebbaceous glands. When transplanted into immunodeficient mice these cells only participate in maintaining the hair follicle itself, and not the sebacceous glands or interfollicular epidermis. However, if these mice are wounded by punch biopsy, the same cells then participate in restoration of the interfollicular epidermis (Nowak et al, 2008). The hair follicle goes through cyclical phases of destruction, rest and renewal during which hair follicle stem cells and melanocyte stem cells go through tightly controlled periods of rest and activation, allowing the co-ordinated production of pigmented hair (Fuchs, 2012). Precise mechanisms are still being revealed.

However, since some areas of the body such as the palms and soles of feet are hairless, hair follicles are unlikely to be the only source of epidermal stem cells. Biedermann et al, 2010 showed that isolated human eccrine sweat gland cells are able to reconstitute an *in vitro* epidermis on collagen gels or wounded athymic rats. Stem cells have also been isolated from the upper hair follicle, hair bulb, upper isthmus and sebacceous glands, as well as the interfollicular epidermis and bulge mentioned previously (Ambler and Määttä, 2009).

Under normal conditions, the continuous replacement of cells in the interfollicular epidermis has been attributed to "epidermal proliferation units" (EPUs) throughout the epidermis which contain at least one stem cell per unit. Stems cells attached to the basement membrane then undergo either symmetric or asymmetric division, producing either two more stem cells or one stem cell and one committed cell respectively. This process is still debated, with opposing models stating that epidermal stem cells provide committed daughter cells through transit amplifying cells (Fuchs and Horsley, 2008) or directly from asymmetrical division (Clayton et al, 2007, Doupe et al, 2010). It has been proposed that the outcome of progenitor division is random, but with equal probability of generating differentiated or

progenitor cells, thus maintaining homeostasis (Doupe et al, 2012). Upon differentiation, these cells detach from the basement membrane into the suprabasal layers and begin to differentiate (Trappmann et al, 2012).

Many different molecular regulators are involved in the maintenance, commitment and differentiation of these epidermal stem cells. Wnt/β-catenin appears to be highly significant, with upregulation of this pathway pushing cells towards a hair follicle lineage and downregulation directing cells to a basal interfollicular epidermis keratinocyte lineage (Lowry et al, 2005). Proteins downstream of β-catenin also appear independently involved, such as c-myc which causes epidermal hyperplasia and hair loss in mice with atopically activated c-myc (Watt et al, 2008). P63 is found in all stratified epithelia in the body, and in the absence of p63, the epidermis fails to form, although the precise nature of this role is not yet understood (Beck and Blanpain et al, 2012). Notch is a cell membrane receptor important in cell-cell communication found in all cellular epidermis layers (Lowell et al, 2000). It is activated by delta 1 and jagged 1 on neighbouring cells or when cleaved jagged 1 is secreted by more distant cells (Urs et al, 2008). Notch signalling appears to induce differentiation of epidermal cells (Estrach et al, 2007) and in a mouse model using inducible Notch intercellular domain, Notch activation by jagged 1 caused epidermal thickening, hair clumping and lymphocyte accumulation in the dermis, indicating several different roles in the skin (Ambler and Watt, 2010).

#### 1.3.1.6 Epidermal Aquaporins

Aquaporins are water-transporting proteins present in epithelial tissues, including the skin, which assist the transporting of water or glycerol into cells. Aquaporin 3 (AQP3) is abundantly expressed in the basal and spinous layers of the epidermis and is involved in skin hydration (Hara-Chikuma and Verkman, 2005) but also plays a role in epidermal proliferation during wound healing. AQP3-null mice display dry skin, increased transepithalial water loss, reduced elasticity and delayed recovery of epidermal barrier function after wounding by removal of the stratum corneum (Hara-Chikuma and Verkman, 2008). Interestingly, although AQP3 is found only in basal and spinous layers, AQP3 expression is important for the concentration of glycerol in the stratum corneum, where it functions as a natural moisturising factor (Hara-Chikuma and Verkman, 2005). Psoriatic epidermis also shows reduced expression of AQP3 compared to healthy controls (Lee et al, 2012).

### 1.3.2 The Spinous Epidermal Layer

Once basal cells detach from the basement membrane, they begin to differentiate, undergoing changes in morphology, keratin expression, organelle formation and lipid synthesis until they are flat, anucleate remnants of cells forming the stratum corneum. Spinous cells form 4-8 layers of the human epidermis and although post-mitotic, these cells are highly metabolically active, synthesising large amounts of proteins involved in epidermal barrier function (Fuchs, 1990).

As shown in Figure 1.1, these spinous keratinocytes begin to synthesise Keratin 1 (type II keratin) and Keratin 10 (type I keratin), which are considered the earliest markers of terminal keratinocyte differentiation (Micallef et al, 2008). Owing to the long half-life of the proteins, keratin 14 and 5 can still be detected in the spinous layers, although they are no longer actively synthesised (Fuchs and Green, 1980, Rugg et al, 1994). Cell transfection experiments have shown that existing K14/5 networks are required for K1/10 networks to form properly as K1 associates to existing K14/5 networks before K10 is then integrated (Kartasova et al, 1993).

Similar to K14 and K5, K1 and K10 are also anchored to desmosomes which attach spinous keratinocytes together, making them essential for skin structure and barrier function. As well as being structural proteins, keratins may play a role in cell proliferation. Santos et al, 2002 expressed K10 under the K5 promoter and demonstrated that the presence of K10 within basal keratinocytes inhibits their proliferation. This is further hinted at during epidermal wounding, where K10 expression is downregulated, possibly to allow more proliferation to occur and repair the wound (Koch and Roop, 2004).

Mutations in Keratin 10 are associated with epidermal ichythoses presenting as skin erosions, scaliness, frequent and fragile blistering and dehydration (Cheng et al, 1992). These mutations can be lethal, causing death by dehydration and infection (Covaciu et al, 2010). Recent evidence (Wallace et al, 2011) demonstrated that double deletion of K1 and K10 in mice does not inhibit stratification or formation of a competent permeability barrier. This is surprisingly, due to the role of keratin attachment to involucrin in the formation of the cornified cell envelope (Candi et al, 2005). Nevertheless, postnatal lethality still occurred in double knockout K1/K10 mice due to increased epidermal fragility leading to lesions. Desmosomal proteins were reduced and denucleation of keratinocytes occurred earlier than normal within

the epidermis of these mice as a side-effect of K1 and K10 deletion and interestingly, the double knockout was not compensated by upregulation of other keratins. K10 knockout alone has been shown (Reichelt et al, 2001) to be compensated by upregulated basal K5 and K14.

Keratinocytes in the upper spinous layer also begin to produce involucrin, first described by Rice and Green, 1979. Involucrin is a 68Kda, rod-shaped protein with an internal region containing 39 repeats of 10 amino acids which provide the substrate for extensive crosslinking (Eckert et al, 1993). Involucrin is important during cornified envelope formation, but only represents 2-5% of the protein in mature human cornified envelopes. During terminal differentiation, involucrin is deposited to the inner surface of the keratinocyte membrane and will eventually form the backbone of the cornified cell envelope after cross-linking by transglutaminase enzymes, also produced by spinous stage keratinocytes (Eckert et al, 1993). This will be discussed in greater detail under the "Cornified Envelope" portion of this Introduction. In this thesis, Keratin 1 and Involucrin will be used as markers of keratinocyte differentiation.

### 1.3.3 The Granular Epidermal Layer

Although only a few cell layers in thickness, the granular zone of the epidermis is where the major transitions between viable, living keratinocytes and flattened remnant skeletons of the stratum corneum occur. This includes the collapse of the keratinocyte cytoskeleton, release of lipids into intercellular spaces and the replacement of the plasma membrane with the cornified envelope (Wickett and Visscher, 2006).

#### 1.3.3.1 Filaggrin

The granular layer is so-called because of deeply-stained keratohyalin granules observed in H&E staining, characterised by Brody, 1957. Keratohyalin granules are synthesised in the granular layer and are composed primarily of pro-filaggrin (400KDa) which is a histidine and arginine-rich, heavily phosphorylated and highly insoluble protein (Rawlings and Harding, 2004). Human pro-filaggrin contains 10-12 filaggrin repeats, joined by hydrophobic linker peptides (Kezic et al, 2011). Upon high extracellular calcium concentration keratinocytes degranulate and pro-filaggrin is processed to release multiple filaggrin monomers (37KDa) (Fleckman and Brumbaugh, 2002). This process requires dephosphorylation of pro-filaggrin,

followed by separation of the N-terminus from the filaggrin repeat domain. Many protease enzymes participate in this process, such as profilaggrin endopeptidase 1 (PEP1), matriptase 1 (MT-SP1) and CAP1 (Sandilands et al, 2009). The cleaved N terminus then translocates to the nucleus during the terminal differentiation of the keratinocyte preceding the loss of the nucleus, possibly suggesting a role in the denucleation of the cell (Ishida-Yamamoto, 2005).

The end-product, filaggrin (**fil**ament **aggr**egating prote**in**) is a protein essential for aggregation of keratin filaments into higher molecular weight parallel structures during the final stages of differentiation where keratinocyte flatten and become anucleate. These tightly-aggregated keratin filaments aid in the collapsing of the keratinocyte into the flattened corneocyte and also form the cytoskeletal base for the attachment of loricrin, involucrin, envoplakin and periplakin to form a scaffold on the inner keratinocyte plasma membrane (Sandilands et al, 2009).

Loss or mutation of filaggrin, profilaggrin or their processing enzymes is relatively common within European populations and is correlated with numerous skin disorders including ichthyosis vulgaris (Morar et al, 2007) but also immune-related disorders such as eczema (Bohme et al, 2012) and atopic asthma (Sandilands et al, 2009). This may be due to increased percutaneous sensitisation to allergen antigens, altered immune reactions to skin surface bacteria or reduced natural moisturising factors (O'regan et al, 2009, Kezic et al, 2011). The precise mechanism between filaggrin mutations and atopic diseases is still not understood, but filaggrin mutations and eczema are one of the mostly strongly correlated gene-to-disease associations currently known (O'regan et al, 2009). Filaggrin may also play a role in maintaining the acidic pH of the stratum corneum, as filaggrin deficient "flaky tail" mice show poor pH buffering when exposed to neutralising agents (Roelandt et al, 2011) which may also contribute towards increased atopic disease through weakening of the skin barrier. Filaggrin mutation may also be linked to inflammatory responses. Kezic and colleagues, 2012, examined 129 patients with atopic dermatitis and found strong correlations between filaggrin mutation severity and increased pH and reduced NMF content. They also detected upregulated IL-1 in the stratum corneum, with possible implications in the inflammatory effects associated with filaggrin mutations.

Patients with ichthyosis vulgaris (IV) have shown abnormalities in the granular layer and lack or keratohyalin granules (Fleckman and Brumbaugh, 2002). In a

comprehensive study of patients with heterozygous and homozygous filaggrin deficient IV, filaggrin genotype was associated with the degree of abnormalities (Gruber et al, 2011). Epidermal skin abnormalities were observed in almost every area of barrier function including increased cornified envelope fragility, intermediate filament retraction, reduction in the number and size of keratohyalin granules, increased skin surface pH, reduced stratum corneum hydration with hyperkeratosis and associated increases in stratum corneum cohesion. These factors combine to increase transepithelial water loss and paracellular penetration, as observed by a tracer dye which passed more readily between flattened corneocytes. These results were confirmed using *in vitro* models formed with filaggrin knockout keratinocytes, demonstrating that filaggrin is a highly important protein in the function of the epidermis. Filaggrin is used throughout this thesis as a marker of late stage keratinocyte differentiation.

#### 1.3.3.2 Lamellar Bodies

Lamellar bodies are an excretory organelle found in keratinocytes of the granular layer, originating from the Golgi. Lamellar bodies are round/oblong packaging organelles which play a key role in terminal differentiation (Bergman et al, 2008). During the process of differentiation, keratinocytes synthesise a number of precursor lipids such as glucosylceramides (GluCer), cholesterol sulphates ($CSO_4$), sphingomyelin (SM) and long chain free fatty acids.

In response to high intracellular calcium concentration in the granular layer of the epidermis, lamellar bodies fuse with the keratinocyte plasma membrane and exocytose their contents into the extracellular spaces (Baroni et al, 2012). This releases lipid precursors into the extracellular spaces between flattening cells. These precursor lipids such as glycosphingolipids, sphingomyelin and glucosylceramides are converted to hydrophobic ceramides by lysosomal enzymes, and most phospholipids are converted into free fatty acids (Proksh et al, 2008, Duan et al, 2012). Transglutaminase enzymes covalently attachment ceramides and fatty acids to proteins such as involucrin to increase hydrophobicity of the epidermal barrier. The result is that terminally differentiated corneocytes are embedded in a matrix of extracellular lipid lamellae of ceramides, free fatty acids (FFA) and cholesterol, forming a highly impermeable barrier (Proksh et al, 2008). This shows that lamellar

bodies are highly important for forming a large component of the epidermal hydrophobic barrier.

These precursor lipids are primarily packaged into lamellar bodies with the aid of ATP-binding cassette transporters, namely at least 11 members of the ABCA12 transporter family (Zuo et al, 2008, Mizutani et al, 2009). The latest evidence suggests that golgi pH receptor (GPHR) also plays some role in either the packaging or excretion of lipids by lamellar bodies, as GPHR knockout mice display abnormal lamellar bodies and reduced ceramide content of the stratum corneum (Tarutani et al, 2012). Mice lacking ABCA12 transporters are unable to transport precursor lipids into lamellar bodies (Zuo et al, 2008). These mice displayed hyperkeratosis of the stratum corneum but lacked mature Ceramide 1/Cer(EOS), possibly because lamellar bodies were not able to transport immature glucosylceramides to a location where they could be converted into mature, hydrophobic ceramides. These ABCA12-null mice die at birth due to rapid dehydration caused by accelerated transepidermal water loss. In humans, ABCA12 mutations cause the devastating disease Harlequin Ichythosis, characterised by hard, plate-like scales over all epidermal surfaces, poor appendage formation and often infant mortality due to lack of temperature regulation, enhanced water loss and bacterial infection (Zuo et al, 2008).

As well as Harlequin Ichythosis, two further disorders are associated with abnormal lamellar body transportation. CEDNIK (cerebral dysgenesis, neuropathy, ichythosis, and palmoplantar keratoderma) syndrome is caused by loss of function mutation in a SNARE protein, responsible for mediating membrane fusion which is utilised heavily in the golgi. This has implications for the entire body, but patient skin shows empty, abnormal granules throughout the epidermis and unsecreted lamellar body contents in cornified cells (Hershkovitz et al, 2008). The second known disorder is ARC syndrome, caused by mutation in VPS33B, a protein which regulates SNARE membrane fusion. In this disorder, intact lamellar granules were found inside the cornified layers, indicating dysfunction in proper secretion (Ishida-Yamamoto and Kishibe, 2011).

As well as precursor lipids, lamellar bodies also contain antimicrobial defensins (Ishida-Yamamoto, 2005), which are released into the extracellular areas of the stratum corneum to aid in the skin's protective role. Lamellar bodies may also play a role in both the formation and degradation of corneodesmosomes in the stratum

corneum, as they have been found to contain corneodesmosin, desquamation enzymes (kallikreins) and inhibitors of those enzymes (Ishida-Yamamoto et al, 2011).

#### 1.3.3.3 Loricrin

Loricrin is a globular 26kDa protein which is expressed late in the granular layer. Loricrin is the main component of the cornified cell envelope where calcium-dependent transglutaminase (TGase) enzymes crosslink loricrin and involucrin (linking glutamine to lysine side chains by isopeptide bonds), followed by other proteins to form an insoluble protein backbone (Steinert et al, 1997). This process is described in more detail in relation to cornified envelope formation.

#### 1.3.3.4 Epidermal Tight Junctions

While epidermal barrier function is largely derived from the flattened cells of the stratum corneum, nucleated cells of the stratum granulosum and lower layers also play an important role. Tight junctions regulate the paracellular diffusion barrier of the epidermis by closely connecting neighbouring nucleated cells in the granular layers. Tight junctions, containing occludin, zonula occludens proteins (ZO-1 and ZO-2), JAM-A, cingulin and claudin-1, claudin-4 and claudin-5, are found in the lower granular layer of the epidermis (Peltonen et al, 2006) and are lost towards the most superficial granular layer (Ishida-Yamamoto et al, 2012). Tight junction proteins are found expressed throughout different layers of the epidermis, but only seem to form mature junctions, capable of trapping hydrophilic tracers, in the lower granular layer (Kirschner et al, 2012). The question of whether differentiation induces tight junction formation, or whether tight junction formation influences differentiation, is yet to be understood and has been posed as a "chicken and egg" situation (Kirschner et al, 2012).

Tight junctions are clearly important in epidermal barrier function, as claudin-1 deficient mice die shortly after birth due to water loss caused by tight junction deficiencies. However, if the epidermis is transplanted onto nude mice, it grows in a hyperproliferative manner (Furuse et al, 2002). Tight junctions may also be able to compensate in epidermis which is affected by other disorders. For instance, in psoriatic lesions, tight junctions are present deeper in the epidermis (into the spinous layers), which was not observed in either normal skin or healed lesions from the same patient (Peltonen et al, 2006).

There is evidence (Kuroda et al, 2010) showing that functional tight junctions play a role in lamellar body secretion, and that disrupting tight junction formation inhibits properly polarised (i.e. towards the stratum corneum) lamellar body release. This suggests a role of tight junctions as guiding lamellar bodies, perhaps acting as a "fence" to prohibit secretion along some axis of the keratinocyte. Calcium is one regulators of lamellar body secretion and disturbances in tight junctions by sodium caprate have been shown to upset the normal epidermal calcium gradient and disregulate the balance between proliferation and differentiation (Kurasawa et al, 2011). This may implicate tight junctions formation in guiding differentiation. However, a recent study (Ishida-Yamamoto et al, 2012) showed that in the sequence of keratinocyte differentiation, lamellar granule secretion occurs before epidermal tight junctions are fully formed which adds further confusion to this interaction.

Tight junctions may play role in the immunological function of the skin. It has been suggested (Kubo et al, 2009) that the tight junctions in the stratum granulosum allow Langerhans cells to present antigens from the stratum corneum while still maintaining epidermal barrier function. Evidence suggests that tight junctions are formed between keratinocytes and Langerhans cells, which themselves express claudin 1. Toll-like receptor 2 (TLR2) activation was also found to increase tight junction formation in the epidermis, further indicating an immune system linkage (Yuki et al, 2011).

Other new evidence (Haftek et al, 2011) shows that tight junctions may compartmentalise the stratum corneum by providing lateral but not horizontal connections between cornified envelopes. As such, the precise roles of tight junctions in the epidermis are not yet fully understood, although they are recognised as important for many aspects of barrier function.

In this thesis, ZO-1 staining will be used to identify tight junctions in cultured keratinocytes.

#### 1.3.3.5 Granular to Stratum Corneum Transition

In the upper granular layer, keratinocytes collapse, become anucleate and expel their contents into the extracellular spaces. This process has been likened to a form of apoptosis, but several differences are noted - apoptosis occurs in individual cells, whereas terminal differentiation is synchronous across multiple cells. Differentiation

also takes many days, whereas apoptosis occurs within minutes. Cells undergoing apoptosis also fragment and display membrane blebbing, but flattening keratinocytes do not (Candi et al, 2005).

During the transition between viable to non-viable keratinocytes, the phospholipid cell membrane of viable keratinocytes is replaced by the cornified envelope and the membrane phospholipids are broken down into free fatty acids by phospholipases. These free fatty acids are then metabolised into other hydrophobic barrier lipids (Fluhr et al, 1992). Cellular proteins such as keratins and filaggrin are deiminated and further degraded into natural moisturising factors which will be discussed later.

### 1.3.4 The Cornified Layer

The stratum corneum has been termed "bricks and mortar" (Elias, 1983) where heavily-crosslinked, insoluble cornified envelopes of protein and lipid form the bricks, embedded in mortar of intercellular lipid lamellae formed primarily by ceramides (Nemes and Steinert, 1999). This mixture provides a structurally robust but flexible , hydrophobic barrier. A schematic diagram of this structure is shown in Figure 1.1. The stratum corneum is approximately 12-16 layers thick on most body sites, although as few as 9 layers on the eyelids and over 50 layers on the palms or soles of the feet (Wickett and Visscher, 2006). This corresponds to approximately 10-100μm thickness depending on body site. In order to pass through the stratum corneum, molecules must weave their way through the extracellular lipids around the insoluble cornified envelopes, or pass directly through the flattened corneocytes (Elias et al, 1981).

Cornified envelope formation is a carefully ordered process which is essential for the proper development of the epidermal barrier. For instance, lamellar bodies locate to the cell membrane to excrete lipids precursors used in cornified envelope formation, but they need to do this before access to the membrane is blocked by the formation of the cross-linked protein barrier (Määttä, 2004).

Cornified envelopes are insoluble structures, 5-20nm in thickness, which have replaced the viable keratinocyte plasma membrane during the process of differentiation. They contain an insoluble inner layer of heavily crosslinked involucrin, loricrin and small proline rich proteins with an outer layer of covalently

attached lipids and represent the end-point of a keratinocyte life cycle in the epidermis - so-called "terminal differentiation" (Proksh et al, 2008).

Involucrin and loricrin have already been discussed, but they are not the only protein constituents of the cornified envelope. There are several small proline rich proteins (SPRPs) ranging from 6-25kDa in the epidermis. Of particular importance are SPRR2G and SPRR4 which function as bridge-forming amino acid donors and receivers during TGase assembly of cornified envelopes (Magdalini et al, 2012). SPRP4 may also play a role in quenching reactive oxygen species in the skin (Vermeij et al, 2010). Other proteins such as trichohyalin, which bears structural similarities to involucrin (Kypriotou et al, 2012) and Kazrin, first described by Groot et al, 2000, also form part of the scaffold on which the cornified envelope is formed. Kazrin binds to periplakin and plays a role in regulating differentiation. Overexpression of kazrinA in human keratinocytes promotes differentiation and knockout of kazrinA impairs differentiation (Chhatriwala et al, 2012). S100 proteins are calcium binding proteins located within the nucleus and/or cytoplasm of keratinocytes. Under the influence of increased intracellular calcium concentration S100 proteins undergo conformational change and bind to target proteins to modify their function. S100 proteins can also act as transglutaminase substrates and cornified envelope precursors (Broome and Eckert, 2004).

Desmosomes appear to be the initiation sites of cornified envelope formation (Di Colandrea et al, 2000). Two of the earliest cornified envelope precursors are envoplakin and periplakin, which begin the process by forming heterodimers and locating to the desmosome where the C-terminus binds intermediate filaments (Sevilla et al, 2007). Periplakin binds kazrin, a protein which localises to the cell membrane, desmosomes or adherens junctions (Groot et al, 2004), and also appears to play a role in initiating differentiation (Sevilla et al, 2008). Transglutaminase enzymes link envoplakin, periplakin and involucrin by iso-peptide bonds, forming a scaffold which bridges the gaps between desmosomes just inside the cell plasma membrane. Late envelope proteins such as loricrin, SPRPs and bundled keratin filaments are then attached to the scaffold (Kypriotou et al 2012).

Interestingly, many of the proteins essential for epidermal differentiation in humans are encoded by genes clustered on chromosome 1q21 in the so-called "epidermal differentiation complex (EDC). These proteins include involucrin, loricrin, small

proline-rich proteins, transglutaminases, S100 family proteins and profilaggrin which constitute the cornified envelope (Kypriotou et al, 2012).

Hydrophobic lipids such as ω-hydroxyceramides are covalently attached onto this protein backbone, thus forming a highly insoluble, hydrophobic matrix which replaces the normal cell membrane (de Koning et al, 2012). There are four TGase enzymes expressed in keratinocytes, each with slightly different functions. Of particular importance is TGase1 which cross-links cornified envelope precursor proteins, and mutations of this enzyme cause lamellar ichthyosis and proliferative hyperkeratosis, leading to increased transepidermal water loss (Kypriotou et al, 2012).

Interestingly, despite the ubiquitous presence of involucrin, envoplakin and periplakin in cornified envelopes, loss of either one does not confer significantly abnormal barrier function (Määttä et al, 2001, Aho et al, 2004). Even knockout of loricrin, which is the most abundant cornified envelope protein, does not cause a serious phenotype (Koch et al, 2000), suggesting compensation mechanisms are able to recover barrier function. Triple knock-out mice with ablated envoplakin, periplakin and involucrin (Sevilla et al, 2007) showed dry, scaly skin, fragile cornified envelopes and reduced ω-hydroxyceramide content, but no fatal barrier dysfunction. Compensation was achieved by downregulation of cathepsin and proteinase enzymes, resulting in reduced desquamation of flattened corneocytes and accumulation of a thicker stratum corneum.

#### 1.3.4.1 Natural Moisturising Factors

The term natural moisturising factors (NMFs) describes a number of hydrophilic amino acids, metabolites and ions which maintain the hydration and acidic pH of the stratum corneum. As well as the protein and lipid barrier of the epidermis, a water gradient is also present across the stratum corneum under normal conditions (Caspers et al, 2001), allowing it to function as a barrier in dry environments. The cellular layers of the epidermis contain approximately 70% water, which drops rapidly to 40-45% in the stratum corneum over a distance of only 15-20μm, with the total stratum corneum being approximately 150μm thick (Caspers et al, 2003). NMF distribution is inversely proportionate to this, with the NMF concentration increasing rapidly shortly after the stratum corneum layer begins and remaining relatively constantly

through the thickness of the stratum corneum itself, aside from the region closest to the surface of the skin, likely due to environmental factors (Caspers et al, 2003).

As mentioned earlier, filaggrin monomers are essential to the NMF as the substrates for deimination and proteolysis. Filaggrin, along with Keratin 1 and other proteins in collapsed keratinocytes, undergoes deimination - the conversion of arginine into citrulline residues by peptidylarginine deiminases (PAD) (Sandilands et al, 2009). After deimination, enzymes such as caspase 14, caplain 1 and bleomycin hydrolase (Kamata et al, 2009) degrade filaggrin peptides into free amino acids (Kezic et al, 2009) that are subsequently converted into trans-urocanic acid (UCA) and pyrrolidone carboxylic acid (PCA) (O'regan et al, 2009 Roelandt et al, 2011). NMFs are formed during the final stages of terminal differentiation at the layers of granular to stratum corneum transition. FLG2 (filaggrin 2) is a member of the S100 fused-type protein family located within profilaggrin lamellar bodies and is involved in barrier maintenance and natural moisturising factor formation (de Koning et al, 2012).

Filaggrin breakdown products comprise approximately 50% of the natural moisturising factors with the remainder formed by lactate, other sugars, urea and many ions including chloride, sodium, potassium and calcium (Rawlings and Harding, 2004). Some of these other products such as urea and lactate arise from sweat glands, and all NMFs can also be diluted in sweat (Caspers et al, 2003). All of the NMF compounds identified so far are water-soluble and low molecular weight, allowing the stratum corneum to effectively "bind" water from the atmosphere and from water evaporating from the cellular epidermis, thus forming a waterproof barrier (Bouwstra et al, 2003). Excessive hydration of the stratum corneum disrupts this ability and increases epidermal permeability (Warner et al, 2003).

NMF formation is a tightly regulated process which is precisely timed to maintain optimal barrier function. Intact filaggrin is present in only 2-3 layers of the granular-stratum corneum and has a half life of roughly six hours in keratinocytes (Kamata et al, 2009). When keratins bind filaggrin during the collapse of the keratinocyte cytoskeleton, they protect it from degradation, but when corneocyte cornified envelopes have sufficiently strengthened and the stratum corneum is sufficiently dry, filaggrin is subject to proteolysis and NMFs are rapidly released. If corneocytes are not sufficiently dried and strengthened by cornified envelopes, osmotic pressures

caused by NMF release may disrupt barrier function rather than improving it (O'Regan et al, 2009). Caspases are ubiquitously expressed, but caspase-14 appears unique to the cornified epithelia, with caspase-14 activation levels correlated with the degree of cornification (Denecker et al, 2008). Caspase-14(-/-) mice show accumulation of filaggrin fragments and a reduction in NMF in the stratum corneum (Hoste et al, 2012). Histidine from filaggrin degradation is converted into urocanic acid which has been shown to play a role in UV radiation protection (Mildner et al, 2000).

Many other factors can affect NMF content of the stratum corneum including reduced profilaggrin synthesis with aging, removal of NMFs by repeated washing or reduction in NMFs by UV exposure (O'Regan et al, 2009). As described earlier, mutations in filaggrin are relatively common and are associated with epidermal structural defects found in ichthyosis vulgaris and atopic dermatitis. However, the structure of filaggrin itself is important as a precursor for the production of NMFs and filaggrin mutations have been associated with abnormalities of filaggrin breakdown products, including NMFs (Kezic et al, 2008). Even in atopic dermatitis patients without any filaggrin mutation present, NMF concentration was significantly reduced due to downregulation of filaggrin (Kezic et al, 2011). In atopic dermatitis patients *with* filaggrin mutations, NMF concentration was correlated with the severity of the clinical condition and so NMFs were proposed as a marker for measuring patient clinical progression and response to treatment. NMFs have typically been measured by tape stripping or biopsy, which is clearly not ideal for patients already presenting with epidermal barrier defects, but recently more non-invasive methods are being developed (Takada et al, 2012).

#### 1.3.4.2 Desquamation of the Stratum Corneum

Cornified envelopes of the stratum corneum are linked by corneodesmosomes which are formed during the granular to stratum corneum layer transition (Ishida-Yamamoto et al, 2011). In the cytoplasm of differentiating keratinocytes, desmosomal attachment plaques become integrated into the forming cornified cell envelope itself and corneodesmosomes express a unique protein, corneodesmosin, which is synthesised by granular cells and packaged into lamellar bodies. After secretion, corneodesmosin is cross-linked with cornified envelope proteins and likely

mediates binding to adjacent corneocytes in the presence of calcium (Jonca et al, 2002).

Desquamation of cornified envelopes is essential for the proper turnover of the epidermis. In the desquamating stratum corneum, corneodesmosin is cleaved by kallikrein-related peptidases (KLKs) and cathepsins. At least 8 different KLK enzymes are expressed in the epidermis and secreted by lamellar bodies, which function as a proteolytic cascade (Komatsu et al, 2006). These KLKs, along with at least three different cathepsins regulate the balance between desquamation and keratinisation, and therefore are expressed differently in various body sites in accordance with varying thicknesses of the stratum corneum (Ishida-Yamamoto et al, 2011). A number of protein inhibitors such as LEKTI, SKALP and SLPI which act on KLKs or cathepsins are also present, further aiding in the regulation of desquamation (Brattsand et al, 2009). These protease inhibitors also act as part of a cascade (Fortugno et al, 2011) and are implicated in disorders, for instance Netherton Syndrome, a skin disorder caused by LEKTI mutation, characterised by ichthyosis due to reduced desquamation (Komatsu et al, 2008). However, as shown earlier (Sevilla et al, 2007), downregulation of desquamation enzymes can rescue the barrier function of mice lacking key structural components of the cornified envelope.

The acidity of the stratum corneum also plays a role in desquamation, with higher pH conditions being associated with increased proteolysis and increased corneodesmolysis (Fluhr and Elias, 2002, Kezic et al 2012). NMFs, discussed previously, may be partly responsible for maintaining the acidic pH of the stratum corneum (O'Regan et al, 2009). The water content of the stratum corneum also plays a role in desquamation, with low humidity environments reducing the action of hydrolase enzymes and reducing the rate of corneodesmolysis (Rawlings et al, 1995). Watkinson and colleagues, 2001, showed that relative humidity regulates the activity of stratum corneum chymotryptic enzyme, with lower desquamation rates occurring in reduced humidity. This was further demonstrated using *in vitro* epidermal models (Bouwstra et al, 2008).

#### 1.3.4.3 Epidermal Lipids

Ceramides represent approximately 35-50% of epidermal lipids by dry weight, and are essential for barrier function (Suhonen et al, 2003, Mizutani et al, 2009). Ceramide upregulation begins in the suprabasal layers of the epidermis and continues

throughout until the stratum corneum which is largely composed of ceramides (Suhonen et al, 2003). Reduced ceramide content of the epidermis causes increased TEWL and barrier dysfunction (Holleran et al, 2006, Zuo et al, 2008). There are four steps towards ceramide-based barrier function - ceramide synthesis, packaging in lamellar bodies, secretion from those lamellar bodies, and processing into final hydrophobic compounds.

As of 2011, there are 12 known ceramides in human skin, although this number increases year-on-year (Smeden et al, 2011). Ceramides basically comprise a sphingoid base and an ester-linked fatty acid and vary depending on which sphingoid base is used and the length of the fatty acid chain attached. These ceramides are given nomenclature N, A and EO indicating non-hydroxy, alpha-hydroxy or ω-hydroxy amide-linked fatty acids, and S, DS, P, H denoting sphingosine (Sph), dihydro-Sph, phyto-Sph or 6-hydroxy-Sph respectively. The ceramides EOS, EOH and EOP (so-called ω-O-acylCer (acylCer)) are unique to epidermis and essential for barrier function due to their extra ester-linked fatty acid chains (primarily linoleic acid) attached to the existing fatty acid chain attached to the sphingol base. This naming system as structural diagrams of each ceramide are reviewed by Mizutani et al, 2009.

The acylCer are bound to involucrin on the external surface of corneocytes, forming the lipid component of the cornified envelope. In essential fatty acid deficiency, linoleic acid in the acylCer is replaced by non-essential fatty acids such as oleic acid, resulting in barrier defects, indicating the importance of these unique ceramides (Uchida et al, 2008).

Epidermal ceramides are synthesised by keratinocytes from basic components (including serine, palmitoyl-CoA and recycled sphingosine from ceramide breakdown) in a multiple-step conversion pathway involving serine palmitoyltransferase, FVT-1, and ceramides synthases 1-6 (CerS1-6) (Mizutani et al, 2009) which occurs primarily at the endoplasmic reticulum membranes (Uchida et al, 2008). CerS3 is the most abundant ceramide synthase enzyme found in keratinocytes, and expression increases dramatically during differentiation (Mizutani et al, 2008). Newly synthesised ceramides are then converted to glucosylceramides by GlcCer synthase and to sphingomyelin by SM synthase at the golgi apparatus. These precursors are then packaged into lamellar granules as described previously (Zuo et

al, 2008) and can act as precursors for stratum corneum ceramide synthesis after excretion at the granular-stratum corneum interface (Uchida et al, 2008).

After excretion from lamellar bodies, β-glucocerebrosidase and sphingomyelinase (SMase) enzymes hydrolyse these precursors into mature barrier ceramides (Mizutani et al, 2009). Mutations in SMase result in a less serious barrier defective phenotype (Holleran et al, $2006_b$). Deficiencies in β-glucocerebrosidase causes barrier dysfunction (Gaucher disease) as all stratum corneum ceramides can be synthesised from glucosylceramides, whereas only two epidermal ceramides (AS and NS) can be synthesised from sphingomyelin by SMase. Gaucher Disease is a neurological disorder which also presents with ichthyosis and poor epidermal barrier function resulting from defective ceramide production (Holleran et al, 1994, 2006).

Ceramides vary by their sphingoid bases and by their amide-linked fatty acid attachments. The 6 known CerS enzymes are each responsible for assembling ceramides with different chain lengths, with CerS2 and CerS3 displaying preference for longer fatty acid chain lengths (Mizutani et al, 2006). Ceramides are located throughout the body but the epidermis is the only location in the body known to have extra long (C28-32) fatty acid chain ceramides. Ceramide NS (Cer 2, or nonhydroxysphingosine) particularly contains these very long fatty acid chains (Mizutani et al, 2009).

As well as barrier function to water loss and compound entry, there is evidence that ceramides also act as signalling molecules in the epidermis. High intracellular ceramides induce apoptosis in keratinocytes which have been exposed to excess UV radiation. This is regulated by ceramide hydrolysis (by ceramidase enzymes) or conversion to non-proapoptotic GluCer which protects against this apoptosis (Uchida et al, 2010).

The most common family of epidermal diseases are termed ichthyoses, which can arise directly from epidermal protein mutations such as filaggrin and keratin or from mutations in enzymes involved in the conversion of precursor lipids into mature barrier lipids (Elias et al, 2012). Therefore, epidermal barriers in patients with ichthyoses display an immature lipid profile such as excessive triglyceride content, inadequate FFA content, insufficient ceramide content paired with high glucosylceramide and reduced cholesterol content (Elias et al, 2012).

For example, X-linked ichthyosis (XLI) is caused by mutations in the steroid sulphatase enzyme and results in elevated cholesterol sulphate levels in the epidermis, coupled with insufficient cholesterol content (Elias et al, 1984 and 2012). More recent studies (Hoppe et al, 2012) have shown altered expression of 27 different genes with a resulting phenotype of corneocyte retention, dry and scaly skin, with impaired barrier function that was not restored by moisturisers. Another ichythosis is neutral lipid storage disease with ichthyosis (NLSDI), also called Dorfman–Chanarin syndrome (DCS). This disorder is often caused by a mutation in CGI-58, an activator of the adipose triglyceride lipase (ATGL) enzyme. This results in an accumulation of triglyceride and a reduction of free fatty acid in the epidermis and has been linked to impaired barrier function (Uchihara et al, 2010).

### 1.3.5 Calcium as a Driver of Differentiation

Calcium has been mentioned several times in the previous pages as a key regulator of protein synthesis and cell behaviour throughout the epidermis. It is essential for many aspects of differentiation such as keratin, involucrin, and loricrin transcription, activation of transglutaminase enzymes (Hitomi, 2005), the processing of pro-filaggrin to filaggrin, triggering of lamellar body release (Elias et al, 2002) and formation of adherens junctions (Gniadecki et al, 2001). Influx of calcium into keratinocytes also activates enzymes responsible for epidermal barrier lipid synthesis and subsequent conversion to more hydrophobic derivatives (Micallef et al, 2008). Calcium is located in the epidermis in three distinct locations - in the extracellular fluid, in the keratinocyte cytosol and inside keratinocyte intracellular organelles such as the endoplasmic reticulum and the Golgi apparatus (Pillai and Bikle, 1991, Celli et al, 2010).

The cellular epidermis contains an extracellular calcium gradient with a low calcium concentration in the basal epidermis rising to the highest concentration in the granular layer at the lower boundary of the stratum corneum (Cornelissen et al, 2007). The calcium ion concentration in the stratum corneum itself is very low due to its dry nature and the inability of corneocytes to dissolve the ions (Baroni et al, 2012). It is not fully understood how this epidermal gradient is formed - i.e. whether it is actively created by calcium pumps in keratinocyte cell membranes (Elias et al, 2002) or tight junction activity (Kurusawa et al, 2011) or whether it is passively

created by the dry upper surface of the stratum corneum causing a water gradient (Adams et al, 2012).

Rising extracellular calcium concentration is detected by CaR **ca**lcium **r**eceptors on the surface of the keratinocyte. This receptor is essential for proper epidermal differentiation, indicating the importance of extracellular calcium signalling. Cells lacking this CaR do not raise intracellular calcium in a normal manner (Tu et al, 2001) and mice lacking this receptor display abnormal epidermal differentiation (Komuves et al, 2002). Rising extracellular calcium triggers a set of events shown in Figure 1.3, initially activated by the CaR. Calcium ions bind the CaR and through second messenger signalling increases intracellular diacylglycerol (DAG) and inositol triphosphate (IP3). Rising intercellular IP3 triggers the golgi and endoplasmic reticulum to release calcium stores, further increasing intracellular calcium concentration. This rising intracellular calcium causes protein kinase C to bind the RACK receptor which in turn activates the keratinocyte calcium ion channels to open and increase intracellular calcium even further as well as activating AP-1 transcription factors (Bilke, 2004). During terminal differentiation, keratinocytes flatten in the granular layer releasing intracellular calcium stores into the surrounding tissue, thus further increasing extracellular calcium concentration (Menon and Elias, 1991). Rising extracellular calcium and subsequent increasing intracellular calcium concentration is also involved in differentiation by action of the Raf/MEK/ERK kinase cascade pathway (Schmidt et al, 2000) as well as inducing growth arrest by inducing p21 (Sakaguchi et al, 2003).

Under *in vitro* conditions, 0.06-0.09mM $Ca^{2+}$ is commonly used as "low calcium" culture conditions for normal cell maintenance and proliferation, as keratinocytes will not proliferate in <0.03mM $Ca^{2+}$. In low calcium conditions, desmosome formation is inhibited and so cells grow as a monolayer (Hennings et al, 1980). 1.1-1.5mM is used as "high calcium" in order to induce differentiation in cell culture conditions (Micallef et al, 2008). However, in the native epidermis, free calcium concentration ranges from only 0.5µM to >20µM, as most calcium is bound to proteins or cellular organelles (Adams et al, 2012). Human free calcium concentration in serum is approximately 1.1-1.4mM, and therefore the concentration referred to as "high" in keratinocyte cell culture closely represents physiological calcium concentration.

Calcium is not the only player in keratinocyte differentiation. Studies mentioned earlier have shown that detachment from the basement membrane (Zhu and Watt, 1996) and increased cell-cell contact (Kolly et al, 2005) are also key players in keratinocyte differentiation, at least *in vitro*. Kolly et al, 2005 found when cultured keratinocytes become confluent, in either high or low calcium conditions, c-Myc is downregulated. High calcium concentration alone was not sufficient to induce cell cycle arrest but adding c-Myc inhibitor to the culture media resulted in immediate cell cycle arrest, indicating the importance of cell-cell contacts in differentiation. Vitamin D also plays a role in differentiation and keratinocytes are the only cell type in the human body with a full profile of vitamin D conversion pathways. They are capable of fully producing the active form of Vitamin D, $1,25(OH)_2D_3$ from 7-dehydrocholesterol (7-DHC) via 1OHase, utilising UV light. Keratinocytes in the stratum basale contain vitamin D receptors and produce their own Vitamin D in levels inversely proportional to their level of differentiation as well as in accordance with regulation by parathyroid hormone (Bikle et al, 1986 and 2004). Calcium, along with AP-1 and Vitamin D metabolites all act in the nucleus to induce transcription and expression of proteins such as involucrin, loricrin and transglutaminase enzymes (which themselves are activated by calcium ions).

However, despite the role of other molecules in the initiation differentiation, calcium is still required for the formation of cornified envelopes, activation of transglutaminase and many other aspects of differentiation discussed previously.

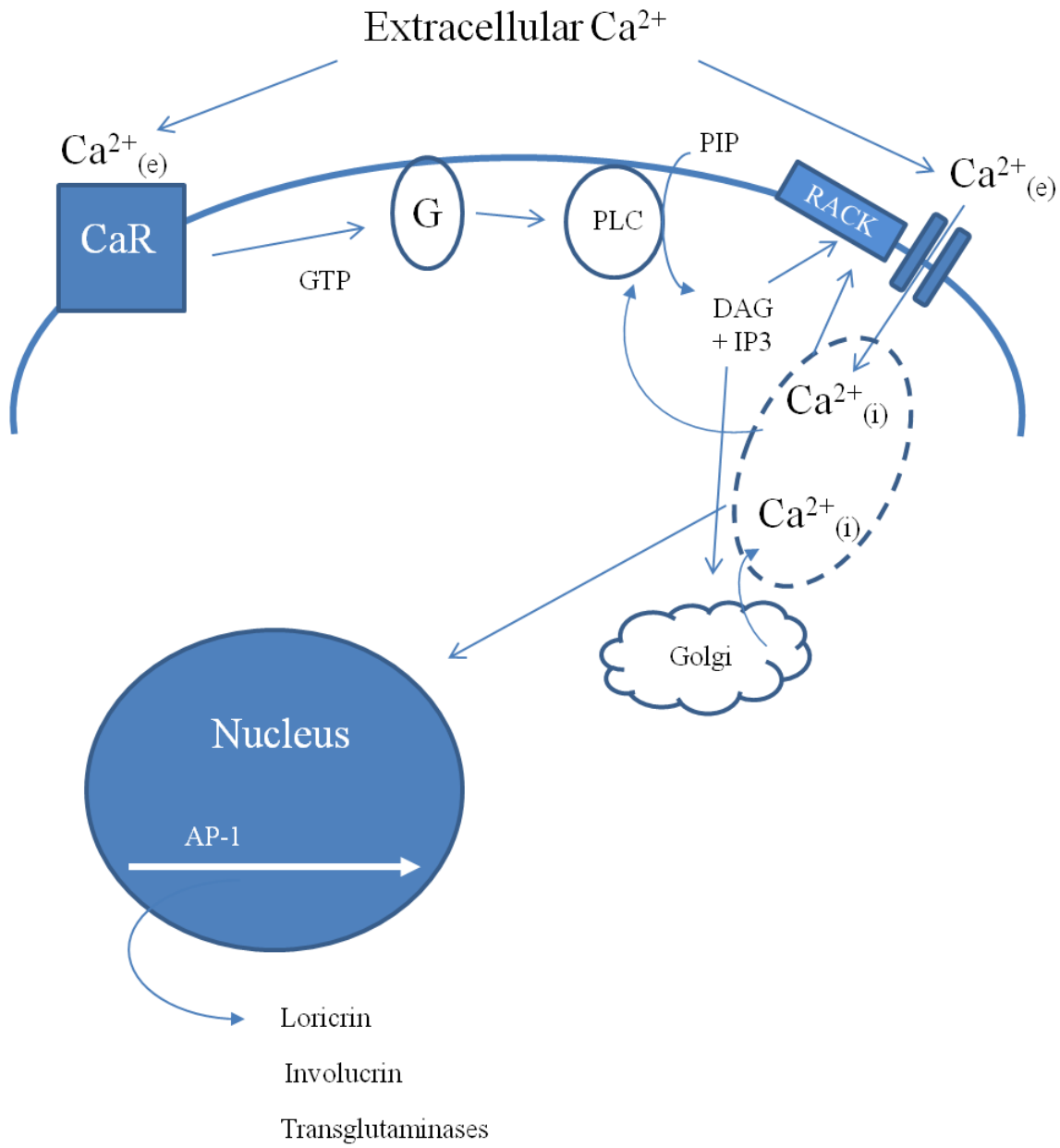


**Figure 1.3. Schematic Diagram of Extra/Intracellular Calcium Signalling**

Rising extracellular calcium ($Ca^{2+}_{(e)}$) is detected by the membrane-bound CaR calcium receptor. Through second messenger signalling, the golgi are stimulated to release calcium stores into the cytoplasm. Simultaneously, keratinocyte membrane-bound calcium channels open, allowing a further increase in intracellular calcium ($Ca^{2+}_{(i)}$)concentration. Calcium acts in the nucleus on calcium response elements (CaREs) and AP-1 to activate transcription of cornified envelope components. Figure based on Bikle et al, 2004.

### 1.3.6 Factors Affecting Epidermal Barrier Function

Several factors can alter epidermal barrier function, including chemical exposure (Kwak et al, 2012), hydration (Warner et al, 2003), moisturisation (de Paépe et al, 2001) and biological molecules. Retinoids are Vitamin A analogues which are involved in proliferation, differentiation and apoptosis in many cell types (Lee et al, 2009). Retinoids have been known to regulate differentiation in the epidermis since Fuchs and Green, 1981. In the epidermis, both natural and synthetic retinoids are known to increase epidermal proliferation and inhibit differentiation - suppressing biosynthesis of epidermal lipids, cholesterol, and long-chain fatty acids as well as cornification (Lee et al, 2009). Retinoids also increase corneodemosomal degradation and downregulation of corneodesmosomal cadherins, thus increasing desquamation (Kim et al, 2011), leading to their consideration and use as therapeutic agents.

Retinoids bind nuclear RXRs (retinoid X receptors) and RARs (retinoic acid receptors), each with multiple isoforms. These receptors form RXR-RAR heterodimers or RXR-RXR homodimers after activation, and then bind DNA retinoid acid response element (RARE) sequences which regulate target genes (Lee et al, 2009). Topical retinoids have been used for the treatment of many skin disorders including psoriasis, acne and even cancers. However therapeutic benefits are often offset by undesired side effects such as scaling, dryness and excessive desquamation, due to increased proliferation of keratinocytes and reduction of lipid content in the epidermis (Lee et al, 2009). Keratinocyte response to retinoids is very rapid, with changes in gene regulation occurring after one hour. Naturally-occurring all-trans retinoic acid (ATRA) has been most commonly used, but is unstable and quickly oxidises under UV light (Barnard et al, 2009).

Due to this, many synthetic retinoid analogues have been developed for possible therapeutic use (Odorisio et al, 2012) and *in vitro* experimentation. The 3D scaffold or other 3D cell culture models represent suitable substrates for testing of compounds such as synthetic retinoids for their effect on cell behaviour before *in vivo* testing is carried out, as in Jean et al, 2011. Such models also represent potential cost-savings for testing, as basic parameters such as speed of action, duration of action and dosage may be calculated using large numbers of *in vitro* models before carrying out smaller-scale *in vivo* testing.

### 1.3.7 Epidermal Permeability and Permeation Enhancers

Transepidermal drug delivery is an appealing method for drug delivery for many reasons. It is non-invasive and can deliver a steady dose of drug, avoiding spikes in bloodstream concentration which is useful in hormone replacement (testosterone gels or oestrogen/progesterone birth control patches), nicotine delivery (skin patches) and steady long-term pain relief (Fentanyl patches) allowing lower doses to be used. Transepidermal delivery also avoids stomach digestion and first pass liver metabolism which are often pharmacokinetic problems in drug design (Chantasart et al, 2007, BNF volume 63).

There are three major routes through the epidermis - transcellular (through corneocytes themselves), paracellular/intercellular (between corneocytes) and appendageal (through hair follicles, sebbaceous glands and sweat glands) (Jampilek and Brychtova, 2010). The appendageal route is a minor route, as these structures occupy only a small fraction of epidermal surface area. However, they represent the most feasible route for passage of large molecular weight compounds (Oshizaka et al, 2012). The transcellular route requires a compound to pass through tough, cross-linked protein matrices, intercellular lipids, cell membranes and natural moisturising factors, all of which confer resistance to most types of compound. However, this is shortest and most direct route through the epidermis (Vavrova et al, 2005). Comparatively, the paracellular route requires compounds to wind their way through the intercellular lipid "cement" between many layers of flattened corneocytes. This increases a 20µm thick stratum corneum into a diffusion pathway of approximately 400µm (Hadgraft, 2001), drastically reducing permeation. Although these routes have historically been defined separately, in reality most compounds applied to the skin travel through a combination of both pathways (Jampilek and Brychtova, 2010).

In order to overcome the epidermal obstacles to drug delivery, chemical penetration enhancers (CPEs) have been developed. Many compounds can increase epidermal permeability, such as dimethylsulphoxide (DMSO), sodium dodecyl sulphate (SDS), acetone, urea, alcohols and other chemicals. However, only a few compounds are commonplace in cosmetic or pharmaceutical products due to toxicity and undesirable side effects such as irritation, dryness or allergy (Ibrahim et al, 2009), as well as regulatory requirements. An ideal permeation enhancer will support the passage of a target compound through the epidermal barrier but only cause a short-term, minimal

disruption to the epidermis. The enhancer should also not pass into the bloodstream itself and also needs to be compatible with the target molecule that it is carrying.

One of the first custom-designed permeation enhancers was Azone (1-dodecylazacycloheptan-2-one), an oily, lipophilic liquid which was discovered in 1976 (Hoogstraate et al, 1999). However, it is still not approved by the FDA for use in humans due to antiviral effects. Azone mechanism of action is still not fully elucidated but it is thought to insert itself and disrupt lamellar bilayers in the stratum corneum or to compete for hydrogen bonds between stratum corneum lipids, thus weakening their structure. As such, many Azone analogues have been developed aiming for the same effects without unwanted side effects (Jampilek and Brychtova, 2010).

Simply altering the pH of the formulation is an effective way of improving permeability of some drugs which are stable in a low pH carrier. For instance, Azeleic acid (an FDA-approved treatment for acne) passed through the epidermis five times more readily in a pH 3.9 formulation compared to the same dose in a pH 4.9 carrier (Li et al, 2012).

Many other compounds and drug carriers are under development, including sucrose laurate which acts as a surfactant (Csizmazia et al, 2011), Transkarbam 12 which degrades in low pH releasing two opposing molecules and $CO_2$ which forms bubbles, interrupting stratum corneum lipid organisation (Novotný et al, 2011) and fluorescent enhancers for research purposes (Seto et al, 2012). Natural alternatives are also increasingly popular such as lemon essential oil, used to deliver water-soluble vitamin B6 and C and fat-soluble vitamins A and E across the epidermis (Vilgimigli et al, 2012).

One direct approach is microneedling (Wu et al, 2006) which uses a roller covered with hundreds of 200-300μm long needles to create micro-pores in the stratum corneum. These needles are too short to stimulate nerves or damage blood vessels, but they increased permeation of large molecular weight anti-inflammatories such as ibuprofen, paracetamol and diclofenac by up to three-fold (Stahl et al, 2012).

## 1.4 Comparison of 2D and 3D Cell Culture

The majority of current cell culture techniques grow cells in monolayers on the surface of flat, rigid 2D plastic dishes or flasks. 2D culture techniques are widespread due to their economy, convenience and generally high cell viability and reproducibility. Cell culture studies in 2D have contributed significantly towards scientific knowledge but if the purpose of cell culture is to draw conclusions about human biology, these flat surfaces are clearly not optimal for accurately portraying the complex native environments of different cell types *in vivo*. Cells i*n vivo* form complex interactions with other cells and a tissue-specific extracellular matrix in order to form three-dimensional structures which cannot be represented fully in 2D. Cells cultured in 2D conditions only form external contacts within restricted dimensions and are forced to adopt polar attachments, forcing cells to adapt to their 2D environment and enforcing a sort of natural selection onto primary cells which are cultured from tissues (Lee et al, 2008). This may alter cell metabolism and functionality in a way that may reduce the accuracy of *in vitro* testing.

3D culture systems can be largely divided into two types - those for clinical use, such as restoring or maintaining injured tissues, and those for *in vitro* cell culture for systemic scientific investigation into cell function to model tissue physiology under normal and disease states. Tissue engineering and regenerative medicine are emerging fields of research, with several biodegradable, biocompatible 3D matrices used as templates for cultured cells which are then implanted back into patients. For instance, tissue engineered bladders formed from urothelial and smooth muscle cells cultured on a collagen/glycolic acid scaffold were successfully implanted into patients (Atala et al, 2006), and collagen/polymer nanofibres have been used to culture skeletal muscle myotubes for potential transplant (Choi et al, 2008).

Of particular interest is clinical treatment of burns and chronic blistering using tissue-engineering. Treatment of burns often requires skin grafts, further injuring healthy portions of skin (which may not be available in severe burns) and increasing risks of infection (Wood et al, 2006). In cultured epithelial autografts (CEAs), combinations of keratinocytes and/or fibroblasts isolated from the patient have been cultured in the lab, then grafted back onto a patient to repair or replace epidermis, dermis or full-thickness skin (Boyce et al, 1999, Supp and Boyce, 2005, MacNeil, 2007). These CEAs reduce the healing time and improve mortality rates of burn

victims. Keratinocytes have been cultured as thin cell sheets (Wood et al, 2005), applied on sub-confluent carrier sheets (Hernon et al, 2006), cultured on porcine dermis, fibrin matrices, or electrospun biodegradable polymers (Ronfard et al, 2000, Zhu et al, 2005, Blackwood et al, 2008, Powell and Boyce, 2009). These electrospun collagen polymers have been shown to be beneficial compared to freeze dried collagen scaffolds in terms of wound healing after full thickness skin damage (Powell et al, 2008). These scaffolds can be used

Recently, a "stem cell gun" and novel wound dressing by Stem Cell Systems, GmbH, has caught the attention of the press as it claims to regrow healthy skin within one week, but as of yet no published scientific data has emerged for this promising-sounding technique. Keratinocytes have been previously sprayed onto wounded tissue (Grant et al, 2002, Zweifel et al, 2008) with positive results.

The 3D scaffold used in this project is non-biodegradable polystyrene and is unsuitable for transplantation. Therefore discussion will focus primarily on *in vitro* 3D models rather than regenerative medicine.

### 1.4.1 Design of 3D Culture Materials

There are several key factors in the design of a 3D material for cell culture including size and shape, porosity, pore size, surface topology, permeability, mechanics (i.e. flexibility, rigidity, degradability), wetability and microscopic surface characteristics (Lee et al, 2008). Surface characteristics include charge, polarity and surface chemistry which can alter the adherence of cells and the cellular deposition of synthesised matrix components (Zeyfert et al, 2009). Ideally, all of these factors would combine to form a 3D structure which models the native environment of those particular cells *in vivo,* bearing in mind that different tissues have specific ECM environments. These factors are best described on different scales - for instance the distribution of nano-scale collagen fibres and the material surface biochemistry are important for cell adhesion, the size of micro-scale pores are important for cell spatial organisation and the macroscopic size, shape and thickness of the whole 3D material itself is important for diffusion of culture media, oxygen and overall "tissue" morphology. Ideally, an *in vitro* 3D model replicates every scale of the *in vivo* environment for maximum relevance.

Several types of 3D culture materials including cell-encapsulating hydrogels, electrospun fibre matrices, fabric-based scaffolds and borosilicate glass matrices have been used for 3D cell culture. An overview is provided below:

#### 1.4.1.1 Encapsulating Gels for 3D Cell Culture

One method of 3D cell culture is termed "encapsulation", where a hydrogel solution is mixed with a cell suspension, which then solidifies or polymerises around the cells, surrounding them with ECM proteins or structural polymer with no porous micro-structure. Similar to cells cultured in the 3D polystyrene scaffold (Bokhari et al, 2007), cells cultured in encapsulated spheroids form structures, and are more resistant to drug-induced apoptosis (Zahir and Weaver, 2004).

Algimatrix (Invitrogen) is a biodegradable "sponge" matrix based on seaweed alginate which encapsulates cells (Shapiro and Cohen, 1997). This gel contains large (70-300µm) pores capable of holding cultured cells, similar to the 3D scaffold used in this project. Algimatrix is 3-4mm thick when fully hydrated (official product information, Invitrogen website) and as there is no porous structure, these gels rely on passive diffusion of molecules through the high water content material. The Algimatrix gel, and indeed most encapsulation-type culture material, is biodegradable (degradable by Versene alone) and highly permeable so that it can maintain cultures of cells inside. Algimatrix has been used to culture many cell types (Mooney et al, 1999, Dvir-Ginzberg et al, 2004) although a literature search revealed no evidence of keratinocyte culture with this product. These types of encapsulation matrix may be suitable for 3D culture of keratinocytes as encapsulated aggregates for other purposes (such as drug toxicity screening) but it would not be suitable for culturing a 3D culture with tissue-like morphology. Another 3D encapsulation product is Perfecta 3D® (3D BioMatrix) hanging drop inserts which can be used to grow cells in 3D inside small pores (Takayama et al, 2011). This product also does not seem to have been tested with keratinocytes (source: 3D BioMatrix product website).

Several forms of synthetic hydrogel have been developed, formed from self-assembling peptides dispersed in water. For instance, DNA has been used to create a 3D hydrogel, formed from a specific DNA sequence which can be repeatedly hybridised to each other by DNA ligase (Um et al, 2006).

Synthetic gels of polymers are able to be more reproducible and can be sterilised before use in tissue culture. However, it should be noted that not every cell type may be cultured inside gels. In order to form structures inside a 3D gel, cells need to cleave extracellular matrix proteins such as collagen and fibrin, but some cells (such as some tumour cells) do not express MMP enzymes, limiting their ability to proliferate, migrate or form structures inside a gel (Hotary et al, 2003).

#### 1.4.1.2 Gel-based Coatings for 3D Cell Culture

MatriGel (BD Biosciences) is a gelatinous protein matrix secreted by EHS mouse tumour cells which was initially used to study cell differentiation (Baatout et al, 1996). It has since been used as general support for cultured cells of many tissue origins as well as a tool to measure carcinoma cell invasion and tissue repair (Hughes et al, 2010). Matrigel is not technically a dermal equivalent or inherently a 3D culture surface, but it has also been used to support human 3D keratinocyte culture. For example, Matrigel was used to manufacture an artificial epidermis for *in vitro* burn modelling (Sobral et al, 2007). Although Matrigel contains many natural biological products, it is heterogenous and variable, and has also been found to contain viruses (Lee et al, 2008). MaxGel (Sigma) is a similar product, forming a gel made of human extracellular matrix components such as collagen, laminin, elastin, proteoglycans and glycosaminoglycans for supporting cell culture. This gel is not inherently a 3D culture system, although it can be applied in a thick coat to a 2D culture dish.

#### 1.4.1.3 Non-biodegradable Scaffolds for 3D Cell Cultures

The 3D scaffold used in this thesis is non-biodegradable. While biodegradable scaffolds are advantageous for some applications (i.e. for tissue engineering (Clark et al, 2007)) or for some laboratory techniques where the scaffold can be removed or digested) biodegradable scaffold are often disadvantageous in terms of practicality - such as instability under long-term culture, limited shelf life, and reduced quality due to improper storage conditions (Lee et al, 2008).

Polymers made from poly(glycolic acid), poly(lactic acid) and co-polymers have been assembled to form 3D matrices where cells can attach and proliferate, similar to the polystyrene of the 3D scaffold (Mikos et al, 1993).

3D CellCarrier (Orlaproteins, UK) is a newly-developed borosilicate 3D glass matrix where cells can be cultured. This scaffold is rigid, non-biological, non-biodegradable and non-permeable, similar to the 3D scaffold used in this project. However, a glass scaffold would clearly not be compatible with some laboratory methods such as paraffin embedding and histology but it is compatible with light microscopy imaging of living cells. The glass scaffold is also thick (4mm) and so may be faced with issues concerning the diffusion of culture media, oxygen and clearance of waste products if the cells inside reach a high confluence.

As described previously, the 3D scaffold is formed by a polyHIPE process. However, there are many other polymer-formation techniques which are capable of developing similar porous 3D structures. For instance, electrospinning can generate polymers formed from multiple layers of laid down fibres with finely controlled diameters, recreating an ECM-like environment (Sun et al, 2006b, Lee et al, 2008). Electrospun scaffolds formed from a variety of natural or synthetic materials have been used in several previous studies for 3D cell culture, and some are available commercially. A product named OrlaMatrix (Orlaproteins, UK), is made of electrospun polyester and appears similar to the 3D scaffold used in this project, however details about this product such as the thickness, pore size and culture mechanism remain unavailable.

Another method of scaffold formation is "particulate leeching" which forms a polymer containing particles which can be dissolved after the polymer has formed, thus leaving a porous structure (often salt or sugar, which is then dissolved by water). However, this method provides problems in sufficient connectivity of the pores formed inside the scaffold, often making a structure which could be classified in between a fully porous structure and an encapsulating structure (Mikos et al, 1994). 3D sponges have also been generated using freeze-drying techniques, which are more similar to the HIPE process used to form the 3D scaffold used in this project. In summary, a polymer solution is mixed with water and then freeze-dried or evaporated, leaving behind a polymer with empty "bubbles" which were previously occupied by water (Whang et al, 1995). Gas-foaming has also been used where high pressure forces gas bubbles into a polymer mixture which is then slowly cooled and gas is allowed to escape, leaving a porous structure behind (Mooney et al, 1996).

#### 1.4.1.4 Mechanics of 3D Culture Materials

The importance of 3D culture material mechanics was initially considered for use in tissue engineering applications, where implanted scaffolds need to withstand the stresses and strains placed onto them after transplantation. Ideally, these scaffolds need to strong enough to withstand stress and movement, but flexible in order to adapt to *in vivo* conditions without interfering with neighbouring tissues after implantation by being excessively rigid. These properties are clearly essential for tissues such as tissue engineered bone grafts, which is highly rigid but also dynamic, and for muscle (i.e. myocardial tissue) which is constantly undergoing contraction and movement (Lee et al, 2008).

However, scientists are increasingly realising the importance of the stiffness, flexibility and compliance of the cellular environment on the behaviour of those cells *in vitro*. Cell surface integrin receptors attach to extracellular matrix and sense the compliance of the surrounding tissues by measuring stresses on the cytoskeleton (Yamada et al, 2007) and it is now becoming clear that these forces act as environmental cues which can alter cell metabolism and differentiation. For instance, human mesenchymal stem cells (MSCs) alter their differentiation lineage based on flexibility of surrounding materials (Engler et al, 2006, Haugh et al, 2011) and chondrocytes display improved viability when cultured on dynamically-loaded porous scaffolds, compared to static scaffolds (El-Ayoubi et al, 2011). The alignment of collagen or polymer fibres on the cell culture surface also appears to influence cell orientation, where skeletal muscle cells aligned to form myotubes on parallel fibres (Choi et al, 2008). In 2D culture, most surfaces are perfectly flat, rigid and have random surface microstructure. Therefore many levels of cellular interaction with the environment are completely lost under traditional culture conditions.

The skin as a whole is clearly a strong but flexible tissue, subjected to constant physical forces such as stretching, compression and abrasions. Keratinocytes themselves are exceedingly strong cells, up to 70x stiffer than "typical" cells such as breast epithelial cells, circulating lymphocytes or connective tissue fibroblasts (Lulevich et al, 2010). Lulevich and colleagues measured the force needed to collapse cultured cells and noted that unfixed, viable keratinocytes were comparable to paraformaldehyde-fixed T-cells in terms of their rigidity and elasticity. This is due to the strength of the keratin cytoskeleton which adapts keratinocytes for their

protective role. It would be surprising if the impact of keratinocytes' cellular environment did not influence their proliferation, differentiation and protein expression as it does with other cell types. Skin clearly shows adaptive properties, such as during birth, pregnancy and wound healing and areas of the skin such as the soles of the feet experience significant mechanical pressure, and palmar keratinocytes express a unique profile of cytoskeletal proteins including keratin 9 which enhances their mechanical strength (Swensson et al, 1998).

Some analyses have been performed in this regard. If keratinocytes are grown to confluence on flexible silicone sheets and then stretched, they show increased proliferation and protein synthesis, aligning themselves in the direction of the force (Takei et al, 1997). Stretching also induces upregulation of adhesion molecules and cell-cell contacts (Knies et al, 2006), indicating that physical forces play a role in barrier formation. Stretched keratinocytes also show downregulation of K10, upregulation of hyperproliferative K6 and enhanced proliferation through EGF-R autophosphorylation and ERK, PI3K pathways in primary human or HaCaT cell line keratinocytes (Yano et al, 2004). However, all of these findings have been based on keratinocytes cultured on two dimensional flexible silicon sheets. Reichelt, 2007 noted that "as fibroblasts show different cytoskeletal properties in 2D versus 3D culture, there is a need to develop experimental settings using 3D culture on mechanotransduction in keratinocytes." In a 3D environment with increased cell-cell contact and improved adhesions, it is likely that these effects initiated by the extracellular environment may be further enhanced. This has implications for the handling of 3D cultures *in vitro* and again shows the value of 3D analysis compared to 2D.

Recently, it was demonstrated that the stiffness of ECM may be one of many factors which regulates epidermal stem cell fate (Trappmann et al, 2012), with cells pulling on the growth surface and sensing the degree of pliability. When stem cells were cultured in high stiffness hydrogels or glass surfaces, they spread out and did not differentiate, but on soft hydrogel substrates, cells rounded up and initiated differentiation. Trappmann and colleagues proposed two pathways through which this occurs - both from inhibition of focal adhesion assembly, reduced integrin clustering and decreased ERK phosphorylation on soft gels and from restricted

spreading on stiff substrates causing reduced G-actin, SRF transcription factor and AP-1 activation.

#### 1.4.1.5 The Effect of 3D Culture On Cell Shape

Epithelial cells *in vivo* are often polarised by their connections to a two-dimensional basement membrane, important for tissue organisation and directional secretion of cellular products - for example in secretory glands or kidney glomeruli (Yamada et al, 2007). However, in 2D culture on flat structureless plastic, forced polarity of attachment causes cells to adopt an abnormal, spread-out morphology, altering their normal shape and secretory pathways (Yamada et al, 2007). Other cells such as fibroblasts are naturally lacking any polarity *in vivo*, but when cultured in 2D are forced to adopt polar attachments on their ventral surfaces, also disrupting their *in vivo* behaviour (Lee et al, 2008). In 2D culture, the ventral side of cells contact the glass or plastic and cells may only form minimal contacts with neighbouring cells that are also adhered to the 2D surface (Bokhari et al, 2007).

Optimisations to 2D surfaces, such as coating with collagen or extracellular matrix components (Cooke et al, 2008), or commercial products such as Matrigel (BD Biosciences), have improved the environment for 2D cultured cells (Hughes et al, 2010), but still do not come close to representing the native cellular environment *in vivo*.

3D culture aims to improve mimic the native cellular environment so that cells function as they would *in vivo*. The importance of the 3D environment is demonstrated by Cukierman et al, 2001 who noted increased numbers of cell-matrix adhesions, enhanced proliferation and more *in vivo*-like morphology almost immediately when cells were cultured inside a 3D environment. When cells were cultured on the surface of same material flattened into a 2D surface, these benefits were lost, showing that the 3D environment itself was essential for cell behaviour. In depth analysis has shown that the scaffold structure, such as fibre thickness and the diameter of spaces between those fibres are important for cell attachment and motility (Sun et al, 2006b).

Cells grown in 3D also display functional differences compared to their 2D counterparts including improved resistance to toxins and increased metabolism (Schmeichel and Bissell, 2003). For instance, keratinocytes were more resistant to

oxidative stress or heavy metal toxicity in 3D cultures compared to their 2D-cultured counterparts (Sun et al, 2006) and hepatocytes cultured in 3D display enhanced albumin production and reduced sensitivity to a hepatotoxic drug than an equal number of cells cultured in 2D monolayers (Bokhari et al, 2007).

In order to more closely mimic the *in vivo* environment, multiple cell types can be cocultured where they participate in mutual cell signalling, improving survival and overall tissue morphology. For example, Sun et al, 2005b cultured combinations of fibroblasts, keratinocytes and endothelial cells in electrospun polystyrene scaffolds and found that when cultured alone in serum free conditions, none of the cells were viable. However, in coculture with fibroblasts but the absence of serum, keratinocytes and endothelial cells were proliferative, indicating the importance of fibroblast signalling in keratinocyte survival. Even more surprisingly, when cultured at the air-liquid interface the cells formed an organised structure even though they were added into the scaffold randomly.

In comparison to animal models, 3D models are also more accessible, more affordable and more suitable for large-scale testing than animal models. They can be used as a surrogate to draw preliminary conclusions in a more realistic environment than 2D culture before carrying out further testing *in vivo* (Yamada et al, 2007). For experimentation where cell motility or cell-cell/cell-matrix interactions are critical (for example carcinoma cell invasion or wound healing), 3D models and co-cultures are ideal. Jacks and Weinberg, 2002 proclaimed that "[s]uddenly, the study of cancer cells in two dimensions seems quaint, if not archaic."

The scaffold utilised in this thesis is a newly-developed porous polystyrene-based structure which enables the culture of cells in 3D (Knight et al, 2011). The structure and properties of the scaffold, as well as a brief overview of the manufacturing process, are described in Chapter Two. Briefly, this polystyrene material is similar to standard 2D culture plasticware, and cells attach directly to the polystyrene and proliferate, migrate and differentiate within pores and voids in the structure, forming three-dimensional connections and laying down extracellular matrix.

This scaffold has been used previously to culture neuronal cells (Hayman et al, 2004 and 2005), liver hepatocytes (Bokhari et al, 2007, Schutte et al, 2011) and adipose-derived stem cells (Neofytou, 2011). In comparisons with 2D culture, all

aforementioned authors noted a more realistic cell morphology of cells cultured inside the 3D scaffold.

### 1.4.2 Problems and Future Developments for 3D Cell Culture

Although advantageous in many aspects, 3D cell culture is not without significant difficulties and challenges when compared to 2D cell culture. These difficulties can influence all aspects of cell culture experiments including cell seeding, cell maintenance (in terms of culture media), cell modifications (such as transfection) and experimental analysis (imaging and assays). As such, even though the advantages of 3D culture are relatively clear and accepted, 3D models have yet to see widespread use.

#### 1.4.2.1 Cell Seeding into 3D Environments

Cell seeding methodologies need to be altered in order to distribute a known number of cells homogenously throughout a 3D material which contains pores and voids of varying sizes. Cells need to adhere to the material quickly so that they are not disturbed or washed away by culture media, and they need to be present in a sub-confluent density which is optimal for their proliferation. Factors such as the pore size, interconnect diameter, porosity and wetability of the 3D material are important for cell seeding, and protocols need to be optimised for individual cell types depending on their size, shape and growth characteristics (Lee et al, 2008). These issues were addressed in Chapter Three of this thesis.

With any novel culture surface, whether glass, hydrogel, natural or artificial polymers or even different brands of standard plasticware, cell adhesion and proliferation may be unexpected, particularly with cells lines which can become "tolerant" to their existing 2D conditions over time (Cukierman et al, 2001, Lee et al, 2008). Therefore, basic investigations need to be performed in order to optimise cell seeding and attachment. For instance, the HaCaT cells used in this thesis were seeded into the 3D scaffold and allowed to adhere for 30 minutes before a larger volume of culture media was added. MET1 squamous cell carcinoma cells, which proliferate rapidly on 2D culture plastic, would not adhere to or proliferate inside the 3D scaffold at all, whereas a different cell line from the same patient (MET4) adhered and proliferated rapidly in the material. Some cell types require surfaces coated with collagen or ECM components, and this will also be addressed in Chapter Three of this thesis.

#### 1.4.2.2 Cell Maintenance in 3D Culture

Cells cultured in 3D are more metabolically active than their 2D counterparts (Schutte et al, 2011), and so place greater stresses on the culture environment - namely the quality of culture media in terms of pH, lactate and glucose content. 3D culture systems are non-vascular and so rely on simple diffusion for transport of oxygen and glucose, as well as clearance of waste materials (Yamada et al, 2007). Therefore, hypoxia is also a real concern with 3D models. The main factors in hypoxia are the distance from the culture media and the number of cell layers separating the culture media from hypoxic cells (Lee et al, 2008).

Standard 2D cultures in Petri dishes are submerged in a uniformly rich distribution of culture media with equal nutritional availability and oxygen concentration across all cells, unlike *in vivo* tissue or 3D cultures which can maintain gradients of nutrition (Yamada et al, 2007). Cells at different distances from culture media can be in different metabolic states (Keith and Simon, 2007) reducing the reproducibility of experiments conducted in 3D. Interestingly, this hypoxia of 3D culture has been useful in modelling some forms of tumour which are hypoxia due to poorly formed vasculature (Hicks et al, 2006). However, for keratinocytes, mild hypoxia has been observed (Weir et al, 2009) to reduce terminal differentiation and involucrin expression in cultured keratinocytes, and should therefore be avoided if a well-differentiated barrier is to be formed.

To address these issues, 3D models need to be designed appropriately for cell nutrition. Materials need to be thin enough (~0.3mm) to permit adequate oxygenation of the interior tissues (Yamada and Cukierman, 2007). As well as thickness, a number of other factors can influence mass transport through the 3D matrix - including the pore size, pore shape, interconnect size, distribution of pore sizes and pore openness (Lee et al, 2008). For instance, a scaffold consisting of large, open pores but small interconnects may have poorer mass transport capability than a scaffold with small pores but more evenly distributed, larger interconnects.

To address these issues caused by lack of vascularisation, the most obvious courses of action are to use larger culture vessels or to change culture media more frequently. However, simply submerging a 3D culture in a larger volume of culture media is likely to have implications for oxygen diffusion unless there is a dedicated oxygen

infusion into the culture itself. Frequent changing of culture media can also upset the concentration soluble signaling molecules produced by the cells (Lee et al, 2008).

Perfusion-type systems have been previously used and have clear benefits in terms of cell viability and reproducibility (Wendt et al, 2009). Such systems can also be used for culturing keratinocytes at an air-liquid interface (Sun et al, 2005a) and perfusion based systems are currently under investigation in our lab for use with the 3D scaffold. However, these systems often utilise custom-made apparatus, and the system needs to be optimised before use (i.e. flow rate, oxygen input rate etc) according to the properties of the culture material and the metabolic demands of the cells. Such systems also utilise greater volumes of culture media than equivalent 2D culture or static 3D culture, increasing the cost of experiments, especially if defined media is required. As previously mentioned, such systems also remove any concentration gradients or soluble signalling molecules which may affect cell behaviour. For 3D cell culture to become more prevalent and replace 2D cell culture as a routine laboratory technique, more standardised equipment and protocols are needed to improve the economy and reliability of cultures to the same level as 2D culture.

#### 1.4.2.3 Experimental Analysis Using 3D Culture Materials

Many 3D culture systems present problems in compatibility with existing lab techniques. In routine 2D culture, the confluence and morphology of cells can be easily visualised with a simple inverted light microscope, but this is not always possible in 3D culture systems which are opaque and display poor optical transmission. Multiple layers of cells also make simple assessments like cell confluence more difficult. Many laboratory techniques such as measuring optical density, using immunofluorescence staining or confocal imaging depend on transparent samples.

The 3D polystyrene scaffold used in this project is 200µm thick, opaque polystyrene and therefore incompatible with simple light microscopy of live cells. Recently, a technique using PicoGreen (Invitrogen, UK) has been developed within our lab for routine assessments of culture confluence, although this still requires creation of standardised protocols and standard curves for multiple cell types. Assays such as the MTS proliferation assay can also be used to measure cell viability in 3D.

In terms of imaging techniques, there are fewer methods for reliably staining and viewing cells cultured in a 3D environment than there are for 2D (Lee et al, 2008). For imaging in this thesis, 3D cultures were treated as pieces of extracted tissue - i.e. fixed, embedded in paraffin, sectioned and then stained with histological stains or immunofluorescence antibodies. While these techniques are suitable for visualising tissue morphology, they require samples to be fixed, thus destroying the viable culture. This places limitations on the use of some 3D materials for live monitoring of cell migration or time-lapse of viable cells. Imaging techniques compatible with 3D culture systems are currently being developed such as multi-photo microscopy, X-ray tomography and optical coherence tomography (Smith et al, 2011, Pappinen et al, 2012). Recently in our lab, techniques have been devised for fluorescent stained confocal imaging of living cells without fixation, as well as Z-stacking techniques to show 3D architecture. Again, more easily accessible standard protocols for culture assessment and imaging are needed if 3D culture is to replace 2D culture as a laboratory standard. However, most of the problems associated with 3D culture imaging are also true for *in vivo* samples which can rarely be analysed without prior excision.

3D culture scaffolds also may reduce the availability of cells for analytical techniques such as protein, DNA or RNA extraction. Where there are multiple cell layers, extraction by simple cell scraping is not possible, and care needs to be taken to ensure that all cells within a 3D material are subjected to equal extraction. The same is true for transfections, where access to cells inside a 3D material may be reduced.

Care must also be taken with regard to interactions between the 3D substrate and lab techniques. For instance, biodegradable protein-based scaffolds may contaminate protein extracts or plastic-based scaffolds may potentially leech plasticisers when exposed to solvents (for instance during lipid extraction). Any 3D culture device must therefore be considered in experimental controls with the empty culture materials being subjected to the same extraction protocols as those containing cultured cells.

Compared to 2D, detachment or removal of viable cells for techniques such as FACS or flow cytometry is almost more difficult. With the 3D scaffold used in this thesis, some cells could be easily trypsinised out from the 3D culture and then re-seeded

onto new material. However, if these scaffolds were then fixed and stained with H&E, most cells in the central portion of the scaffold remained inside. This may be then bias a cell extraction towards those cells with less developed adhesions to the material, or it may simply be due to physical constraints of cells trapped inside a complex porous structure. As prolonged exposure to trypsin enzymes is toxic to cells, other methods for cell detachment using non-enzymatic methods are under investigation in our lab.

### 1.4.3 In vitro Models of Epidermis

Since the work of Reinwald and Green in 1975-1977, keratinocytes have been cultured *in vitro* for the purpose of studying the epidermis. Keratinocyte culture has been used to provide therapies for skin disorders such as cultured epithelial autografts for treatment of burns or chronic blisters as described earlier. However, the 3D scaffold utilised in this thesis is not suitable for autografting techniques due to its rigid, non-biodegradable nature.

Shortly after keratinocytes were cultured in 2D, Fusenig, 1978, Regnier, 1981 and Prunieras et al, 1983 cultured keratinocytes at an air-liquid interface using de-epidermised dermis (DED) or contracted collagen and fibroblast gels as a support and noted improved keratinisation, stratification and epidermal-like morphology. The air-liquid interface partially replicates *in vivo* conditions where basal keratinocytes are fed from the dermal blood supply on the ventral side and the skin (or *in vitro* model) is exposed to the dry atmosphere on the outer side. Keratinocytes grown in this manner form a stratified epidermis-like structure. Fibroblasts were found to induce keratinocytes to produce basement membrane components (Lee and Cho, 2005) and keratinocyte-fibroblast interactions were found to dictate many aspects of keratinocyte behaviour such as MMP expression (Nova et al, 2003) and differentiation (Mak et al, 1991).

Since those early studies, numerous models of three-dimensional keratinocyte culture have been developed which have provided an invaluable tool for the investigation of keratinocyte function and skin biology under more suitable conditions than submerged 2D culture. Even recently, collagen gel and DED-based organotypic cultures are still in widespread use (Lee and Cho, 2005, Ojeh et al, 2008).

These cultures have been used to investigate keratinocyte cell signalling (Liang et al, 2012), disease modelling (Barker et al, 2004, Semlin et al, 2010, Mildner et al, 2010), irritancy testing (Netzaff et al, 2005), growth factor interactions (Amjad et al, 2007), protein interactions (Vermeij et al, 2010, Yoneda et al, 2012), stromal interactions (Maas-Szabowski et al, 2003, Ikuta et al, 2006), bacterial colonisation (de Breij et al, 2012) and many more investigations.

The focus of this thesis is the study of epidermal barrier function and in this regard numerous models have been developed in laboratories and several are sold commercially for *in vitro* testing of epidermal permeability (Pasonen-Seppanen et al, 2001, Netzaff et al, 2005, Yan-feng Xu et al, 2005, Pappinen et al, 2008 and 2012, Vilgimigli et al, 2012).

Commercial demand for epidermal equivalents for use *in vitro* is increasing, due to public perception of animal testing as well as European Union legislation. For instance, EU Directive 2010/63/EU article 4 states "Member States shall ensure that, wherever possible, a scientifically satisfactory method or testing strategy, not entailing the use of live animals, shall be used instead of a procedure." Article 86/609/EEC states that " Member States should actively support the development, validation and acceptance of methods which could reduce, refine or replace the use of laboratory animals." The European Reference Laboratory On Alternatives To Animal Testing (EURL ECVAM) are responsible for assessing *in vitro* models and their suitability for replacing animal or human studies. They have recognised and validated some models for use in epidermal barrier permeability studies, including EpiDerm (Mattek, USA) and Episkin/RHE (SkinEthic/L'Oreal) which have been approved for use in preliminary epidermal toxicity testing by the OECD and ECVAM (ESAC peer review, 2006).

Epidermal models are designed to replicate as many aspects of native epidermis as possible - namely morphology, a stratum corneum, expression of barrier proteins and a lipid profile representative of native epidermis. However, to date, no organotypic model is able to fully replicate the structure and properties of human epidermis. Most *in vitro* models form a thick stratum corneum (Ponec et al, 2000, Poumay and Coquette, 2007) but stratum corneum thickness is not necessarily related to barrier permeability, with conflicting studies in the area (Stahl et al, 2009). Studies have shown mixed results with *in vitro* equivalents showing either variability and some

unreliability (Ponec et al, 2000) or showing excellent reproducibility and comparability with human and porcine epidermis (Schäfer-Korting, 2008). Native human tissue is also variable in properties, depending on age, gender, race and body sample site (Darlenski and Fluhr, 2012), leading to wide definitions of "normal" epidermis in terms of thickness, lipid composition and barrier permeability.

In order to provide a reliable substrate for testing of novel compounds, *in vitro* equivalents need to be stable and reproducible, as well as successful in predicting the action of a compound on human skin - whether in terms of permeability, irritation or physiological effect. Efforts are now concentrating on culture systems which can be duplicated in large scale and repeated by multiple labs (Poumay and Coquette, 2007).

Many other commercial keratinocyte culture models utilising collagen gels are available, such as EpiDermFT (MatTek, USA), TestSkin (LSE, USA) and AST-2000 (CellSystems, Germany). All models are based on similar principles of culturing human keratinocytes on a collagen-contracted gel at the air-liquid interface. Other models utilise a 2D collagen-coated surface, such as a well-developed rat keratinocyte organotypic culture model which has shown reliable prediction of native human skin penetration (Pappinen et al, 2012).

Keratinocytes have also been cultured in 3D without a cellular dermal equivalent. Commercial models such as EpiDerm (Mattek, USA), SkinEthic (Skinethic Labs, France), EST-1000 (CellSystems, Germany) (recently renamed epiCS) have cultured keratinocytes on polycarbonate membranes to form *in vitro* epidermal equivalents and use supplemented culture media rather than fibroblast feeder cells. These models have been used to study keratinocyte differentiation (Chaturvedi et al, 2006), skin irritation (Welss et al, 2003) or barrier permeability (Pappinen et al, 2003).

**Table 1.1 Summary of Leading Commercial and Non-commercial Epidermal Models**

| Model | Culture material | Cell type(s) used | Information | References |
|---|---|---|---|---|
| **Commercial Models** | | | | |
| */**Epiderm (MatTek, USA) | Inert polycarbonate membrane | NKEH | 6-8 living cell layers (28-43µm) with 16-25 layers (12-28µm) of stratum corneum (Netzlaff et al, 2005). Manufacturer, 8-12 viable layers and 10-15 stratum corneum. This is the longest standing commercial model (since 1992) and the first to be ECVAM validated. | Poumay and Coquette, 2007, Netzlaff et al, 2005, Ponec et al, 2000 |
| */**SkinEthic Rhe (Laboratoire Skinethic, France) (SkinEthic are subsidiary of L'Oreal) | Inert polycarbonate membrane | NKEH air-lifted for 17 days | 5-9 living cell layers (23-59µm) with 14-24 layers (15-32µm) of stratum corneum | Netzlaff et al, 2005, Ponec et al, 2000 |
| */**EpiSkin/Invitrosk in (Episkin SNC, France) | Type I bovine collagen matrix topped with Type IV human collagen | NKEH submerged for 3 days and air-lifted for 13-20 days | 15-24 living cell layers with 600-100 layers (73-102µm) stratum corneum | Netzlaff et al, 2005, Ponec et al, 2000 |

| | | | | |
|---|---|---|---|---|
| StrataTest, (Stratatech, USA) | NHDF in collagen I on hyaluronic acid membranes in well-inserts | NIKS keratinocyte progenitor cell line and NHDF-collagen based dermal equivalent | NIKS (normal immortalised keratinocytes) are a spontaneously immortal neonatal foreskin-derived cell line. The model shows a thick, highly stratified epithelium (>20 layers) which stains positive for differentiation markers | Slavik et al, 2007, Rasmussen et al, 2010. Zhang and Michniak-Kohn, 2012 |
| Epiderm FT (MatTek, USA) | Collagen matrix in cell culture membrane insert | NKEK and NHDF | Full thickness model. Produces 8-12 epidermal cell layers, not including stratum corneum. Includes well developed basement membrane and hemidesmosomes at DEJ | Hayden et al, 2005. Manufacturer product information |
| *epiCS/ Epidermal Skin Test 1000 (EST1000), (CellSystems Biotechnologie GmbH) | Permeable cell culture membrane insert | NHEK | More than 4 viable layers, more than 5 cornified layers. ECVAM validated for corrositivity. Model shows accurate locations of major differentiation markers (K10, profilaggrin, TGase and involucrin) and K14, organised into well-defined layers | Hoffman et al, 2005. Manufacturer product information |
| **Non-Commercial Models** | | | | |
| ROC (Rat Organotypic Culture) | Collagen gel | Rat keratinocytes air-lifted for 21 days with | Well-characterised model with physiologically similar lipid profile and | Suhonen et al, 2003 Kuntsche et al, 2008 |

| | | | | |
|---|---|---|---|---|
| | | 40µg/ml ascorbic acid | predictable barrier properties which have been tested against an extensive range of permeants | Pappinen et al, 2007<br>Pappinen et al, 2008 |
| Michniak group HSE | Bovine collagen matrix | NHDF and NHEK | Full thickness model. Overestimates caffeine and hydrocortisone permeability | Batheja et al, 2009 |
| LHE (Leiden Human Epidermal) Model | PEGT/PBT biodegradable scaffold 300µm thick, 70-80% porosity with 50-210µm pore diameter. With or without collagen | NHDF and NHEK | Cultured in presence of lipid supplement and 40µg/ml ascorbic acid | El Ghalbzouri et al, 2005 |
| HaCaT-based model | Contracted collagen type I gel containing 2-3x$10^5$ fibroblasts/ml. | L929 murine dermal fibroblasts and HaCaT keratinocytes. 7 days submerged, 14 days air-liquid interface | Model shows positive staining for differentiation markers and has been used for permeability testing. Results for the compounds tested (ibuprofen) showed permeability approximately 20x higher than native epidermis. | Specht et al, 1998 |

| | | | | |
|---|---|---|---|---|
| RHE (Reconstructed human epidermis) | Inert polycarbonate filter | NHEK cultured for 14 days at air-liquid interface in high calcium | Model displays differentiation markers and clear progression of epidermal layers. TEM analysis reveals lamellar bodies and keratohyalin granules | Poumay et al, 2004 |
| RE-DED | De-epidermised dermis | NHEK cultured for 5 days submerged and 14 days at air-liquid interface, supplemented with 50µg/ml ascorbic acid | Displayed many similarities with in-vivo epidermis including SC organisation and presence of physiological lipids, including ceramide profile | Ponec et al, 1997 |
| CSS (Cultured Skin Substitute) | Collagen-GAG matrix | NHDF added to collagen-GAG matrix and NHEK seeded onto surface | When cultured submerged or without additional supplements (such as ascorbic acid, linoleic acid etc), these models displayed an incomplete set of barrier lipids, poor lamellar body formation and lipid vacuoles present inside keratinocytes. Addition of supplements restored normality to the cultures. | Boyce and Williams, 1993 |

** = ECVAM validated for OECD Test Guideline 431 (Skin corrosivity), ** = ECVAM validated for OECD Test Guideline 439 (Skin irritation)*

**** = lipid supplement of 20µM palmitic acid, 15µM linoleic acid, 7µM arachodonic acid and $2.4x10^{-5}$ BSA*

Detailed analysis of many epidermal equivalents are presented by Pappinen et al, 2012, Zhang et al, 2012, Poumay and Coquette, 2007, Ponec et al, 2000 and Ponec et al, 1997. It is also worth noting that some models such as Skin2TM, (Advanced Tissue Sciences, USA) (Rheins et al, 1994) and EpiSkin (L'Oreal, France) are no longer commercially available. The withdrawl of these commercial models have likely incentivised some active research groups to develop their own reproducible in-house models where future access and consistency can be guaranteed (Poumay and Coquette, 2007).

The 3D scaffold used in this thesis is a porous 3D material and cells remain inside the structure throughout the entire culture period, which makes it considerably different to the models mentioned previously. This material has been used previously for culture of neuronal cells (Hayman et al, 2004 and 2005), liver hepatocytes (Bokhari et al, 2007, Schutte et al, 2011) and adipose-derived stem cells (Neofytou, 2011) but not yet keratinocytes. Therefore, this thesis will by evaluating the potential of this new material as the basis for forming an *in vitro* epidermal model with a suitable barrier function for permeability testing.

## 1.5 Hypotheses

In this project I will examine the following hypotheses:

- Keratinocytes are able to proliferate and differentiate inside a porous 3D polystyrene scaffold, given suitable culture conditions
- Keratinocytes are capable of producing cornified envelopes and a lipid profile similar to native epidermis, given optimal culture conditions
- Keratinocytes can form a specialised epidermal barrier inside this porous 3D scaffold
- The created model will be useful for testing compounds which affect keratinocyte behaviour
- Differentiation in the 3D environment can be accelerated by inhibition of the JNK pathway, which has been previously shown to increase differentiation in 2D cell culture. This increased differentiation is hypothesised to increase the barrier function of the 3D cultured keratinocytes.

## 1.6 Aims of the Current Project

- To modify existing laboratory analytical techniques for use with the 3D scaffold. This includes integrating collagen gels or coatings into the material and establishing optimal culture conditions such as the number of cells to be seeded, culture duration and culture media volume.

- To utilise the 3D polystyrene scaffold as a cell culture device to induce keratinocyte differentiation at the air-liquid interface. This will involve further modification to the culture conditions and checking cell viability, morphology and differentiation under different conditions.

- To characterise the 3D model in terms of viability, differentiation and proliferation, morphology (including ultrastructure) and barrier lipid profile under various conditions. Methods of optimising keratinocyte behaviour from published literature will be tested against the new model

- To form a reproducible keratinocyte model by consistently applying the optimised culture conditions. The stable nature of the polystyrene scaffold and of HaCaT cells will help to accomplish this.

- To assess the epidermal barrier function by functional testing using a diffusion chamber and a common, biologically relevant permeant. The permeability coefficient can then be compared against published data for human epidermis and other *in vitro* epidermal models.

- To use the newly created model to examine the effect of compounds known to affect keratinocyte differentiation. This will show whether the model is useful for predicting the action of unknown compounds.

- Throughout the thesis, results 2D cell culture and 3D cell culture will be compared

# 2 Chapter 2

# Materials and Methods

All materials were purchased from Sigma, UK unless otherwise stated.

# 2.1 Routine 2D Cell Culture

## 2.1.1 Cell Maintenance

### 2.1.1.1 HaCaT Cells

HaCaT cells, isolated by Fusenig et al, 1978, were obtained via Cell Line Services, GmbH, Eppelheim, Germany. HaCaT cells were grown routinely in T75 flasks (Greiner, Bio-One, UK) in Dulbecco's Modified Essential Medium (DMEM) with 10% fetal bovine serum (FBS) and 1% Penicillin/Streptomycin (P/S) at 37°C in 5% $CO_2$. This medium is pre-supplemented with stabilised L-glutamine. For routine passaging, cells were washed twice with PBS, trypsinised with 0.25% v/v trypsin/EDTA and split at a 1:4 ratio into new flasks following standard cell culture methods. Cells were maintained between 20-80% confluence and discarded if over-confluent. For long-term storage, cells were trypsinised as stated above and centrifuged at 1000g for 5 minutes, then re-suspended at $10^6$ cells per 900µl culture media and mixed with 100µl dimethyl sulphoxide (DMSO) in a cryovial. Cryovials were mixed thoroughly, then placed in an insulated container in a -80°C freezer for up to six months of storage and -130°C for long-term storage. For thawing, vials were defrosted in a 37°C water bath, then mixed with fresh culture media, centrifuged at 1000g for 5 minutes and re-suspended in fresh cell culture media and seeded into a T25 flask. When 80% confluent, cells were then trypsinised and seeded into T75 flasks.

### 2.1.1.2 3T3 Cells

3T3-NIH cells were grown routinely in T75 flasks in Dulbecco's Modified Essential Medium (DMEM) with 10% v/v bovine serum and 1% v/v penicillin/streptomycin at 37°C in 5% $CO_2$. For routine passaging, cells were washed twice with PBS, trypsinised with Versene (Invitrogen, UK) and seeded at a 1:5 ratio. Cells were not allowed to reach >90% confluence. Cells were stored and thawed in the same way as HaCaT cells.

### 2.1.1.3 Mouse Wild Type Keratinocyte (WTK) Culture

Mouse keratinocytes, originally isolated from the back epidermis of 3 month old C57 black mice were donated by Dr Carrie Ambler, Durham University. These cells were originally cultured with 3T3-J2 mouse fibroblast "feeder" cells in T25 flasks

although for the purpose of this study they were cultured independently so that they could be grown in the 3D scaffold without the complication of a supporting feeder layer. Mouse keratinocytes cells do not grow in DMEM and were more sensitive to calcium concentration than HaCaT cells. The optimal growth conditions were determined to be calcium free Epilife culture medium (Cascade, UK and Invitrogen, UK) supplemented with 0.06mM $Ca^{2+}$ and 1% v/v Epilife Defined Growth Supplement (Invitrogen, UK). Undifferentiated cell morphology was preserved, but the rate of growth was very slow. Addition of FBS provided quicker growth but induced differentiation. Addition of chelexed, calcium free FBS (cFBS) preserved normal cell morphology while increasing the rate of proliferation to a usable level. 1% v/v antibiotic/antimycotic was later added to the culture media and showed no detrimental effect on cell morphology or behaviour. After 40 passages, cells were deemed a stable cell line continuously maintaining normal cell morphology and differentiation potential. Cells were frozen, stored and thawed in the same way as HaCaT cells.

#### 2.1.1.4 MET Cell Culture

MET1 and MET4 squamous cell carcinoma cell lines (Proby et al, 2000) were cultured, subcultured and stored frozen in the same way as HaCaT cells although subcultured more frequently due to their rapid proliferation.

## 2.1.2 Cell Culture Media Preparation

### 2.1.2.1 Cell Culture Media Additives

During the course of this project, several modifications to standard culture media were made. A list of additives and concentrations are summarised below. More information is discussed where appropriate alongside relevant data in the results chapters.

**Table 2.1. Summary of Cell Culture Additives**

| Additive | Concentration | Supplier | Notes |
|---|---|---|---|
| Calcium | 0.06/1.5mM | Sigma, UK | Diluted with PBS, sterile filtered. Stored at -20°C |
| SP600125 JNK inhibitor | 0.5-100µM | Calbiochem/ Sigma, UK | Stock solution in DMSO. 0.1% v/v DMSO added to culture media for every 10µM concentration. Stored at -20°C in the dark |
| Ascorbic Acid | 100µg/ml | Sigma, UK | Diluted with PBS, sterile filtered. Stored at -20°C |
| Linoleic Acid | 10µM | Sigma, UK | As used in Ponec et al, 2003 |
| Palmitic Acid | 25µM | Sigma, UK | |
| Arachadonic Acid | 7µM | Sigma, UK | |
| Bovine Serum Albumin (BSA) | 2.4mM | Sigma, UK | Diluted with PBS, sterile filtered. Stored at -20°C |
| EpiLife Defined Growth Supplement (EDGS) | 1% | Cascade, UK/ Invitrogen,UK | Stored at -20°C in the dark. |

**SP600125 is a selective, reversible, competitive inhibitor of cJun N-terminal kinase (JNK) with respect to ATP, designed and characterised by Bennett et al, 2001. SP600125 inhibits all three isoforms of JNK and displays at least a 100-fold selectivity for JNK as opposed to a panel of other inflammatory or stress-related kinase enzymes. SP600125 is poorly soluble in water and so was diluted in DMSO, stored and used at concentrations recommended by the manufacturer (Calbiochem, UK) and Bennett et al, 2001. Controls were given the appropriate amount of DMSO.*

#### 2.1.2.2 Calcium Chelated FBS (cFBS)

To generate cFBS, 200g "Chelex 100" resin was washed by stirring into 1.3L Milli-Q dd$H_2O$ and adjusting to pH7.4 with 6M HCl. Resin was then allowed to settle for 30 minutes and water removed. The washing procedure, minus pH adjustment, was carried out a further two times with dd$H_2O$ and a further two times with sterile PBS. 1L of 4$^oC$ FBS was mixed with the washed resin and stirred in the dark at 4$^oC$ for 1 hour to bind calcium in the serum. To remove Chelex from the media, the solution was filtered through a 0.45µm filter, then again through a 0.22µm filter for sterilisation. cFBS was then aliquoted and stored at -20$^oC$ until use (Turksen et al, 2005). Before routine use, the cFBS-based media was tested on WTK cells grown on coverslips and checked for cell viability and examined for differentiation markers.

## 2.2 3D Cell Culture

### 2.2.1 The 3D Polystyrene Scaffold

The 3D scaffold utilised and referred to throughout this thesis is a porous, polystyrene-based disc, 25mm in diameter and 200µm thick. It is designed and manufactured by Reinnervate, UK, who are the CASE industrial partner and partial sponsor for the work carried out in this thesis. All 3D scaffold materials used in this thesis were provided by Reinnervate, or by their academic partners at Durham University.

Cells adhere to the 3D scaffold material and are cultured inside the pores of the material in three dimensions. Scaffolds were manufactured by technicians in our lab or in an external facility. A brief outline of the manufacture process is outlined below.

#### 2.2.1.1 Manufacture of the 3D Scaffold

3D scaffolds were manufactured by a high internal phase emulsion (HIPE) process as detailed in Hayman et al, 2005, Bokhari et al, 2007 and Zeyfert et al, 2009. Briefly, styrene, divinylbenzene (DVB) and sorbitan monoleate were mixed into an oil phase. This was stirred into a solution of d$H_2O$ with surfactants and mixed vigorously into an emulsion. This mixture was poured into a 25mm diameter tube and allowed to solidify at 60°C for 5 hours. This solid monolith was washed in dd$H_2O$ followed by several changes of isopropyl alcohol (later modified to acetone). The monolith

cylinder of hardened polymer was then sectioned into 200µm thick slices using a Leica Vibratome. Properties of the scaffold such as pore size, void diameter and overall porosity can be varied by changing the concentration of surfactants or altering the stirring speed and duration, as described in Bokhari et al, 2007[a] ,2007 [b] and Carnachan et al, 2008.

Figure 2.1 shows the structure of the 3D scaffold used throughout this project. Image A shows a 25mm diameter monolith before sectioning and image B shows a single 200µm thick section. Image C shows an SEM image of the 3D scaffold, showing numerous pores and voids forming a 3D structure. Cells attach to the surface and are cultured inside the pores and voids. Voids inside the 3D scaffold are approximately 30-80µm which is large enough to accommodate cells, and all voids show several 10-20µm interconnects, allowing cell infiltration and migration into the material.

As the pores voids of the 3D scaffold are formed by vigorously mixing oil and water phases, the distribution and size of pores is essentially random, but can be controlled within a certain range of specifications. This is opposed to a synthetic scaffold formed from regular repeating subunits which would be uniform in structure and distribution, such as those formed by solid free-form (SFF) fabrication (Hollister, 2006). Therefore, quality control (QC) steps were taken to monitor the size and overall porosity of each batch of polyHIPE scaffolds. QC was carried out internally by our technicians, using SEM imaging to measure pore diameter and mercury porisimitery to measure porosity. Results were shared within the lab and batches of scaffolds which failed QC analysis were discarded. All 3D scaffolds used in this study conformed to internal specifications for porosity (shown in Figure 2.2) and morphology, visualised by SEM. In later stages of development, each batch of 3D scaffold was tested for cell culture by MTS assay after 48 hours of a number of different cell lines. Batches which failed QC testing were discarded. All scaffolds used in this study were from batches which had passed cell culture QC.

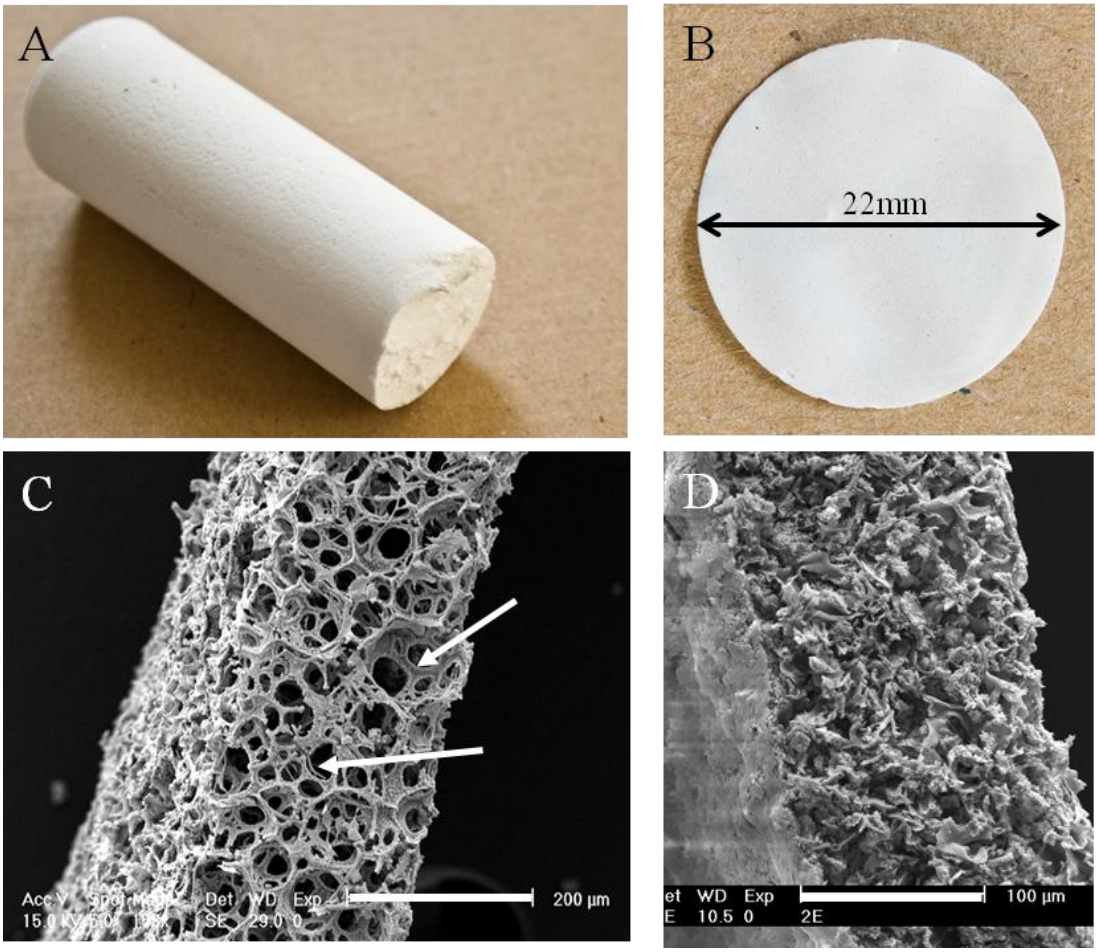


**Figure 2.1. Ultrastructure of the 3D Polystyrene Scaffold**

A) 22mm diameter polystyrene monolith, from which the 200µm sections are cut with a vibratome; B) 22mm diameter scaffold, formed from cutting a 200µm thick section of the monolith; C) Scanning Electron Micrograph of 3D scaffold showing pores and voids (indicated) in which cells can proliferate. The highly porous structure of the scaffold is clearly visible. Scale bar 200µm; D) SEM image of 3D scaffold with HaCaT keratinocytes cultured for 7 days, showing that cells have filled the pores through the full depth of the scaffold. Scale bar 100µm.

#### 2.2.1.2 Development of the 3D Scaffold

The 3D scaffold is a developing commercial product which has undergone changes for several years, continued throughout the duration of this project. During this time, the process for manufacturing the 3D scaffold, and therefore the properties of the scaffold itself, have altered. Initially, 3D scaffolds were manufactured in the laboratory in one-off quantities (the "in-house" phase). These showed pinholes and variable porosity, indicated in Figure 2.2. Production was later scaled up to a larger-scale manufacturing process utilising larger mixing vessels, a new stirring speed and modified washing procedures using acetone rather than isopropyl alcohol. QC was also introduced at this stage (the "1G" phase). These scaffolds showed an increased total porosity, and smaller, more tightly controlled pore sizes. Finally, production was moved to an external manufacturing facility and the procedure was fully adapted for large-scale manufacture (the "2G" phase). These scaffolds have smaller interconnect and pore sizes and a narrower variability in size. A summary of these three main phases along with changes to the scaffold properties and culture apparatus are detailed in Figure 2.2. For instance, moving from in-house to 1G scaffold, the pore size reduced from 60-80µm to 40-65µm, which may reduce infiltration and migration of some cell types. However, the porosity of the scaffold increased from 73% to 93%, which would allow better diffusion of culture media and oxygen through the 3D culture as well as allowing more cell-cell contact due to less polystyrene material.

In order to obtain consistency of results, all replicates and repeats of the same experiment in this project were performed with scaffolds from the same manufacturing batch. Where possible, the series of related experiments were carried out using the same batch of 3D scaffolds, although this was not always possible due to the timing of experiments and availability of materials.

In order to address issues surrounding cell maintenance in 3D (discussed in Chapter Three), several different culture methodologies were utilised over the course of this study, including custom-designed plasticware to hold the 3D scaffold and deeper well plates or dishes to hold a greater volume of culture media. An overview of the different 3D scaffolds and culture apparatus used in this study is shown in Figure 2.3 and 2.4.

| Pre-1G. 100-200µm thick sections | | 2008 |
|---|---|---|
| 12 well format only | | |
| Grown on Wire grids in 6-well plates with 4ml culture media | | |
| VOID: 60-80µm | Interconnect: n/a | Porosity 70-90% |
| No QC performed. Showed pinholes | | |
| Ethanol washed before use | | |

Introduction of 1G single well-insert holders for 6 well plates. These form a continuous ring around the scaffold and separate the inner/outer areas. Shown in Figure 2.3

Pinholes through whole scaffold visible

| In-house-1G. 200µm thick sections | | |
|---|---|---|
| 12 well and 6-well insert formats | | |
| Grown in in-house sealed plastic holders – deep wells | | |
| VOID: 40-65µm | Interconnect: 10-20µm | Porosity ~93% |
| In-house QC ranges used | | |
| Plasma-treated in-house immediately before use | | |

Introduction of 1G triple well-insert holders for 3 well deep petri dishes. These form a continuous ring around the scaffold and separate the inner/outer areas. They allow growth of cells in much larger media volumes. Shown in Figure 2.4C

Uniform appearance

| 2G. 200µm thick sections | | 2012 |
|---|---|---|
| 12 well and 6-well insert formats | | |
| Grown in open-sided plastic holders – deep wells | | |
| VOID: 35-50µm | Interconnect: 12-15µm | Porosity ~90% |
| Full QC – cell growth, mercury porosimetry, SEM morphology | | |
| Sterile packed and ethanol washed before use | | |

Introduction of 2G well-inserts holders for 12-well and 6-well sized scaffolds. These now feature ports to allow diffusion of media from the inside and outside of the insert. Shown in Figure 2.3B

**Figure 2.2. Timeline of 3D Scaffold Development**

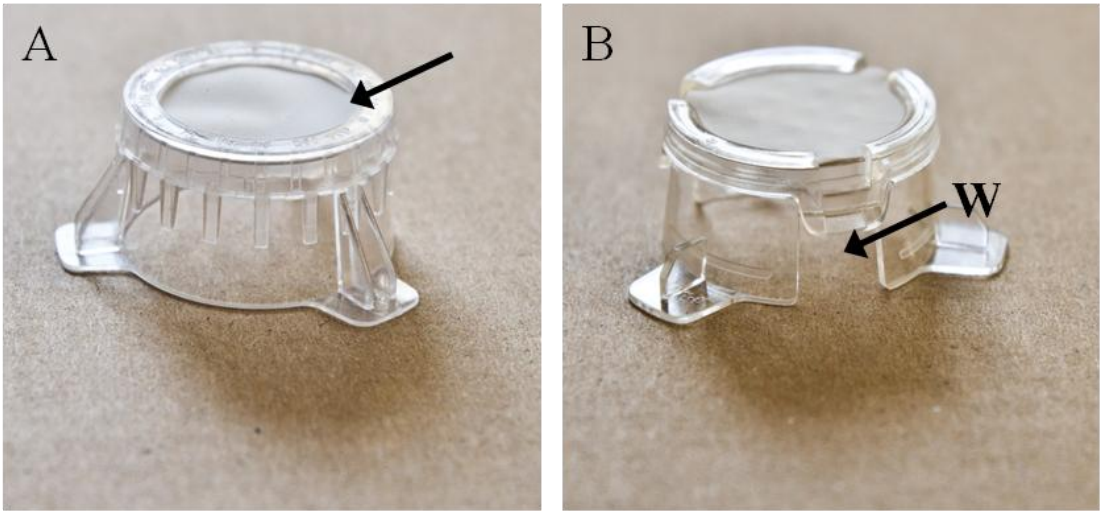


**Figure 2.3. 3D Culture System Well-inserts**

**A)** Well insert type 1 with a solid seal between the upper and lower sides of scaffold, shown inverted. The scaffold is slightly recessed on the underside and does not lie flat with media while at air-liquid interface (indicated with arrow); **B)** Well insert type 2 with three "windows" (labelled **W**) to allow culture media exchange between the upper and lower sides of the scaffold or separate media compartments on the upper and lower sides of the scaffold. The underside of the insert is less recessed and so the scaffold can maintain flat contact with media at the air-liquid interface. Scaffold diameter 22mm.

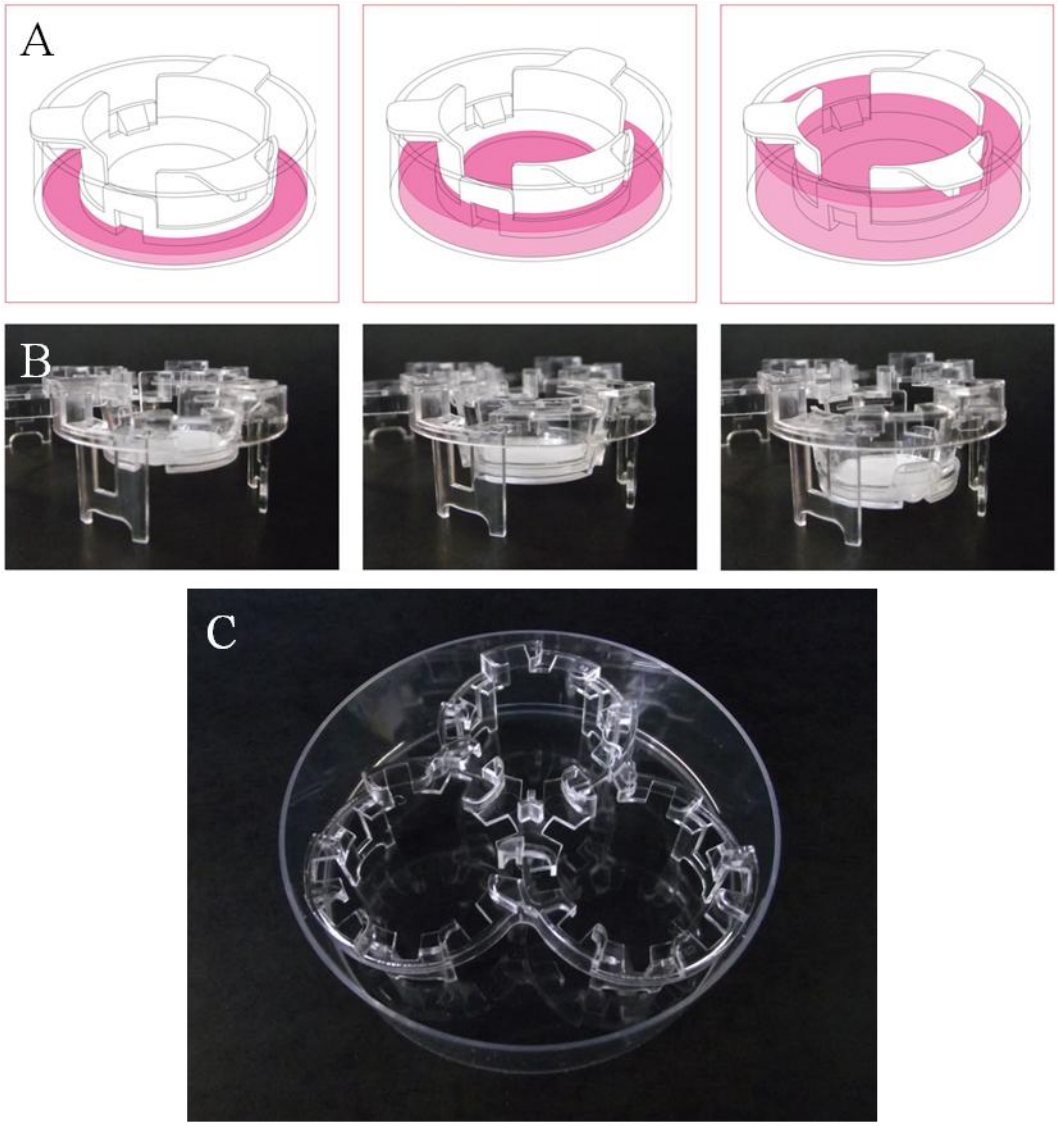


**Figure 2.4. Custom Cell Culture Apparatus**

A) Well insert type 2 set to three different media levels showing how culture media passes through the window of the well-insert when the scaffold is submerged. B) Well inserts type 1 and 2 can both be set to high, medium and low levels. This allows different amounts of culture media to be placed underneath the scaffold at the air-liquid interface (20ml, 34ml and 48ml respectively) or 70ml, 80ml and 92ml when submerged; C) Tri-well insert which holds three well-inserts inside a 86mm diameter 25mm deep Petri dish. Images reproduced with permission from Reinnervate Ltd, UK.

### 2.2.2 Preparation of the 3D Scaffold for Cell Growth

The polystyrene material that forms the 3D scaffold is very hydrophobic and solutions of water, PBS or cell culture media will simply form a bead on top. Therefore the scaffold must be prepared for cell culture by either pre-wetting with ethanol or by plasma treatment.

#### 2.2.2.1 Ethanol Pre-wetting of the 3D Scaffold

70% v/v ethanol was added to the scaffold for 10 minutes under sterile conditions, then washed away by 3 washes of tissue culture grade PBS, without the scaffold being allowed to dry. The scaffold was then stored under PBS until use. This treatment also sterilises the scaffold for cell culture. Before seeding cells, the scaffold was removed from PBS, and a cell suspension immediately added before the scaffold becomes dry and hydrophobic.

#### 2.2.2.2 Plasma Treatment of the 3D Scaffold

To plasma treat the 3D scaffold, a 12 well plate or a plate of scaffolds in 6-well sizes inserts were oxygen plasma treated individually with an Emitech Plasma Asher (K1050X) for 5 minutes at 40W, 30ml/min $O_2$ for same-day use, or 30 minutes at 10W, 30ml/min $O_2$ for long term (maximum one week) storage. This method of plasma treatment shows no detrimental effect on the scaffold structure (confirmed by in-house SEM analysis) although higher energy plasma treatment can adversely affect the structure of the scaffold by "melting" some surface voids, blocking cells from successfully entering the scaffold. Internal QC showed that plasma treatment also suitably sterilises the scaffolds and plasticware for cell culture. Plasma treatment of this 3D scaffold is discussed in more depth in Zeyfert et al, 2007.

In this study, both ethanol pre-wetted and plasma treated scaffolds were used. During the course of this project plasma treatment of the scaffold was still undergoing development and QC testing. In a comparison of ethanol wetting against plasma treatment shown in Chapter Three, plasma treatment was found to provide better cell growth. Where possible, plasma treated scaffolds were used preferentially in this study. However, due to the developmental nature of this project as well as time and equipment constraints, this was not always possible. However, all scaffolds used within one particular experiment, or in three repeats of the same experiment were always prepared by the same method. The preparation method will be noted where relevant throughout this thesis.

### 2.2.3 Cell Seeding in the 3D Scaffold

The 3D scaffold is a novel culture device and so a seeding method, quantity and density of cells needed to be determined. These were analysed in Chapter Three.

#### 2.2.3.1 Concentrated Cell Seeding Method

Cells were suspended at high density in a small volume of media and added to the centre of a scaffold. It was hypothesised that capillary action will draw the media and cells into the scaffold and fill the thickness of the scaffold. The approximate fluid volume of a 200µm thick, 25mm diameter scaffold is 68µL (in-house QC data) and so 50-100µl was typically used as the volume for seeding cells. This results in a high density of cells in the centre area of the scaffold.

#### 2.2.3.2 Diffuse Cell Seeding Method

In order to achieve a more even distribution of cells, cells were suspended into 2ml for a 12-well plate or 4ml for a 6 well plate and added to the scaffold. This would result in a more even distribution of cells over the surface area of the scaffold but potentially less penetration inside the scaffold.

### 2.2.4 Collagen Coating of the 3D Scaffold

In order to optimise the 3D scaffold as a dermal equivalent, it was combined with collagen in a variety of ways to form a gel, film or a filbrillar network. Type I rat tail collagen supplied at 2.12mg/ml in 0.6% acetic acid, (First Link,UK) was used. When the pH of the solution is neutralised by NaOH and the temperature is raised, the collagen can form a gel. The following five methods for collagen gel formation were used in this study:

**1) Fibroblast-contracted Gel.** 7:1:1:1 collagen, 1M NaOH, MEM and 3T3 cells ($5x10^5$ per ml) were mixed on ice and pipetted onto a prepared scaffold. All pipette tips were pre-cooled on ice to prevent early solidification of the gel. Scaffolds with collagen mixture were incubated at 37°C for 15 minutes to form a soft gel, then submerged in media and grown for 10 days with media changes every two days in accordance with Ojeh et al, 2008.

**2) Stable Chondroitin Sulphate and Collagen Gel.** A more stable gel was formed by mixing, on ice, 10:1:1 parts collagen, 1M NaOH, DMEM containing chondroitin-6-sulphate (final concentration of choindroitin 10% w/v) and pipetting onto a plasma-treated or ethanol-washed scaffold, based on a modification of the method by

Osborne et al, 2008. This forms a thick gel which solidifies quickly. This is discussed in more detail in Chapter Three.

**3) Ammonium Chamber Collagen Coating.** An ammonium chamber was used to form collagen fibres inside the scaffold rather than forming a sheet around the outside surfaces. Collagen solution was kept on ice and diluted in ice cold 0.6% acetic acid to 0.2mg/ml. To coat a scaffold, it was submerged in this mixture on ice for 15 minutes, then moved to a Petri dish containing a cotton ball soaked in ammonia. This was air-sealed at room temperature for 15 minutes to solidify.

**4) Collagen Coating in PBS or Ethanol.** Collagen was diluted into 1xPBS or 70% ethanol. 500µl was added to the scaffold in a 12 well plate. The solution was allowed to evaporate under sterile culture conditions.

**5) Pre-Neutralising with NaOH.** In order to prevent the collagen solution gelling prematurely outside of the scaffold, 100µl 1M NaOH solution was added to the scaffold and evaporated to leave a coating of NaOH throughout the scaffold. A dilute collagen concentration of 0.2mg/ml was then added to the dry scaffold and incubated at 37°C for 3 hours.

#### 2.2.4.1 Coomassie Brilliant Blue Staining for Collagen Coating

Collagen coating of the scaffold was quickly assessed by staining with Coommassie Brilliant Blue (40% v/v methanol, 10% v/v acetic acid, 0.1% v/v Coomassie Brilliant Blue G-250) for 5 minutes and removing excess with with de-stain solution (40% v/v methanol, 10% v/v acetic acid in $dH_2O$). As a control, an un-coated scaffold was used and all samples were washed in destain until the control showed no blue staining.

## 2.3 Analytical Methods

### 2.3.1 Imaging Methods

#### 2.3.1.1 Immunofluorescence Staining

Cells were seeded and grown on glass coverslips (VWR, UK) with one coverslip per 24 well plate submerged in 1.5ml cell culture media. To fix cells for analysis, cell culture media was aspirated and adherent cells were washed 3x with PBS then fixed in 2ml 4% w/v paraformaldehyde (Agar Scientific, UK) per well for 15 minutes at room temperature. Fixed coverslips were then washed 3x with sterile PBS and stored at 4°C in PBS for a maximum of 7 days before analysis.

For immunofluorescence staining, cells were permeabilised with 0.5% or 1.0% v/v Triton X-100 (Fisher Scientific, UK) for 15 minutes then blocked with a mixture of 0.5% v/v fish skin gelatin, 0.1% v/v Triton X-100 and 1% w/v Bovine Serum Albumin (BSA). Primary antibodies shown in Table 2.2 were then diluted to manufacturer specifications in blocking solution and added to coverslips for 1 hour at room temperature, or overnight at 4°C in a humidified chamber. Coverslips were then washed 4x 5 minutes with PBS to remove non-specific primary antibody, then inclubated for 1 hour at room temperature in appropriate secondary antibodies conjugated to a fluorophore i.e. Alexa488/594. Controls coverslips were stained with secondary antibody only. Coverslips were then mounted, cell side down, onto glass microscope slides with ImmuMount (Thermo Scientific, UK) with 1:1000 4', 6-Diamidino-2-phenylindole, (Invitrogen, UK).

#### 2.3.1.2 3D Scaffold Fixation, Embedding and Paraffin Sectioning

The following protocol was developed in-house for the 3D scaffold. 3D cultures were removed from culture vessels, fixed in 4% PFA overnight, then washed 3x in PBS for 5 minutes each. The central strip of the scaffold was then cut out and dehydrated through 30%, 50%, 70%, 80%, 90%, 95% and two washes of 100% v/v ethanol for 15 minutes each, cleared in Histoclear II for 15 minutes and embedded vertically in paraffin wax. Wax blocks were allowed to dry overnight. 10µm sections were cut as standard for histology and immunofluorescence staining with a Leica microtome, floated onto a waterbath at 45°C and adhered to histobond glass microscope slides. Sections were dried overnight on a slide drier at 40°C.

#### 2.3.1.3 Haematoxylin and Eosin (H&E) Staining

10µm thick, paraffin-embedded sections were de-waxed in Histoclear II (RA Lamb, UK) for 10 minutes. If sections were not fully de-waxed, they were placed into a second Histoclear II bath for 5 minutes. Sections were then re-hydrated through 100%, 95%, 80%, 70% v/v ethanols for 2 minutes each and moved into $dH_2O$ for 2 minutes. Sections were then stained in Mayers Hematoxylin for 6 minutes, washed in $dH_2O$ for 30 seconds, nuclei differentiated in alkaline alcohol (70% ethanol with 1% v/v ammonia) for 15 seconds, moved through 70% and 90% v/v ethanols and counterstained in 1% eosin solution for 15 seconds. Sections were then washed twice in 95% v/v ethanol and twice in 100% v/v ethanol for 30 seconds each. Finally, sections were cleared in Histoclear II for 5 minutes each, then mounted with a coverslip in DePeX (VWR, UK).

#### 2.3.1.4 Immunofluorescence Staining of 3D Cultures

The following protocol was developed in-house for the 3D scaffold. 10µm thick, paraffin-embedded sections were de-waxed with Histoclear II and rehydrated through graded ethanols and $dH_2O$ as above. In order to retrieve antigens blocked during fixation, sections were then subjected to antigen retrieval in citrate buffer at pH 6.5 with 6 minutes in the microwave at 900W, 5 minutes of cooling at room temperature, and a further 2 minutes at 900W. Sections were left to cool for 10 minutes, then washed in three changes of room temperature PBS for 10 minutes each. Sections were marked off with an ImmuEdge hydrophobic marker pen (Vector Scientific, UK), permeabilised with 0.5% v/v Triton-X100 in PBS for 15 minutes and blocked with blocking buffer (PBS/1% w/v bovine serum albumin/ 5% v/v fish skin gelatin, v/v 0.1% Triton-X100). Samples were incubated with primary antibodies in a humidified chamber at room temperature for 1 hour or overnight at 4°C depending on manufacturer reccommendations, washed 3x with PBS for 10 minutes each and then incubated with AlexaFluor 488 or 594 labelled secondary antibodies in a dark, humidified chamber for 1 hour at room temperature, following manufacturer reccommendations. Control sections were stained with secondary antibody only. Sections were then washed in PBS with 5 minutes and mounted with coverslips using ImmuMount mounting media with 1:1000 DAPI.

A summary of antibodies used for 2D and/or 3D immunofluorescence staining is shown in Table 2.2:

**Table 2.2. Summary of Antibodies Used in this Project**

| Antibodies | Target | Manufacturer | Type | Dilution |
|---|---|---|---|---|
| **Primary** | Filaggrin | Abcam ab24584 | Rabbit Polyclonal | 1:1000 |
| | Involucrin | Abcam ab28057 | Rabbit Polyclonal | 1:1000 |
| | Desmoplakin | Abcam ab71690 | Rabbit Polyclonal | 1:200 |
| | ZO-1 | Zymed 61-7300 | Rabbit Polyclonal | 1:100 |
| | Periplakin | In-house* | Rabbit Polyclonal | 1:500 |
| | E-cadherin | BD Bioscience | Mouse Monoclonal | 1:500 |
| | Ki67 | Novacastra NCL-L-Ki67-MM1 | Mouse Monoclonal | 1:100 |
| | Keratin 1 | Abcam ab93652 | Rabbit polyclonal | 1:500 |
| | Keratin 14 | Abcam ab53115 | Rabbit polyclonal | |
| **Secondary** | AlexaFluor 594 | Invitrogen A21207 | Donkey anti-rabbit | 1:800 |
| | AlexaFluor 488 | Invitrogen A11059 | Rabbit anti-mouse | 1:800 |
| **Other** | DAPI | Sigma, UK | | 1:1000 |

** BOCZ-1 antibody generated by Boczonadi and Määttä, 2012, pending publication.*

All fluorescent slides were then imaged on a Zeiss Axioskop 40 microscope equipped with 10x, 20x and 40x NEOFLUAR objectives. Images were taken with a AxioCam MRm camera and AxioVision 3.1 software. Scale bars were added in ImageJ using the "Spatial Calibration" plug-in for ImageJ (available at http:// *rsbweb.nih.gov/ij/download.htm*) and composite images and panels created in Adobe Photoshop CS4 or Microsoft Powerpoint. Linear adjustments to brightness and/or contrast were made where necessary.

#### 2.3.1.5 Scanning Electron Microscopy (SEM)

Karnovsky's Fixative was freshly prepared before use as follows: 25ml dd$H_2O$ was

heated at 60°C and 2g paraformaldehyde and 4 drops 1M NaOH were added. The solution was cooled and 5ml 50% w/v glutaraldehyde and 20ml 0.2M sodium cacodylate buffer were added. The solution was adjusted to pH 7.2-7.4 and stored frozen before use. 3D scaffold cultures were fixed in Karnovsky's fixative for 1 hour at room temperature, washed 3x in PBS and fixed for a further 30 minutes in osmium tetroxide at room temperature. Samples were cut into smaller pieces for analysis and dehydrated through graded ethanol series (30%, 50%, 70%, 80%, 90%, 95%, 2x100% v/v) for 30 minutes each, then critical point dried from 100% ethanol. Samples were gold-coated and observed using a Philips XL30 ESEM.

#### 2.3.1.6 Transmission Electron Microscopy (TEM)

Samples were fixed in Karnovsky's Fixative and osmium tetroxide and dehydrated as above. Small sections of samples were then embedded in LR White resin and cut into ultrathin sections by technicians using a Leica microtome. Samples were observed using a Hitachi H7600 TEM. Composite images were made in Adobe Photoshop or Microsoft Powerpoint.

### 2.3.2 Cell Viability Assays

#### 2.3.2.1 MTS Assay for Cell Metabolic Activity

3D cultures were removed from their culture vessels, washed 3x with sterile PBS and placed into 12 well plates. 2ml fresh DMEM/10% v/v FBS was mixed with 100µl MTS reagent (CellTiter 96 AQueous One Solution Cell Proliferation Assay, Promega UK) to make a final solution of 159µg/ml MTS reagent. 2ml of this MTS reagent was added to each 3D culture in a well of a 12 well plate. Empty 3D scaffolds were used as negative controls. Plates were placed into the cell culture incubator at 37°C for 2 hours. After 2 hours, the solution in each well was mixed thoroughly and 100µl samples pipetted into 96 well plates in triplicate. The plate was then read immediately on an Anthos Lucy-1 96-well plate reader at 490nm. The mean of three readings was then calculated. Assays on 2D cultured cells were performed as above, although MTS reagent was added directly onto cells cultured on the bottom of 24 or 12 well plates. All experimental MTS assays were repeated a minimum of three times. The MTS reagent contains a tetrazolium compound which is bioreduced by viable cells into a soluble formazan product which absorbs at 490nm. Absorbance is directly proportional to the metabolic activity of living cells in the scaffold. Graphs

were plotted as either absorbance at 490nm, or as percentage change against a control.

#### 2.3.2.2 Viacount Assay for Apoptosis

ViaCount assay uses a two membrane-permeable DNA dyes in combination with flow cytometry. The primary dye stains all nucleated cells, but ignores anucleate or dead cells and the secondary dye stains only damaged cells with breaches in the plasma membrane, indicating apoptosis or cell death. Media containing floating cells was centrifuged at 1000g for 5 minutes and adherent cells were trypsinised, re-suspended into PBS and pooled with non-adhered cells. Cells were counted and re-suspended into 1.0ml PBS and kept on ice. The Guava ViaCount analyser was auto-cleaned and passed relevant QC procedures before use. Cells in PBS were diluted 1:10 in ViaCount assay reagent into 96-well plates. The assay was then performed, with the machine counting individual cells for 120 seconds or until a minimum of 1000 cells had been counted. Wells which contained a small number of cells (<200) were rejected. After performing analysis on control beads provided by the manufacturer, the apoptosis gate was set manually. Results were exported as a Microsoft Excel spreadsheet for further analysis.

### 2.3.3 Assessment of Epidermal Barrier Maturity

#### 2.3.3.1 Cornified Envelope Extraction from 2D Cultures

Cornified envelopes were extracted according to methods in Määttä et al, 2001 and Sevilla et al, 2007. Culture media from 2D cultures in T25 or T75 flasks was collected and centrifuged at 1000g for 5 minutes to pellet differentiated and non-adhered cells in the culture media. Cells adhered to culture flasks or dishes were scraped into PBS and pooled with pelleted non-adhered cells. Floating and adherent cells were resuspended and centrifuged for a further 5 minutes at 1000g. The pellet was re-suspended in cornified envelope extraction buffer (20mM TrisHCl, 5mM Ethylenediaminetetraacetic acid (EDTA), 10mM dithiothreitol (DTT) and 2% w/v Sodium Dodecyl Sulphate (SDS) and boiled at 95°C for 20 minutes. This mixture was repeatedly washed by centrifugation at 5000g for 5 minutes, removing the supernatant and re-suspending in cornified envelope extraction buffer with 0.2% w/v SDS. Finally, the pellet was resuspended in 50µl of PBS for imaging. Cornified

envelopes are imaged by dropping 10µl of extract onto a glass slide and observing using phase contrast microscopy. For imaging with Nile Red, cornified envelopes were spotted onto a glass microscope slide, then mounted in ImmuMount with 0.5mg/ml Nile Red in acetone, adapted from Hirao et al, 2001 and Rawlings, 2003.

#### 2.3.3.2 Cornified Envelope Extraction from 3D Cultures or Tissue

For 3D cultures, culture media was collected and centrifuged as above. The 3D scaffold or mouse ear tip tissue samples were cut into smaller pieces using sterile scissors and added to cornified envelope extraction buffer for 20 minutes at 95°C. 3D scaffolds were pooled with pelleted cells from the culture media. The pieces of polystyrene scaffold were then removed, and the mixture was centrifuged at 1000G for 5 minutes. The rest of the extraction was carried out as described for 2D extractions.

#### 2.3.3.3 Protein Extraction and Quantification

For 2D or 3D cultures, flasks of cells or 3D culture dishes were placed on ice. Culture media was removed and spun at 1000g for 5 minutes to pellet floating cells. 3D cultures were removed from culture apparatus and placed into 6 well plates. Cells adhered to flasks or 3D scaffolds in 6 well plates were washed 3x with ice cold PBS. A drop of 2x Laemmli (Laemmli, 1970) protein lysis buffer with DTT (50mM Tris-HCl pH6.5, 20% v/v glycerol, 1mM EDTA, 1% SDS, 1M DTT) was added to re-suspend the cell pellet while 600µl cell lysis buffer was added per T75, 10cm dish or scaffold in a 6 well plate. Cells were scraped into lysis buffer using a cell scraper. For scaffolds, a sterile pestle and mortar was used to break up the scaffold with protein lysis buffer. The resulting mixture was pipetted into a 1.5ml Eppendorf tube and boiled for 5 minutes. After boiling, the mixture was passed back and forth through a 25 gauge needle, transferred to a new tube and frozen at -20°C. An empty scaffold was used as a control.

The total of proteins extracted as above was quantified with the bicinchoninic acid (BCA) assay reagent kit (Pierce, UK). This kit uses the reduction of $Cu^{+2}$ to $Cu^{+1}$ by protein in an alkaline medium (Biuret reaction) and detects the $Cu^{+1}$ with a colorimetric reagent. Ten standards between 0.0-2.5mg/ml protein were made using a provided bovine serum albumin solution. Standards were mixed with the colorimetric reagent, incubated at 37°C for 30 minutes and cooled before absorbance was measured at 562nm. A standard curve of absorbance vs concentration was generated.

Samples were analysed with the same methodology and diluted if necessary to fit within the linear range of the assay. These protein concentrations were then used to standardise the amount of lipid extract applied to TLC plates.

#### 2.3.3.4 Lipid Extraction from 2D Cell Culture

HPLC-grade reagents, MilliQ water and glass tubes and pipettes were used throughout. Flasks of cells were washed twice in PBS for 2 minutes, then scraped into 1ml ice-cold PBS. This was then added to 4ml 2:1 methanol:chloroform and placed onto a rotator at room temperature for 1 hour, then spun at 5000g for 5 minutes. The supernatant was discarded and the pellet resuspended in 4ml 1:1:1 50mM citric acid: dd$H_2O$: chloroform. This mixture separates into three phases and was vigorously mixed on a shaker for 1 hour at room temperature then spun at 5000g for 20 minutes to fully separate different layers. The top layer (water/methanol) and the solid layer of protein were discarded. A fresh, glass pipette was then used to move the lower phase containing chloroform and extracted lipids (approx 1ml) into a new glass tube. The solvent was then evaporated under sterile conditions, leaving an opaque coating of lipid in the tube. This was re-suspended in 2:1 chloroform:methanol and stored, double-sealed to prevent evaporation, at -20°C until required.

#### 2.3.3.5 Lipid Extraction 3D Cell Culture

3D cultures were removed from culture vessels, washed in PBS and added to 2:1 methanol:chloroform with 1ml PBS. The scaffolds were then broken apart with sterile, chloroform-methanol washed metal tweezers and mixed for 1 hour at room temperature. The mixture was then centrifuged at 5000g for 5 minutes. The supernatant and pieces of scaffold were removed and discarded, and pellet resuspended in 4ml 1:1:1 50mM citric acid: dd$H_2O$: chloroform. The procedure was then carried out and samples were stored as above. An empty scaffold was used as a control in each batch of extractions to ensure that chloroform:methanol was not leeching styrene or other plastics from the scaffold. No bands or streaks were visible on TLC plate with the development and staining protocols used.

#### 2.3.3.6 Lipid Extraction Mouse Epidermis

C57BL/6 mice were shaved, killed by cervical dislocation and skin samples removed from the back. Samples were handled to avoid folding and contamination of the epidermis with subcutaneous fat. Skin sections were washed for 30 seconds in

hexane to remove surface lipids, then adhered to Whatmann filter paper and stored in 2x PBS with 2% antibiotic/antimycotic. To separate the epidermis from intact skin samples, sections of skin were floated onto 0.25% trypsin at 4°C overnight. The epidermis was then peeled and scraped off. Alternatively, skin samples were floated onto a 70°C waterbath for 20 seconds, then sandwiched between two pieces of filter paper and twisted to separate the epidermis. The epidermis was then scraped off into an eppendorf tube and lipid extraction carried out as above.

#### 2.3.3.7 Thin Layer Chromatography

A 20x20cm 0.25mm silica gel-coated TLC plate (Merck, UK) was divided into separate 1cm wide lanes by scraping off the silica gel coating. Extracted lipids, standards and control samples (from empty scaffolds) were suspended in 2:1 chloroform:methanol were spotted into each lane 2.5cm from the bottom edge of the plate, using calibrated 2µl glass capillary tubes. Samples were added in 2µl spots in total amounts equalised against protein concentration from samples of the same treatment group. Solvent was allowed to evaporate between each 2µl application in order to apply a small, concentrated spot of lipid into the silica coating. All markings on the TLC plate were made in pencil.

A three-phase development profile (Wertz and Downing, 1990, Pappinen et al, 2008) was chosen for best separation of epidermal lipids - particularly ceramides, free fatty acids and cholesterol as shown in Table 2.3:

**Table 2.3. Three-phase Development Protocol for TLC Lipid Separation**

| Solution | Solvents | Distance run |
|---|---|---|
| A | 40:10:1 chloroform:methanol:water | 0-10cm |
| B | 190:9:1 chloroform:methanol:acetic acid | 0-16cm |
| C | 70:30:1 hexane, diethylether and acetic acid | 0-20cm |

HPLC-grade solvents and glass pipettes were used throughout all lipid analyses. A large glass TLC development tank was filled with 200ml (approximately 1cm deep) of solvent along with blotting paper soaked in that solvent. The tank was then sealed and allowed to fill with vapours for five minutes before the TLC plate was then added to the tank and the tank was air-sealed. Each solvent was allowed to run up the plate to the distances shown above. Between each solvent run, the plate was removed and allowed to dry thoroughly in a fume hood. After the final run, a 2µl spot of each extracted sample was added to an unused area of the plate. A schematic diagram is shown in Figure 2.5.

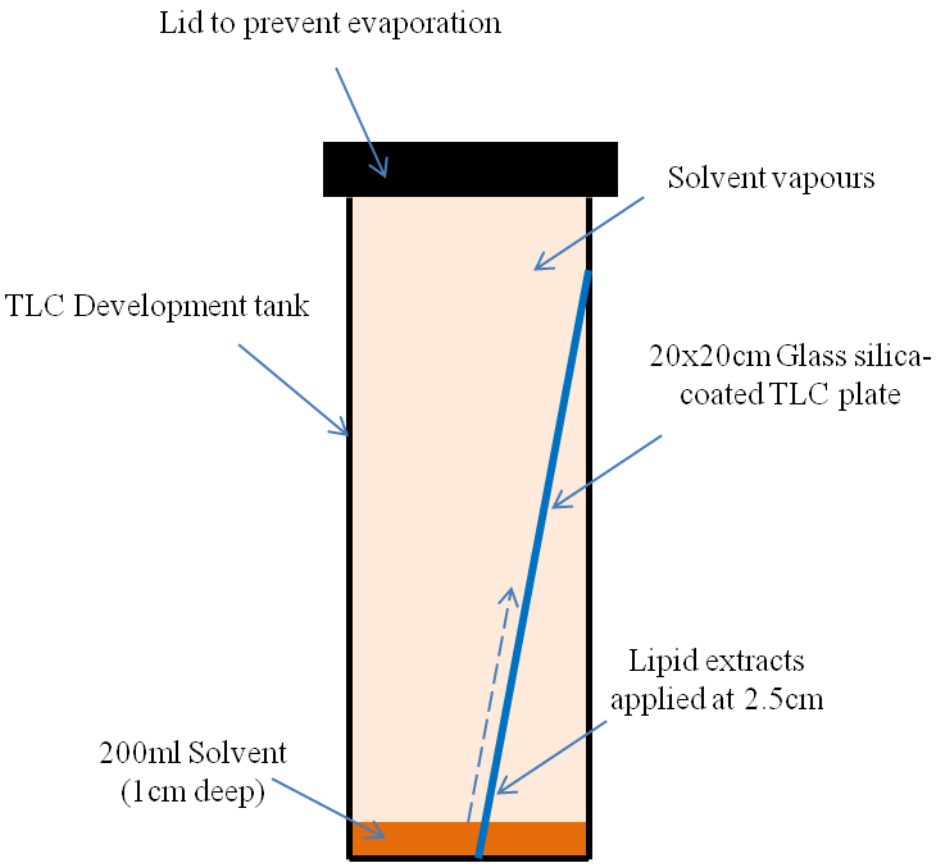


**Figure 2.5. Thin Layer Chromatography Development**

Schematic diagram of TLC development tank containing 20x20cm TLC plate. The tank was filled to 1cm depth with solvent and the lid was attached. The insides of the tank are lined with absorbent filter paper soaked in solvent and the tank was allowed to fill with solvent vapours. Samples are applied to the plate 2.5cm from the bottom, and then submerged into 1cm of solvent. The lid was replaced and the solvent runs up the TLC plate. After the solvent front reaches a certain distance on the plate, the plate was removed and dried, and the solvent and filter paper replaced with the next solvent. The chamber was then allowed to fill with vapour and the process repeated until the plate was fully developed by all three phases.

#### 2.3.3.8 Lipid Quantification

In order to visualise lipids on the plate, the plate was dipped into a solution of 0.001% Phloxine B in 70% ethanol and allowed to dry overnight at room temperature in the dark. The plate was then visualised face-down under UV light and images were captured using a BioRad GelDoc with QuantityOne software. The image was flipped horizontally, inverted and background-reduced in ImageJ. Band density was quantitated by a rectangular selection around the entire lane. "Plot profile" was then used to generate a plot of peaks for the entire lane. The area of each peak was then used to calculate the relative amount of lipid contained in that peak. An example of this is shown in Figure 2.6. For individual spots of lipid applied directly to the plate from extracted samples, the measure tool was used to measure the integrated density of each selection.

#### 2.3.3.9 Lipid Identification

Bands on the plate were identified by the known standards Cholesterol, Cholesterol Oleate and Sodium Cholesterol Sulphate (Sigma UK). These standards were applied at 10µg/ml to the TLC plate alongside extracted lipid samples. They were then separated and visualised with the same procedures as extracted samples. The retardation factor (Rf) value was then calculated as the distance which the standard travelled, divided by 20cm. Rf values were recorded, and used to identify bands on the TLC plate arising from lipid sample separation. Other bands were identified by ASAP-MS and reference to published literature.

#### 2.3.3.10 Atmospheric Solids Analysis Probe-Mass Spectrometry

In order to further confirm the identity of separated lipids, lipid standards suspended in chloroform were also analysed by atmospheric solids analysis probde - mass spectrometry (ASAP-MS). Bands of silica gel containing lipids were scraped from the glass TLC plate into a glass sample tube, then vortex mixed with chloroform for 5 minutes to resuspend the lipid into solution. These samples were then immediately analysed by ASAP-MS on a Waters Xevo QTOF analyser. Analysis was performed by technicians using the appropriate methods for each sample. m/z values and peaks from standards were compared bands scraped from the TLC plate and to those found in published literature (Duh et al, 1992, Masahiro and Masao, 2007, Tachi and Iwamori, 2008). Phloxine B was also tested and found not to interact or interfere with the ASAP-MS identification of lipids.

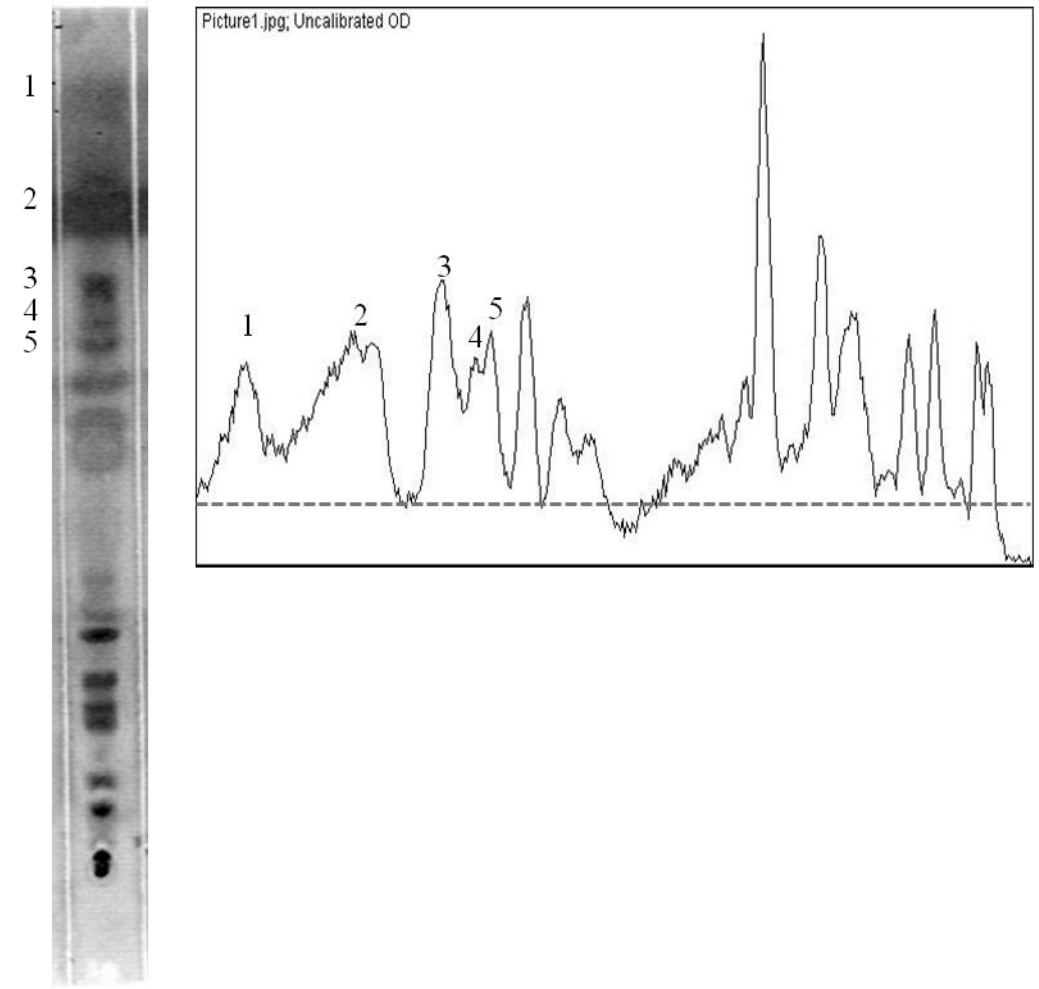


**Figure 2.6. Quantification of TLC Bands**

ImageJ "plot profile" of selected band (left). The plot profile is viewed from right to left and the TLC plate is run from top to bottom. Each peak corresponds to a lipid on the TLC plate and the area under each peak corresponds to the integrated density of that peak, as shown. Therefore the amount of lipid present in that band can be calculated. In ImageJ, the line tool was used to separate each band, then the "measure" tool used to calculate the area inside that peak. Background was subtracted by a horizontal line forming a new X-axis, as shown by the dotted line.

### 2.3.4 Measuring Epidermal Barrier Permeability

#### 2.3.4.1 Diffusion Chamber Analysis

A custom-made side-by-side diffusion cell (PermeGear, USA) was used to measure barrier permeability of 3D cultures. The diffusion cell comprises two 4ml capacity glass chambers with opposing ground glass interfaces and a 6mm diameter diffusion portal between them. Photographs and a schematic diagram of the diffusion cell are shown in Figure 2.7.

To assess permeability, samples were clamped firmly between the two chambers and sealed with waterproof silicon annealing tape. The diffusion cell was placed onto a magnetic stirrer with white paper underneath to visualise any leaking of culture media from either chamber. Donor and recipient sides of the chamber were each filled with 4ml of sterile DMEM culture media at 37°C as diluent, with a permeant compound of 15,000pg/ml corticosterone present in the donor side. Both sides of the chamber were mixed equally on a customised magnetic stirrer for the full duration of the experiment.

Diffusion experiments were initially carried out at 37°C until equilibrium was reached, but due to the long time-frame of these experiments (>48 hours), results became variable due to the degrading quality of the submerged cultures. Therefore, all diffusion experiments presented in this thesis were carried out at 37°C and both donor and recipient sides were both sampled (100µl) every hour for three hours and the removed volume was replaced with DMEM. This short-sample technique has been used in published studies (Schreiber et al, 2005) to measure epidermal permeability. Cultures were monitored for air bubbles, and cultures where DMEM leaked from the seal between the two chambers were discarded. Aliquoted samples from donor and recipient chambers were frozen at -20°C until used.

#### 2.3.4.2 Corticosterone Assay

Corticosterone concentrations were calculated using a Corticosterone EIA kit (Enzo Scientific ADI-900-097) in a 96 well plate. Standard solutions of 20,000, 4,000, 800, 160 and 32pg/ml were made in DMEM culture media then 100µl added to wells of the 96 well plate in triplicate with 100µl of diluent. 50µl of each assay buffer, conjugate and antibody were added to each well. Internal controls were performed for maximum and minimum absorbance. The plate was incubated at room

temperature for 2 hours on a shaker. Wells were then emptied and washed three times with 400µl wash solution. Wells were aspirated and dried, then 200µl pNpp substrate added to each well and incubated for 1 hour. Finally, 50µl of stop solution was added per well and the plate read immediately after at 405nm. Absorbance readings were corrected against blank wells and the percentage of bound antibody was calculated from the maximum absorbance control wells. A standard curve of percentage bound against concentration was made using standards, and unknown samples calculated from the equation of the line of best fit.

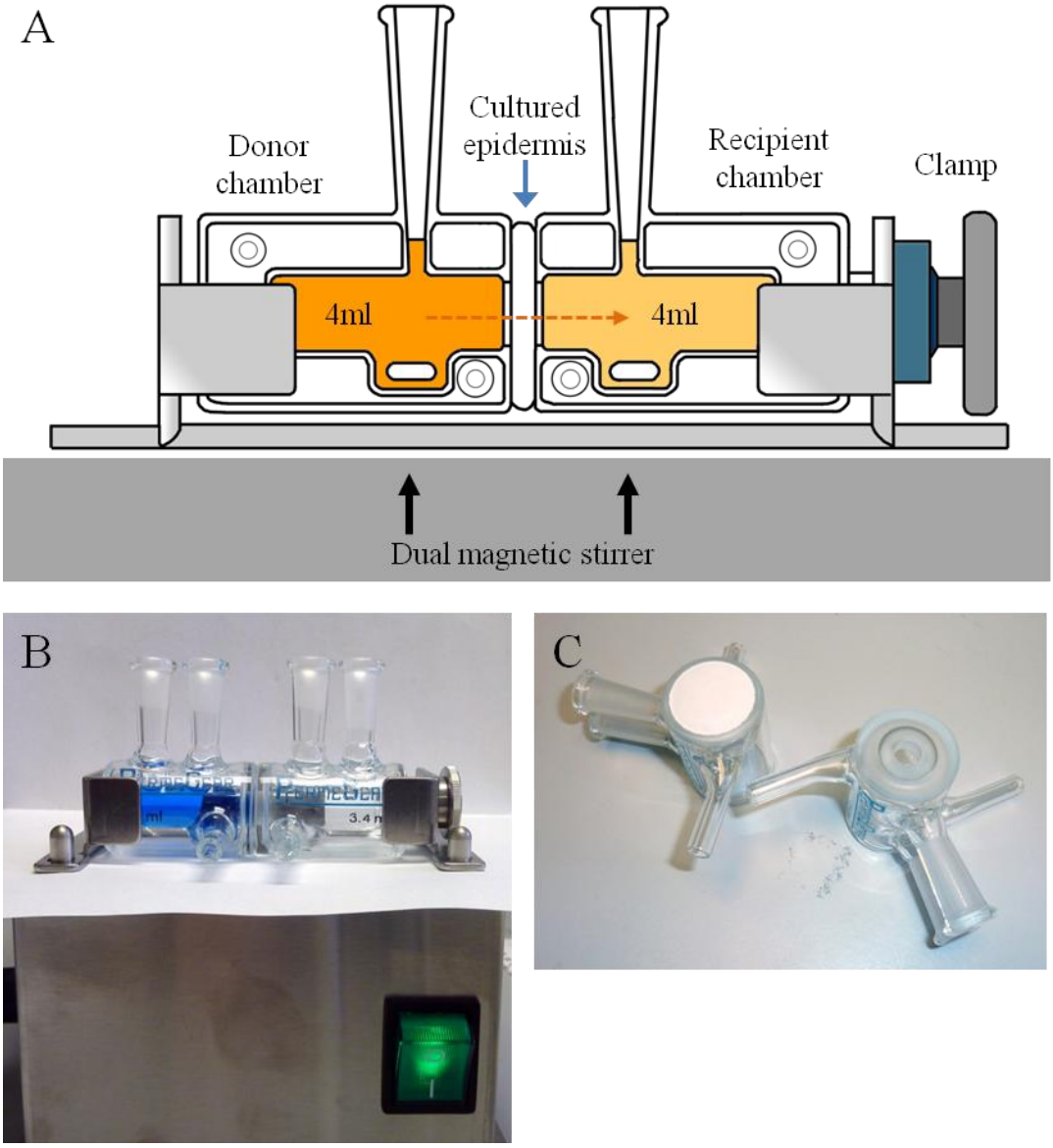


**Figure 2.7. Side-by-side Diffusion Chamber**

A) Diagram of side-by-side diffusion chamber from PermeGear, USA. Each side contains 4ml of cell culture media with a 6mm diameter diffusion orifice separating the two chambers. Each side has a dual sampling ports which are sealed to prevent evaporation during the experiment. The apparatus sits on a custom dual magnetic stirrer so that both chambers are continuously mixed. B) Photograph of the apparatus on magnetic stirrer with blue dye added to visualise the barrier effect of the 3D culture between the two chambers; C) Photograph of separated diffusion chambers with 6mm orifice visible. 22mm diameter scaffold size and placement shown for reference.

### 2.3.4.3 Calculation of Permeability Coefficient

The permeability coefficient for each culture was calculated by plotting a graph of the cumulative amount (µg) of permeant in the recipient chamber versus time (seconds). Permeability coefficient was then calculated as follows

$$P = \frac{1}{AC_D} \frac{dQ}{dt}$$

P = permeability coefficient (cm/s)

A = Diffusional area ($cm^2$). Diameter of diffusion orifice in the chamber 6mm = $0.2827 cm^2$

$C_D$ = Initial concentration in donor chamber (µg/ml) = 0.015µg/ml

dQ/dt = Slope of linear region of cumulative permeant amount (µg) over time (s) where $r^2$ = 0.941-1.000. Equation y=mx+c used to determine slope.

# 3 Chapter 3

# Development of a 3D Culture System for HaCaT Keratinocytes

## 3.1 Introduction

### 3.1.1 Aims, Objectives and Overview

The long-term aim of this project was to engineer an *in vitro* 3D epidermal equivalent using a 3D polystyrene scaffold. This epidermal equivalent can be used for *in vitro* investigations into keratinocyte differentiation, with emphasis on epidermal barrier function. The aim of this chapter was to establish a culture method for keratinocytes using the 3D scaffold which had not previously been cultured on this material. To this end, an experimental approach involving optimization of several different aspects of cell culture was adopted.

Previous experiments have demonstrated that HepG2 hepatocytes (Bokhari et al, 2008) and *TERA2*.cl.*SP12 cells* (Hayman et al, 2005) cells can be cultured within the polystyrene scaffold, but the growth of keratinocytes in this porous polymer structure had not been analysed in depth previously. It should be possible to utilise the scaffold as the basis for 3D organotypic culture of keratinocytes, given optimised conditions. Therefore, fundamental procedures such as the type and number of cells to be seeded, the method of seeding and the length of culture period were addressed initially. As mentioned in Chapter Two, the scaffold and 3D culture system were under development throughout the course of this project and initial investigations were performed using wire grids to raise the scaffold to the air-liquid interface. These were later followed by use of a custom well-insert device. These culture methods were compared experimentally in this chapter.

Another optimisation step involved the preparation of the scaffold itself before the use. The polystyrene-based material is highly hydrophobic and requires pre-wetting with ethanol and washing with PBS before use (Hayman et al, 2005, Bokhari et al, 2007). However, this has inherent disadvantages to well-distributed cell seeding and therefore a more recently developed technique of plasma treatment (Zeyfert et al, 2009) was investigated as means to generate a uniform surface hydrophilicity in the scaffold.

Many cell lines, particularly primary cells, require culture surfaces coated with collagen for attachment and proliferation. Collagen gels also represent the current standard for the dermal component in 3D full thickness *in vitro* skin models. Likewise, co-culturing keratinocytes with fibroblasts is also required for some

primary keratinocytes and has been shown to improve the growth of HaCaT keratinocytes in un-supplemented 3D cultures (Ikuta et al, 2006, Schoop et al, 1999). Therefore, preliminary experiments with collagen coating and fibroblast co-cultures were set up to explore the full potential of the 3D scaffold system.

Due to the number of different conditions tested, the outcomes were assessed by histology and MTS cell viability assays. Once optimised culture conditions were established, more in-depth analyses into investigate barrier assembly and barrier function were performed in Chapter Four and Chapter Five. A summary of culture conditions investigated in this chapter are summarised in Table 3.1.

**Table 3.1. Culture Conditions Testing in this Chapter**

| **Condition Tested** | **Comparison** | **Methodology** |
|---|---|---|
| Collagen coatings and gels | Gel recipe and methods of applying gel to 3D material | Collagen gel tested for morphology |
| Collagen/Chondroitin gel | Gel thickness and method of application | Tested for gel morphology and ability to support cell culture |
| Pre-treatment of scaffold | Plasma treatment compared to ethanol pre-washing | Tested based on collagen deposition |
| Cell-seeding number and method | Diffuse and concentrated seeding methods. Cell numbers ranging from $0.5\text{-}4.0\text{x}10^6$ per scaffold | Assessed based on morphology, MTS assay and immunofluorescence staining |
| Growth Period | Duration submerged and at the air-liquid interface | Assessed based on MTS assay and morphology |
| Culture Method | Wire grids compared to well inserts | Assessed based on cell morphology |
| Culture of skin cells | 3T3 fibroblasts, MET cells and mouse keratinocytes | Tested for morphology in 3D scaffold |

### 3.1.2 HaCaT Cells as an Experimental Model for Epidermal Keratinocytes

HaCaT cells are a stable, immortal human keratinocyte cell line first derived by Boukamp et al (1988) from the outside periphery of a melanoma from a 62yr old man - although HaCaT cells themselves are non-tumorigenic. HaCaT cells were shown to maintain the ability to proliferate beyond passage 140 while retaining the ability to differentiate indicating that this cell line offers a stable model for studies on keratinisation and differentiation (Boukamp et al, 1988). In a following study, the original authors (Boukamp et al, 1997) reported culturing HaCaT cells to beyond passage 300 with the majority of changes (i.e. increasing serum dependence, reduced population doubling time, increasing chromosomal translocations) occurring after passage 100. HaCaT cells tested at passage 80 could still form an organised, differentiated epidermis in organotypic culture. In the studies presented in this thesis, all HaCaT cells were earlier than p65. It should be noted that HaCaT cells are not a complete replication of normal human keratinocytes primary cells (NHK), which are typically isolated from human neonatal foreskin.

Maas-Szabowski and colleagues, 2003 showed that NHK cells form a more ordered 3D epidermis under *in vitro* organotypic co-culture conditions than HaCaT cells. This was shown to be because of reduced interactions with dermal fibroblasts, initiated by the HaCaT cells. HaCaT cells produce significantly less IL-1 than NHK cells, therefore reducing the production of KGF/FGF and GM-CSF from fibroblasts. HaCaT cells also produced less TGF-alpha. Addition of IL-1, KGF, FGF and TGF-alpha to culture media enabled HaCaT cells to produce an epidermis more similar to NHK cells. In this thesis, serum-containing culture media or growth factor supplemented media was used for maintaining cultured cells and in all experimental studies, aside from where indicated.

In a direct comparison with NHK cells, Micallef et al, 2008 showed that HaCaT cells have a delayed response to calcium concentration, and that they present abnormalities in their cell cycle. Under low calcium conditions, HaCaT cells and NHK cells showed similar behaviour in terms of cell cycle distribution and the balance between proliferation and differentiation (i.e. expression or basal keratins and differentiation markers). Upon stimulation with high (1.3mM) calcium, NHK cells were much more rapid in their calcium-induced responses such as

morphological changes, formation of stratified sheets and increased cell-cell contact when compared to HaCaT cells. The same is true for the expression of differentiation markers. NHK cells showed a more rapid increase in mRNA and protein expression of involucrin, K1 and K10. However, importantly, HaCaT cells still showed full terminal differentiation capacity when stimulated by high calcium, albeit more slowly than NHK cells.

One further note is that HaCaT cells also begin to undergo structural changes associated with differentiation when grown at high confluence (Boukamp et al, 1988). Therefore, HaCaT cells shown in this study were always sub-cultured at a confluence of 70-80% in 2D and not allowed to become too confluent.

Bearing these differences to NHKs in mind, HaCaT cells were selected for the majority of analyses in this chapter. Despite differences when compared to NHK cells, HaCaT cells have been shown to exhibit all major functional activity and characteristics of NHK cells including the ability to differentiate and form stratified epidermal structures (Boukamp et al, 1998). Furthermore, HaCaT cells have been previously used successfully over many years for the three-dimensional organotypic culture of epidermis *in vitro* (Rosdy, 1990, Smola et al, 1998, Schoop et al, 1999, Zinn et al, 2006, Ojeh et al 2008). These data support the concept of using HaCaT cells for 3D culture with the aim of engineering an epidermal barrier.

## 3.2 Results

### 3.2.1 Assessment of the HaCaT Clone Used in this Study

Extracellular calcium concentration has been shown to modulate the activation of keratinocyte differentiation (Micallef et al, 2008). Namely, keratinocytes can be maintained in a proliferative state at low calcium (<0.1mM) concentration and differentiated by the presence of a high calcium (>1.0mM) concentration in the culture media. During differentiation, HaCaT cells undergo morphological changes, altered protein expression (increased K1/K10, involucrin etc) and the formation of desmosomes and adherens junctions. (Micallef et al, 2008).

As the main aim of this project was to engineer an epidermal barrier model, reliant on cell differentiation, it was important to ensure that the HaCaT clone used in the study had retained its differentiation capacity and the ability to express epidermal barrier proteins. To this end, HaCaT cells were allowed to proliferate in low calcium (0.06mM) DKSFM culture media on glass coverslips, then switched to 1.5mM calcium media as described (Ojeh et al, 2008). Live cells were examined by light microscopy (Figure 3.1), then fixed and stained at various time points for differentiation markers as described in Chapter Two.

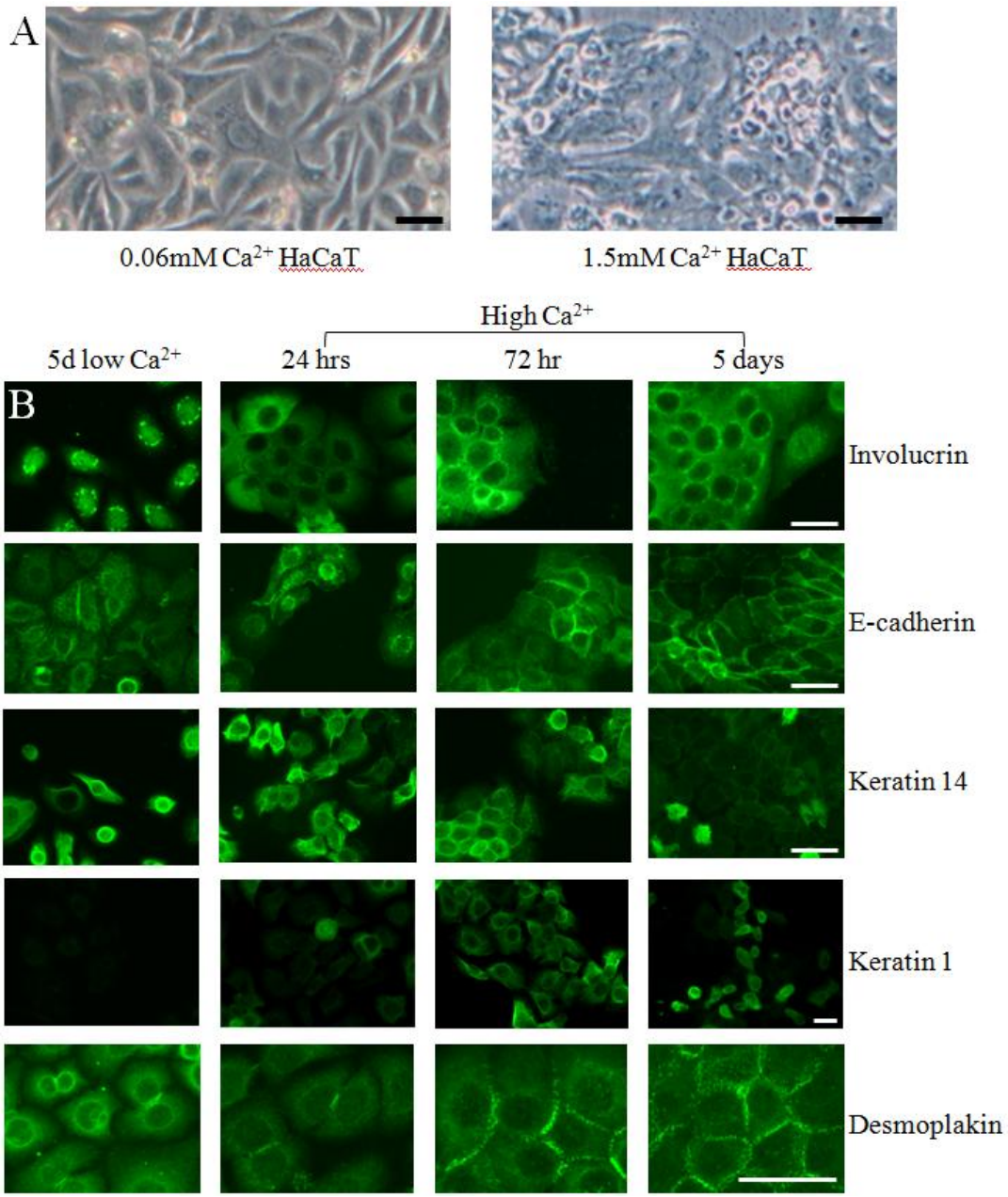


**Figure 3.1. Characterisation of HaCaT Clone in 2D Culture**

A) Light microscopy images of HaCaT cells grown in low (0.06mM) and high (1.5mM) calcium for 48 hours; B) Immunofluorescence staining of HaCaT cells grown for 24 hours, 72 hours and 5 days in high calcium culture media on 2D glass coverslips. Control cells were grown in low calcium culture media for 5 days. Scale bars 50µm.

Light microscopy images of HaCaT cells in low calcium (0.06mM) and high calcium (1.5mM) conditions (Figure 3.1A) show a marked difference in morphology between the two growth conditions. Under low calcium conditions, the HaCaT cells have formed a confluent monolayer of elongated or oblong shaped cells, with occasional rounded cells undergoing cell division. Boundaries between the cells are clearly visible and cells appear darker and opaque. Under high calcium conditions, the HaCaT cells have formed a layer of flattened, more transparent (thinner) cells which occupy a larger surface area of the coverslip. Boundaries between the cells are also less clearly visible by light microscopy and the number of detached cells floating in the culture media has increased. It also appears that the number of cells present may have increased. This would be in line with previous findings by Walker et al, 2006 and Micallef et al, 2008, who unexpectedly found that HaCaTs were more proliferative in media containing high calcium than when cultured in low calcium conditions.

Immunofluorescence staining (Figure 3.1B) shows clear changes in cell morphology after 5 days in the high calcium culture medium. Involucrin, an early differentiation marker, usually located in keratinocytes of the spinous and granular layers of the epidermis, shows a pronounced increase in expression and a re-distribution in the cytoplasm over time. E-cadherin, a cell adhesion protein, shows increased expression as expected as well as re-location to the cell-cell boundaries as time in high calcium media increases. After 5 days, E-cadherin expression is present at almost all cell-cell boundaries. Some E-cadherin staining at cell borders is visible after 5 days in low calcium media. Desmoplakin, a desmosomal plaque protein involved in the connection of keratin intermediate filaments to the desmosomal cadherins, also shows a similar change in expression and re-location to cell boundaries. This is important for the growth of the HaCaT cells in the 3D environment - showing that they are able to form adherence junctions and desmosomes with other cells, vital for the barrier acquisition. K14, a keratin found predominantly in proliferative basal layers of the epidermis, shows a decrease but not a total loss in expression over 5 days in high calcium, owing to the long half-life of the protein. Similarly, K1, a differentiation marker in keratinocytes, shows a general increase in expression but is not found in every cell. This confirms that this HaCaT cell line may be suitable for growth in the 3D scaffold with the intention of forming an epidermal barrier and is in line with other published studies in HaCaT cell differentiation.

### 3.2.2 Integration of Collagen Coatings into the 3D Scaffold

Many cell types, including keratinocytes, may benefit from being cultured on collagen coated surfaces or on collagen itself. Contracted collagen gels and collagen-fibroblast gels have been used to culture keratinocytes in 3D since the 1980's (Prunieras et al, 1982, Bell et al, 1983,) and are still used currently (Ng et al, 2011). They, along with de-epidermalised dermis (Cumpstone et al, 1989, Mak et al, 1991), represent the gold standard in organotypic culture of keratinocytes. Therefore methods of combining the 3D scaffold with collagen coatings and collagen gels were investigated. Two different approaches for collagen coating of the 3D scaffold were tested:

1) Deposition of collagen fibres within the scaffold. This involves coating the surfaces of the polystyrene scaffold and allowing better attachment and proliferation of cells. This is similar to coating of a 2D surface such as a Petri dish or cell culture flask.

2) Using the scaffold as a solid base for a contracted collagen gel. Cells are then cultured on the surface of the gel at the air-liquid interface. This is similar to using a porous membrane (often made of porous acetate cellulose, polycarbonate or PTFE) such as the Nucell (Nucleopore), Transwell (Costar) or MilliCell (MilliPore) as a collagen support. These supports function as a stable and culture media-permeable base for the contraction of a semi-solid collagen gel, which may also include fibroblasts as feeder cells. Keratinocytes can then be seeded into the surface of the collagen gel and lifted to the air-liquid interface for organotypic culture. Typically wire grids or raised well-inserts are used for lifting cultures to the air-liquid interface.

A solution of Type I rat tail collagen provided in 0.6% acetic acid can be solidified into a stable gel by neutralising with NaOH and warming to 37°C. Collagen solution was diluted to various concentrations in 0.6% acetic acid, then added to ethanol/PBS pre-wetted scaffolds and warmed to 37°C for 30 minutes. Scaffolds were then stained with Coomassie Brilliant Blue and de-stained to visualise collagen deposited in the scaffold. A negative control was performed by using a scaffold submerged into 0.6% acetic acid without collagen, which was also stained and then de-stained along with the other samples, until it showed no residual staining. All other scaffolds were then removed from de-staining at this point and the amount and distribution of collagen deposition can be approximated by the blue staining. However, this staining

does not show the depth of penentration of collagen fibres and was only used to determine a starting point for further collagen experimentation. Penetration will be assesed by more advanced methods in subsequent experiments.

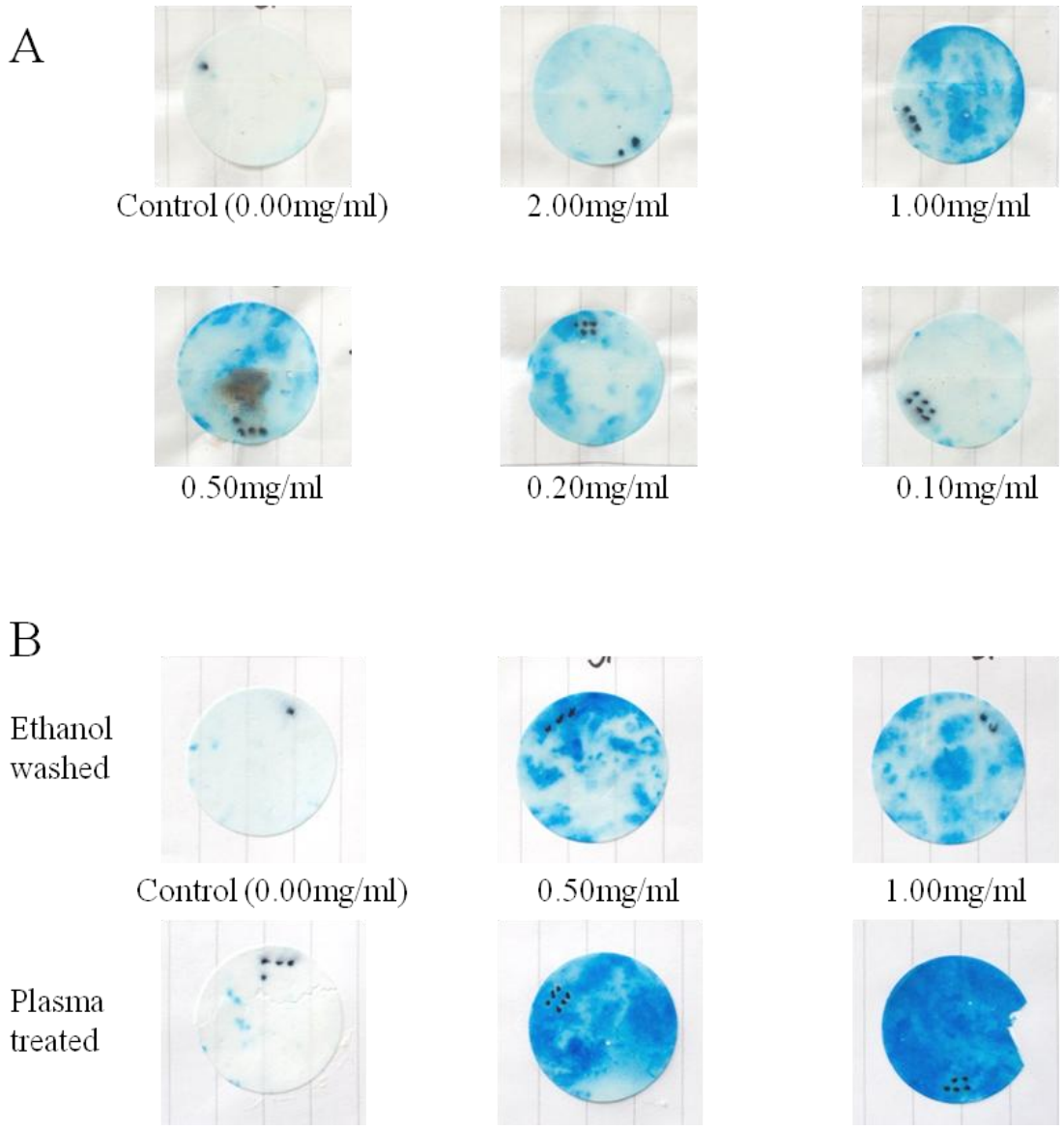


**Figure 3.2. Collagen Coating of Ethanol-Washed and Plasma Treated Scaffolds**

A) Ethanol-washed, 200µm thick, 22mm diameter 3D scaffolds coated with collagen by addition of 200µl neutralised collagen solution diluted to concentrations between 0.00-2.00mg/ml. Scaffolds were then stained with Coomassie Brilliant Blue and de-stained until the control scaffold (0.00mg/ml) was fully de-stained. Blue staining shows the location of collagen deposition on top or inside the scaffold. 1.00mgml and 0.50mg/ml of collagen show the best deposition of collagen. It is likely that 2.00mg/ml is too viscous to properly coat the scaffold, and less than 0.50mg/ml is too dilute; B) Plasma treated scaffolds show better collagen deposition than ethanol washed scaffolds, as indicated by stronger, more evenly distributed staining. 1.00mg/ml provides the optimal collagen deposition.

The staining in Figure 3.2A shows that the most even deposition of collagen is when the solution is diluted to between 0.50mg/ml and 1.00mg/ml. With an undiluted sample of 2.00mg/ml, it is likely that the collagen solution is too viscous to penetrate the 3D structure of the scaffold. Before de-staining, large clumps of blue staining were observed on the surface of the scaffold, which then washed off during de-staining. With 0.50mg/ml or 1.00mg/ml collagen concentrations, the collagen is optimally diluted and reasonably well distributed throughout the scaffold. At 0.20mg/ml and 0.10mg/ml concentrations the solution is likely to be too dilute to deposit sufficient fibres within the scaffold. The negative control only shows slight background staining.

One observed problem was that even with the optimal collagen concentrations of 1.00mg/ml and 0.50mg/ml, the collagen was unevenly distributed within the scaffold. One potential reason for this maybe that the scaffold is already wet due to the pre-wetting with ethanol and PBS before use. Therefore, when a solution of neutralised collagen solution is added, it needs to displace the PBS which is already in the scaffold. Due to the random distribution of pores and voids within the 3D scaffold, the distribution of collagen may become uneven because the collagen solution is viscous and begins to solidify quickly before it can displace the PBS. It may also be that liquids already present inside the scaffold are further diluting the collagen solution, or altering the pH and interrupting gelation.

To overcome these problems, the collagen coatings were repeated with concentrations of 0.50mg/ml and 1.00mg/ml using 3D scaffolds which had been plasma-treated as described in Chapter Two. Therefore, collagen solution was applied to dry plasma-treated scaffolds and these were compared with scaffolds prepared by the pre-wetting and washing method. A negative control for each group was carried out as above. Results are shown in Figure 3.2B. The results clearly shows a more even distribution of collagen in the plasma treated scaffolds compared to ethanol washed scaffolds. Ethanol washed scaffolds show a distribution of collagen similar to the previous experiment, as expected. However, at 0.50mg/ml the staining of the plasma treated scaffold is more even than the ethanol pre-wetted scaffold, although still uneven. At 1.00mg/ml the staining is evenly distributed and noticeably more strongly stained than the other samples. This indicates that the plasma treatment is a better method for the preparation of the scaffold, allowing

solution to be added to a dry scaffold where capillary action will draw it inside. This also confirms that 1.00mg/ml collagen is optimal for distribution of collagen inside the scaffold.

It is likely that the penetration of collagen can act as a proxy for the penetration of cells into the 3D scaffold. When seeding cells into the scaffold, liquid inside the scaffold will reduce the penetration and distribution of cells, whereas with plasma treatment, cells suspended in culture media can more easily penetrate the dry plasma-treated scaffold.

#### 3.2.2.1 Organisation of Collagen Coatings

Staining with Coomassie Brilliant Blue shows the gross coverage of collagen fibres and approximate amount of deposition, but it cannot be used to determine the structure of collagen or the depth of penetration inside the scaffold. Therefore, plasma treated scaffolds coated with 1.0mg/ml of collagen solution were fixed and prepared for SEM analysis. In the results, shown in Figure 3.3A, collagen fibres are clearly visible within the 3D scaffold with a relatively even distribution. They appear to be deposited along surfaces of the scaffold although some webs of collagen (panel B) are deposited inside the scaffold in a way which may restrict cells from entering the voids.

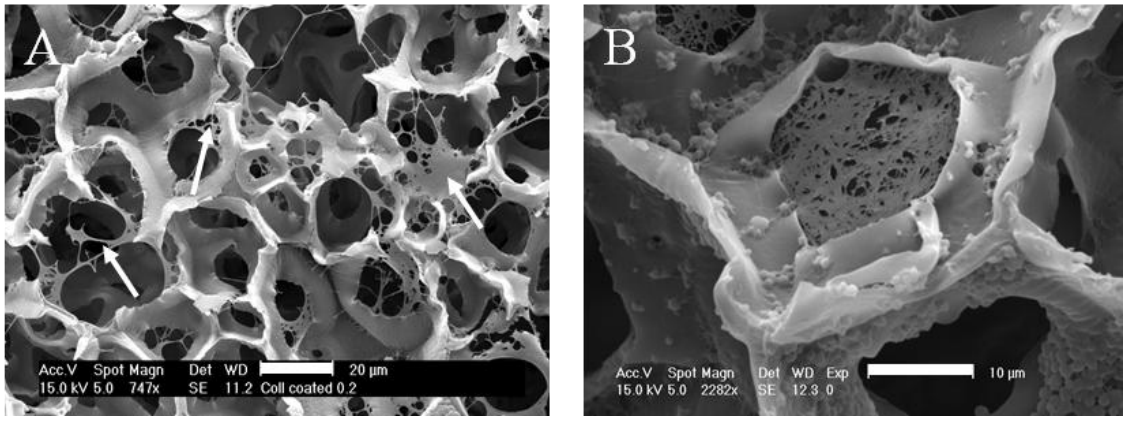


**Figure 3.3. Organisation of Collagen Coated Scaffolds**

1.0mg/ml collagen neutralised with NaOH and added to plasma treated scaffold for 30 minutes at 37°C. A) Image showing collagen fibres (indicated with white arrows) coating surfaces of the scaffold. Scale bar 20µm; B) Image showing collagen fibres blocking void within scaffold. Scale bar 10µm.

### 3.2.2.2 Integration of Collagen Gels with 3D Scaffold

In order to create a solid gel and use the scaffold as a base similar to a porous membrane, a number of different gel formulas from published literature were utilised. One standard formula used is a 7:1:1:1 ratio of collagen:1M NaOH:MEM:3T3 cells (6x $10^5$ fibroblasts/ml gel, determined to be the optimal number for organotypic HaCaT growth by Maas-Szabowski et al, 2003). 300µl of this solution was added to a plasma treated scaffold, allowed to contract initially for 30 minutes at 37°C, then gently submerged in culture media and cultured for 7d at 37°C to allow contraction of the gel. Samples were then fixed and visualised by SEM. A representative image of the structure of this gel is shown in Figure 3.4B.

The low magnification SEM image (Figure 3.4D) shows that the collagen has formed a sheet on top of the scaffold but has not penetrated inside the scaffold. One problem observed with the collagen gel formation was that much of the solution simply passed through the 3D scaffold when it was initially added. Permeable culture membranes such as MilliCell utilise pore sizes of 0.4µm, 1.0µm, 3.0µm or 8.0µm (MilliPore website). These pores sizes are too small for cells to fall through the membrane, and will slow down the penetration of viscous liquids, allowing the collagen solution time to gel before it can pass through the membrane. However, the 3D scaffold is highly porous, designed to contain pores and voids of up to 80µm, which are large enough to accommodate multiple cells. This means that the majority of the collagen solution may be passing through the scaffold when it is initially added. When the scaffold is then submerged in culture media, the collagen solution may be diluted or simply washed out of the scaffold.

Other methods to integrate collagen gels with the 3D scaffold were utilised and representative images shown in Figure 3.4. A collagen solution was diluted in 70% ethanol, pipetted onto the scaffold and allowed to evaporate in a tissue culture cabinet (Figure 3.4A). This method is similar to the standard methods for coating of 2D plasticware. Ethanol is also able to penetrate the scaffold without pre-wetting. However, SEM analysis showed very little deposition of collagen inside the scaffold.

1M NaOH solution was added to the scaffold, evaporated, then collagen solution was added in acetic acid and the scaffold placed into an incubator at 37°C. This was designed to delay gel formation until the collagen solution fully entered the scaffold, where it will combine with NaOH, neutralise and being to form a gel inside the

scaffold. The SEM analysis in Figure 3.4C shows that most collagen gel formation is on the lower surface of the scaffold. It is likely that the solution still did not gel immediately and began to fall to the bottom of the scaffold. Through surface tension, the solution clings to the bottom of the scaffold where it begins to gel.

In a fourth method, the collagen solution was applied to the scaffold without being neutralised by NaOH. The whole scaffold coated with collagen solution was incubated in a chamber containing ammonium vapours. Neutralising the collagen solution a with a gas rather than a liquid was theorised to allow the collagen to gel inside the scaffold by removing problems associated with poor mixing of the gel or the gel solidifying before penetrating the scaffold fully. However, the SEM analysis shown in Figure 3.4B, the gel formed on the upper and lower surfaces of the scaffold, and higher magnification showed no collagen present inside the 3D scaffold. This surface should still be able to support keratinocyte culture, with the polystyrene scaffold structurally supporting the collagen gel and acting as a wick to take up culture media.

#### 3.2.2.3 Stable Gels Containing Chondroitin-6-Sulphate

The collagen formula was modified to include 20% chondroitin-6-sulphate (C6S). After optimising the ratio of collagen and C6S, a solution of 10:1:1 collagen solution in 0.6% acetic acid:1M NaOH: DMEM with 20% C6S was determined to provide the quickest gelation time. This solution was prepared on ice using cooled tissue culture equipment to slow down gelation, then 500µl was added to the scaffold and allowed to solidify for 30 minutes at 37°C. This solution formed a much thicker and more solid gel. This was then fixed and prepared for SEM analysis.

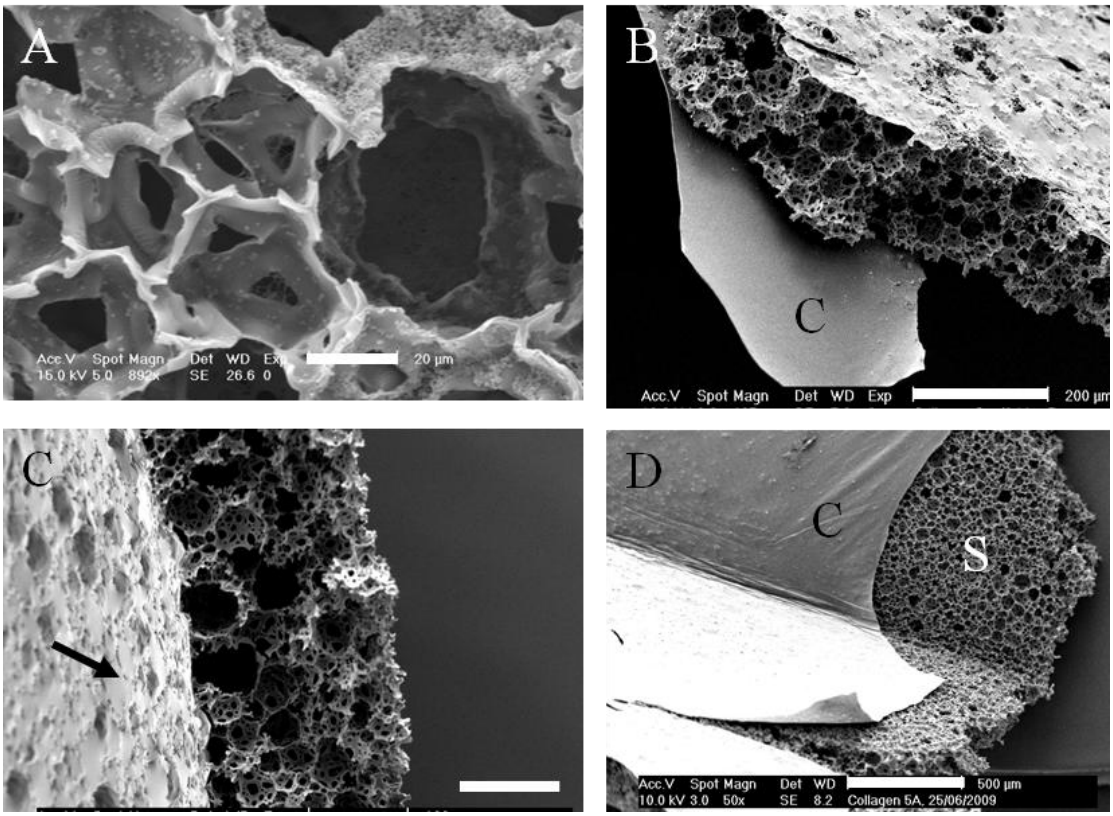


**Figure 3.4. Morphology of Collagen Gels On the 3D Scaffold**

Low magnification SEM micrgraph showing (A) collagen solution added in 70% then evaporated. Very little collagen is observed inside the pores and voids of the scaffold. Scale bar 20µm; (B) Collagen solution was neutralised in an ammonium chamber and has formed a sheet on the upper and lower surfaces of the scaffold, but not penetrated inside. Scale bar 200µm; (C) NaOH added to the scaffold, then evaporated and collagen added. Most collagen is visible on the upper surface, indicated with a black arrow. Collagen has not penetrated inside the scaffold. Scale bar 100µm; D) Low magnification SEM showing a sheet of collagen (C) on the surface of the 3D scaffold (S). This sheet was present across the entire surface of the scaffold and appears smooth and uniform, which should be capable of supporting cultured keratinocytes. Scale bar 500µm.

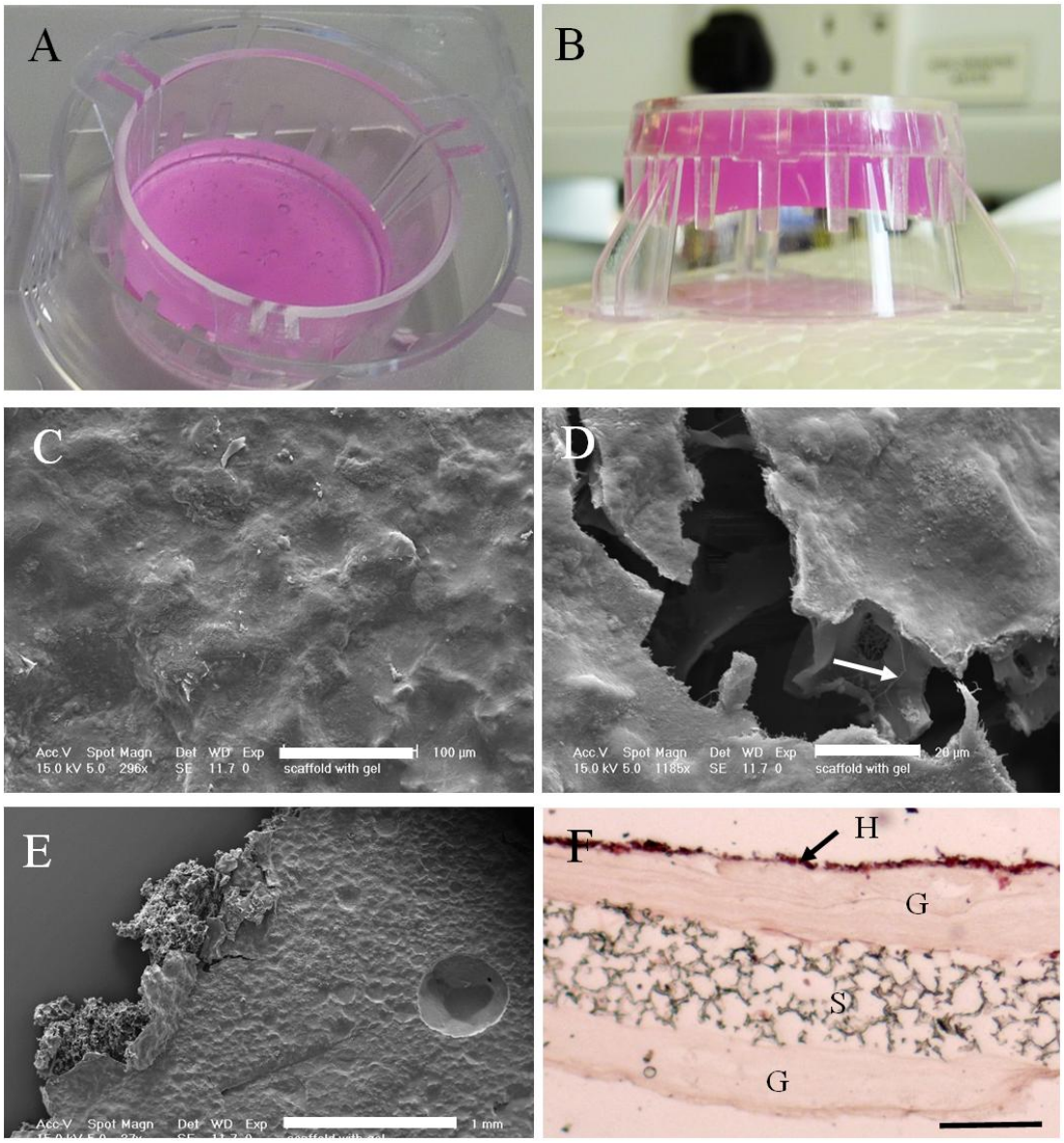


**Figure 3.5. Formulation of Chondroitin-6-Sulphate Collagen Gel on 3D Scaffold**

A) 4mm thick collagen and chondroitin-6-sulphate gel on top of 22mm diameter 3D scaffold inside well-insert; B) The scaffold and well-insert is inverted, showing the high stability of the gel; C) SEM image of collagen and chondroitin-6-sulphate gel on top of a scaffold. The solid gel completely covers the surface of the scaffold and should provide a surface for keratinocytes to adhere and proliferate. Scale bar 100µm; D) SEM image showing gel on the surface of the 3D scaffold and sparse collagen fibres (indicated by white arrow) inside the porous scaffold structure. Scale bar 20µm; E) Low magnification image showing coverage of collagen gel. Scale bar 1mm; F) Collagen and chondroitin-6-sulphate gel (G) on 3D scaffold (S), with $10^6$ HaCaT cells (H) grown at the air-liquid interface for 14 days. The cells are clearly shrunken and disorganised, with no signs of stratification. Scale bar 200µm.

Collagen-C6S gels formed on top of the scaffold inside the well insert were stable and approximately 4mm thick (Figure 3.5A and B). The surface of the gels was relatively rigid but semi-permeable, tested by the addition of a drop of culture media which slowly soaked into the gel (data not shown). The stability of the gels is demonstrated by inverting the 3D scaffold in panel B and the surface of the gel appears solid and covers the whole 3D scaffold Figure 3.5C-E). In some preparations (Figure 3.5D) the collagen gel appears to be in a thin, shrunken layer on the surface of the scaffold. This shrinkage is likely due to the fixation, ethanol dehydration and critical point drying involved in preparation for SEM which removes the water content of the gel. Overall, however, this surface appears to be stable and distributed well enough to maintain a culture of keratinocytes.

To test the ability of the scaffold-supported collagen gels to function as a dermal equivalent, $1x10^6$ HaCaT cells were seeded in a spot of 100µl culture media into the centre of the top surface of collagen/C6S gel prepared under sterile tissue culture conditions by the method above. The keratinocytes were allowed to settle for 30 minutes in the culture incubator at 37°C, before culture media was gently added. The culture was then submerged for 2 days and raised to the air-liquid interface for 14 days, then fixed and prepared for H&E staining, shown in Figure 3.5F. Cell growth on top of the gel is very poor, with only a small amount of shrunken cells remaining. It is not clear whether these cells are viable or not and there is no evidence of any stratification of the cells. The thick collagen gel is visible on both the upper and lower surfaces of the 3D scaffold, approximately 200µm either side. This means that the cells are approximately 0.6mm away from the culture media when at the air-liquid interface. Although the collagen gel appeared semi-permeable to initial testing, it is possible that the gel is too thick and impermeable for the cells to be sufficiently supplied by the culture media when at the air-liquid interface. As shown in Figure 3.5 by SEM, there is no evidence of collagen inside the scaffold itself.

Therefore a thinner collagen coating was then made by diluting the solution 2:1 in DMEM and applying 150µl of solution to the scaffold, rather than 500µl. This gel formed more slowly than the previous model but still appeared stable. SEM revealed that there was a thin film of collagen deposited on the surface of the scaffold which was considerably thinner than those shown in Figure 3.5. However, these cultures also showed showed sporadic cell growth on top of the scaffold.

### 3.2.3 Generation of Keratinocyte-Only Epidermal Model

As a result of the previous experiments, no further work with collagen gels with the 3D scaffold was carried out. Simultaneous experiments utilising keratinocytes with the 3D scaffold alone were promising - showing that keratinocytes could be cultured directly inside the 3D scaffold. This is a more rapid method than contraction of a collagen gel before keratinocyte seeding. Therefore, the remainder of this project focused on creating a 3D culture model using the 3D scaffold and keratinocytes only.

#### 3.2.3.1 3D Cell Culture of HaCaT Keratinocytes

In order to culture HaCaT cells in the 3D scaffold, the cells need to be in a high enough density to proliferate and form an inter-linked layer of cells. In the paper where HaCaT cells were first described (Boukamp et al, 1988), confluence was described as a key factor in the proliferation and differentiation of HaCaT cells. For the purposes of these experiment in the 3D scaffold, it is preferential for the cells to be added in a uniform manner, in order to improve the reproducibility of the cultures.

The scaffold is a 22mm diameter circular disc, occupying the same two-dimensional surface area as a 12-well plate, ($3.8cm^2$). The scaffold is 200μm thick, which roughly corresponds to 15-20 cell layers. The 3D scaffold is also around 90% porous (i.e. 10% of the total dimensions of the scaffold is made from solid material). At a seeding density of 20,000 cells per $cm^2$, this equates to a capacity of roughly $1.3x\ 10^6$ cells per scaffold. Therefore, a range of seeding densities were chosen either side of this number.

One recognised difficulty with a rigid, non-biodegradable 3D scaffold is achieving even cell distribution (Wendt et al, 2009). Cells were seeded at varying densities using the traditional "diffuse" method and alternatively a "concentrated" method, as described in Chapter Two. The "diffuse" method seeds cells into a large volume of culture media allows cells to settle onto the scaffold and fall inside by gravity in the same way that cells are subcultured in 2D, whereas the "concentrated" seeding method adds cells in a highly concentrated spot of 100μl culture media. This allows cells to be rapidly drawn inside the 3D scaffold by capillary action. In order to determine the optimal seeding density for HaCaT cells in the 3D scaffold, the following conditions were set up in triplicate.

**Table 3.2. Seeding Densities of HaCaT cells for 3D Cell Culture**

| Diffuse method | Concentrated Method |
|---|---|
| 0.25x $10^6$ cells | 0.25x $10^6$ cells |
| 0.5x $10^6$ cells | 0.5x $10^6$ cells |
| 1x $10^6$ cells | 1x $10^6$ cells |
| 2x $10^6$ cells | 2x $10^6$ cells |
| 4x $10^6$ cells | 4x $10^6$ cells |

*NB: Pre-1G scaffolds were used for this experiment. The air-liquid interface was reached using wire grids.*

Cells were grown in the scaffold under standard culture conditions for 2 days submerged. Media was then removed and the cultures lifted to the air-liquid interface on 6-well-sized wire grids. Approximately 2ml media was added to the well, underneath the wire grids until the air-liquid interface was achieved. Media was replaced every two days. After each time point, cultures were removed from the grid and placed into a 12 well plate and the MTS assay was performed. Each culture was grown in triplicate, and the experiment was repeated three times. Duplicate cultures were also fixed and processed for H&E staining. MTS analysis results are shown in Figure 3.6A.

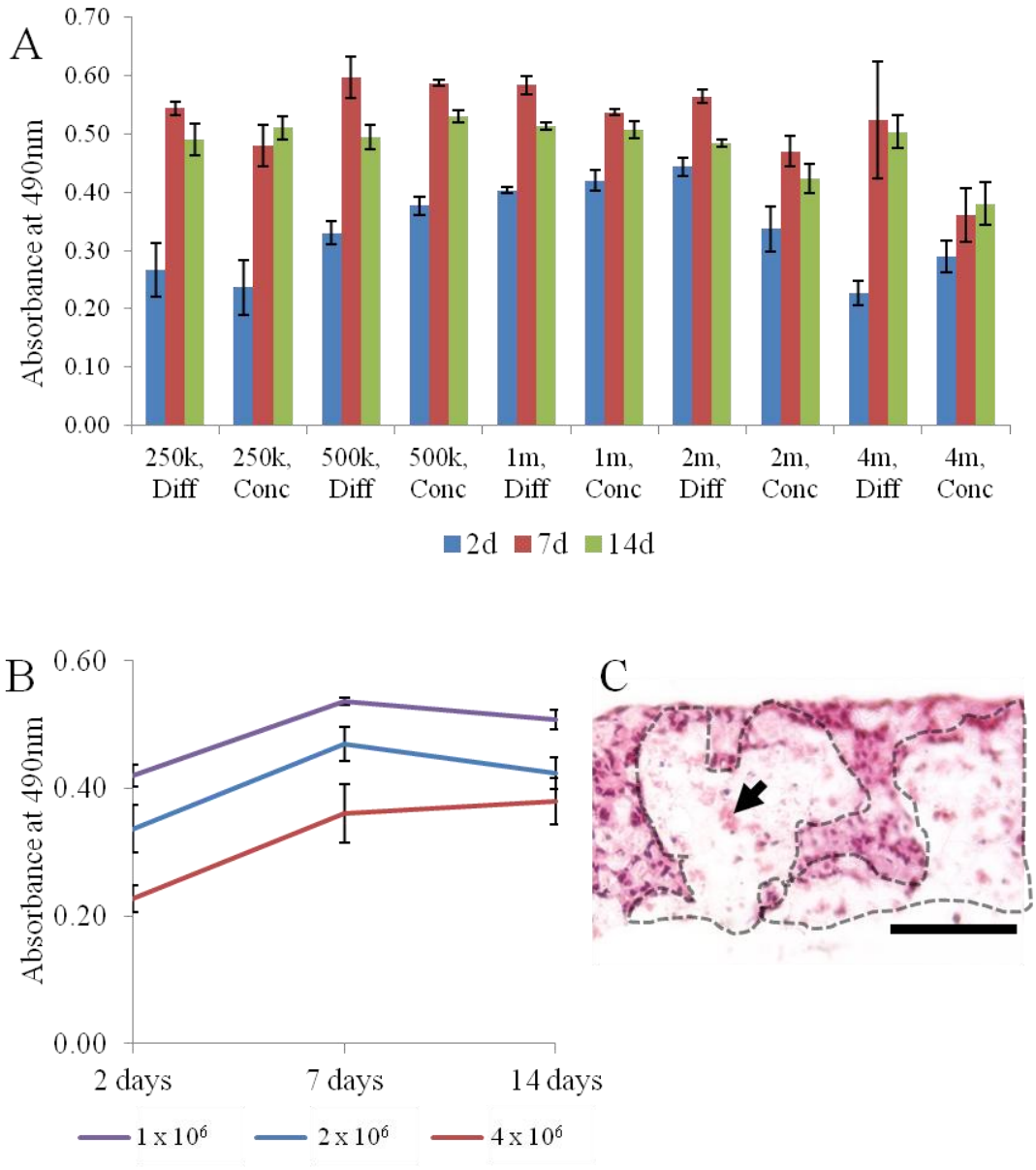


**Figure 3.6. MTS Assays of Different Seeding Densities for 3D Culture**

A) MTS cell viability of different 3D culture seeding methods of HaCaT cells. MTS assays were performed on 3D cultures after 2, 7 and 14 days. Concentrated and diffuse seeding methologies have similar viability and all cultures have higher viability after 7 days than after 2 days. $4x10^6$ keratinocytes have lower viability than other cultures; B) MTS cell viability over time of $1x10^6$, $2x10^6$ and $4x10^6$ HaCaT cells in the 3D scaffold seeded by the concentrated method; C) $4x10^6$ spot-seeded HaCaT cells seeded in 3D scaffold and grown for 7 days at the air-liquid interface. Large white areas of suspected cell necrosis are visible, encompassed by dotted black lines. An area of unknown pink cytoplasmic eosin staining are indicated with black arrow. These are possible cell remnants. Scale bar 100µm. Error bars show SEM.

The MTS assay results in Figure 3.6A show that after two days, $10^6$ or $2x10^6$ cells show the most cell viability in 3D cultures. Predictably, lower initial seeding densities showed lower MTS assay activity than higher densities. Interestingly, $2x10^6$ cells per scaffold seeded by the concentrated method showed a reduction in viability of the population of cells in the culture compared to the same number seeded by the diluted method. This may be because some areas within the scaffold become so densely populated that cells are unable to attach and proliferate normally. Alternatively, too many cells may have depleted the culture media prematurely. In 2D, it has been shown that HaCaT cells which become too confluent undergo changes in cell morphology as if beginning early stages of differentiation (Gniadecki et al, 2001). This is also likely to be the case in a 3D environment, if not more pronounced due to improve cell-cell contact and communication.

Cell growth within the 3D scaffold also requires sufficient penetration of culture media, diffusion of oxygen and clearance of waste products of metabolism. If cells are densely packed, the ability of cells to receive nutrition and clear waste products may be restricted, leading to a reduction in cell viability measured by MTS assay.

After 7 days, proliferation has increased in all treatment groups, with most treatment groups showing roughly equal proliferation. The highest density seeding method again showed the lowest activity, and the $4x10^6$ diffuse seeding method showed much larger variability than other groups. This is predictable, as the distribution of a large number of cells through the scaffold is likely to be more variable.

After 14 days, all culture groups show similar or less viability than at 7 days. This may be because cells have reached a high degree of confluence inside the scaffold and therefore slow down their rate of proliferation. This is similar to their behaviour in 2D cell culture. Alternatively, cells may be differentiating, and are therefore flattening, losing their nuclei and not able to metabolise the MTS reagent, resulting in a reduction of the measured viability. Alternatively, cells may have reached a density which becomes a limiting factor in terms of oxygen, nutrient and waste product diffusion, therefore limiting proliferation and reaching an equilibrium. It is expected that a culture of highly differentiated cells will result in a lower proliferation assay result.

The results show that for shorter periods of growth in the 3D scaffold, the number of cells initially seeded into the scaffold is a key factor. However, after longer culture periods at the air-liquid interface, this becomes less important. For instance, $0.25x10^6$ cells showed the lowest proliferation after 2 days, but increased rapidly after 7 days of culture. This suggests that the limitation of cell proliferation rate is the culture system itself, rather than the number of cells seeded into the system. This may be because of the availability of culture media, diffusion of oxygen, or that the maximum density of cells in the scaffold has been reached.

A simplified line graph of three seeding densities (0.5, 1.0 and 2.0 x $10^6$ cells) is presented in Figure 3.6B, showing that $1.0x10^6$ cells consistently show the most proliferative cultures with the least variation.

An image of $4x10^6$ HaCaT cells after 7 days in the 3D scaffold is shown in Figure 3.6C. This sample shows large white areas throughout the whole thickness of the scaffold, with shrunken nuclei and blotchy pink staining, possibly from cell remnants. This corresponds to reduced MTS assay activity seen in Figure 3.6A. It is likely that diffusion of nutrients, oxygen and waste products is limited by high cell numbers, causing some cells to become necrotic.

### 3.2.3.2 Optimisation of the 3D Scaffold Culture System

As the scaffold is relatively thick and is constructed from a rigid, non-porous, non-biodegradable polystyrene, there are several factors to bear in mind such as the availability of glucose, clearance of waste products, and the adequate diffusion of oxygen into the culture. Growing 3D cultured keratinocytes on a wire grid in a 6 well plate allows for approximately 2.0ml of culture media underneath the scaffold when at the air-liquid interface. Given that there are $1x10^6$ cells initially seeded in the scaffold, and subsequent cell divisions will increase this number, 2ml of culture media is likely to be inadequate for optimal proliferation and differentiation of the keratinocytes.

In response to this, custom well inserts (shown in Figure 2.3A) were developed. These allow for a greater amount of culture media per scaffold and provides a more reproducible system (i.e. a horizontal, fixed height for every culture) for maintaining the air-liquid interface. They also allows for three 3D cultures to be maintained in the same deep Petri dish, in the same culture media which will improve the reproducibility of cultures by reducing experimental error. In the well insert system, three 3D scaffolds can be held in one holder and cultured in 45ml culture medium i.e. around 15ml per scaffold, as shown in Figure 2.4. This is 7.5 times more culture media per scaffold than the wire grid system allow, which should lead to improved cell growth and morphology.

Therefore, the wire grid system was compared to the newly developed well insert system. $1.0x10^6$ HaCaT cells per 200µm thick, 22mm diameter 3D scaffold have been previously determined as the optimal seeding number. Therefore, $1x10^6$ cells were seeded in 100µl culture media per scaffold, grown submerged for 2 days and then lifted to the air-liquid interface for 14 days by either the wire grid or well insert method. Cultures were fixed and stained for H&E after 2, 7 and 14 days. Representative sample images for the wire grid system are shown in Figure 3.7 and for the well inserts in Figure 3.8.

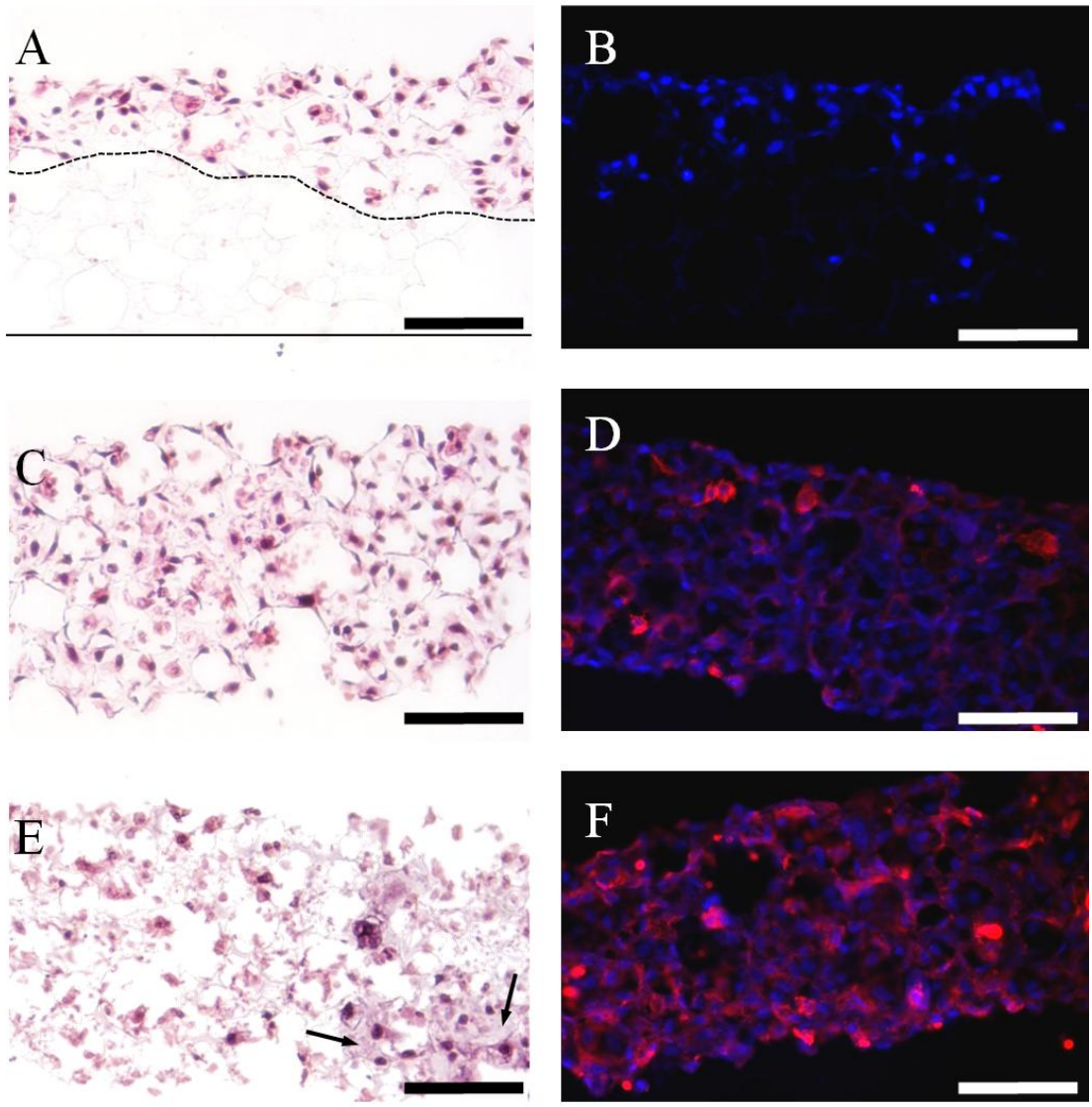


**Figure 3.7. 3D Scaffold Cultures Grown on Wire Grids**

A, C, E) $10^6$ spot-seeded HaCaT cells after 2 days submerged, 7 days at the air-liquid interface and 14 days at the air-liquid interface respectively. Cell penetration in the submerged sample (A) is marked by a dotted line and the bottom of the scaffold is approximated with a solid line. HaCaT cells have penetrated an average of 45% (90µm) into the 3D scaffold after 2 days. Areas of cellular staining with no nuclei are indicated with arrows. After 14 days at the air-liquid interface (E), there are less nucleated cells visible. It is unclear whether these cells are differentiated and have lost their nuclei, or have undergone necrosis; B, D, F) Keratin 1 staining of $10^6$ HaCaT cells grown for 2 days submerged, 7 and 14 days air-liquid interface on wire grids. Arrows show areas of pink staining without visible nuclei. All scale bars 100µm.

As seen in the H&E staining in Figure 3.7A, after two days the HaCaT cells are located mostly in the upper regions of the scaffold and have not fully penetrated the full 200µm depth of the scaffold. This depth is marked with a dotted line and was measured as an average of 45% (90µm) penetration by assessing various points along the length of the section. Noticeably, all cultures show cells with a shrunken appearance, with little cytoplasm surrounding the nuclei. After 7 days (Figure 3.7C), cells are now present through the whole depth of the scaffold, which corresponds to the increase in MTS cell counts (Figure 3.6). This shows that HaCaT cells are capable of proliferating to fill the three-dimensional area provided to them although it is not clear from these results alone whether cells have migrated throughout the scaffold, or have proliferated to fill the available space. Again, cells still show a slightly shrunken morphology with less cytoplasm surrounding the nucleus than would be expected. After 14 days (Figure 3.7E), there is little visible increase in the cellular bulk inside the scaffold, although there are larger areas of pink staining with no visible nuclei (indicated by black arrows). It is unclear from this staining alone whether this is cell necrosis or an area of differentiated cells which have flattened and lost their nuclei.

The shrunken appearance of the cells may be explained by the low amount of culture media available to the cells. The culture media was changed frequently (every 48 hours), but only 2ml of culture media was present at any one time, which may be limiting cell viability in the 3D environment. It is already known that cells grown in a 3D environment have higher metabolic requirements than those grown in 2D (Bokhari et al, 2008). Although 3D scaffolds were only in contact with the culture media from the underneath, no clearly visible differences between cells located at either the top or bottom of the scaffold in terms of morphology.

Sections were also stained for the early proliferation marker keratin 1 (K1). This can give insight into the MTS data and show whether a drop in the cellular metabolism (measured by conversion of MTS substrate) of the culture is due to cell differentiation or from cell death related to poor media quality or necrosis.

The K1 staining results show that after two days (Figure 3.7B), there are no cells staining positive for K1. This is expected, as the cells are still submerged and proliferative. This corresponds with earlier 2D data, showing that HaCaT cells do not express basal K1 staining. At 7 days (Figure 3.7D), there is some positive K1

staining, indicating that some cells are undergoing differentiation in the 3D environment. At 14 days (Figure 3.7F), K1 staining is clearly visible around the nuclei of many cells, and there is clearly more staining than after 7 days, indicating that more time at the air-liquid interface increases cell differentiation. However, there appears to be little organisation in K1 staining. In the stratified epidermis, K1 staining is found in the suprabasal layers (Wallace et al, 2011), but in the 3D scaffold, K1 staining appears to have no clear pattern of expression. It is clear from these results that 3D cell culture has been achieved in all samples, but there is room for improvement of cell morphology and the organisation of differentiation.

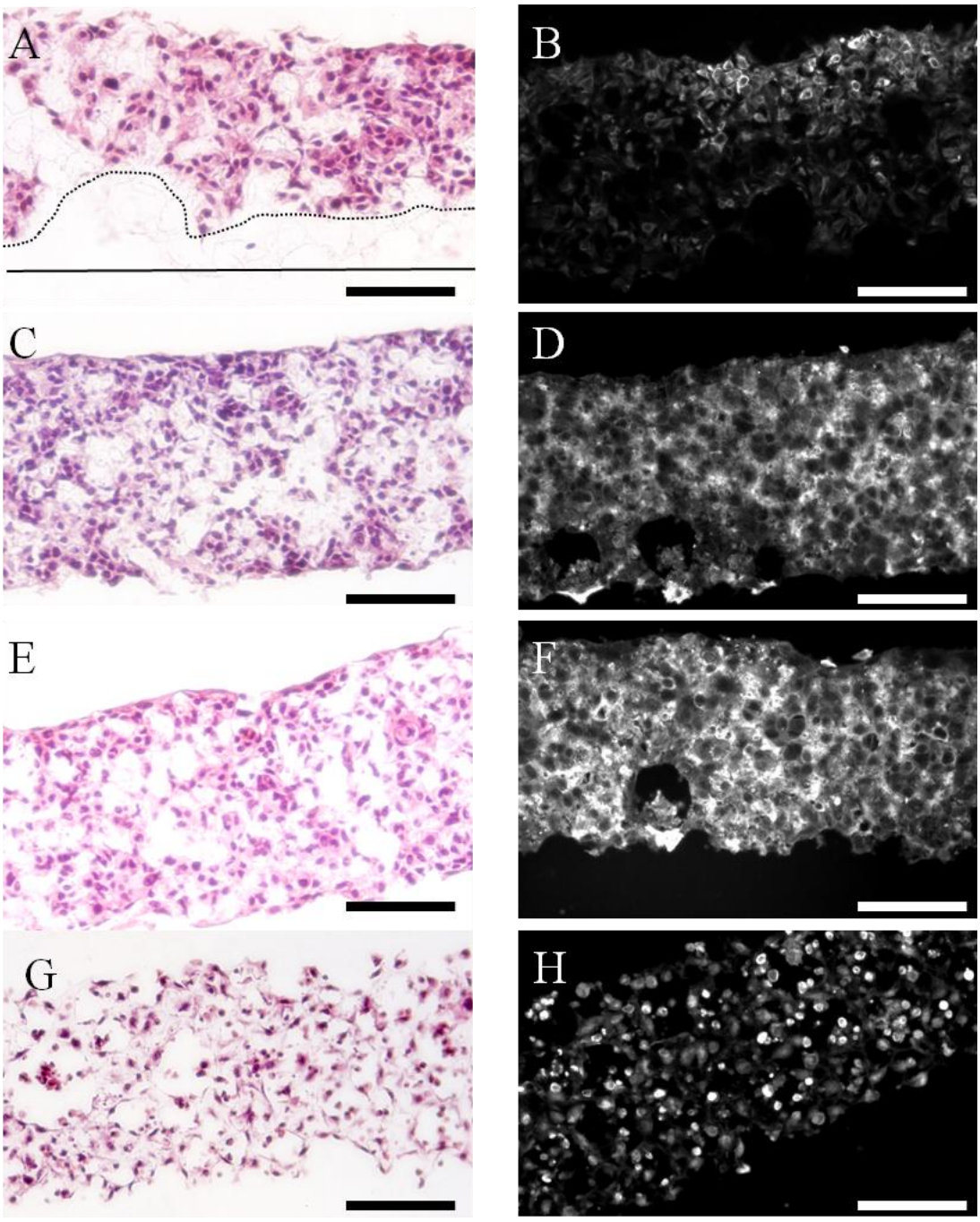


**Figure 3.8. 3D Scaffold Cultures Grown in Custom Well-Inserts**

A, C, E) $10^6$ spot-seeded HaCaT cells after 2 days submerged, 7 days and 14 days at the air-liquid interface respectively. Cell penetration is marked by a dotted line and the bottom of the scaffold is indicated with a solid line. HaCaT cells have penetrated an average of 71% (142µm) into the depth of the 3D scaffold after 2 days; B, D, F) K1 stained sections from 2d submerged, 7 and 14d at air-liquid interface respectively; G, H) H&E and K1-stained cultures of $10^6$ HaCaT cells submerged for 14d. K1 staining shows clearly less positive staining than 14d at the air-liquid interface. All scale bars 100µm.

Compared to wire grid cultures (Figure 3.7), there is a noticeable change in cell morphology after all time points. After 2 days submerged (Figure 3.8A), cells still do not penetrate the entire depth of the scaffold, but they do show more penetration into the scaffold than the wire grid system (marked with a dotted line, and the bottom of the scaffold with a solid line). Cells have penetrated an average of 71% (142µm) into the scaffold using the well insert system compared to 45% (90µm) with the wire grid system. The cells pictured in H&E staining appear larger, with more visible stained cytoplasm than those grown in the wire grid culture system. Methodology for histological preparation was the same as previous samples and so it is likely that shrunken cells were caused by poor nutrition by the culture media rather than any artefact induced by dehydrating the cells too rapidly. K1 staining after 2 days submerged (Figure 3.8B) shows sporadic K1 positive cells, located mostly in the upper layers of the culture.

After 7 days at the air-liquid interface (Figure 3.8C), H&E staining shows that the cells have filled the entire depth of the scaffold. The cells in the scaffold appear all to have similar morphology and there is a limited number of flattened cell layers on the surface of the scaffold. K1 staining (Figure 3.8D) reveals many differentiating cells.

After 14 days at the air-liquid interface (Figure 3.8E), H&E staining shows that the cells are still occupying the entire scaffold and appear very similar to the 7d cultures. There are some flattened cells on the top of the scaffold, but no visible stratum corneum on the surface of the scaffold. However, there is more K1 staining in the 14d air-liquid interface culture (Figure 3.8F) than in the 7d culture, indicating that time spent at the air-liquid interface increases the number of differentiated keratinocytes inside the 3D scaffold.

Control samples were left submerged for the full 14 day time period, with media changes at the same time as cultures at the air-liquid interface. H&E staining (Figure 3.8G) shows that cells have penetrated the full thickness of the scaffold but are slightly shrunken and are not filling voids as readily as in cultures lifted to the air-liquid interface. K1 staining (Figure 3.8H) shows sporadic individual cells located randomly throughout the scaffold. This shows that submerged cultures of HaCaT cells do not generally differentiate, even after 14 days. Previous 2D experiments showed that occasional HaCaT cells express differentiation markers, even when submerged in 2D in low calcium culture media (Figure 3.1).

In overall comparison to the results on wire grids (Figure 3.7), it is clear that cultures grown with the well-inserts and deep cell culture dishes show a better morphology than those grown on wire grids as well as more keratinocyte differentiation.

In all samples, it is clear that 3D cell growth has been achieved. HaCaT cells have proliferated to fill the thickness of the scaffold and areas of the section which cut through multiple adjacent cells show cells in contact with each other and a "tissue-like" appearance. Interestingly, the K1 staining indicates that keratinocyte differentiation has occurred inside the scaffold, but there are no stratified cell layers on the upper air-exposed surface of the scaffold.

For further investigation into the 3D culture of HaCaT cells, samples cultured in the deep well culture dishes at the air-liquid interface for 7d were fixed and prepared for SEM analysis, shown in Figure 3.9. SEM analysis confirms finding from H&E staining that cells can grow through the full thickness of the scaffold, and are capable of growing within voids. Low magnification SEM imaging (Figure 3.9A) shows cells occupying the full thickness of the scaffold in three dimensions. The overall appearance represents a "slab" of 3D cultured cells, with the keratinocytes and 3D scaffold closely integrated. Figure 3.9B shows a higher magnification transverse section of the 3D scaffold, showing that HaCaT cells are present at all depths of the scaffold after 7 days at the air-liquid interface, which corresponds with findings by H&E staining. These SEM images confirm that the cells are growing in a 3D manner and have attachments to the 3D scaffold and to other cells.

For further characterisation of the model, cultures were grown using the optimised conditions and prepared for immunofluorescence staining of differentiation markers.

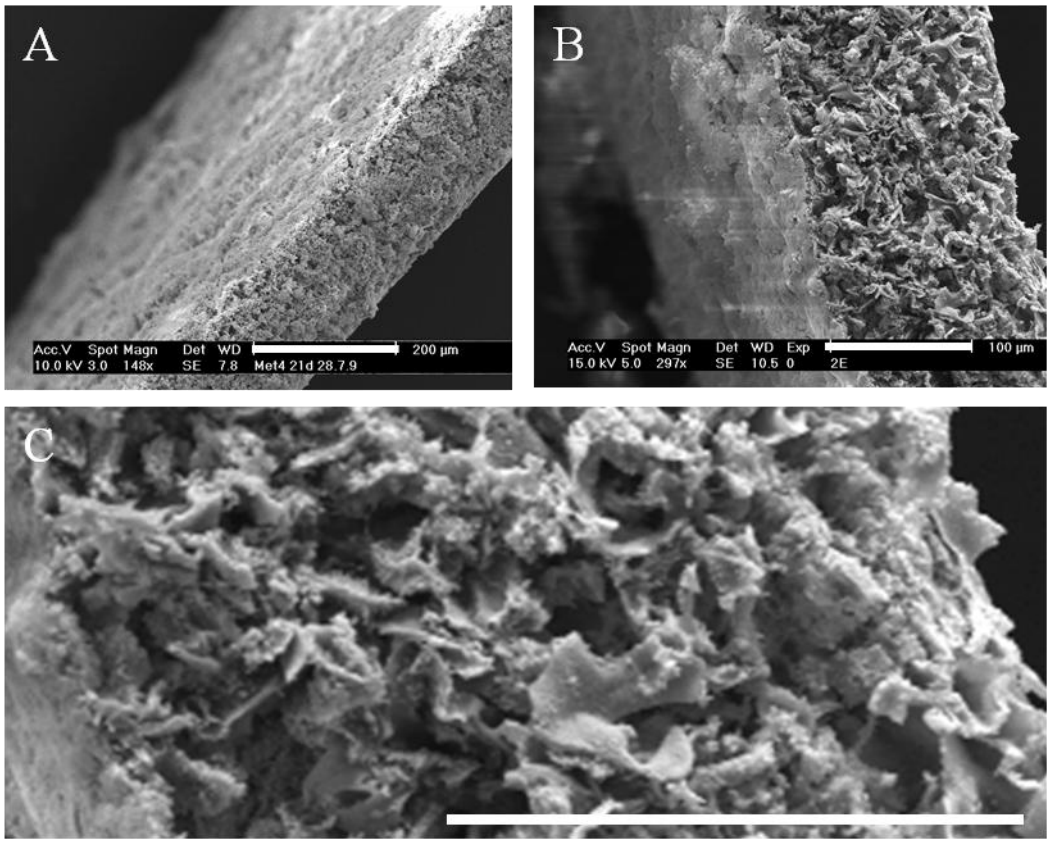


**Figure 3.9. SEM of 3D Cultured HaCaT Cells**

Images from $10^6$ HaCaT cells grown in the 3D scaffold for 7 days showing evidence of 3D cell growth. A) Low magnification transverse section showing cells have penetrated through the full depth of the scaffold and are covering a large area of the scaffold. Scale bar 200µm; B) Intermediate magnification transverse section showing cell that cells have penetrated the full thickness of the scaffold. Scale bar 100µm; C) High magnification image showing cells throughout thickness of scaffold. Scale bar 100µm.

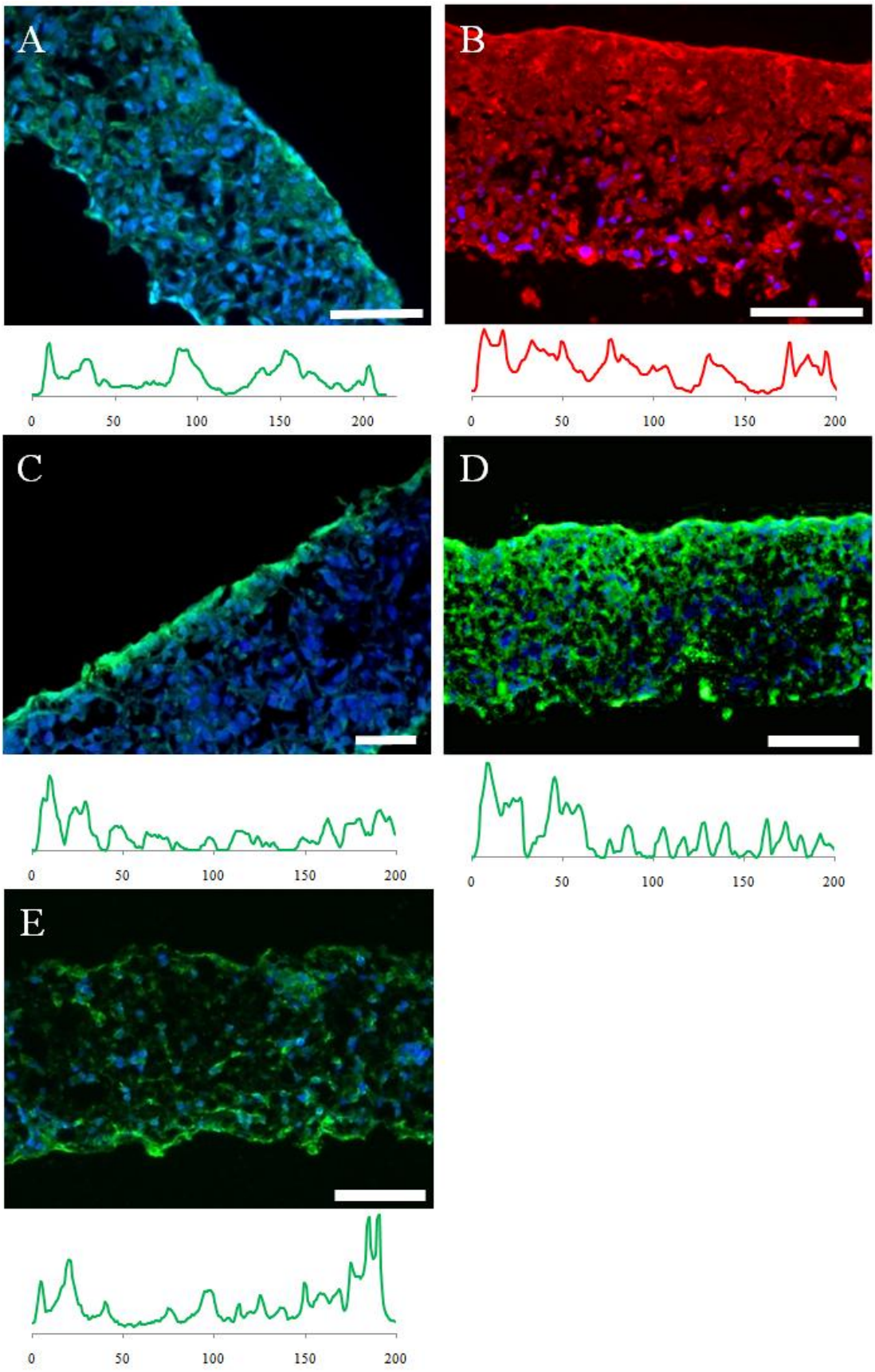


**Figure 3.10. Differentiation Markers of 3D Cultured HaCaT Cells**

Immunofluorescence of $10^6$ spot-seeded HaCaT cells grown in the 3D scaffold for 2d submerged, then 14d at the ALI in deep well culture inserts. Stained for A) E-cadherin; B) involucrin; C) desmoplakin; D) keratin 1 and E) keratin 14. All scale bars 100µm. Graphs underneath each image show relative intensity of staining for each marker, through the 200µm thickness of the 3D scaffold with 0 representing the upper surface and 200 representing the lower surface

Figure 3.10 shows the expression of the differentiation markers E-cadherin, involucrin, desmoplakin and keratin 1 in many cells inside the 3D scaffold, confirming that cell differentiation is occurring at the air-liquid interface. E-cadherin and involucrin staining are distributed throughout the 3D scaffold with no clearly stronger staining areas. Involucrin would normally be concentrated in the suprabasal layers of the epidermis. Desmoplakin staining (Figure 3.10) shows a more concentrated staining on the air-exposed surface although the staining does not look strongly desmosomal. Analysis of the gradient of staining intensity through the thickness of the scaffold shows Keratin 1 is stronger in the upper layers of the 3D scaffold, closer to the air-exposed surface and Keratin 14 staining shows some preference for the submerged lower areas of the 3D scaffold. This approximates the location of Kertain 1 and Keratin 14 in normal human epidermis where Keratin 1 is present in differentiating cells and Keratin 14 present in basal proliferative cells. This staining for differentiation markers shows that differentiation is clearly occurring, however it appears disorganised, with no clear gradients of differentiation markers towards the air-exposed surface of the culture, which would be expected in native epidermis. Nor are there any clearly divisible layers such as the basal or granular layers. The histology results alone do not show how differentiating HaCaT cells are organised within the scaffold or whether there are flattened cells layers on the air-exposed surface of the culture. In the next chapter, SEM will be used to determine the organisation of cells within the scaffold and look for evidence of flattening keratinocytes.

Figure 3.10E shows that the basal Keratin 14 is still found in the cultures, even after 14 days at the air-liquid interface when numerous differentiation markers are observed.

### 3.2.4 Growth of Other Skin Cells in the 3D Scaffold

In order to test the 3D scaffold as a cell culture device, many other cell types were tested in our lab for their ability to proliferate and form tissue-like structures in this material. These cells types included Chinese Hamster Ovary (CHO-K1) cells, embryonal carcinoma (*TERA2*.cl.*SP12*.) cells, liver hepatocyte (HepG2) cells, osteoblasts (MG63) and breast cancer epithelial cells (MCF-7). I carried out some initial testing of other skin cell types in the 3D scaffold - specifically, squamous cell

carcinoma MET cells, primary mouse keratinocytes and 3T3-NIH mouse fibroblasts were cultured in the 3D scaffold using the protocols developed in this chapter.

MET cells are a series of human cell lines derived from a squamous cell carcinoma (SCC) by Proby et al, 2000. The cells were named MET1, 2, 3 and 4 according to their various stages of SCC development from the same adult patient. MET1 cells originate from the primary cutaneous tumour on the hand, MET2 and MET3 from two local re-occurrences, and MET4 were isolated from a metastases on the axillary lymph nodes. MET cells are keratinocyte-like cells, with similar morphology and growth properties to normal human keratinocytes. However, after isolation from the patient they were shown to proliferate more quickly, and did not require feeder layers, even when initially isolated. Further experimentation showed that MET cells are unable to differentiate and that they express an altered keratin profile - for example no suprabasal K1/K10. As they cannot differentiate, they are unable to form an organised, stratified epidermis (Proby et al, 2000).

Of the four MET cell lines, MET1 and MET4 cells represent the most different subtypes, and so they were selected to be cultured in the 3D scaffold. As they are similar to keratinocytes, they were cultured following the same protocols previously developed for HaCaT cells.

Keratinocytes from the back skin of C57 mice were kindly donated by Dr Carrie Ambler, Durham University. These cells were initially supplied with fibroblast feeder layers but were subsequently cultured in defined keratinocyte media, Epilife, supplemented with 10% chelexed FBS, Epilife Defined Growth Supplement (EDGS) and 0.06mM calcium. Initial growth was slow, but after several passages, these cells improved in their proliferation rate while maintaining an unaltered basal keratinocyte morphology. After p>15, these keratinocytes were deemed to be a stable, immortal cell line and named WTK (wild type keratinocyte) cells. These WTK cells were then grown in the 3D scaffold utilising the same protocols as HaCaT cells.

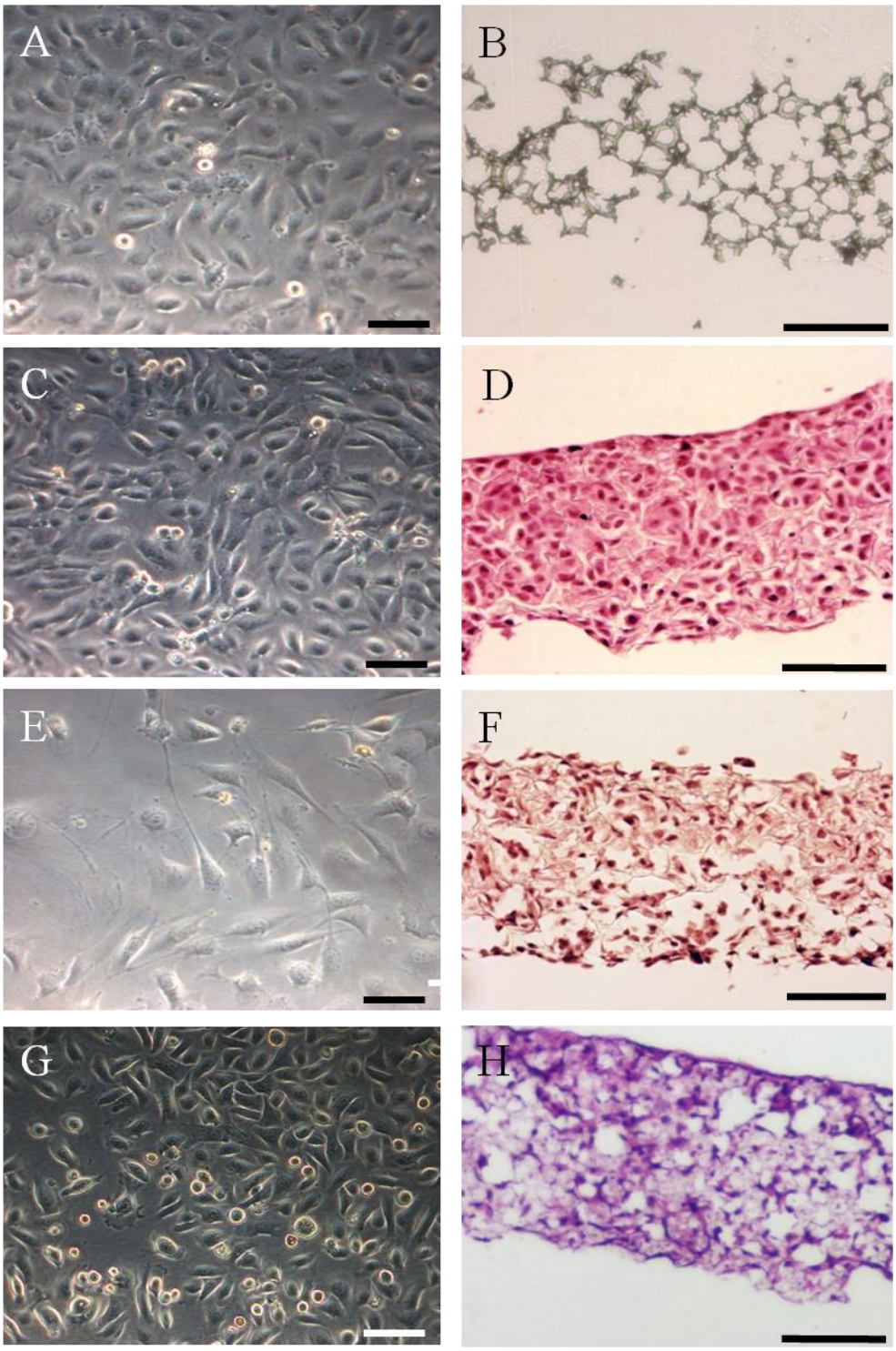


**Figure 3.11. Culture of Other Skin Cell Types in the 3D Scaffold**

2D light microscopy images and H&E stained images 3D cultures of MET1 (A,B); MET4 (C-D); 3T3-NIH (E, F) and Mouse Primary Keratinocytes (G,H) cells grown for 14 days in the 3D scaffold. MET1, MET4 and 3T3-NIH cultures were cultured submerged and mouse keratinocytes were grown at the air-liquid interface. Scale bar 100µm.

As seen in Figure 3.11B, MET1 cells did not adhere to the 3D scaffold at all. The reason for this is unknown, although MET1 cells are noted to maintain very little cell-cell contact in 2D culture. They were also observed to proliferate poorly on glass cover slips (data not shown). A study by Margulin et al, 2006 found that when squamous cell carcinoma keratinocytes deficient in intercellular adhesion proteins (such as E-cadherin) were cultured in 3D, they displayed a more invasive phenotype. This lack of adhesion proteins might explain why MET1 cells showed poor adhesion to many materials, including the 3D scaffold. Interestingly, these findings do not correspond with the MET1 origin as the original tumour which had not yet become invasive.

On the other hand, MET4 cells (Figure 3.11D) have proliferated very well inside the 3D scaffold, and occupy the entire depth and width of the scaffold. When cultured in 2D (panel C), MET4 cells continue to proliferate, even when confluent. When 100% confluence is reached it appears that MET4 cells "push" other cells off the surface of the culture dish and continue to proliferate. As MET4 cells are unable to differentiate they have continued to proliferate and fill the 3D scaffold.

3T3 cells (Figure 3.11F) have shown moderate growth inside the 3D scaffold. They have occupied the full depth of the scaffold but are less "dense" than MET4 cells or HaCaT cells shown previously. 3T3 cells are substantially larger cells than keratinocytes and so the seeding methods utilised may not have been optimal and further optimisations may improve the morphology of the culture. Nevertheless, 3D growth has been achieved and many cells are present within the scaffold.

WTK cells (Figure 3.11H) have proliferated well within the 3D scaffold, similar to HaCaT cells. In experiments similar to Figure 3.1, WTK cells maintained a proliferative phenotype when maintained in low calcium culture media and strongly expressed markers of differentiation when switched to high calcium. As mentioned earlier, HaCaT cells have limited differentiation capacity and continue to proliferate while differentiating, but they are convenient for experimentation due to their robust nature, non-fastidious growth requirements and stable behaviour. WTK cells require defined culture media with growth supplements and proliferate much more slowly. In future chapters, WTK cells will be used in experiments alongside HaCaT cells where relevant and where possible with regard to time and cost.

## 3.3 Discussion

### 3.3.1 Results Summary

This chapter investigated the 3D growth of the HaCaT human keratinocyte cell line with the goal of forming a differentiated 3D epidermal equivalent using a novel cell culture scaffold. This 3D culture aims to have a barrier function suitable for *in vitro* permeability testing of various compounds. It may also be used to investigate the effect of pharmacological agents on the proliferation and differentiation of keratinocytes.

Investigations began by optimising basic culture conditions such as the number of cells to be seeded, the method of seeding and the length of the culture period. These were simple but essential steps in successful tissue engineering with any novel system. MTS assays were used to measure viability of cells in the 3D scaffold. Generally the populations of cells cultured in the 3D scaffold were sufficiently viable, unless cultures became too confluent or the media quality became insufficient. Another possible line of investigation would have been to examine the quality of the culture media by testing glucose utilisation, lactate concentration and pH of the culture media. However, the DMEM culture media utilised is pH buffered and contains phenol red indicator which changes colour if the pH falls below the specified range. Culture media was also changed frequently.

The culture system itself underwent developments. Initially, wire grids were used to lift cultures to the air-liquid interface in 6 well plates. This method did achieve 3D growth of HaCaT cells but Figure 3.7 and Figure 3.8 demonstrate that a well-insert apparatus with deep culture wells providing more culture media to each scaffold is clearly a more effective system. Cells grown in this system maintained a better morphology with no cell shrinkage that was observed using the wire grid system. In terms of preparing the scaffold pre-culture, plasma treatment was preferable to ethanol and PBS pre-washing, although due to equipment constraints, it was not possible to use plasma treated scaffolds for every experiment.

By the end of work presented in this chapter, an optimised system for 3D culture of HaCaT cells has now been developed. The resulting culture shows signs of epidermal differentiation which will be further investigated in the following chapters.

**Table 3.3. Optimal Culture Conditions for 3D Scaffold Cultures**

| Method Tested | Optimal Condition | Comments |
|---|---|---|
| Pre-treatment of scaffold | Plasma treatment | More effective than ethanol pre-washing |
| Cell seeding density | $1x10^6$ cells per 200µm thick, 22mm diameter scaffold | The most consistent viable cell number |
| Cell seeding method | Cells seeded in 100µl culture media to centre of scaffold | Cells allowed to settle for 30 minutes before culture media added |
| Growth period | 2d submerged. 14d at air-liquid interface | Filled the full 200µm scaffold depth and stained positive for differentiation markers |
| Culture method | Tri-well insert in deep Petri dish | Better cell morphology than wire grids |

#### 3.3.1.1 Summary of HaCaT Cell Culture in the 3D Scaffold

The data gathered in this chapter have confirmed previous findings (Boukamp et al, 1988, Micaleff et al, 2008) that HaCaT cells maintain the ability to proliferate in routine 2D culture and can be induced to differentiate when stimulated by high calcium or by culture at the air-liquid interface (Boelsma et al, 1999). The air-liquid interface was essential for differentiation, as found in previous studies (Koria and Andreadis, 2005). A summary of the optimal culture conditions is shown in Table 3.3.

HaCaT cells were seeded into the 3D scaffold using a concentrated method where $10^6$ cells were suspended in 100µl culture media and applied to the centre of the scaffold. This overcame difficulties in achieving an even HaCaT cell distribution in the 3D material by using capillary action to draw the cells inside the material (Wendt et al, 2009). HaCaT cells adhered to the material and were able to proliferate inside the porous structures, as visualised by H&E staining and SEM imaging (Figure 3.8 and Figure 3.9). Modification of the culture conditions with custom-designed well inserts and a larger volume of culture media improved the morphology of the keratinocytes in the scaffold. When cultured submerged, the cells remained

undifferentiated, but at the air-liquid interface, HaCaT cells expressed proteins such as involucrin, desmoplakin and keratin 1, as visualised by immunofluorescence staining.

HaCaT cells cultured in this scaffold showed 3D growth and routine methods such as MTS assay, paraffin embedded histology and immunofluorescence staining were shown to be compatible with the material after some small modifications to standard lab methodologies. For instance Xylene, commonly used as a clearing or de-waxing agent, had an adverse effect on the polystyrene-based scaffold and Histoclear was used instead.

Within the studied time period, it is unclear whether HaCaT cells fully acquired a flattened morphology. While the cells expressed differentiation markers visualised by immunofluorescence staining, there was no visible stratum corneum on the surface of the culture, and no clearly defined epidermal layers which are observed in some epidermal models (Ponec et al, 2000, Pasonen-Seppanen et al, 2001, Mazar et al, 2010). Instead, it appears that HaCaT cells are differentiating inside the porous 3D scaffold structure, even when at the air-liquid interface. One possible reason for this is the fact that cells appear to remain adherent to the 3D scaffold through the culture period.

HaCaT cells in the 3D scaffold also retained some characteristics of proliferating cells such as basal keratin 14 expression and a high cell viability when cultured at the air-liquid interface. This may be partly due to the choice of cell line, as HaCaT cells have been shown to maintain some elements of a proliferative phenotype (including K14 expression) during differentiation (Micallef et al, 2008). Nevertheless, HaCaT cells in the 3D scaffold are clearly differentiating when cultured at the air-liquid interface and the extent of this differentiation will be fully characterised in the following chapter.

It was also possible to culture other cell types within this scaffold such as fibroblasts, MET squamous cell carcinoma cells and mouse keratinocytes (Figure 3.11). Each cell type displayed their own growth characteristics in the 3D scaffold and resulting cultures displayed morphological differences in line with the properties of the cell lines used. Mouse keratinocytes formed a 3D culture similar to HaCaT cells and in 2D observations they appeared to be more similar to normal human keratinocytes

than HaCaTs. Therefore, these mouse keratinocytes were used in some future experiments when time permitted.

### 3.3.2 Integration of Collagen Gel with the 3D Scaffold

Bearing in mind the popularity and acceptance of collagen gel-based models for keratinocyte culture, initial experiments in this chapter focused on utilising the 3D scaffold in a similar way - namely as a support for a fibroblast-contracted collagen gel. Many different methods were utilised to integrate the 3D scaffold with collagen gels, but none of these methods fully achieved that goal. Using a standard collagen gel formula from published methodology (Turksen et al, 2005), the gel would simply run through the pores in the 3D scaffold, as the pore size (~80µm average) is much larger than semi-permeable membrane inserts which are typically used for this purpose.

Increasing the solidity, gelation speed and stability of the gel was investigated as a way to form a contracted collagen gel around the 3D scaffold. The formula was altered to include choindroitin-6-sulphate ($Ch6SO_4$). Chondroitin-6-sulphate is a glycosaminoglycan which acts as a cross-linker of collagen fibres and has been shown (Osborne et al, 1997) to increase the physical and biological stability of collagen gels. Incorporation of 20% C6S into a collagen gel was shown to increase the speed of collagen crosslinking and gelation, as well as increasing the proliferation of keratinocytes on the surface (Osborne et al, 1998). Another study showed that human keratinocyte and dermal fibroblast attachment to collagen matrices is improved by the addition of glycosaminoglycans (Grzesiak et al, 1997). In this chapter, collagen and C6S were introduced to the 3D scaffold and a highly stable, rigid gel was formed (Figure 3.5). When examined under SEM, this surface covered large areas of the scaffold and appeared relatively uniform. However, this gel would not support cell culture. This was theorised to be due to the thickness of the gel affecting culture media diffusion, but reducing the thickness and amount of the gel was still incompatible with cell culture.

In preliminary experiments earlier scaffold prototypes (50-100µm thick with higher porosity) had been successfully used to culture keratinocytes on scaffold-supported collagen gels. However, these results were not repeatable with the current scaffold

model which is manufactured by different methodology. Therefore, it seems that the scaffold structure utilised in the experiments in this thesis is unsuitable for combining with a collagen gel to form an organotypic culture. It is likely that the manufacturing process for the scaffold could be altered to create a more optimal material for collagen coating, although this is beyond the scope of this thesis. A technique called "layer by layer" (LBL) coating may be appropriate, where a material is alternately submerged into oppositely charged solutions to sequentially coat it (Decher, 1997). Vapour phase deposition is another technique which could potentially be used to surface coat porous polymers such as the 3D scaffold (Chen et al, 2006).

### 3.3.3 Culture of Keratinocytes without Dermal Component

It is clear that in terms of keratinocyte culture, this 3D scaffold is best suited for the direct culture of cells, and not as a support for collagen matrices. The 3D scaffold allows the three dimensional culture of keratinocytes at an air-liquid interface without a dermal equivalent or fibroblasts. This is a faster method for 3D keratinocyte culture without waiting for collagen gel contraction before cell seeding. Secondly, collagen gels are inherently unstable with limited shelf life and stability in culture conditions, and thirdly, collagen gels are inherently variable in quality due to their reliance on cultured fibroblasts.

However, there are some sortcomings of a model based on keratinocytes only; lack of dermal-epidermal (i.e. keratinocyte-fibroblast) interactions being the largest. Bearing this in mind, the following chapters will use supplemented culture media to promote optimal proliferation and differentiation of keratinocytes. The second clear shortcoming is that none of the cultures grown so far have shown evidence of layers of organised stratifying cells, as would be expected in human skin and are readily found in published epidermal models. This is because it appears that keratinocytes are differentiating inside the 3D scaffold rather than forming stratified layers on the air-exposed surface. The following chapter will investigate this in more detail, to determine whether keratinocytes are organised in the 3D scaffold and whether they are still able to produce barrier lipids and form cornified envelopes under these conditions. These experiments will investigate whether keratinocytes alone are capable of forming an epidermal barrier within the confines of the 3D scaffold.

### 3.3.4 Conclusion

There are many different systems available for the 3D culture of keratinocytes - each with different properties, allowing for many different analytical methods and investigations, as well as the preferences of researchers. The 3D scaffold presented in this thesis has shown suitability for the rapid 3D culture of keratinocytes at the air-liquid interface without a dermal equivalent. Keratinocytes are contained within the scaffold, rather than forming multiple flattening layers on top of the culture. The resulting culture stains positive for differentiation markers, indicating that differentiation, and likely an epidermal barrier, is formed, although these markers were not distributed in an organised manner, such as in native epidermis. Chapter Four will use the information gained during Chapter Three (such as seeding method, cell number, duration of growth and culture apparatus) and progress to investigate the cell morphology and ultrastructure, cornified envelope formation and lipid synthesis of keratinocytes in 3D culture. These results will be compared to those from 2D culture and optimisations will be made to adapt the model for barrier permeability testing.

# 4 Chapter 4

# Characterisation of Barrier Components of the 3D Epidermal Culture System

## 4.1 Introduction

#### 4.1.1.1 Aims, Objectives and Overview

Results in Chapter Three have shown that, under optimised conditions, HaCaT cells can be cultured inside a novel 3D scaffold and induced to differentiate by raising the culture to the air-liquid interface. In response to this, cells differentiated and expressed barrier proteins that were visualised by immunofluorescence staining. Expression of proteins such as involucrin, keratin 1 and filaggrin is in common with the majority of epidermal models in the commercial market (Pappinen et al, 2012). In this chapter, keratinocytes will be analysed in detail by TEM and SEM to reveal ultrastructure associated with differentiation. Lipid analysis will assess the barrier lipid profile of keratinocytes cultured under various conditions, including after the addition of supplements to the culture media in both 2D and 3D.

#### 4.1.1.2 Morphology and Ultrastructure of Cells in the 3D Scaffold

The previous chapter showed that differentiation marker expression occurred throughout the thickness of the 3D model, but there was no clear organisation into definable epidermal layers. In most organotypic keratinocyte cultures, the resulting epidermal equivalent shows clearly defined layers - noticeably the granular and stratum corneum layers. However, this layered organisation is clearly not possible within the confines of a porous 3D polystyrene material. Therefore, this chapter further characterises the 3D scaffold keratinocyte model with scanning and transmission electron microscopy (SEM/TEM) techniques to visualise the organisation and ultrastructure of keratinocytes in this material. Cells were examined for changes in cell morphology associated with each epidermal layer, including keratin bundling, lamellar bodies, keratohyalin granules and cell flattening. These findings show the organisation of keratinocytes in the 3D scaffold as well as the extent of cell differentiation. The presence and location of desmosomes was also noted, due to their increasingly recognised importance in epidermal barrier function as well as their roles in diseases (Naoe et al, 2009).

#### 4.1.1.3 Cornified Envelopes as Evidence of Terminal Differentiation

Cornified envelopes are insoluble protein and lipid structures formed during terminal keratinocyte differentiation by covalent attachment ceramides and fatty acids to a tough protein matrix formed from involucrin, loricrin and small proline-rich proteins (Proksh et al, 2008). Cornified envelopes can be visualised under the membrane of

flattened corneocytes and serve as markers of terminally differentiated keratinocytes. Therefore, 3D cultures were analysed for their ability to produce cornified envelopes, as other epidermal models have been assessed previously (Nolte et al, 1993). Cornified envelopes were extracted from cultures after different periods of grown at the air-liquid interface and compared to those from mouse epidermis and from differentiated 2D cultures. A Nile Red lipid stain was used to visualise the lipid content of the cornified envelopes and they were classified as mature or immature depending on their morphology.

#### 4.1.1.4 The Role of Lipid Metabolism in the Epidermis and *in vitro* Equivalents

Although proteins such as involucrin are essential to barrier function, they alone are not enough to create a model with barrier permeability representative of *in vivo* epidermis. Investigations by Ponec et al, 2000, Netzlaff et al, 2005, Pappinen et al, 2012 and others have compared commercially available *in vitro* epidermal equivalents to native human epidermis. In all cases, *in vitro* equivalents showed morphological evidence of differentiation (such as flattening and stratification) as well as protein markers of differentiation (involucrin, K1/K10). However, all epidermal equivalents had some form of defect in lipid composition such as abnormal ceramide profile, elevated triglyceride content or insufficient FFA content. Lipids are often the main area of weakness in the barrier permeability of 3D epidermal equivalents, limiting their usefulness as *in vitro* models of epidermal permeability (Pappinen et al, 2003, Netzlaff et al, 2007, Godin et al, 2007, Zhang and Michniak-Kohn, 2012). In most cases, *in vitro* epidermal equivalents contain more cell layers and are several times thicker than native human epidermis, yet most of these models still display poor barrier function (Schmook et al, 2001, Pappinen et al, 2012). This highlights the importance of the lipid content of the epidermal equivalent as well as morphology.

The overall epidermal lipid profile is formed as the end result of many complex lipid metabolic pathways in the body such as processing dietary triglyceride and cholesterol into precursors and providing essential fatty acids. In the epidermis, keratinocytes synthesise lipids from intermediate products of their own metabolism, as well as those supplied from the diet such as essential fatty acids (Elias, 2006, Duan et al, 2012).

#### 4.1.1.5 Using the 3D Scaffold Model to Investigate Lipid Synthesis

The lipid content of the epidermis is closely linked to epidermal barrier function and examining the lipid content of the epidermis can be used as a measure of maturity. To investigate further into the maturity of 3D culture lipid profiles, HaCaT cell lipid synthesis was measured by lipid extraction and thin layer chromatography (TLC) in both 2D and 3D conditions. The profile of 3D cultured HaCaTs was compared to mouse epidermis, as well as published literature concerning human epidermis.

As part of this assessment, the 3D keratinocyte culture model was cultured with culture additives and pharmacological agents which have been shown to affect keratinocyte differentiation and lipid composition. The effect on cell morphology, viability and lipid synthesis in both 2D and 3D was analysed. This serves two purposes - firstly, to improve the existing model through modifying culture conditions for optimal barrier lipid production *in vitro*, and secondly to test the effects of culture additives on the 3D culture system in comparison to 2D cell culture.

## 4.2 Results

### 4.2.1 Morphology of 3D Cultured HaCaT Cells

3D cultures were grown with the protocol developed in the previous chapter, as follows: $10^6$ HaCaT keratinocytes were seeded in 100µl culture media into dry plasma-treated 3D scaffolds. Cultures were submerged for 48 hours, then raised to the air-liquid interface for 14 days in tri-well inserts in a deep cell culture dish. Culture media was replaced every three days for the duration of the experiments.

For a detailed examination of the morphology of the 3D culture, cultures were processed for Toluidine Blue staining, as well as H&E staining. Toluidine Blue sections are embedded into a hard resin and are cut to 1µm thin sections, rather than 10µm paraffin sections. Toluidine Blue stains nucleic acids and all proteins which also shows a sharper, more detailed cell morphology that H&E staining. Representative images of H&E and Toluidine Blue stained cultures are shown in Figure 4.1.

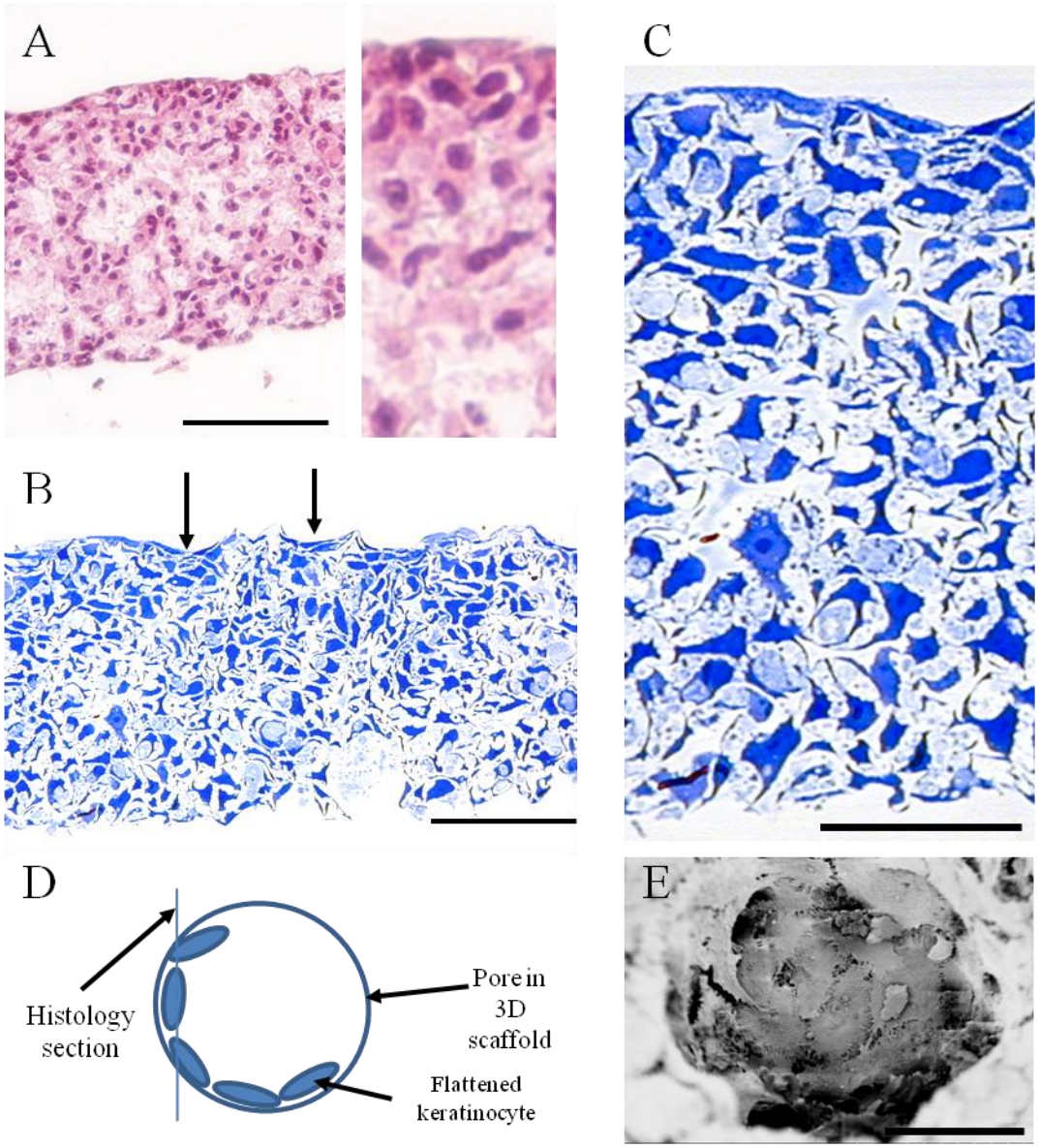


**Figure 4.1. Morphology of 3D Cultured HaCaT Cells**

A) H&E stained section of $10^6$ HaCaT cells cultured at the air-liquid interface with high magnification inset. Scale bars 100µm; B) Thin Toluidine Blue stained section of $10^6$ HaCaT cells cultured at the air-liquid interface. Flattened cells indicated; C) High magnification Toluidine Blue stained section showing cell morphology throughout the thickness of the scaffold. Scale bar 50µm; D) Schematic showing flattened cells inside a pore of the 3D scaffold; E) SEM image showing cells inside a pore of the 3D scaffold. Scale bar 40µm.

The H&E staining in Figure 4.1A show that HaCaT keratinocytes have completely filled the depth and length of the 3D scaffold. In this H&E section, there are no visible gaps or pores, indicating that the scaffold should be able to form a suitable epidermal barrier. There is no evidence of cell necrosis or death visible in the H&E image and cells have a clearly defined nucleus and cytoplasm.

The Toluidine Blue section (Figure 4.1B) shows more detailed cell morphology more clearly than the H&E section and shows keratinocytes inside the scaffold in various orientations. However, from these results alone it is not possible to tell whether HaCaT cells are undergoing differentiation, although previous immunofluorescence suggests that this is the case. In Figure 4.1C, a number of flattened cells are seen throughout the 3D culture, but it is unclear whether these cells are actually flattened, or this observed morphology is due to the orientation of the cells in the section. In real epidermis, flattening keratinocytes are oriented horizontally, in parallel to the skin surface, but inside the 3D scaffold the cells are likely to be adhering to the surface of the scaffold pores and voids and flattening along the surfaces in many orientations. It may be that the rigid nature of the 3D scaffold itself is constraining cell morphology and organisation. and keratinocytes are flattening *inside* the pores of the scaffold in various orientations. A schematic diagram of this is shown in Figure 4.1D. SEM imaging, shown in Figure 4.1D supports this, with a pore inside the scaffold showing multiple flattened cells in various orientations along the inner surfaces of the pore.

At the upper air-exposed surface of the scaffold, there is more evidence of horizontally oriented flat cells (indicated with arrows in Figure 4.1B), which would support positive differentiation marker staining seen previously. However, only 1-2 layers of fully flattened cells are observed. These flattened cells are not present on the underside of the scaffold, showing that the flattened cells are in response to the dried upper surface from culture at the air-liquid interface and not simply from being at the edge of the 3D scaffold.

#### 4.2.1.1 SEM Imaging of 3D Culture Ultrastructure

Therefore, higher magnification imaging was used to examine the upper surfaces of the scaffold for flattened keratinocytes and for examining the cells in the mid-portions of the scaffold for signs of proliferation or differentiation. Representative images are shown in Figure 4.2.

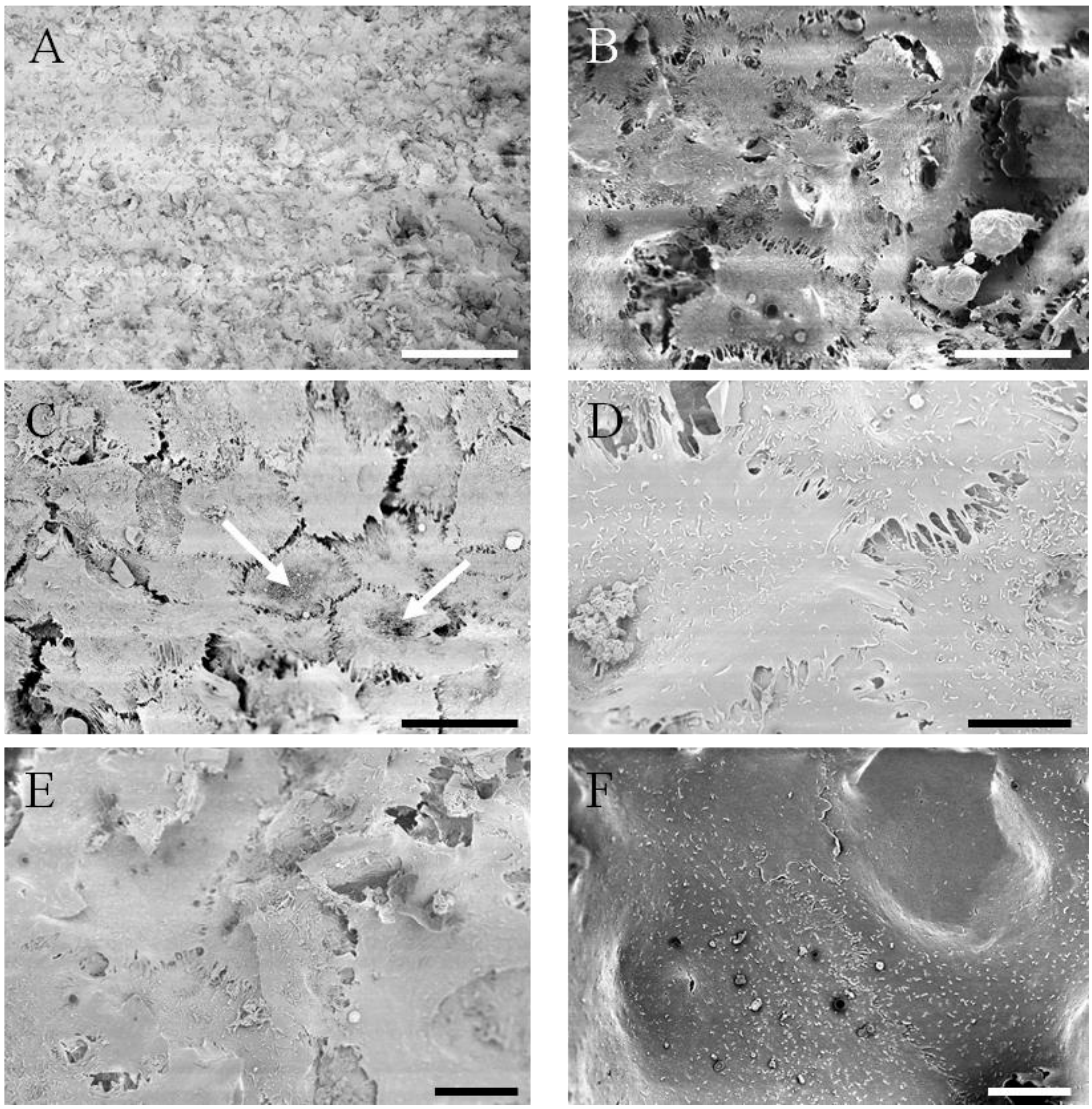


**Figure 4.2. SEM of Surface of 3D Cultured HaCaT Cells**

A) Low magnification SEM image of the surface of 3D scaffold showing wide coverage of cells. Scale bar 150µm; B, C) Intermediate magnification SEM image of the surface of 3D scaffold showing polygonal flattened corneocytes. Probable nuclear remnants indicated with arrows. Scale bars 20µm; D) High magnification SEM image showing three flattened corneocytes. Scale bar 10µm; E) High magnification image showing multiple layers of flattened corneocytes. Scale bar 10µm; F) High magnification image showing tightly-assembled corneocytes. Scale bar 5µm. All cultures grown with $10^6$ HaCaT cells for 14 days at the air-liquid interface.

The low magnification image in Figure 4.2A shows the surface of the 3D scaffold after $10^6$ HaCaT cells were grown for 14 days at the air-liquid interface. The image shows cells consistently covering of an area approximately 700µm in diameter. There are large areas of flattened cells and with some areas of more rounded cells still present. This was observed over the central portion of the 22mm diameter scaffold. Intermediate magnification images in panels B and C show flattened pentagonal or hexagonal shaped corneocytes with distinct cell boundaries. The majority of these corneocytes are clearly anucleate, indicative of terminally differentiated corneocytes. These cells are flattened and covering an area approximately 40µm in diameter. Image B shows that a minority of cells were not completely differentiated. There are also flattened cells with remnants of nuclei remaining (panel C, indicated with white arrows). It is unclear from these images how many layers of flattened cells are on top of the scaffold, although there are at least two layers visible.

The high magnification image in panel D shows flattened cells, one of which has remnants of the cell nucleus remaining. Corneocytes are attached by stitch-like connections around the periphery. Panels E and F show an area which appears more "cobblestone" with less clear corneocyte boundaries and "tighter" assembly of each corneocyte. The overall appearance of these areas is more smooth, and more similar to human cornified epidermis (Naoe et al, 2008). Patches of these "cobblestone" and "stitched" areas of corneocytes were found throughout the surface of the 3D scaffold with no identifiable patterns of distribution. This is perhaps due to processing for SEM, or from slight differences in exposure to the dry air-interface across the scaffold during culture.

#### 4.2.1.2 TEM Imaging of 3D Culture Ultrastructure

In order to look more closely at the ultrastructure of cells and to determine the thickness of layers of flattened cells, cultures were fixed and processed into ultrathin sections for TEM. Representative images showing key observed features are shown in Figure 4.3, Figure 4.4 and Figure 4.5.

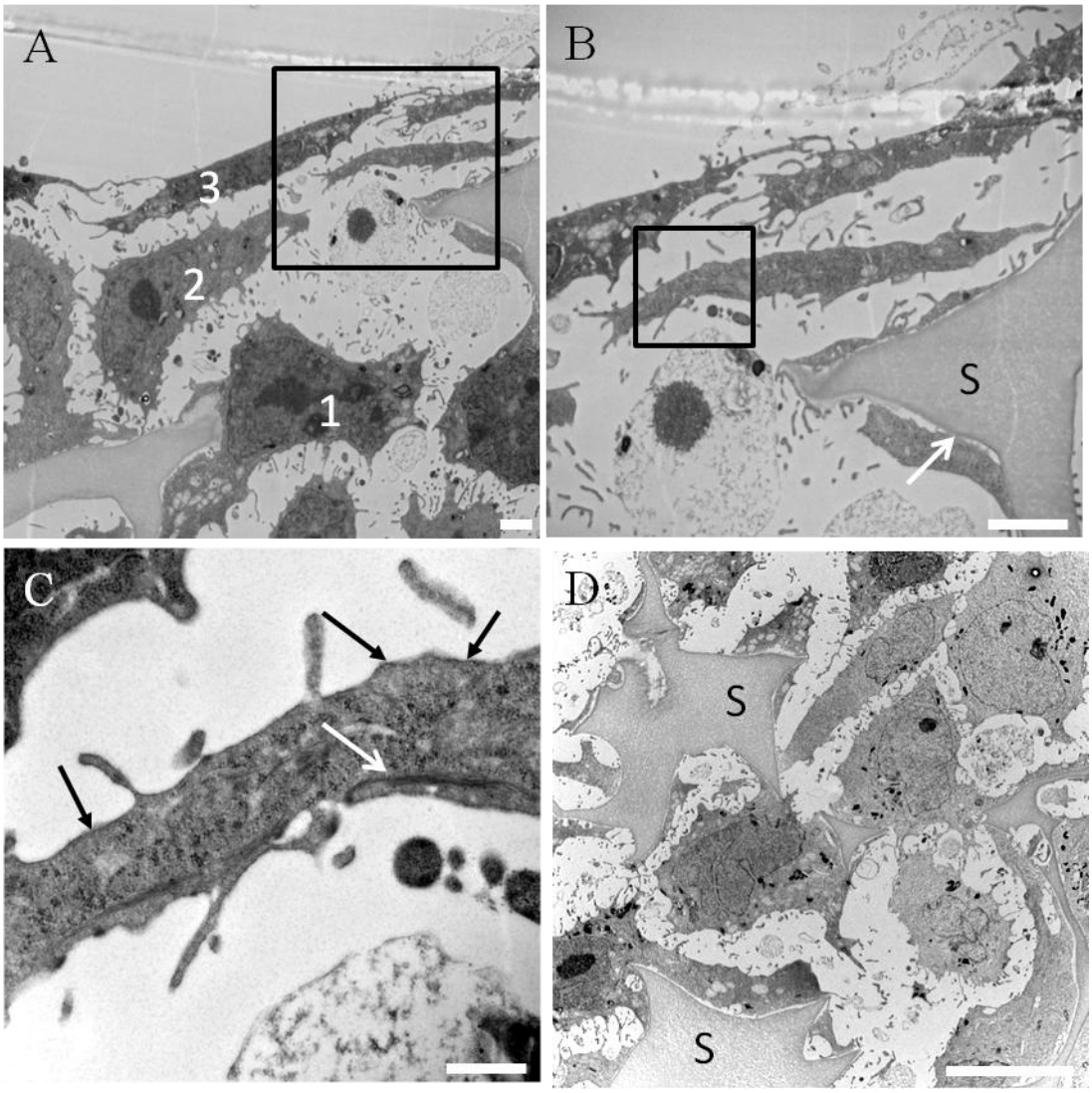


**Figure 4.3. TEM of Keratinocytes on the Surface of Air-Exposed 3D Cultures**

Image showing flattened cells on air-exposed top of 3D scaffold structure. In this image, three cells at various stages of transition from normal to flattened morphology are clearly visible, labelled 1, 2 and 3. Scale bar 2µm; B) Higher magnification view of the area marked in image (A). The scaffold (S) is annotated, and flattened cells are seen attached to the surface (white arrow). Scale bar 2µm; C) High magnification image showing flattened keratinocyte with no visible nucleus. Keratin bundling is annotated with a white arrow and cornified envelope formation with black arrows, visualised by dark staining under the flattened corneocyte membrane. Scale bar 500nm; D) Central region of the 3D scaffold showing cells with various morphologies around the scaffold (S). Scale bar 10µm.

Figure 4.3 shows TEM images of HaCaT cells at the air-exposed surface of the 3D culture. In panel A, a low magnification TEM image of the upper surface shows three cells at various stages of transition from normal to flattened morphology. Cell (1) is rounded with a fully formed nucleus and cytoplasm, as well as cytoplasmic organelles. This cell is attached to the 3D scaffold and is similar in appearance to a proliferative HaCaT cells shown by Gniadecki et al, 2001. Cell (2) has a shrunken nucleus. Cell (3) is completely flattened and is anucleate.

A higher magnification view of the area marked in panel A shows how cells are attached to multiple surfaces. As predicted from Toluidine Blue sections earlier, flattened cells are seen adhered to the surface of the scaffold. The cell annotated with a white arrow is approximately 1.0µm thick. In panel C flattened, anucleate cell ultrastructure is visible, showing evidence of keratin bundling, indicated with a white arrow. Keratin bundling increases the mechanical stability of the cells and occurs during keratinocyte differentiation (Windoffer et al, 2011). This cell is approximately 1µm thick, which corresponds to the correct size for a corneocyte (Wickett and Visscher, 2006). It was not possible to see a clearly defined keratinocyte cornified envelope, but the dark line around the border of the cell, underneath the cell membrane (indicated by black arrows) is potentially indicative of cornified envelope formation.

TEM analysis confirmed that differentiation is taking place deep within the scaffold. Figure 4.3D shows an area approximately 100µm deep inside the cross section of the scaffold. Here, several cells are pictured which match the descriptions of differentiating HaCaT cells according to Gniadecki et al, 2001. Cells appear with an irregular, dark edged nucleus with vacuoles in the cytoplasm. These are noted by Boelsma et al, 1999 to be indicative of differentiating HaCaT cells. This is opposed to proliferative cells which show a rounded/oval nucleus and organelle rich cytoplasm. It is also clear that cells are fully integrating with the 3D scaffold and are adapting their shape around the surface of the scaffold. These results support earlier immunofluorescence staining for differentiation markers which showed differentiation throughout the 3D scaffold and not just at the upper air-exposed surfaces (Figure 3.10).

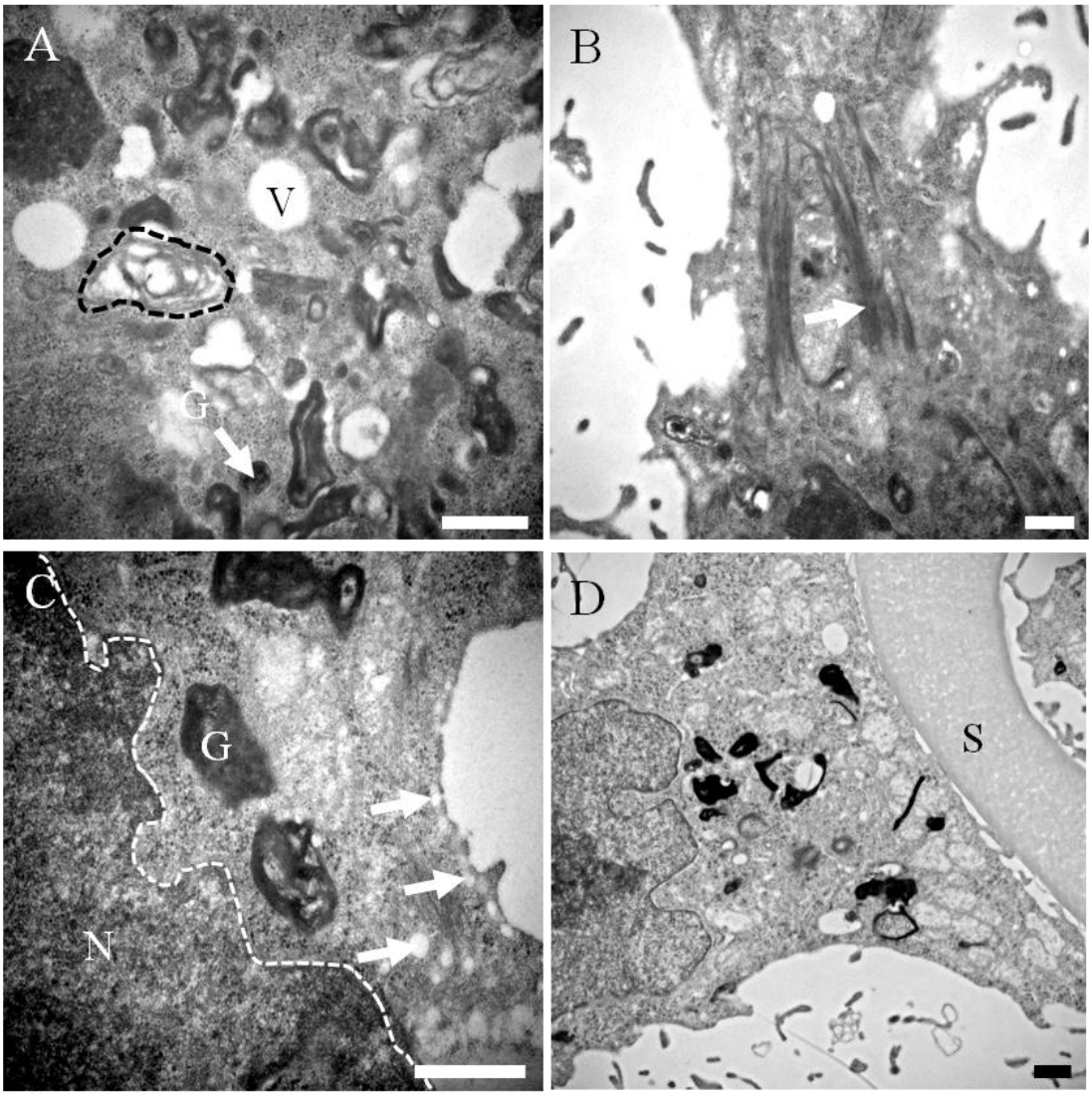


**Figure 4.4. TEM Imaging of HaCaT Cells inside 3D Scaffold**

A) HaCaT cell inside 3D scaffold showing large amounts of lamellar bodies (dotted area), lipid vacuoles (V) and keratohyalin granules (G) inside the cytoplasm; B) Keratin bundling (labelled) inside a flattening keratinocyte; C) Image showing emptied lamellar bodies and excreted lipid vacuoles (labelled with arrows). The nucleus is labelled (N) and the border marked with a dotted line; D) HaCaT cells growing inside 3D scaffold, attached to the scaffold (labelled (S)), showing several differentiated-associated organelles and lipid vacuoles. Organelles identified by images from Rosdy et al, 1990 Boeslma et al, 1999, Stark et al, 1999 All scale bars 500nm.

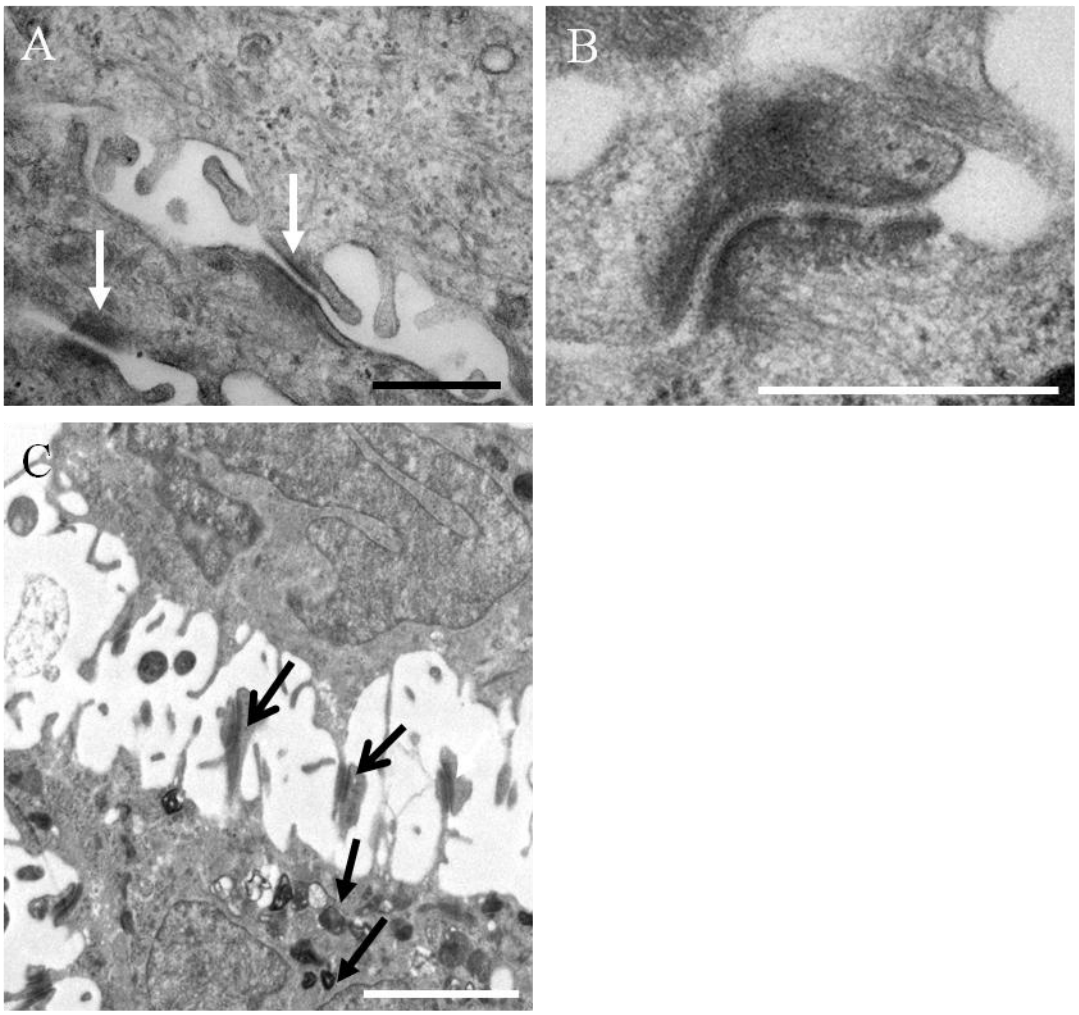


**Figure 4.5. Evidence of Desmosome Formation by HaCaT Cells in 3D Scaffold**

A) TEM image showing three flattened keratinocytes connected by desmosomes, indicated by white arrows. Scale bar 500nm; B) High magnification image of a desmosome. Scale bar 500nm; C) The interface between two cells shows several desmosomes, labelled with open headed arrows. The lower cell also shows a large volume of lamellar bodies and keratohyalin granules, labelled with black arrows. Scale bar 2µm. Similar images of desmosomes in 3D cultured epidermis are found in Smith et al, 2010.

In Figure 4.4, the ultrastructure of various cells from regions inside the 3D scaffold are presented. Panel A shows a high magnification image of keratinocyte located approximately 80µm deep inside the 3D scaffold. The cell cytoplasm shows extensive lamellar bodies (L), as well darkly stained ~400nm diameter rounded keratohyalin granules (G) and white, empty, lipid vacuoles (V), as identified by images in Rosdy et al, 1990 Boeslma et al, 1999, Stark et al, 1999 and descriptions in Ishida-Yamamoto et al, 2011. These organelles are indicative of a keratinocyte which is undergoing cell differentiation, corresponding to approximately the stratum granulosum layer of normal epidermal differentiation. This cell is likely to be capable of producing and excreting barrier components such as extracellular lipids into the surrounding area. Cytoplasmic lipid vacuoles will show as white unstained areas due to the solvent and ethanol washes involved in processing for TEM imaging (Ponec et al, 2000) and several such vacuoles were observed in cells throughout the 3D culture.

A high magnification section (Figure 4.4B) shows a keratinocyte located approximately 40µm deep inside the 3D scaffold. This cell is located closer to the air-interface and may be expected to be further along the pathway of differentiation than the previous cell in image A. This cell shows keratin fibre bundling and organisation inside the cytoplasm. This occurs during cell differentiation, when keratin fibres line up to contract and flatten the cells, confirming that cells are differentiating and flattening inside the 3D scaffold and not only at the air-exposed surface. An image from deeper inside the 3D scaffold (Figure 4.4C) shows a keratinocyte approximately 80µm deep which still has a nucleus, labelled "N" (border indicated) and shows darkly stained keratohyalin granules (G). There are also numerous lamellar bodies and excreted lipid vacuoles inside the cytoplasm, characteristic of the granular layer of normal epidermis. This again shows evidence of lipid production and excretion by the HaCaT cells grown in the 3D environment. Panel D shows another keratinocyte attached along the surface of the 3D scaffold with numerous cytoplasmic organelles.

Many desmosomes were observed throughout the 3D culture. Figure 4.5A shows three anucleate HaCaT cells with flattened morphology, connected by desmosomes. These corneodesmosomes are essential for barrier function of the epidermis, although desmosomes are expected to degrade in fully differentiated cells, allowing

for desquamation. Panels B and C show high and intermediate magnification images of desmosomes observed in the nucleated cell portions of the 3D culture. Panel C shows two cells connected by several desmosomes in one plane. Similar images of desmosomes in 3D cultured epidermis are found in Smith et al, 2010.

#### 4.2.1.3 Conclusion of 3D Culture Morphology

It is clear from examining these sections that after 14 days at the air-liquid interface, keratinocytes throughout the 3D scaffold are differentiating. On the upper, air-exposed surface of the scaffold, keratinocytes are generally more differentiated (i.e. flat, anucleate) than those contained within the scaffold. Flattened cells were observed through the scaffold, but appeared to be more prevalent towards the upper air-exposed surface. The majority of non-flattened keratinocytes observed inside the 3D scaffold still show signs of differentiation such as desmosomes, keratohyalin granules, lamellar bodies and keratin bundling. These organelles show a general trend showing a more differentiated morphology in closer proximity to the air-interface however the whole 3D culture is not easily divided into distinctive layers such as the spinous, granular or stratum corneum layers.

It is clear that the rigid, non-biodegradable nature of the scaffold itself is a key factor in keratinocyte behaviour. In most 3D *in vitro* epidermis equivalents utilising collagen gels or de-epidermalised dermis, and in samples of real human epidermis, cells can be clearly identified as being part of a greater architecture, with clearly divisible layers. However, in the 3D scaffold, differentiation is occurring but cells are differentiating inside the 3D scaffold itself rather than forming an series of layers of increasing differentiation.

### 4.2.2 Cornified Envelope Extraction and Characterisation

Both TEM imaging in Figure 4.3C and Toluidine Blue staining of ultrathin sections (Figure 4.1) showed the presence of flattened corneocytes and possible cornified envelope formation located under the cell membranes of flattened cells.

Therefore a series of cornified envelope extractions were performed on 3D cultures. Due to their resilient and insoluble nature, cornified envelopes can be isolated by treating whole epidermal sections (or 3D scaffold cultures) with reducing agents and surfactants (SDS and DTT), followed by boiling and repeated washing all soluble debris away. Cornified envelopes were extracted, imaged by phase contrast light microscopy, counted and classified as fragile or mature depending on their morphology. Objectivity was achieved by a colleague labeling each sample with a code before classification of cornified envelope morphology. Cornified envelopes were stained with 0.5mg/ml Nile Red lipid stain. Cornified envelopes from 2D cultures and from mouse ear tip epidermis were also extracted for comparison. Representative images from each experiment are shown in Figure 4.6 and Figure 4.7.

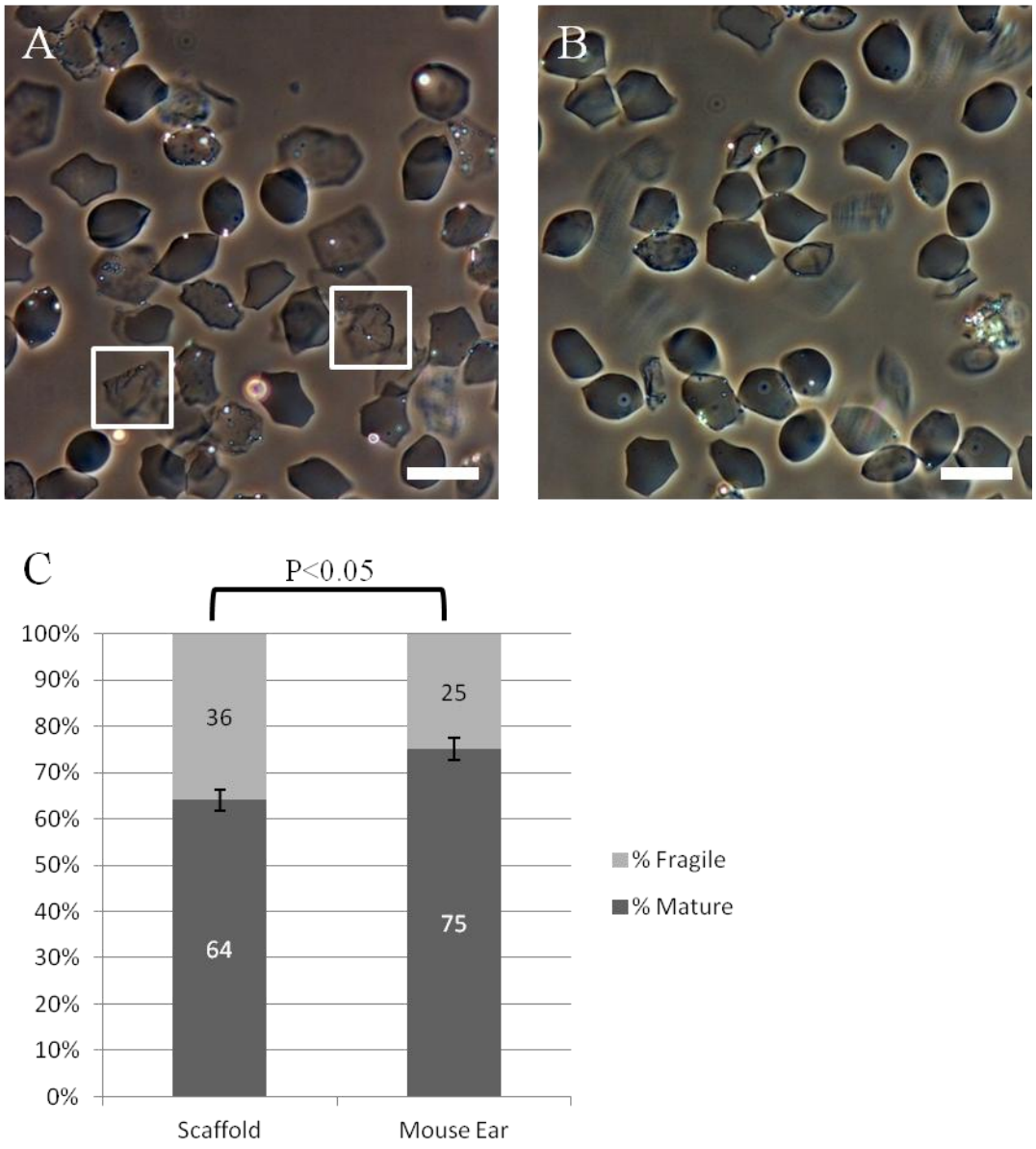


**Figure 4.6. Properties of Cornified Envelopes From 3D Culture**

Phase contrast microscopy images of cornified envelopes from A) HaCaT cells cultured in the 3D scaffold for 14d at the air-liquid interface and B) mouse ear tip epidermis. White boxes show examples of cornified envelopes with fragile morphology. Scale bars 50μm; C) Graph showing percentage of fragile and mature cornified envelopes from three repeats of cornified envelope isolations from 3D culture (n=509) and mouse ear tip epidermis (n=622). Error bars show SEM.

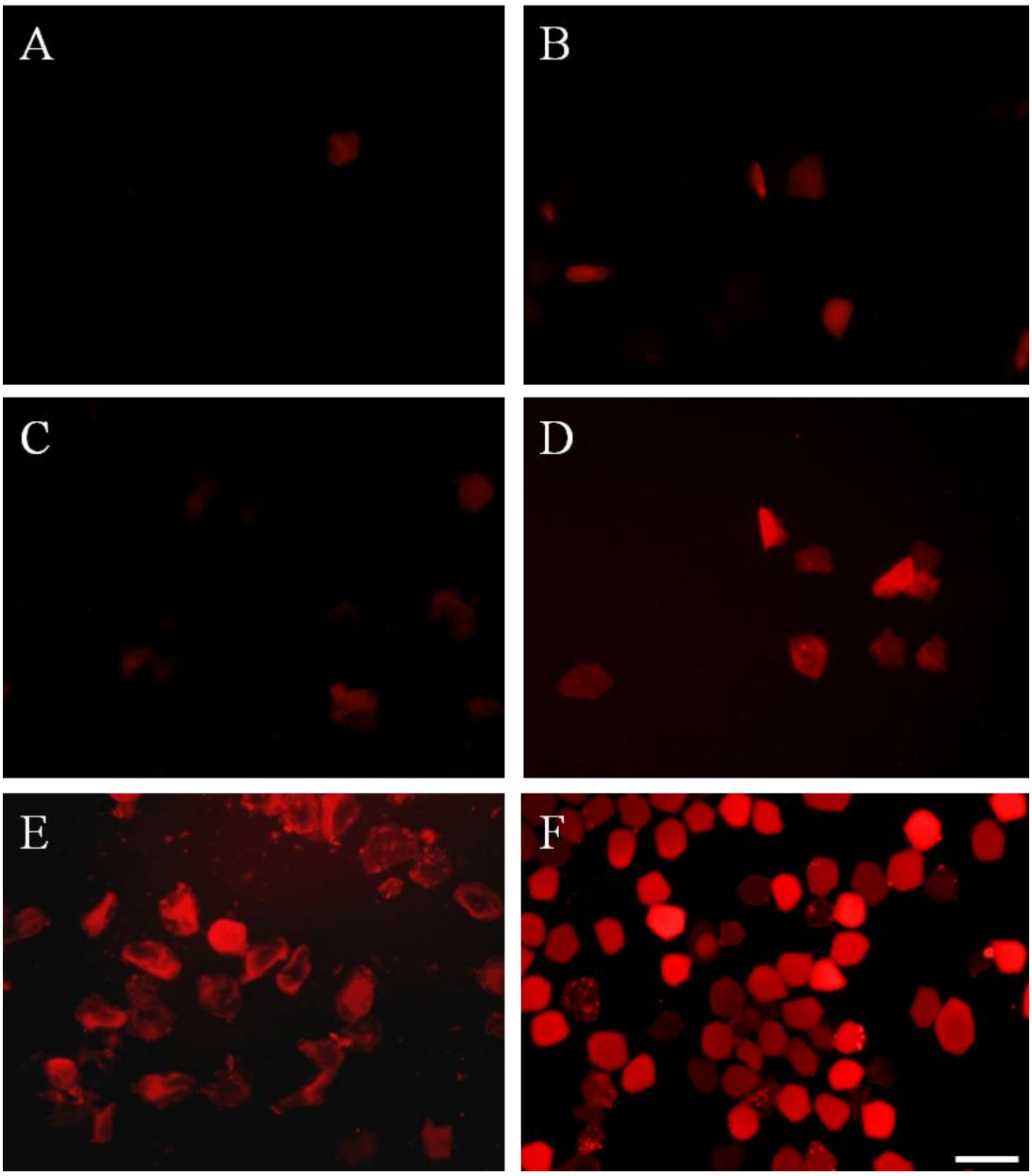


**Figure 4.7. Comparison of Cornified Envelopes from 2D and 3D Culture**

Cornified envelopes isolated from A) 2D low calcium; B) 2D high calcium; C) 3D scaffold 2 days submerged; D) 3D scaffold 7d air-liquid interface; E) 3D scaffold 14d air-liquid interface; F) Mouse ear tip. All cornified envelopes stained with Nile Red for lipids and imaged at equal exposure for comparison. Scale bar 50µm for all images.

In Figure 4.6, samples of 14d 3D cultured CE and mouse ear tip CE were visualised by phase contrast microscopy for examination of their morphology.

Published studies (Koch et al, 2000, Hirao et al, 2001 and Sevilla et al, 2007) have observed that cornified envelopes may be categorised into two main types: mature/rigid or immature/fragile. Mature cornified envelopes are of a relatively homogenous polygonal shape, with clearly defined rigid edges, larger size and stronger staining by Nile Red (Rawlings, 2003). Fragile or immature cornified envelopes taken on a more hetergenous morphology - usually being smaller, with irregular edges and a more rounded, less polygonal shape, sometimes with inclusions.

A mixture of both mature and fragile cornified envelopes is visible in both samples. Cornified envelopes were counted from 10 fields of 3 samples each of 3D cultured cornified envelopes (n=509) and mouse ear tips (n=622) and categorised as mature or immature morphology. Results in Figure 4.6 show that the cornified envelopes isolated from the 3D scaffold are 64:36 mature:immature, whereas cornified envelopes from mouse ear tips are 75:25 mature:immature. This difference is statistically significant ($P<0.05$). This indicates that, on average, keratinocytes cultured within the 3D scaffold are displaying a more immature morphology than those from mouse epidermis. The 3D scaffold is much thicker than the epidermis of mouse ear tips, and the difference in the ratio shows that not all cells inside the scaffold are fully differentiated. In a comparison of size, the immature CE were found to be an average of 22% smaller than mature CE and the average diameter of mature CE was 38μm.

#### 4.2.2.1 Visualisation of Cornified Envelope Lipids

Nile Red is a red fluorescent lipid probe first described by Greenspan et al, 1985 and characterised by Klinkner et al, 1997. It has been used previously (Hirao et al, 2001, Rawlings, 2003) to identify cornified envelopes with covalently attached lipids. Immature/fragile cornified envelopes stain inconsistently with Nile Red due to less covalent attachment of lipids (Hirao et al, 2001). Figure 4.7 shows cornified envelopes isolated from 2D and 3D cultured HaCaT cells as well as mouse ear tip epidermis.

Keratinocytes grown in 2D cultures (Figure 4.7) show very few cornified envelopes after 7 days in either low calcium (Panel A) or high calcium (Panel B) culture media. This is to be expected, as 2D culture generally does not produce matured cornified envelopes, even in the presence of high calcium concentrations.

After 2 days submerged in the 3D scaffold (Figure 4.7C), the extraction shows similar results to 2D cultures, which is to be expected as cells do not differentiate when submerged (as desmonstrated in Figure 3.8). However, after 7 days at the air-liquid interface (Figure 4.7D), there were more cornified envelopes extracted from the 3D scaffold cultures. These cornified envelopes also show more Nile Red staining than previous samples, indicating that they are more mature and have more covalently attached hydroxyceramides.

After 14 days at the air-liquid interface (Figure 4.7E), there are many cornified envelopes extracted from the cultures. These cornified envelopes are more strongly stained with Nile Red than previous samples, however compared to those extracted from mouse ear tips (Figure 4.7F), the morphology of 3D cultured cornified envelopes is irregular and Nile Red staining is less intense, confirming the lower percentage of mature envelopes observed in Figure 4.7.

In comparison to the cornified envelopes from mouse ear tips, the morphology of the 3D scaffold-cultured cornified envelopes is quite variable. The morphology of the 14d cultured CEs are generally larger, with less consistent Nile Red staining, mostly located around the periphery of each CE. By comparison, mouse ear tip CEs are smaller, more mature in polygonal shape and clearly stronger stained with Nile Red. Again, this probably reflects the constraints that the scaffold imposes on the cell morphology.

### 4.2.3 Synthesis of Epidermal Lipids in the 3D Scaffold

Cornified envelopes from 3D cultures were shown to have covalently attached lipids and ultrastructure of cells in 3D culture showed organelles such as lamellar bodies associated with lipid production and extrusion. As mentioned previously, the lipid profile is a useful measurement of the maturity of the epidermal barrier, and is also defective in many *in vitro* equivalents (Ponec et al, 2000). Most investigations into *in vitro* epidermal equivalents have focused on the quality of the dermal equivalent

such as the type, number and treatment of various fibroblast feeder cells. These experiments have been based on optimising the feedback between keratinocytes and fibroblasts in order to improve keratinocyte differentiation. However, when keratinocytes are cultured inside the 3D scaffold with no dermal equivalent or feeder cells, the main area for optimisation is the culture media itself. It has been shown that addition of compounds to the cell culture media can alter the differentiation of HaCaT cells (Breiden et al, 2007).

Therefore, the 3D scaffold model was cultured in various conditions listed in Table 4.1. The experiments were designed to separate factors influencing differentiation, such as the air-liquid interface, serum in the culture media, calcium concentration, and two additives shown to alter lipid metabolism.

**Table 4.1. Culture Media Tested for Modifying 3D Keratinocyte Lipid Synthesis**

| Culture Media | Calcium (mM)* | FBS (%) | Ascorbic acid (µg/ml)** | FFA*** |
|---|---|---|---|---|
| SF low | 0.06 | - | - | - |
| SF high | 1.50 | - | - | - |
| High | 0.06 | 10 | - | - |
| Low | 1.50 | 10 | - | - |
| High AA | 1.50 | 10 | 100 | - |
| High FFA | 1.50 | 10 | - | Yes |

* 0.06mM or 1.5mM Calcium. Calcium concentration has been previously used to differentiate keratinocytes. Breiden et al, 2007, found that human keratinocytes grown under low calcium conditions synthesise only a simple profile of ceramides, including 50% more immature ceramide precursors. Under high calcium conditions, ceramide production increased and immature ceramide precursors reduced.

** 100µg/mL Ascorbic Acid was initially shown to have a photoprotective effect against UV-b induced damage in keratinocytes (Miyai et al, 1996) and has since been widely used to improve the performance of 3D cultured epidermal equivalents. Ponec et al, 1997, showed improved lipid profile and barrier function in a DED-based 3D model. Pasonen-Seppanen et al, 2001, cultured a rat epidermal keratinocyte (REK) model with 40µg/ml ascorbic acid and reported improved morphology of the stratum corneum, increase quantity and organisation of lipids in the stratum corneum, and improved barrier function (50% reduction of TEWL) in their model. Uchida et al, 2001 demonstrated that ascorbic acid stimulated sphingolipid production, increased lamellar body formation and increased omega-hydroxylated ceramides. Boyce et al, 2002 showed that cultured epidermal substitutes with ascorbic acid showed improved viability and barrier function.

*** FFA is a mixture of free fatty acids with bovine serum albumin as a carrier for fatty acids. This mixture comprises 10µM Linoleic Acid, 25µm palmitic acid, 7µm arachidonic acid and 2.4mM BSA, following the protocol of Ponec et al, 2003, who demonstrated that supplementation with these lipids increased the lipid synthesis of *in vitro* epidermal cultures, as well as altered the ceramide profile. This cocktail was also utilised by El Ghalbzouri et al, 2004 who noted increased differentiation and a lipid profile more similar to *in vivo* epidermis.

Serum was also considered as a factor, as it is the main source for precursors. Therefore low and high calcium serum free cultures were set up as controls.

#### 4.2.3.1 Viability of 2D Cultured Keratinocytes in Modified Culture Media

In order to determine the effect of these culture conditions on keratinocytes, a series of analyses were performed. Firstly, cell viability in 2D was assessed using the MTS

assay to highlight any culture conditions which lead to detrimental effects on viability of the culture such as cell toxicity and death. HaCaT cells were cultured in 24-well plates for 24 hours, then switched into different culture media as shown in Table 4.1. An MTS assay was performed after 6 hours, 2, 4 and 7 days in the culture media. The experiment was repeated three times, averaged and the SEM was calculated. The results shown in Figure 4.8 indicate that after 6 hours, all treatment groups are similarly viable. ANOVA analysis showed that there is no significant difference in viability of any treatment group, for instance from cell toxicity. This shows that no groups are having an immediate toxic effect on HaCaT cells.

After 2 days, some small differences in cell viability were noted, with serum free conditions displaying lower viability than those containing serum. After 4 days, all cultures are more proliferative than after 2 days, as expected and HaCaT cells grown in both serum-containing and serum-free low calcium media are utilising significantly more MTS reagent than those grown in high calcium. High calcium culture media with serum leads to higher viability than serum-free high calcium media. However, these differences were slight. Culture media with ascorbic acid was not significantly different to other serum containing culture conditions, aside from the FFA group which had slightly higher viability. However, variability in viability with all treatments is low, with no evidence of toxicity.

After 7 days, all cultures are more metabolically active than after 4 days, but the increase in activity is reduced compared to the increase from 2 to 4 days as the cultures have become more confluent. After 7 days, there is no significant difference in MTS viability after 7 days between any of the treatment groups. These results show that all culture conditions are capable of maintaining cultures of cells, without causing toxicity. Some small differences in viability appear between groups after 2-4 days, but they do not result in any significant differences to the overall cell number in the culture after 7 days of culture.

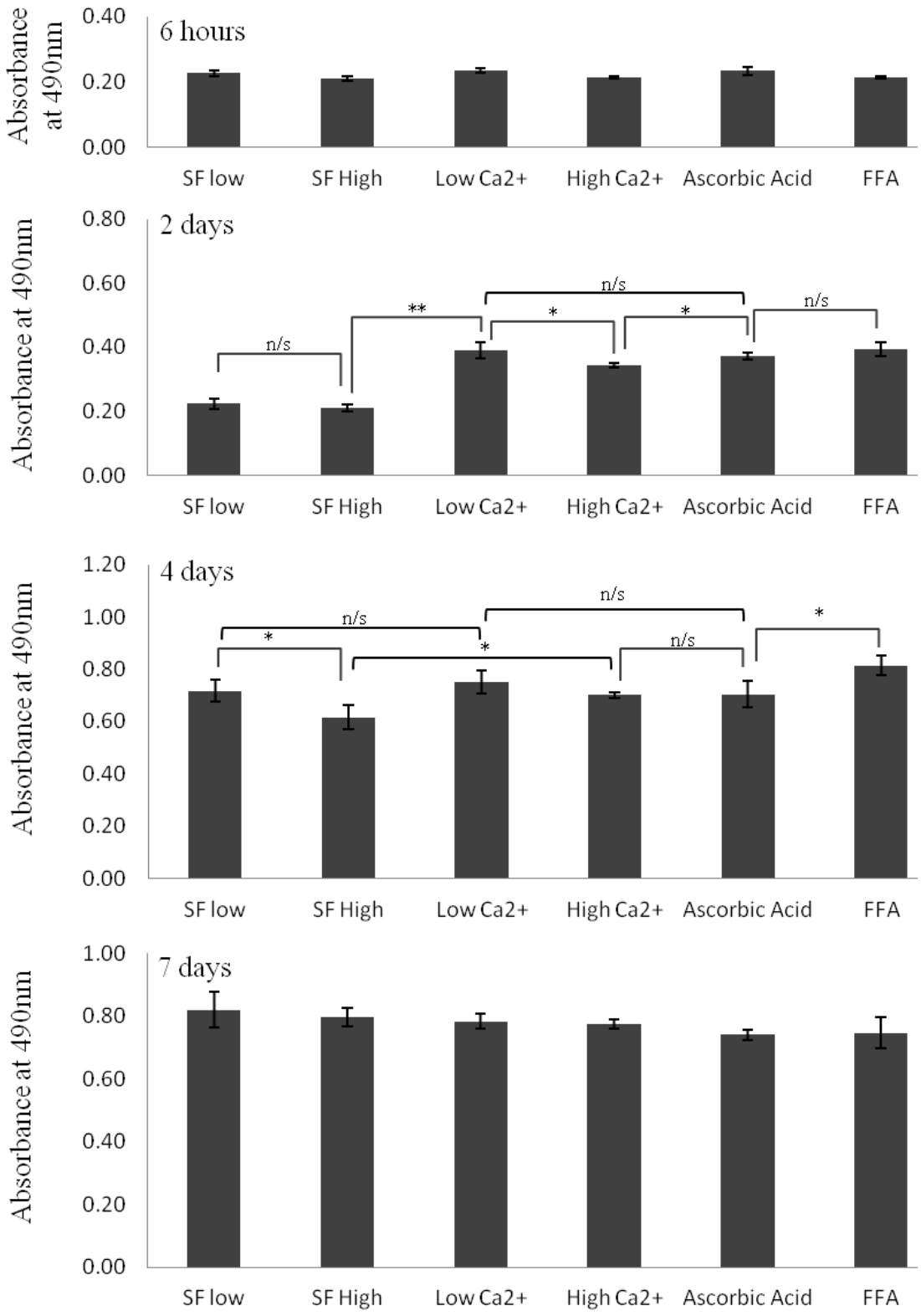


**Figure 4.8. MTS Assays of HaCaTs Cultured in Various 2D Conditions**

MTS assay of HaCaT cells grown in 2D for 6 hours, 2, 4 and 7 days under various culture conditions. Note several changes in y-axis. Error bars show SEM. * = $p<0.05$, ** = $p<0.01$, n/s = not significant. No significant differences observed between different culture conditions at 6 hours or 7 days.

#### 4.2.3.2 Effect of Culture Media on Keratinocyte Lipid Synthesis in 2D

In order to examine the effect of each culture condition of the lipid production of HaCaT cells, T25 flasks of HaCaT cells were grown for 5 days to approximately 80% confluence in each media type. Cell number was approximated by counting and lipids were then extracted, analysed and quantitated as detailed in Chapter Two. Results from three replicate experiments are experiments are expressed as the total amount of lipids normalised against cell number and standardised against the low calcium, serum free treatment as 100%.

The results in Figure 4.9 show that calcium concentration is a key determinant in the lipid production of HaCaT cells. Under serum free and serum-containing conditions, the addition of calcium significantly increases lipid production ($p<0.01$). This is in line with published literature (Breiden et al, 2007). Addition of serum also increases the amount of lipid that could be extracted from HaCaT cells under high and low calcium conditions ($p<0.01$). This is to be expected, as the serum itself contains lipoproteins, cholesterol, FFA, triglycerides and phospholipids which can act as substrates for conversion into cellular lipids. Serum also contains proteins such as bovine serum albumin (BSA) which may aid in the transport and uptake of serum lipids into the cells (Price & Gregory 1982).

The addition of ascorbic acid or bovine serum albumin did not increase lipid production compared to high calcium and serum alone. This is contrary to published data (Pasonen-Seppanen et al, 2001, Breiden et al, 2007), which suggests that lipid production should have increased. However, this may be because HaCaT cells are limited in their lipid production capability in the 2D environment.

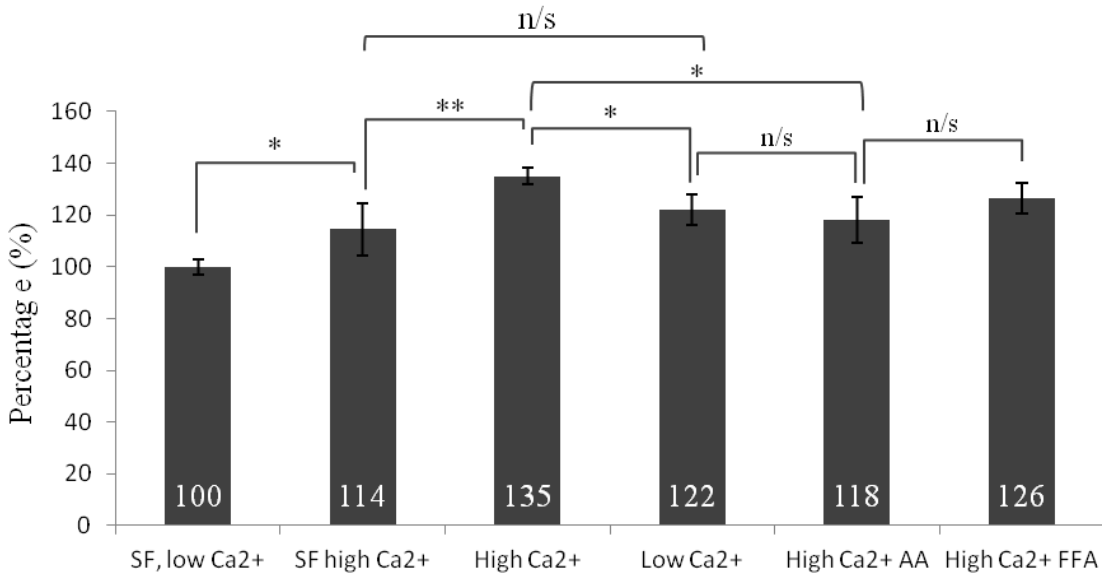


**Figure 4.9. Lipids Extracted from 2D Cultured HaCaT Cells**

Total lipid amount extracted from HaCaT cells grown in 2D for 5 days compared against serum free low calcium conditions and standardised against cell number. Error bars show SEM. * = P<0.05, ** = P<0.01, n/s = not significant. SF = serum free. High/low $Ca^{2+}$ = 1.15mM/0.06mM, AA = 100µg/ml ascorbic acid, FFA = added cocktail of free fatty acids.

#### 4.2.3.3 Identification of Epidermal Lipids by ASAP-MS and TLC

Quantitation of total lipid production does not reveal the types of lipids produced (i.e. FFA, ceramides, cholesterol etc). Therefore the proportion of each lipid was measured by separating whole cell lipid extracts on a thin layer chromatography (TLC) plate. Lipid extracts from the previous analysis were used and a three phase separation was carried out with three different combinations of solvents (as in Suhonen et al, 2007), and bands in the lanes of the TLC plate were identified by known standards, ASAP-MS and relevant literature.

Figure 4.10 shows annotated lanes from a TLC plate showing two known standards (cholesterol and cholesterol oleate) which were separated on the plate. The RF values for these standards were calculated and lined up next to a lane of a whole cell lipid extract. Data on RF values from literature (Suhonen et al, 2007) was used to identify other lipids. To further verify the identification of lipids, Atmospheric Solids Analysis Probe - Mass Spectrometry (ASAP-MS) was used to confirm the identity of some bands on the TLC plate.

Figure 4.11A shows an ASAP-MS scan of a 99.9% pure cholesterol standard which was analysed by ASAP-MS in powder form. There is a strong peak at m/z 369.3. A structural diagram of the cholesterol molecule is included as a reference. According to an ASAP-MS database at the Department of Chemistry, Durham University, this value corresponds to cholesterol (personal communication, Dr J. Mosely). When identifying the compounds corresponding to the m/z values, predictable changes to the molecule, such as loss of an OH group from cholesterol, were taken into account. This identification is also supported by m/z values in published literature (Astarita et al, 2011 and Piehowski et al, 2008). Figure 4.11 B shows an ASAP-MS scan from a sample scraped from the TLC plate at RF 0.65, corresponding to cholesterol. The cholesterol molecule is still detected in this scan, albeit with more background peaks from the solvents and silica gel coating on the TLC plate. This confirms that the band located at RF 0.65 is cholesterol.

Ceramide NS (Figure 4.12A and B), cholesterol sulphate (Figure 4.12C) and cholesterol ester (Figure 4.13) were also subjected to ASAP-MS analysis in order to confirm their identifications from the TLC plate.

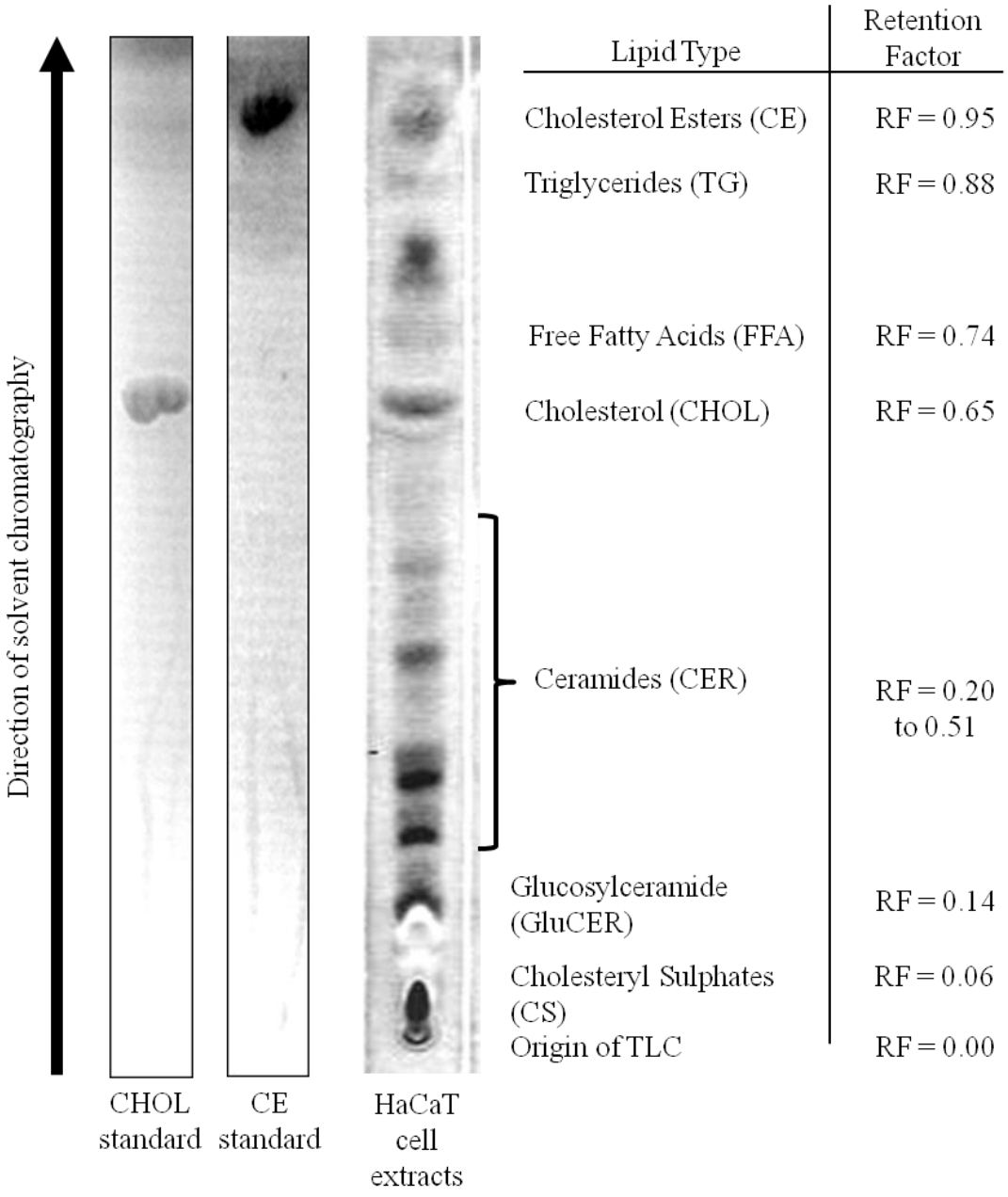


**Figure 4.10. Identification of Epidermal Lipids by TLC**

Figure showing thin layer chromatography (TLC) separation of lipids from 3D Cultured HaCaT cells, along with cholesterol and cholesterol oleate (a cholesterol ester) standards. Other lipids identified by ASAP-MS and published literature (Suhonen et al, 2007). Lipid types and RF values are indicated.

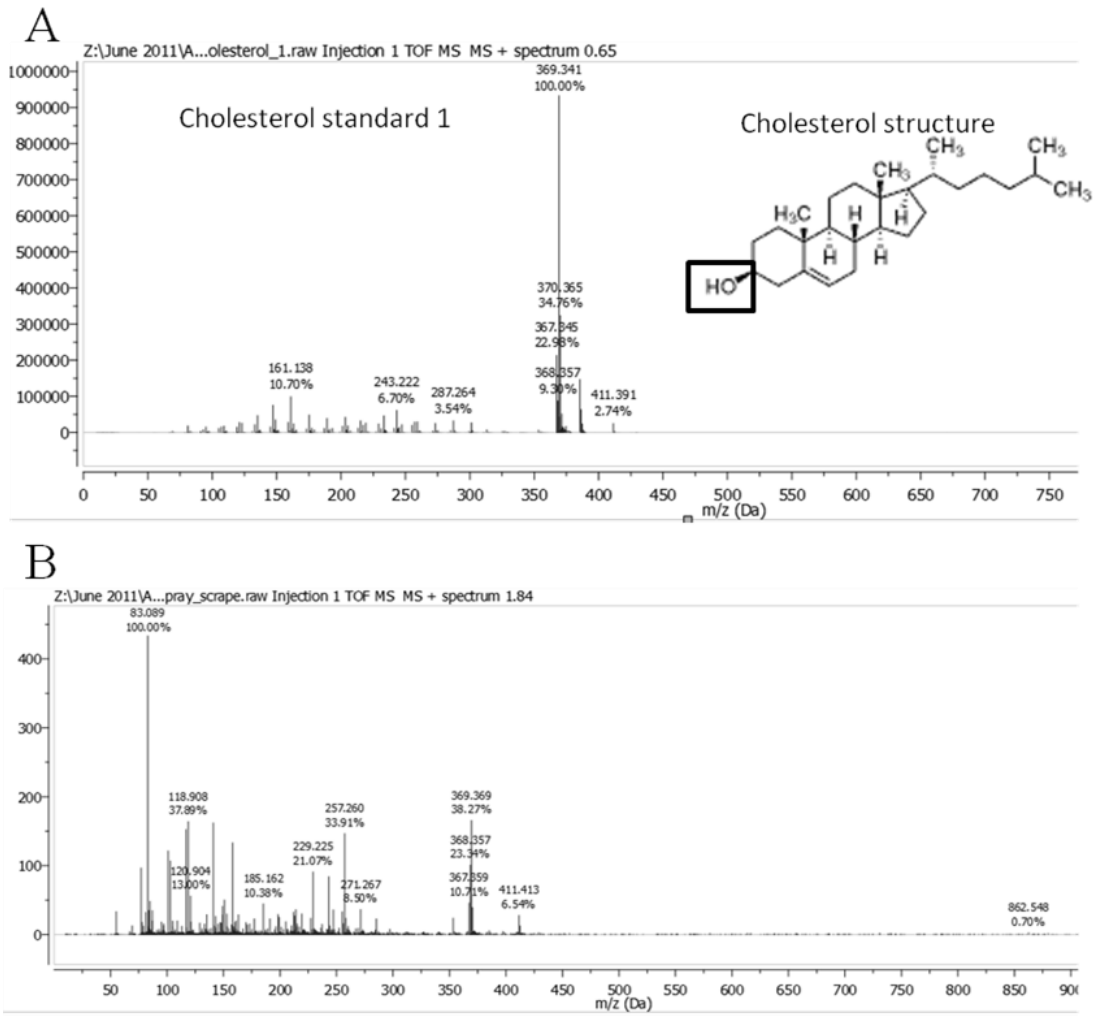


**Figure 4.11. ASAP-MS Analysis of Cholesterol Sample and Standard**

A) ASAP-MS scan of 99.9% pure cholesterol standard. The sample shows a high purity with low amounts of background. The strong peak at 369.3 corresponds with Durham University internal library data for cholesterol. The cholesterol molecule is presented, with the OH group indicated as the likely cleavage site (source: manufacturer data sheet for standard molecule); B) 3D cultured HaCaT cell lipid extract separated on the TLC plate and a band at RF = 0.65 (corresponding to cholesterol) scraped from the TLC plate and subjected to ASAP-MS analysis. There is more "background", likely from the solvents used in TLC separation, as well as the silica gel coating of the TLC plate. However, a peak at 369.3 is still observed. Note that the peak at 411.4 present in both samples is the contaminant plasticiser Diiooctyl phthalate, found in rubber/plastic tubing of the analyser (source: Durham University internal standards).

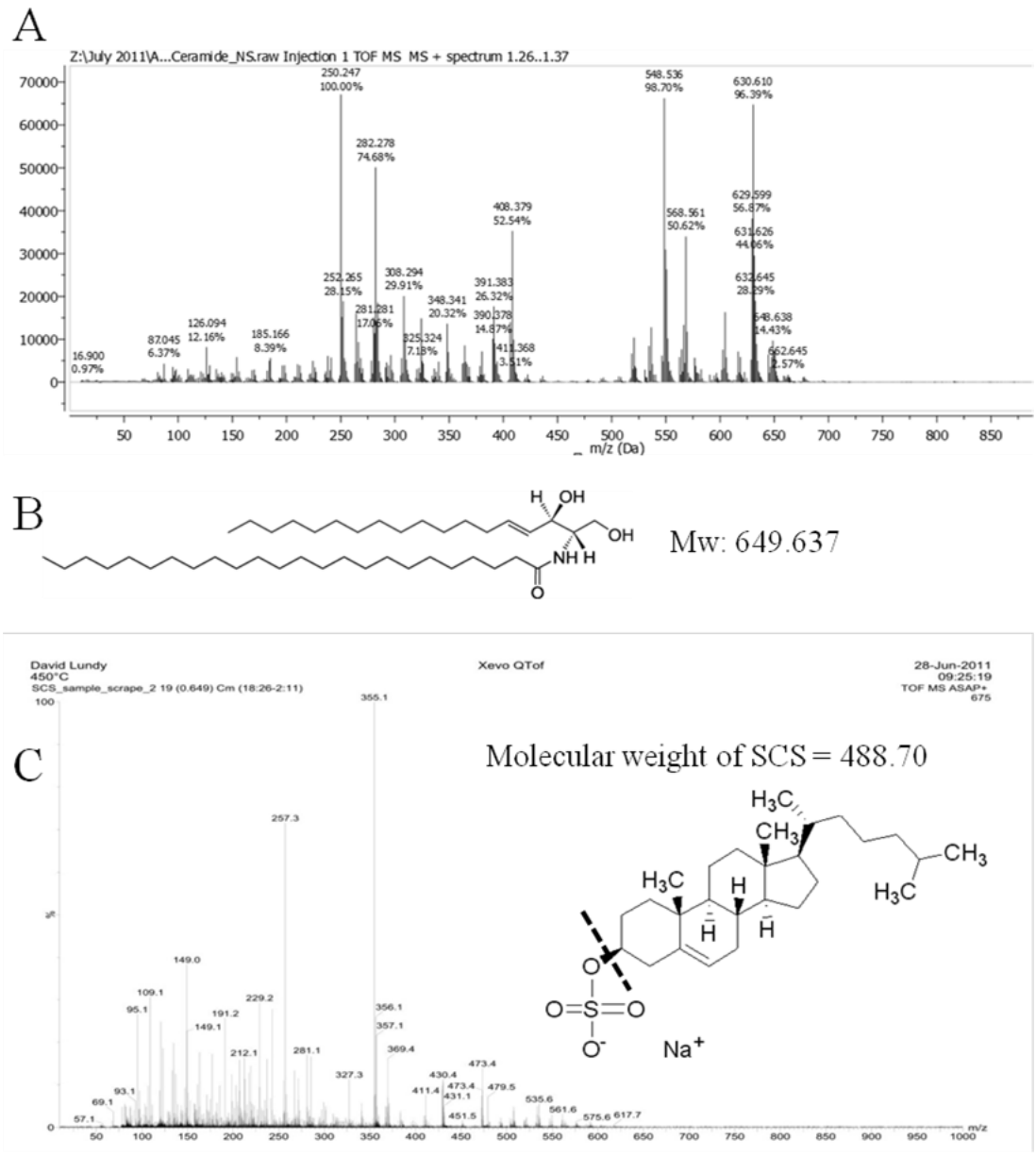


**Figure 4.12. ASAP-MS Analysis of Sodium Cholesterol Sulphate and Ceramide**

A) Mass spectra of nonhydroxyceramide (Ceramide NS) band scraped from TLC plate. The largest two bands are m/z = 548.5 and 630.3. Both correspond to ceramide NS. B) Structure of ceramide NS molecule with molecular mass 649.637; C) Mass spectra of sodium cholesterol sulphate (SCS) scraped from TLC plate. The largest peak is at 355.1. The structure of SCS molecule is shown with the likely breakage point indicated by a dotted line (source: manufacturer data sheet for standard molecule).

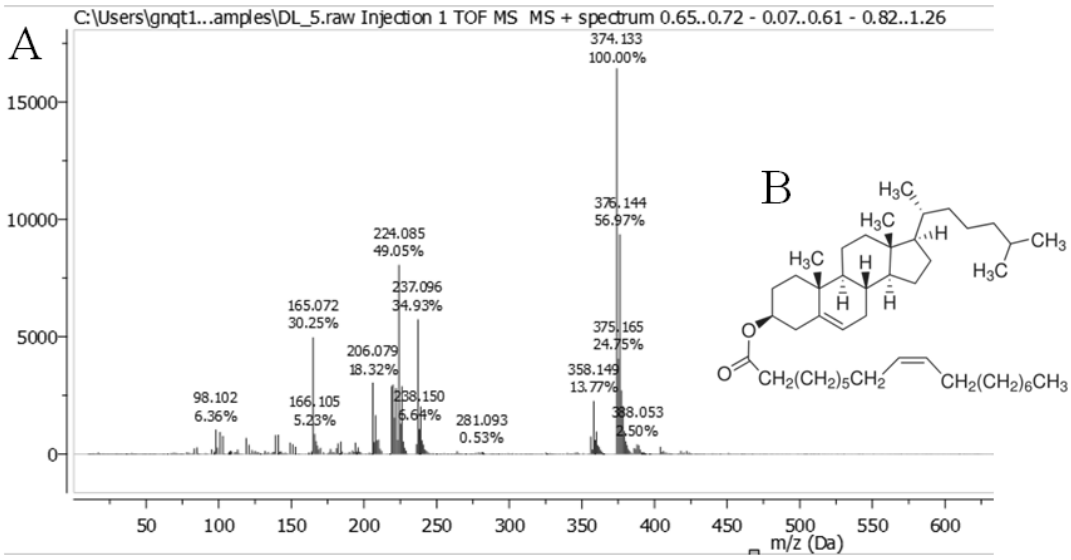


**Figure 4.13. ASAP-MS Analysis of Cholesterol Ester (Cholesterol Oleate)**

A) Mass spectra of cholesterol ester band identified by Rf value and scraped from TLC plate. The largest band is m/z = 374.1; B) Diagram of the cholesterol oleate molecule for reference (source: manufacturer data sheet for standard molecule).

Figure 4.12A shows the mass spectra for ceramide NS which was extracted from HaCaT cells, separated by TLC, scraped from the TLC plate and analysed by ASAP-MS. Evenly spaced peaks 16 Da apart (364.4-348.3),(324.3-308.3),(536.5-520.5) are from cleavage of the long carbon chains in the molecule. Literature confirms the band at m/z = 630.3 (Astarita et al, 2011) and 548.5 (Duh et al, 1992) to both be ceramide ions. A small band is visible at 648.6, corresponding to exactly the mW of the intact ceramide molecule, minus one hydrogen. This confirms that bands identified as ceramide on the TLC plate are indeed ceramides.

Figure 4.12C shows the ASAP-MS results for sodium cholesterol sulphate. This molecule has a mW of 488.7 but is based on a cholesterol molecule of mW 386.6. The most likely breakage point for the molecule is the loss of the SO4 group (mW 96.0) as well as the $Na^+$ molecule (23.0), annotated in Figure 4.12C. This leaves 369.7 - i.e. the m/z for cholesterol, which is detected in a small amount in the shown mass spectra. Furthermore Wu-Nan Wu, 2006 confirms that m/z 355.1 corresponds to cholesterol sulphate.

Figure 4.13 shows the mass spectra for cholesterol oleate, a cholesterol ester representing 45% of cholesterol esters in adult epidermis (Masahiro and Masao, 2007, Tachi et al, 2008). The dominant peak is 355.1, which corresponds to cholesterol esters (Onorato et al, 2012). The cholesterol ester band on the TLC was already confirmed by the RF value for a standard as shown in Figure 4.10.

In summary, these ASAP-MS results show that the main epidermal lipids cholesterol, cholesterol sulphate, cholesterol ester and ceramides have all been identified correctly on the TLC plate and verified by a second technique. Using the RF values of these known compounds, it is possible to use published literature to identify other bands on the TLC plate which fall between the known bands.

#### 4.2.3.4 Lipid Profile of 2D Cultured Keratinocytes

Cell lipid extracts from HaCaTs grown in 2D conditions were separated on a TLC plate, bands identified by Rf value and each band quantitated by densitometry in ImageJ. Results are summarised in Figure 4.14.

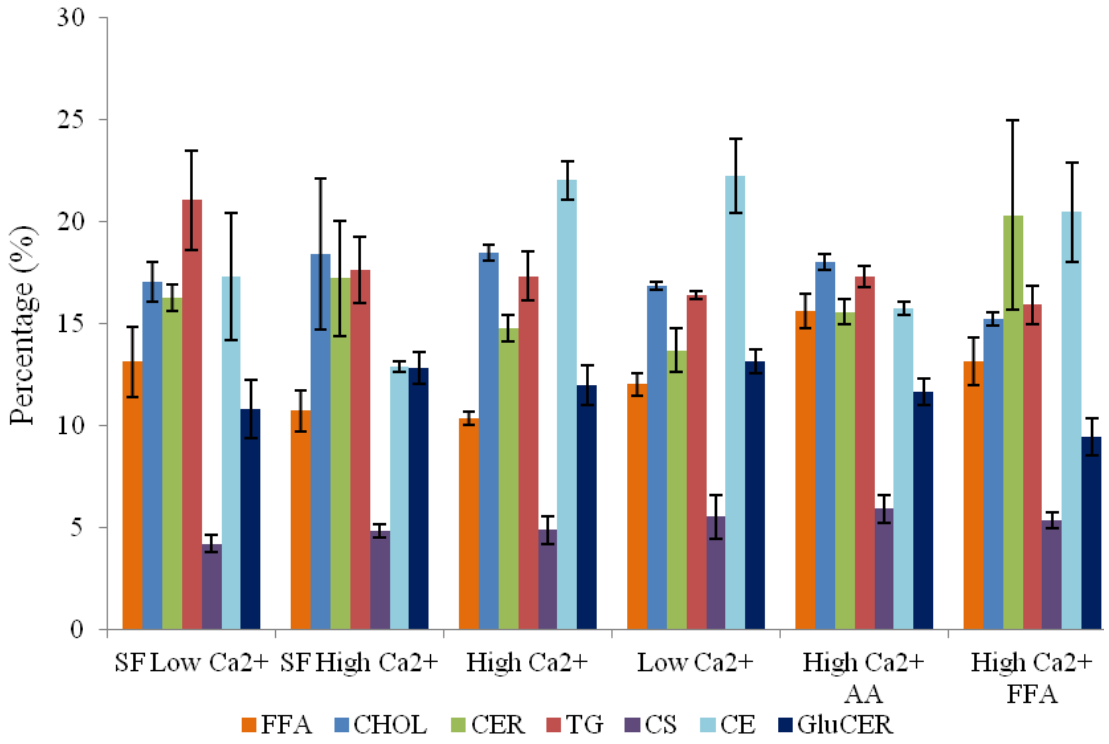


**Figure 4.14. Lipid Profile of HaCaT Cells Cultured in 2D**

Lipid extracts from HaCaTs grown in 2D for 7 days under various conditions. SF = serum free. High/low $Ca^{2+}$ = 1.5mM/0.06mM calcium, AA = 100µg/ml ascorbic acid, FFA = added mixture of free fatty acids. CER = ceramides, CHOL = cholesterol, FFA = free fatty acids, TG = triglycerides, CE = cholesterol esters, CS = cholesterol sulphate, GluCer = glucosylceramides. Error bars show SEM.

Lipids isolated from 2D HaCaT cells display an immature lipid profile, as expected. Findings are summarised in **Table 4.2**:

**Table 4.2. Lipid Composition of 2D Cultured Keratinocytes**

| **Lipid** | **% in 2D cultures (lowest-highest)** | **% in human epidermis or stratum corneum*** |
|---|---|---|
| Cholesterol esters | 12-22 | 6-10% |
| Cholesterol | 16-18 | 20-25% (30% of SC) |
| Triglyceride | 16-21 | 6-12% |
| Ceramides | 13-18 | 30-50% (30-50% of SC) |
| Free Fatty Acids | 10-15 | 8-20% |
| Cholesterol sulphate | 3-5 | 5% (1% of SC) |
| Glucosylceramides | 10-13 | 2-3% |

**Data combined from Moghimi et al, 1996, Netzlaff et al, 2005, Pappinen et al, 2008, Elias et al, 2012.*

Although cholesterol esters are some of the most hydrophobic lipids found in the epidermis (Masahiro and Mirao, 2007), 2D cultures produced an increased proportion of cholesterol esters which, conversely, is indicative of immature epidermis (Netzlaff et al, 2005). Cholesterol content was similar, albeit slightly lower than human epidermis in all samples. There was also no significant difference in cholesterol proportion between any of the culture groups in 2D, even though high calcium and supplemented ascorbic acid and FFA would have all been expected to increase cholesterol production.

Triglyceride production was much higher than human epidermis, which may be associated with an immature epidermal barrier or a defect in lipid conversion pathways (Demerjian et al, 2006). Cholesterol sulphate ($CSO_4$) levels are similar in 2D cultures and human epidermis, but both are greater than in human stratum corneum. In human epidermis, cholesterol sulphate is mostly located in the granular layer, and is only present at low concentrations in the stratum corneum (Lampe et al, 1983, Masahiro and Masao et al, 2008). This again suggests an immature profile of lipids.

Ceramide is mostly synthesised during later stages of differentiation (Baroni et al, 2012) and in all 2D cultures, ceramide content was significantly lower than human

epidermis or stratum corneum. In the FFA culture condition with added linoleic acid, ceramide content was a significantly greater percentage than found in other culture conditions, which is in line with findings by Breiden et al, 2007. Glucosylceramides were also found in higher concentrations in 2D culture conditions compared to human epidermis.

In summary, cells cultured in 2D display a lipid profile of immature epidermis, including a higher proportion of lipid precursors such as glucosylceramides, and lower proportion of mature end-products such as ceramides or cholesterol. The addition of supplements to the culture media did alter some properties of the lipid profile (as well as increasing the total amount of lipid produced (Figure 4.9)), but none were able to produce a lipid profile corresponding to mature epidermis. This corresponds to data shown previously (Figure 4.7) where HaCaTs are unable to fully differentiate in 2D culture. However, they can terminally differentiate and produce cornified envelopes when grown in the 3D scaffold.

#### 4.2.3.5 Effect of Culture Media on Keratinocyte Differentiation in 3D

The previous experiment was repeated using HaCaT cells cultured in the 3D scaffold using methodology described earlier. The 3D environment provides a more favourable environment for the differentiation of HaCaT cells by providing a longer culture period, a greater number of cells, increased cell-cell communication as well as an air-liquid interface which was shown (Figure 3.8) to induce differentiation and cornified envelope formation (Figure 4.7).

The 3D scaffold model is serving two main purposes: firstly for testing compounds on the 3D model described so far to better understand their effects, and secondly for optimising the current model for lipid synthesis and barrier function. By testing in 2D and 3D, the effect of the environment on how HaCaT cell differentiation and lipid production is altered by culture conditions can be determined.

Lipids were extracted from 3D cultures by an adaptation of the previous protocol, described in the materials and methods chapter. A bar chart showing the total amount of lipids isolated after 14 days at the air-liquid interface in Figure 4.15. Separate scaffolds from the same treatment groups were also fixed and processed for H&E staining (Figure 4.16) and involucrin staining (Figure 4.17) to examine the effect of each treatment on cell morphology and differentiation.

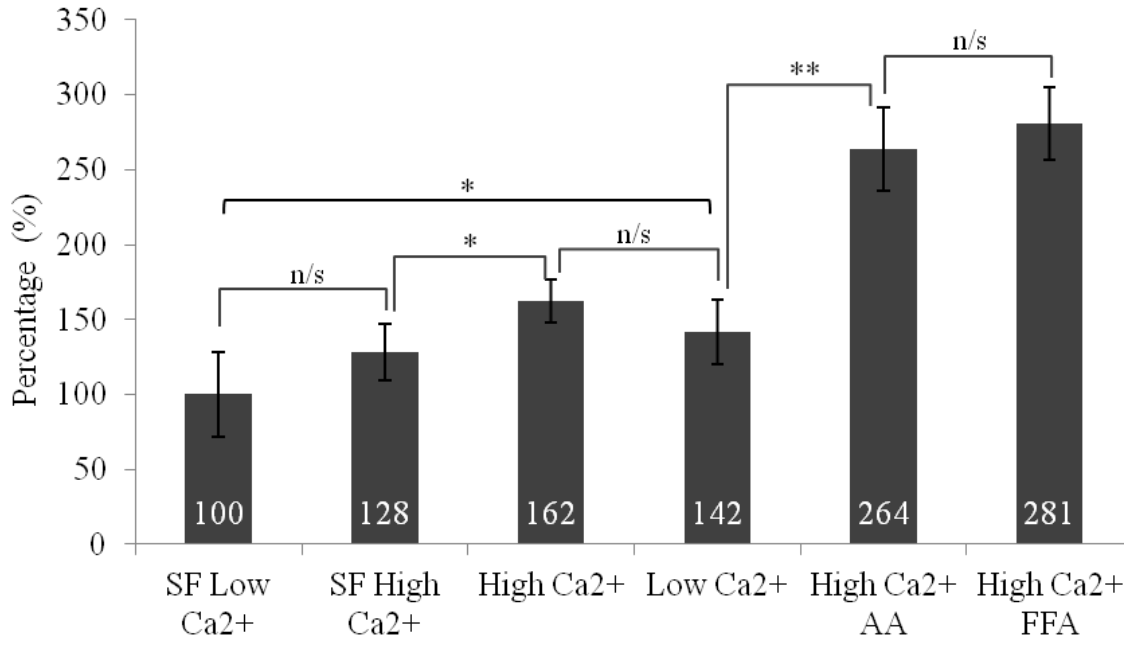


**Figure 4.15. Total Lipids Isolated from 3D Cultures**

Lipids isolated from 3D cultures grown for 14 days at the air-liquid interface. Normalised against protein concentration and the total lipid extracted from serum free low calcium culture conditions. SF = serum free, High/low Ca2+ = 1.5mM/0.06mM, AA = 100µg/ml ascorbic acid, FFA = added cocktail of free fatty acids. Error bars show SEM. * = P<0.05, ** = P<0.01, n/s = not significant.

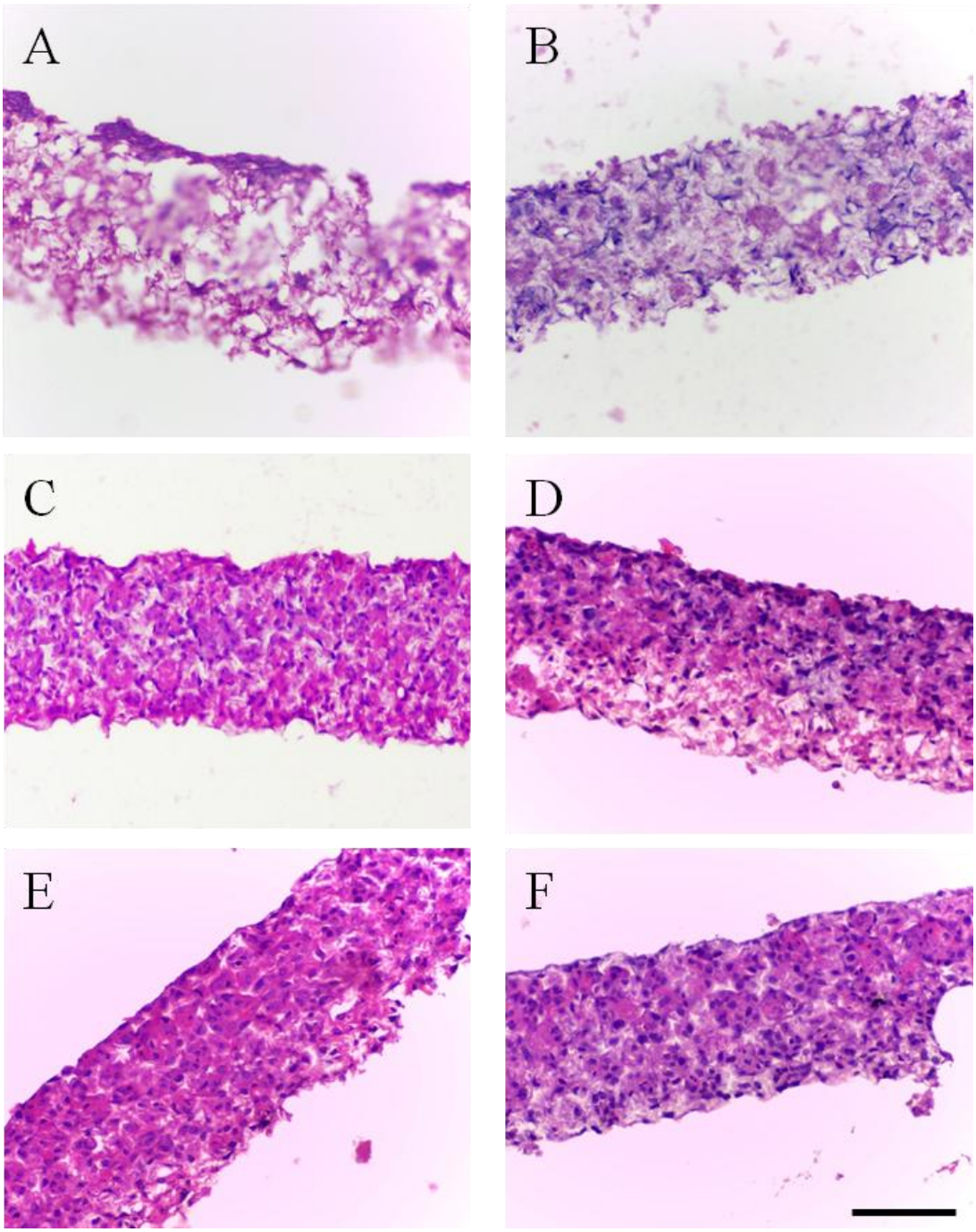


**Figure 4.16. H&E Images of 3D Cultures in Modified Culture Conditions**

H&E images from HaCaTs grown in 3D scaffold for 14 days at air-liquid interface under A) low calcium, serum free; B) high calcium, serum free; C) high calcium 10% FBS; D) low calcium, 10% FBS; E) As C with 100µg/ml ascorbic acid; F) as C with FFA. All cultures appear intact although comparatively few nuclei are observed in A and B. Scale bar 100µm for all images.

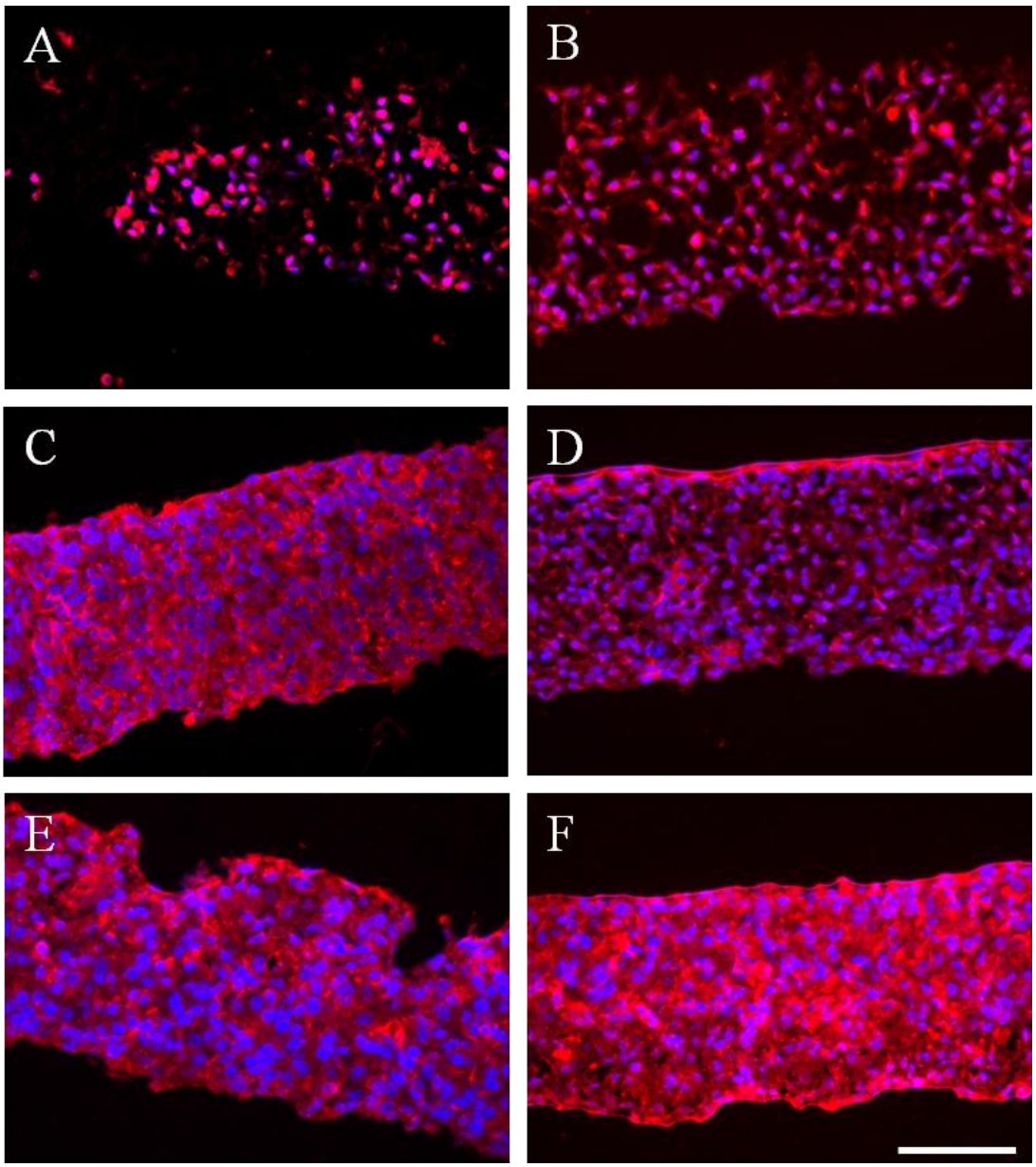


**Figure 4.17. Involucrin Immunofluorescence of 3D Cultures in Modified Culture Conditions**

Involucrin stained sections from HaCaTs grown in 3D scaffold for 14 days at air-liquid interface under A) low calcium, serum free; B) high calcium, serum free; C) high calcium 10% FBS; D) low calcium, 10% FBS; E) As C with 100µg/ml ascorbic acid; F) as C with FFA. Scale bar 100µm for all images.

It was found that the pattern of lipid production is similar in 3D compared to 2D, although the differences between groups are more pronounced in the 3D environment (Figure 4.15). For example, in 2D the addition of 1.5mM Ca2+ increased lipid production by 14%, but in 3D this difference was 28%. In 2D, the addition of serum increased lipid content by 22% for low calcium and 21% for high calcium, but in 3D the increase was 42% and 46% respectively.

The addition of serum or high calcium concentration significantly increased the amount of lipid produced by HaCaT cells in the 3D cultures. Interestingly, where the addition of ascorbic acid or FFA slightly reduced the lipid production of HaCaT cells in 2D (compared to high calcium with serum), it increased the lipid production significantly in 3D. Compared to high calcium and FBS alone, the addition of 100µg/ml increased lipid synthesis in the 3D culture by 63% and FFA supplementation increased lipid synthesis by 73%. These increases are in line with published literature (Uchida et al, 2001, Breiden et al, 2007).

H&E images (shown in Figure 4.16) from HaCaTs grown in the 3D scaffold under these conditions show that all cultures were able to proliferate and fill the scaffold, although there are visible differences in the morphology of some culture conditions. Due to serum free growth conditions, panels A and B show less visible nuclei and more "debris" than images C, D, E or F. Cells in grown in high calcium but serum free condition (Figure 4.16B) show sparse flattened nuclei among large amounts of non-specific cytoplasmic staining. All scaffold cultures grown with 10% FBS (Figure 4.16C, D, E and F) show a healthy morphology with no distinctly visible differences in appearance.

In order to quickly approximate the level of differentiation of these cultures, sections were stained for the differentiation marker involucrin. Images were taken at the same exposure, so that a comparison of expression can be made. These images (Figure 4.17) show a definite increase in involucrin expression when serum is added to the culture conditions. Panels A and B show very little involucrin staining whereas images C, D, E and F all show strong staining. Panel C (high calcium with 10% serum) staining clearly visible in cell cytoplasm throughout the full thickness of the scaffold with generally more staining towards the upper surface of the scaffold. Image D shows an interesting pattern of involucrin expression, where comparatively less staining is observed throughout the scaffold, and the majority is found on the

flattened, air-exposed surface. This is more in line with Involucrin distribution in native human epidermis. Image E (100µg/ml ascorbic acid with high calcium) shows a involucrin staining throughout the scaffold, although slightly less than in image C whereas image F (high calcium, with serum and FFA) shows an largely increased amount of involucrin. It is clear from these images that differentiation is occurring, and is increased by the presence of 10% FBS, high calcium concentration and free fatty acids in the culture media. Due to the lack of stratified layers and nucleated corneocytes observed in TEM analysis, the focus of these experiments was on increasing keratinocyte differentiation, which conditions C and F in particular have appeared to accomplish. However, in hindsight it is probable that this differentiation is too accelerated and that culturing the cells for a longer duration at the air-liquid interface in low calcium media (condition D) may have been optimal. This is due to reduction in the barrier function associated with premature differentiation observed in Chapter Five.

#### 4.2.3.6 Keratinocyte Lipid Synthesis in 3D

The lipid extracts from 3D cultures were then subjected to separation on TLC plates. A sample of mouse back epidermis was also subjected to lipid extraction and quantification. Examples of these separations are shown in Figure 4.18. Visual comparison of the TLC lanes from HaCaT cells cultured at the air-liquid interface (Figure 4.18A) and mouse epidermis (Figure 4.18B) show a strong overall similarity. Hexane washing of mouse epidermis was found to reduce the amount of contamination from subdermal lipids (primarily triglycerides) as well as sebum and wax and allowed clearer separation of epidermal lipids into distinct bands. All major lipid classes were observed after hexane washing.

Lipid profiles for both submerged and air-liquid interface 3D cultures at several time points were quantified and expressed as a bar chart, shown in Figure 4.19B. The lipid composition of mouse epidermis was also quantified and is shown for comparison.

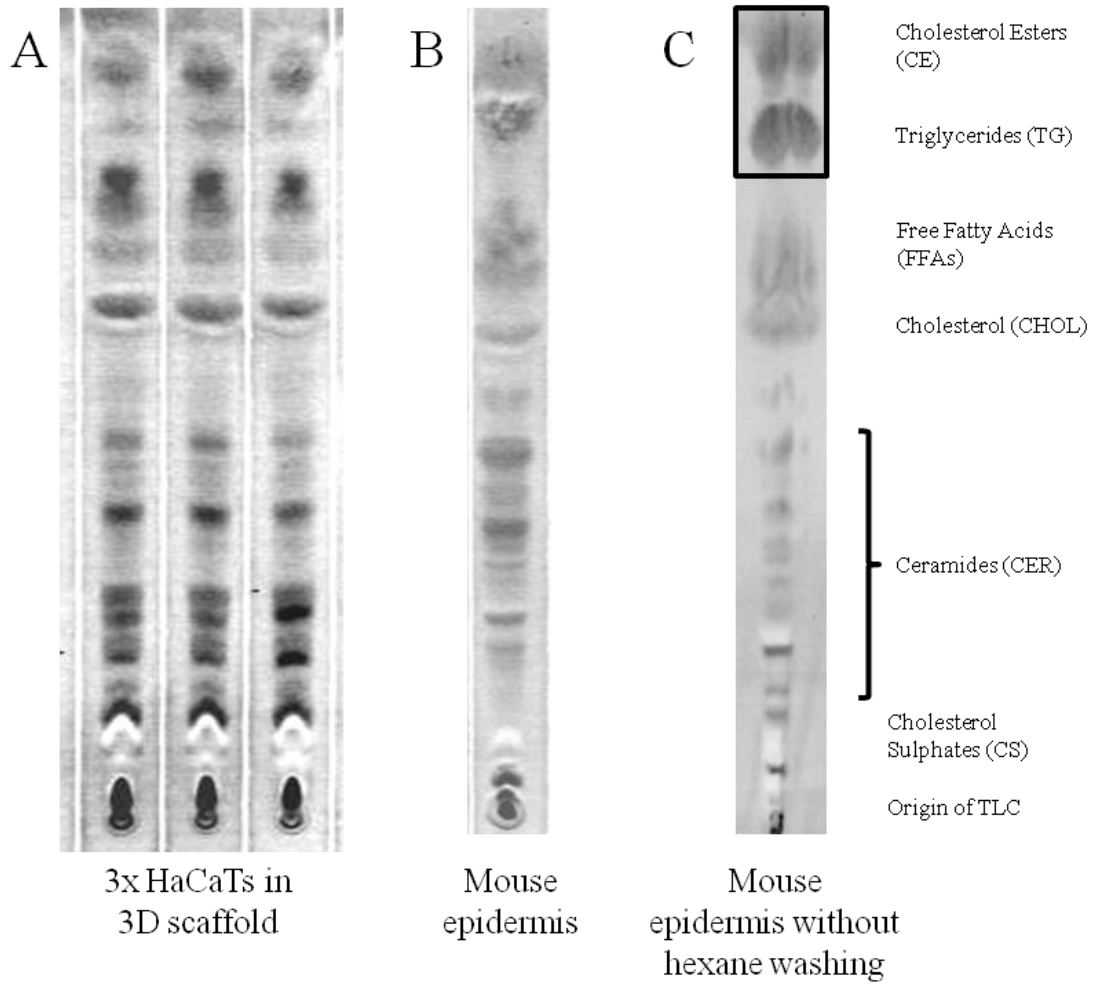


**Figure 4.18. TLC Lanes from 3D HaCaT Culture and Mouse Epidermis**

Images showing sample TLC separation of lipids extracted from A) 3D cultured HaCaT cells; B) mouse epidermis; C) non hexane-washed mouse epidermis. Similarities in the lipid content of 3D cultures and mouse epidermis are evident, although the distribution of individual ceramides appears different.

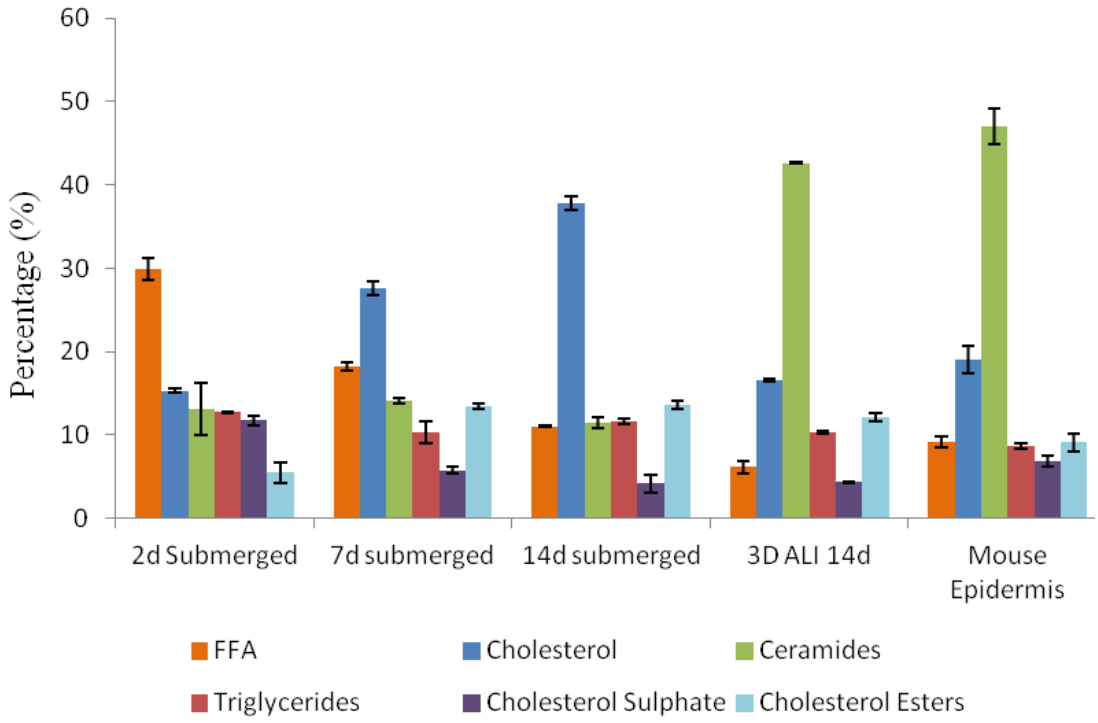


**Figure 4.19. TLC Analysis of 3D Cultured HaCaT Cells**

Table showing % lipid composition of 3D cultured HaCaT cells after 2, 7 or 14 days submerged or 14 days at the air-liquid interface compared to mouse epidermis. It is apparent that submerged cultures display a different lipid profile than those cultured at the air-liquid interface.

After 2 days submerged in the 3D scaffold, (Figure 4.19), the most predominant lipids found in HaCaT cells are free fatty acids. In comparison to mouse epidermis and HaCaTs grown at the air-liquid interface, the lipid profile of the submerged keratinocytes is profoundly different. Submerged cultures show a higher proportion of FFA and less cholesterol and ceramides. This is a similar profile to the lipid profiles observed in 2D culture shown in Figure 4.14. Interestingly, highly hydrophobic cholesterol esters were found in lower proportions in submerged 3D cultures than in standard 2D cultures.

After 7 and 14 days in submerged cultures, the most predominant lipid produced is cholesterol (28% and 38% respectively) which is markedly higher than the cholesterol content of mouse epidermis. Ceramides in submerged cultures (14% and 11% after 7 and 14 days respectively) are significantly lower than the proportion in mouse epidermis. As mentioned previously, low ceramide content indicates an immature epidermal barrier. Earlier data (not shown) showed that between 7 to 14 days submerged, the total amount of lipid produced by submerged HaCaT cells does not change. However, the lipid profile after 7 and 14 days in submerged cultures are slightly different overall. Through 2 to 14 days of submerged culture, the proportion of FFA in the culture decreases while the proportion of cholesterol increases. However, ceramides remain in very low proportions (11-14%) in all submerged cultures.

In contrast, after 14 days of culture at the air-liquid interface, the overall profile is significantly different submerged cultures and is much more similar to mouse epidermis. In 3D cultures at the air-liquid interface ceramides make up the majority (43%) of the epidermal lipids, similar to mouse epidermis (47%) and published data for human epidermis (30-50%, Pappinen et al, 2008). This shows that the air-liquid interface has a profound effect on the lipid composition of HaCaT cells. Previous experiments have shown that HaCaT cells inside the 3D scaffold undergo a small amount differentiation when submerged (as determined by involucrin and K1 staining), but these data show that the air-liquid interface is an important factor in lipid production. Even though there are still differences between the 3D cultured HaCaT cells and mouse epidermis, the 3D air-liquid interface cultured sample is clearly the closest of all the conditions examined. Therefore, both samples were expressed side by side in a comparative bar chart, shown in Figure 4.20.

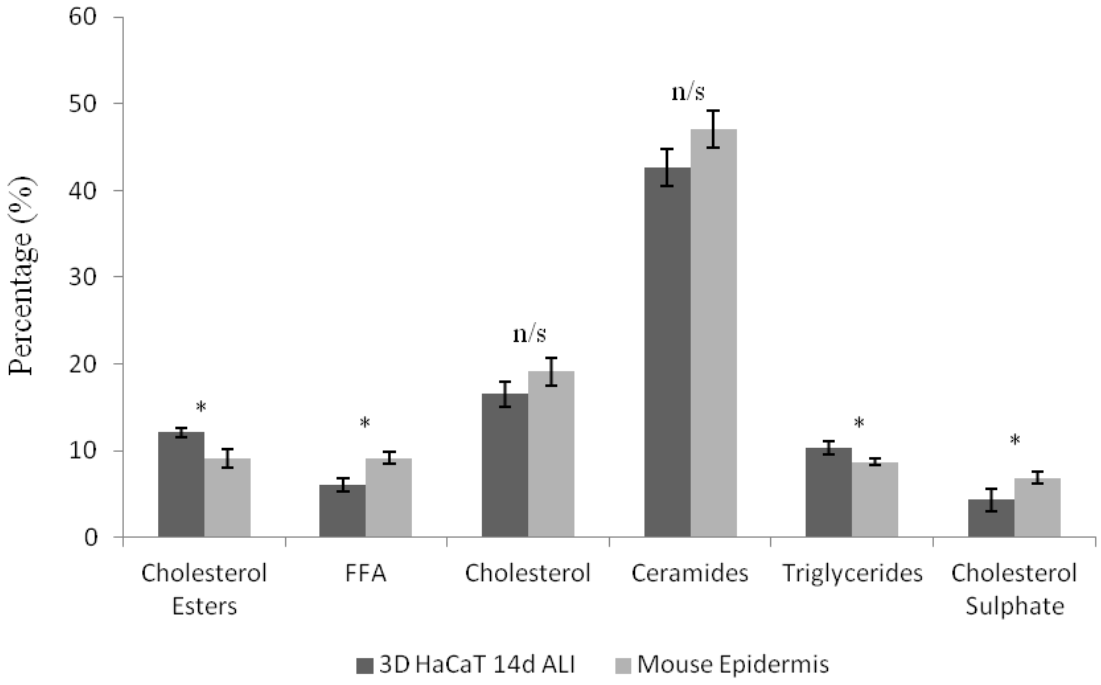


**Figure 4.20. Lipids of 3D Scaffold Cultures Compared to Mouse Epidermis**

Graph showing % lipid composition of 3D HaCaT culture (14 days air-liquid interface) compared to mouse epidermis. Error bars show SEM. * = $P<0.05$, n/s = not significant.

Analysis by t-test in Figure 4.20 shows that significant differences ($P<0.05$) are observed in the proportion of free fatty acids, triglycerides, cholesterol esters and cholesterol sulphate. However, cholesterol and ceramides show a statistically similar proportion. This shows that HaCaT cells cultured at the air-liquid interface for 14 days in the 3D scaffold display a mature lipid profile, similar to native epidermis in many aspects, aside from the proportion of FFA in the cultured epidermis samples are significantly lower than human epidermis (usually 10-15%, Pappinen et al, 2008).

#### 4.2.3.7 Effect of Culture Media on Lipid Synthesis in Keratinocytes Cultured at the Air-liquid Interface

3D cultures were then grown in the 6 different culture medias outlined previously in Table 4.1. Cultures were grown submerged for two days in standard culture conditions, then raised to the air-liquid interface and changed into the above media where they were kept for 7 or 14 days. Lipids were extracted, separated by TLC and quantitated as previously shown. Results for cells cultured for 7 and 14 days were expressed in a series of bar charts shown in Figure 4.21.

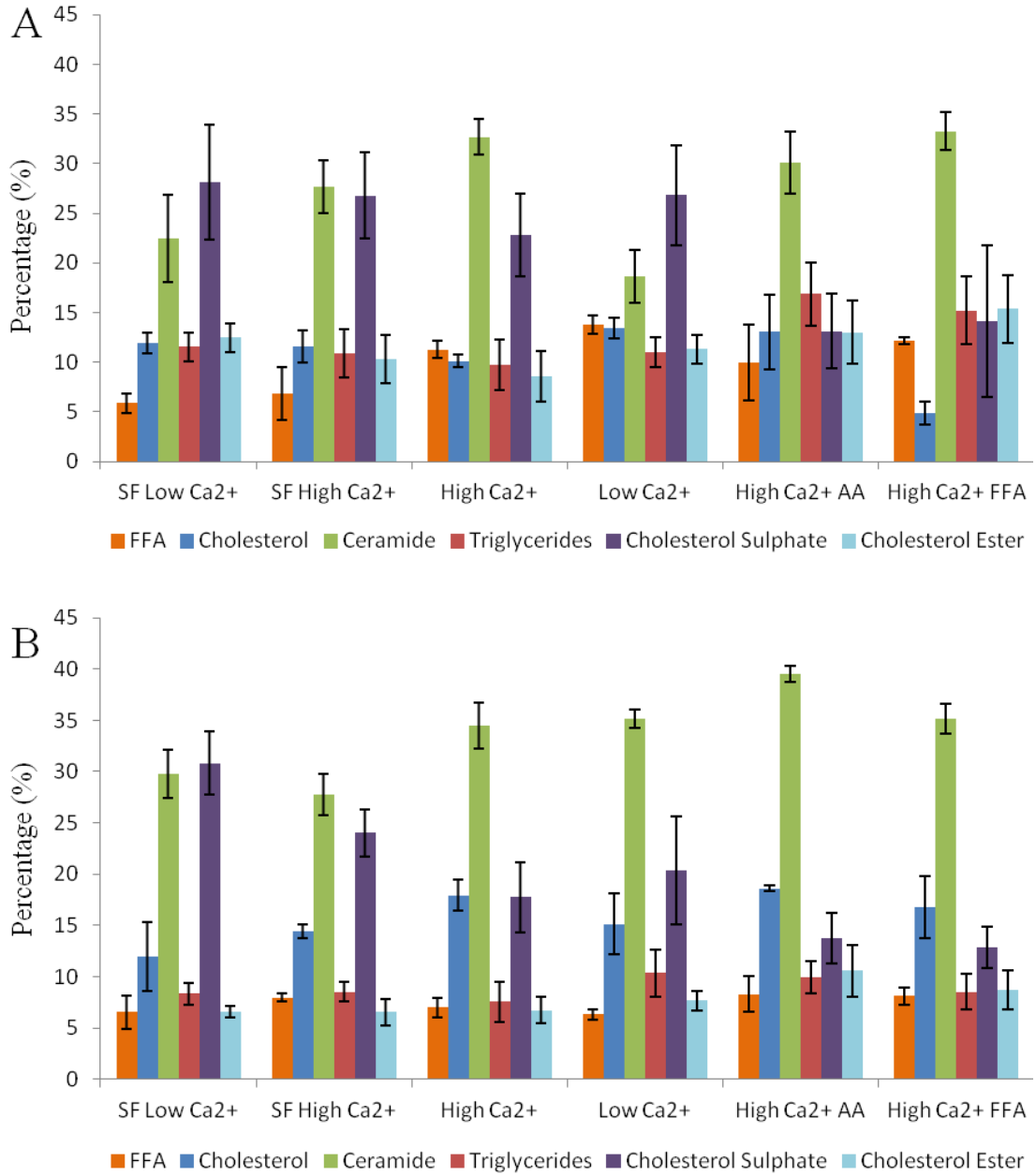


**Figure 4.21. Lipid Composition of 3D Culture HaCaT Cells After 7 and 14 days**

Graphs showing lipid composition of HaCaT cells after A) 7 days at the air-liquid interface and B) 14 days at the air-liquid interface in various culture conditions. Culture conditions as follows; SF = serum free, Low/Hight $Ca^{2+}$ = 0.06mM/1.5mM Ca2+, AA = 100µg/ml ascorbic acid, FFA = free fatty acids. Error bars show SEM.

A summary of the results in Figure 4.21 are shown below:

**Table 4.3. Summary of 3D Cultured Keratinocyte Lipid Profiles**

| **Lipid** | **% in 7d ALI (lowest-highest)** | **% in 14d ALI (lowest-highest)** | **% in human epidermis or stratum corneum*** |
|---|---|---|---|
| Cholesterol esters | 9-15% | 6-11% | 6-10% |
| Cholesterol | 5-15% | 12-19% | 20-25%<br>(30% of SC) |
| Triglyceride | 10-17% | 8-10% | 6-12% |
| Ceramides | 19-33% | 28-40% | 30-50%<br>(30-50% of SC) |
| Free Fatty Acids | 6-14% | 6-8% | 8-20% |
| Cholesterol sulphate | 16-27% | 13-30% | 5% (1% of SC) |

Figure 4.21 shows the lipid composition of 3D cultured HaCaT cells after 7 days and 14 days at the air-liquid interface. The increasing maturity of the epidermal barrier with time is apparent - for instance, the lipid composition of the culture comprises 18-33% ceramide after 7 days, whereas this has increased to 28-40% after 14 days. Cholesterol ester content decreases from high levels to physiologically normal levels between 7 and 14 days and cholesterol sulphate also decreases in most culture conditions. However, the proportion of FFA does not increase with time at the air-liquid interface, which would have been expected.

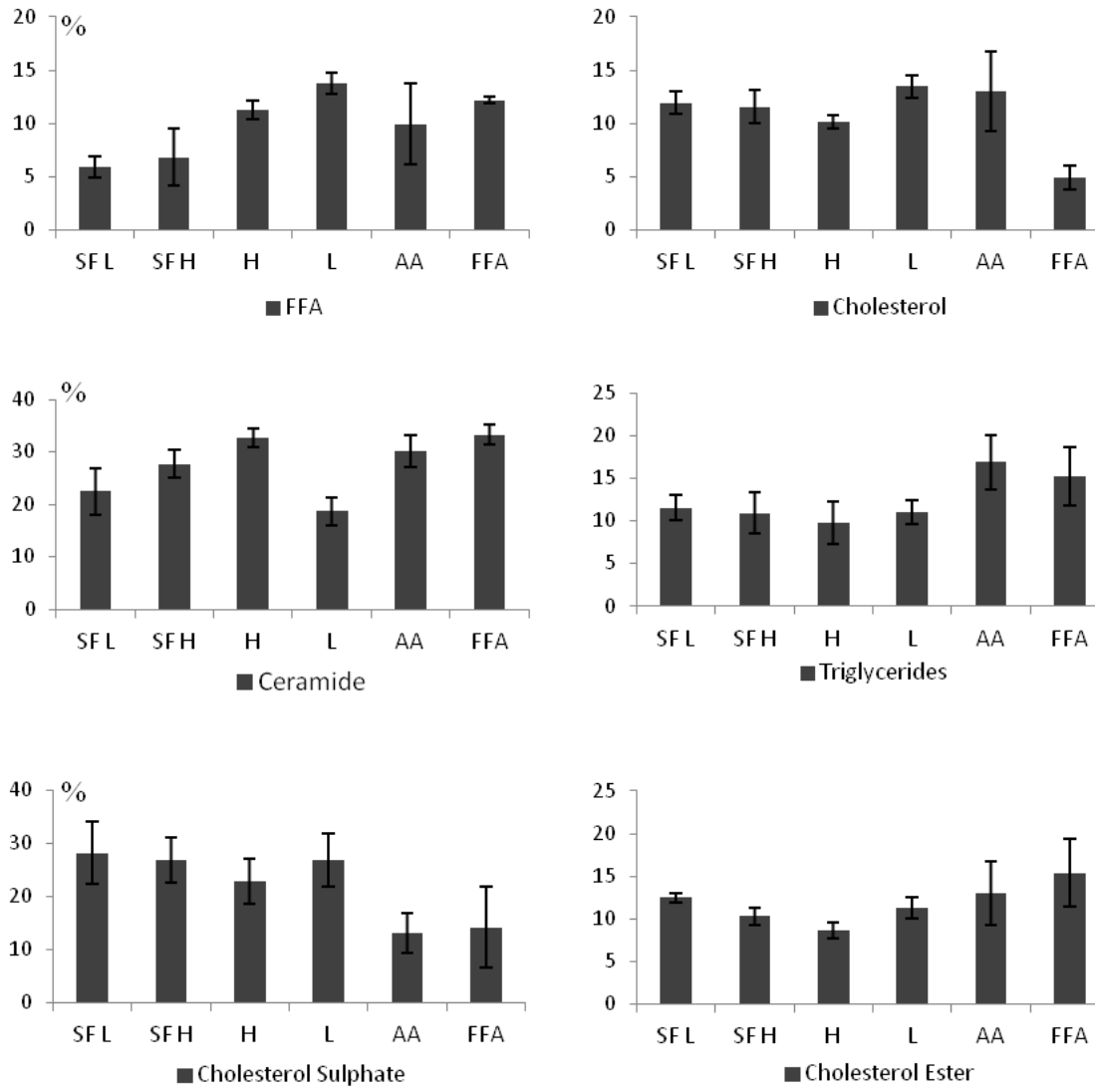


**Figure 4.22. Lipid Composition of 3D Cultured HaCaT Cells After 7 Days**

Graphs showing percentage lipid composition of HaCaT cells after 7 days at the air-liquid interface in various culture conditions. The percentage of each lipid is then compared separately for each culture condition. Culture conditions as follows; SF – serum free, L/H = 0.06mM/1.5mM $Ca^{2+}$, AA = 100µg/ml ascorbic acid, FFA = free fatty acids. Note changing y-axis throughout. Error bars show SEM.

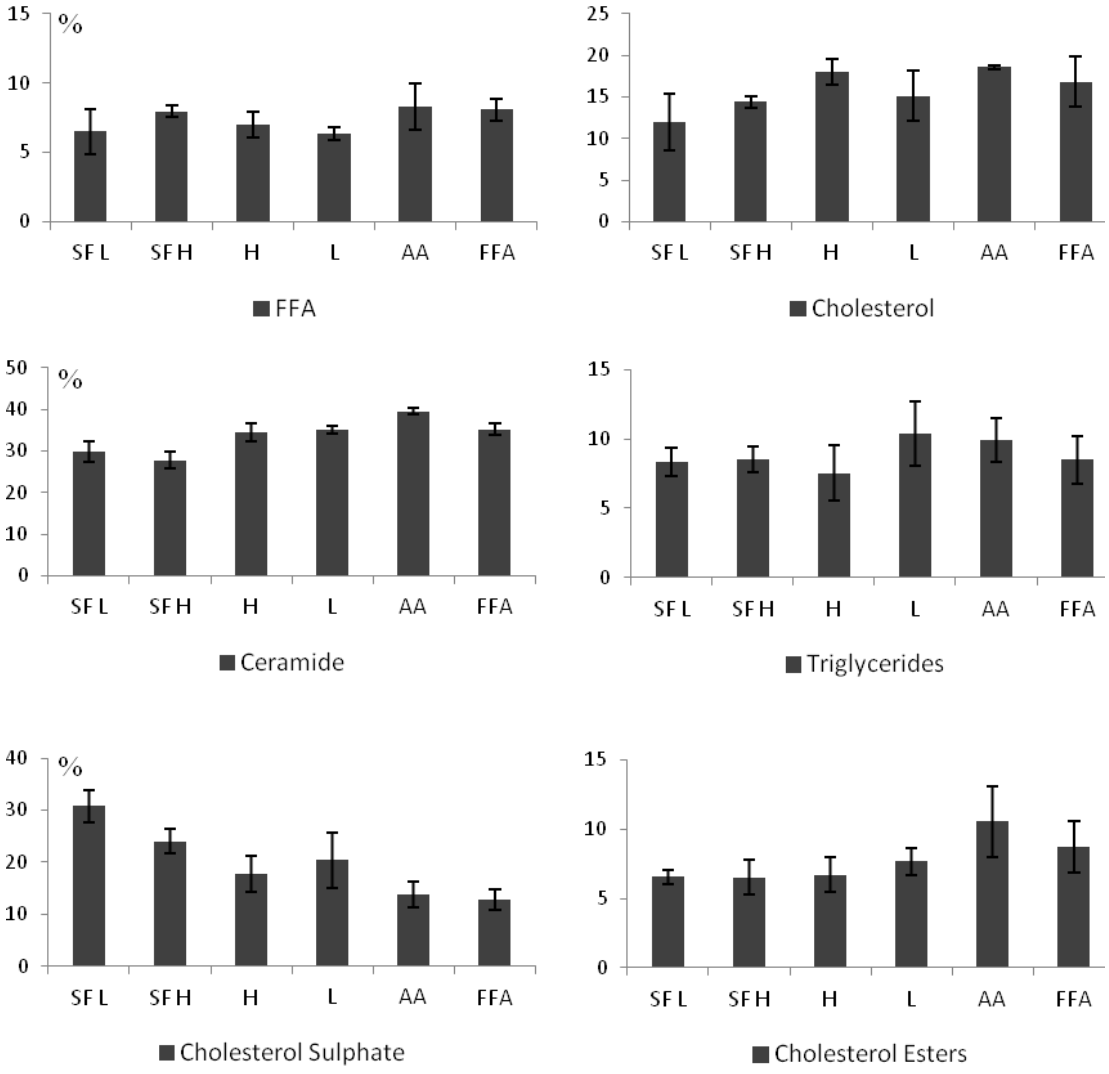


**Figure 4.23. Lipid Composition of 3D Cultured HaCaT Cells After 14 Days**

Graphs showing lipid composition of HaCaT cells after 14 days at the air-liquid interface in various culture conditions. The percentage of each lipid is then compared separately for each culture condition. Culture conditions as follows; SF = serum free, L/H = 0.06mM/1.5mM $Ca^{2+}$, AA = 100µg/ml ascorbic acid, FFA = free fatty acids. Note changing y-axis throughout. Error bars show SEM.

Lipid extracts from 7 days and 14 days at the air liquid interface are shown in Figure 4.22 and 4.23 respectively. After 7 days at the air-liquid interface, the addition of 10% serum to the culture media significantly increases FFA, as expected. Ascorbic acid and supplementation with FFA do not have any further effect on the total proportion of FFA produced by the cells. Calcium concentration does not appear to cause an increase in FFA, as neither the differences between SF-L and SF-H or H and L are significantly different to each other after 7 or 14 days at the air-liquid interface.

For cholesterol, no significant differences were observed between treatment groups after 7 days apart from the FFA-supplemented culture condition which has significantly lower cholesterol content. The reason for this is unknown. After 14 days there are no significant differences between treatment groups, including the FFA-treated cultures. Compared to 7 days, the cholesterol content of the 3D cultures has increased as a whole (12-19% at 14 days compared to 5-15% at 7 days).

For ceramide content, all cultures display a relatively high proportion of ceramide after 7 days (19-33%) which is close to native epidermis (30-50%). Again, the addition of serum and calcium are key factors in the proportion of ceramide in the lipid profile. Both low calcium culture conditions show the lowest percentage of ceramide content (19 and 22%) while high calcium culture conditions contain 30-33% ceramide. After 7 days, the addition of 100µg/ml or FFA to the culture media does not further increase the total ceramide content of the 3D culture compared to the high calcium only condition. After 14 days, ceramides have increased as a proportion of the lipid profile from 7 days (19-33%) to 14 days (28-40%), which is more physiologically accurate. The addition of serum makes the largest difference to the proportion of ceramides, although supplementation with 100µg/ml ascorbic acid also significantly increased ceramides, as predicted (Uchida et al, 2001).

After 7 days, triglyceride content varies between 10-17% with no significant difference between culture conditions, aside from 100µg/ml ascorbic acid which increased triglyceride content. After 14 days, no significant differences were observed between groups. Compared to 7 days, triglycerides fell slightly, ranging from 7.5-10.4%

Cholesterol sulphate content is quite high in all cultures after 7 days at the air-liquid interface, ranging from 13% to 27%, compared to around 5% in native human epidermis. This is interesting, as the addition of serum and/or high calcium makes no significant difference to the high proportion of cholesterol sulphate after 7 days at the air-liquid interface. However, ascrobic acid and FFA-supplemented culture conditions display the lowest cholesterol sulphate proportion. After 14 days, some of the treatment groups (high and low calcium with serum) show significantly lower cholesterol sulphate proportions than after 7 days, demonstrating increased maturity. Ascorbic acid and FFA-treated cultures display a significantly lower level of cholesterol sulphate compared to other treatment groups, reduced by almost 50%. This may indicate that these cultures are more differentiated, or alternatively the conversion of cholesterol sulphate into other derivatives is accelerated.

Cholesterol esters are also found in a high proportion in some cultures after 7 days at the air-liquid interface, ranging from 9-15% (native human epidermis 6-10%). After 14 days at the air-liquid interface, cholesterol ester content is lower than after 7 days. However, in the case of ascorbic acid and FFA-treated cultures, cholesterol ester content has slightly increased.

Overall, all cultures show a lipid profile broadly comparable to mouse epidermis or native human tissue. All cultures display a more mature lipid profile after 14 days at the air-liquid interface compared to 7 days and differences lipid profile were observed in accordance with the culture media composition. Serum and ascorbic acid or FFA being the biggest determinants of lipid composition. On the other hand, calcium concentration did not appear to be a large determinant of lipid composition after 14 days. However, Figure 4.15 showed that high calcium culture conditions induce keratinocytes to synthesise more lipids in total, therefore showing that calcium is still a factor in keratinocyte lipid production.

## 4.3 Discussion

### 4.3.1 Summary of Results

Results have shown that keratinocytes can be cultured and induced to differentiate at the air-liquid interface in the 3D scaffold. Thin Toluidine Blue sections showed flattened cells throughout most of the thickness of the scaffold and SEM and TEM both confirmed that flattened keratinocytes were present in the 3D cultures. These methods also gave insight into the organisation of cells inside the 3D scaffold, showing that the keratinocytes are not organised into layers such as in native epidermis. Nevertheless, TEM imaging confirmed that most cells contain organelles associated with differentiation such as lamellar bodies and keratohyalin granules, and desmosomes were also observed throughout the culture, including attaching the flattened corneocytes. TEM imaging showed possible cornified envelope formation under the cell membranes of flattened, anucleate keratinocytes, and this was confirmed by cornified envelope extraction. Nile Red staining demonstrated that these cornified envelopes contained covalently attached lipids and that a mixture of mature and fragile cornified envelopes were present. An experiment demonstrated the importance of the 3D air-liquid interface in cornified envelope formation, as cells cultured in 2D did not produce cornified envelopes, even when induced to differentiate.

An investigation was performed to desmonstrate the effect of culture conditions on keratinocyte lipid synthesis. Results in 2D showed that keratinocytes cultured in serum-containing media or in high (1.5mM) calcium produced more lipids. These results were quantified by thin layer chromatography and the identities of lipid bands on the plate were confirmed by a mass spectrometry technique. As expected, cells cultured in 2D did not produce a physiologically accurate lipid profile in comparison to native epidermis, although supplementation of culture media with ascorbic acid and FFAs did improve this slightly.

When cultured in 3D, cells produced a markedly different lipid profile. Cultures which were left submerged for 14 days displayed an immature lipid profile, similar to 2D cultures, but those cultured at the air-liquid interface displayed a different, and more mature, lipid profile. When the culture media was altered, some morphological differences in the cultures were apparent and the amount of lipid extracted from cells

was dramatically increased, with cells in optimised conditions synthesising almost three times as much lipid than those in control conditions.

In terms of the lipid profile, a general improvement in the physiological accuracy of the profile was noted as the culture period extended from 7 to 14 days. In retrospect, a longer time period such as 21 or 28 days may have been beneficial. The addition of ascorbic acid and FFA to the culture media altered the lipid profile, increasing ceramides and reducing cholesterol sulphate.

#### 4.3.1.1 Ultrastructure and Cornified Envelope Formation

These results demonstrated that HaCaT cells are capable of reaching terminal differentiation inside the 3D scaffold. The flattened corneocytes observed by SEM in Figure 4.2 are similar to those observed by SEM in published literature (Mihara, 1988, Kunii, 2003) although the corneocytes in the 3D cultures appear more variable in size and have less smooth surfaces compared to those from human epidermis. They also appear less tightly connected, with more visible "stitching" around the edges of each corneocyte compared to human skin which shows a more "cobble stone" appearance (Naoe et al, 2008). This may be due to processing, such as the dehydration and critical point drying procedures carried out before SEM imaging. The polystyrene material of the scaffold can become charged (as visible by SEM image banding in Figure 4.2B) and so during preparation for SEM, a thicker layer of gold is applied during sputter coating which may have altered the surface of the sample.

SEM and TEM imaging also showed the possible presence of occasional nucleated, immature corneocytes on some of the air-exposed surface of the 3D cultures. These were sporadic but indicate that terminal differentiation is not uniformly complete across the whole surface of the culture. These immature, still-nucleated corneocytes have been linked by Kunii et al, 2003 to barrier dysfunction, measured by elevated transepidermal water loss (TEWL). Kunii et al, 2003 also found that when the epidermal barrier is defective from immature corneocytes, the ratio of cholesterol to ceramide content of the stratum corneum increases. Interestingly, this pattern of high cholesterol and low ceramide is found in a number of *in vitro* models (Ponec et al, 2000) although not in the 3D scaffold model as shown in Figure 4.20.

Lamellar bodies are characteristic of the stratum granulosum region of the epidermis and contribute towards the differentiation process and barrier formation by secretion of enzymes, proteins and barrier lipids (Ishida-Yamamoto et al, 2011). Lamellar bodies were noted in cells located throughout the 3D scaffold after fourteen days at the air-liquid interface, potentially indicating that many cells are in this stage of differentiation.

Some cells contained large number of vacuoles (Figure 4.4). These are a normal feature of differentiating epidermis, but excessive lipid vacuoles inside cells, particularly inside flattened cells or the stratum corneum, are indicative of a disorder of excess triglyceride retention (Ujihara et al, 2010). The overall triglyceride content of the 3D cultures was shown in Figure 4.21 to be marginally higher than native epidermis, although likely not high enough to indicate a pathogenic-type defect in lipid metabolism. TEM imaging only showed vacuoles inside nucleated cells and did not show any lipid vacuoles inside flattened corneocytes.

TEM imaging has been used by researchers to examine the lamellar bilayer organisation of the stratum corneum. In organised layers of the stratum corneum Warner et al, 2003 showed TEM images of stratum corneum with organised banding of lamellar lipids filling intercellular spaces between corneocytes. In TEM images, this is observed as alternating bands of electron dense and electron lucid layers. However, in the 3D scaffold model, this pattern of organisation was not observed because cells differentiate inside the polystyrene structure and do not form these layered structures. This is an interesting property of the epidermal equivalent formed by the 3D scaffold - showing that terminal differentiation (evidenced by cornified envelope production) can occur even without this layered organisation. It is likely that the absence of these organised lipid bilayers may have impact on the epidermal barrier function possible with the 3D scaffold. The barrier permeability of these cultures will be measured in the following chapter.

Numerous desmosomes were observed throughout the 3D cultured keratinocytes. Desmosomes in native epidermis normally degrade so that desquamation of the upper layers of stratum corneum can occur. These degrading desmosomes have been observed by Warner et al, 2003 as electron dense "mushy" desmosomes, as opposed to those shown in Figure 4.5. Neither desquamation or any desmosome degradation was observed in any 3D cultures subjected to TEM analysis. As an observation, more

desmosomes were observed in cultures maintained at the air-liquid interface compared to those which were submerged (data not shown).

Hydration of the epidermis is an important factor in barrier function. In particular, over-hydration of the stratum corneum causes structural changes in corneocytes, accelerated corneodesmosome degradation (Rawlings et al, 1995) and delaminated intercellular lamellae (Warner et al, 2003), which is an issue for certain occupations and for infants wearing nappies as it may lead to dermatitis. The data shown so far in this thesis again highlights the importance in the air-exposed surface and the drying of the upper layers of the 3D culture. Submerged cultures are morphologically different, show less evidence of differentiation, and produce a completely different profile of lipids (Figure 4.19).

Figure 4.6 and Figure 4.7 showed that cornified envelopes can be extracted from the 3D cultures to assess barrier maturity (as performed in Nolte et al, 1993, Sevilla et al, 2007). When compared to those from mouse ear tip epidermis, cornified envelopes from the *in vitro* 3D scaffold model displayed a more immature, fragile morphology and less lipid content. Michel et al, 1990 performed tape stripping experiments where the cornified layers of the epidermis are removed layer by layer. They found that fragile immature cornified envelopes are more prevalent in the deeper layers of the stratum corneum, whereas rigid, mature cornified envelopes are found in the outer layers of the stratum corneum. This varies by body site with fragile cornified envelopes observed more frequently in areas of epidermis with reduced barrier function such as the face or lip, compared to areas such as the upper arm which contained more mature cornified envelopes.

By comparing the images from Michel et al, 1990 and Hirao et al, 2001 with those in Figure 4.6 and Figure 4.7, an estimate about the maturity of the cornified envelopes can be made. Cornified envelopes extracted from 2D cultures (shown in panels A and B) appear most similar to those extracted from the 25th stripping (i.e. deep layers of the stratum corneum) whereas those from 3D cultures appear most similar to those extracted from between the 5th and 15th tape strippings. A similar tape stripping experiment with the 3D culture would be interesting but this technique is not possible with the 3D scaffold as the cells differentiate inside the rigid scaffold. Therefore the cornified envelopes collected from 3D scaffolds represent an *average* sample from the whole 200µm thickness of the scaffold and cannot be attributed to certain layers.

It is not clear whether there is any ordered distribution of mature and immature cornified envelopes inside the 3D scaffold or whether they are located throughout the full thickness of the scaffold.

The ratio and location of mature and immature cornified envelopes has implications in skin conditions. In psoriasis and keratoderma, immature corneocytes are more often found in the outer layers of the stratum corneum and these patients often display poor epidermal barrier function in those affected areas (Ishida-Yamamoto A et al, 1995). With hindsight, a longer culture time at the air-liquid interface would have been interesting to observe further changes in morphology and to determine if cornified envelopes became more mature with longer exposure to the air-liquid interface. An alternate method of electron microscopy, such as cryo-SEM preparation may also have been beneficial to observe any intracellular lipids which would likely be removed during the alcohol and solvent-based preparation techniques used for standard SEM.

#### 4.3.1.2 Lipid Synthesis in 2D Cultures

Overall, 2D cultures produced a lipid profile which is not representative of native epidermis. The addition of serum, high calcium, ascorbic acid or FFA made some differences to the total amount of lipid produced, as well as the overall profile. However, these changes were minimal and no 2D cultures showed a mature lipid profile comparable to 3D-cultured keratinocytes, mouse epidermis or published data concerning human epidermis. This shows that the 3D environment is critical for keratinocyte production of epidermal barrier lipids.

Low cholesterol content in 2D culture may be because cells in 2D are limited in their production of cholesterol such as the activity of the HMG-CoA reductase enzyme (Harris et al, 2000). HMG-CoA reductase is also inhibited by high $CSO_4$ levels, which were found in all of the 2D culture conditions. Alternatively, cells in 2D may simply be producing very little cholesterol in the form of a barrier lipid, with the cholesterol in this analysis being mainly from cell membranes. As shown in Figure 4.7, keratinocytes cultured in 2D do not terminally differentiate to produce mature cornified envelopes and so a mature lipid profile with a high percentage of ceramides would be unexpected.

Glucosylceramides are polar lipids found inside lamellar bodies, but after extrusion they are converted into ceramides by cleavage of the polar head (Pappinen et al, 2003, Masahiro and Masao, 2007). The glucosylceramide to ceramide ratio is an indicator of barrier function (Chan et al, 2011) with high glucosylceramide content indicating immature epidermal barrier function. All 2D cultures showed higher than normal glucosylceramide levels, again indicating immaturity of lipid synthesis.

#### 4.3.1.3 Lipid Synthesis in 3D Cultures

**Table 4.4. Summary of 3D Culture and Mouse Epidermis Lipid Composition**

| Lipid | 3D 2d sub | 3D 7d sub | 3D 14d sub | 3D 14d ALI** | Mouse Epidermis |
|---|---|---|---|---|---|
| FFA | 29 | 18 | 11 | 6 | 9 |
| CHOL | 15 | 28 | 38 | 17 | 19 |
| CER | 13 | 14 | 11 | 43 | 47 |
| TRIG | 13 | 10 | 12 | 10 | 9 |
| CS | 11 | 6 | 4 | 4 | 7 |
| CE | 6 | 13 | 14 | 12 | 9 |
| Others* | 13 | 11 | 7 | 8 | - |

** Including glucosylceramides, lanosterol and phospholipids*
*** ALI = air-liquid interface*

Overall, the lipids extracted from 3D cultures are more physiologically accurate than those extracted from 2D-cultured keratinocytes. Table 4.4 also shows that the air-liquid interface is was key factor in differentiation as submerged 3D cultures were shown to produce significantly more cholesterol but less ceramide than those at the air liquid interface.

The results in this chapter showed that supplementing the culture media with serum, high calcium, ascorbic acid or FFA can alter the lipid profile produced by keratinocytes. This is immediately obvious in the total amount of lipid extracted from cultures (Figure 4.15) but also in the proportions of each synthesised lipid. While keratinocytes can independently synthesise some barrier lipids, they are still dependent on precursors from the diet, supplied by serum, particularly essential fatty acids. After 14 days of culture at the air-liquid interface, serum free cultures (Figure

4.21) showed a less mature profile than their serum containing counterparts. Noticeably, the addition of high calcium concentration to serum free culture conditions did not significantly alter the overall lipid composition. This shows that even when cells are actively induced to differentiate by high extracellular calcium concentration, they are unable to form a mature lipid profile. Particularly noticeable are the lower levels of ceramides in comparison other cultures, as well as significantly elevated cholesterol sulphate content, highly indicative of an under-developed epidermal barrier (Elias et al, 2012).

With regard to calcium concentration, results shown in Figure 4.15 showed that the total amount of lipid produced by high calcium conditions was significantly larger than by low calcium conditions after 14 days. Results in Figure 4.21 show that after 7 days, high calcium concentration alters the lipid profile by increasing ceramide production. However, after 14 days the differences in lipid composition between high and low calcium conditions were only slight, with high calcium conditions showing a marginally more mature profile. This indicates that the air-liquid interface alone is sufficient to induce keratinocytes to produce barrier lipids. However, under high calcium conditions, the cells produced more lipids in total. Analysis of ceramide production by keratinocytes (Breiden et al, 2007) showed that in low calcium concentrations, keratinocytes can only synthesise some of the normal epidermal ceramides. However, the data shown previously in this chapter only addresses the total proportion of ceramides, and not the presence or absence of each individual ceramide found in human epidermis (12 in total, according to van Smeden et al, 2011).

These results showed that ascorbic acid and FFAs altered the lipid profile of 3D cultured keratinocytes in line with a more mature epidermal lipid profile. For instance, 3D cultures supplemented with ascorbic acid displayed the highest ceramide and cholesterol content, which were also the most physiologically accurate. This is in line with findings by Uchida et al, 2001. The 3D scaffold cultures treated with ascorbic acid also displayed the most physiologically accurate cholesterol sulphate content. However, ascorbic acid treated cultures displayed a significantly higher proportion of cholesterol esters than native epidermis.

All 3D scaffold cultures still displayed a relatively low proportion of free fatty acids in comparison to published data for human epidermis (Pappinen et al, 2008). There

were also no significant differences in FFA proportion between treatment groups after 14 days. This suggests that there may be a limitation of HaCaT cells' ability to produce FFA (for instance if cells are utilising glucose in the culture media for ATP production rather than FFA synthesis). Alternatively, despite FFA supplementation (linoleic acid, arachadonic acid and palmitic acid) and fetal bovine serum in the culture media, the culture media may not contain all precursors for adequate FFA synthesis.

In human epidermis, cholesterol sulphate is found in very low concentrations in stratum corneum in comparison to the rest of the epidermis. This indicates that the cultures with lower cholesterol sulphate content can be classified as more mature than those with higher cholesterol sulphate content. As mentioned previously, a high proportion of cholesterol sulphate in native epidermis is indicative of an immature epidermal barrier (Elias et al, 1984). Cholesterol sulphate is found predominantly in the granular layers of human epidermis (Higashi et al, 2004), and so the high proportion observed in these 3D cultures may indicate that many cells are in approximately this phase of differentiation. All 3D cultures showed higher than physiological levels of cholesterol sulphate, although the ascorbic acid and FFA-supplemented culture conditions showed much lower levels which were closer to physiologically accurate.

Linking these lipid profiles to involucrin staining (shown in Figure 4.17) shows that there is some link between a 3D culture with stronger involucrin staining and a more mature lipid profile, but this is not absolute. For example, under low calcium, serum free conditions the culture shows very little involucrin staining and has a correspondingly immature lipid profile with a high percentage of cholesterol sulphate as well as low cholesterol and low ceramide percentages. However, the "high $Ca^{2+}$ FFA cultures showed very strong involucrin staining present throughout the entire scaffold but a lipid profile which was no more mature than other, lesser staining, cultures such as "high $Ca^{2+}$" or "high $Ca^{2+}$ AA" which contained ascorbic acid.

With hindsight, it is possible that the cultures utilising ascorbic acid and the FFA cocktail may be over-differentiated, i.e. differentiated too quickly in an uncontrolled manner. The focus for most of the experiments in this thesis were based on increasing the amount of differentiation, as well as the rate, with the assumption that the barrier properties of the 3D cultures would be improved by more differentiation.

This was because previous results have shown that cornified envelopes were less mature than those from native epidermis, some flattened cells still contained nuclei and that there were only 2-3 layers of flattened cells on the surface of the culture - all indicating incomplete differentiation. Therefore experimentation focused on increasing the differentiation of the cultures. However, the results shown in Chapter Five support the idea that differentiating keratinocytes too quickly may result in reducing barrier function, even though markers such as involucrin and the amount of epidermal barrier lipids produced rise.

### 4.3.2 Factors Affecting Lipid Synthesis in the 3D Scaffold

Lipid synthesis and metabolism is clearly essential for proper epidermal barrier formation and this complex process of epidermal barrier assembly is overviewed in the Introduction Chapter of this thesis. Experiments in this chapter have shown that the profile of lipids produced by keratinocytes is dependent on many factors such as the availability of precursors (i.e. culture media with serum), calcium concentration and the drying caused by the air-exposed upper surface. These conclusions are in line with information gained in animal models or human studies - for instance, dietary sphingolipid intake (and thus provision of raw materials for lipid synthesis) affects skin barrier function (Duan et al, 2012), and exposure of the skin water causes increased epidermal barrier permeability (Warner et al, 2003).

Investigations in this chapter showed that 3D cultures produce an overall profile of barrier lipids which are approximately physiologically accurate to native human epidermis. It is worth noting that the relatively wide-ranging reference figures used for "native epidermis" (i.e. ceramide content of 30-50% or FFA of 8-20%) is due to large variation in human samples. These are due to several factors which may include age, gender, race, geographical location, body sampling site and more - although many of these factors are still not fully understood (Darlenski et al, 2012). Even the time of day may affect the composition of epidermis, as evidenced by Le Fur et al, 2001.

Optimised 3D cultures showed a lipid composition comprising almost 50% ceramide in total. This high proportion of ceramide is associated with the final stages of epidermal differentiation, as the ceramide content in the basal, spinous and granular layers of human epidermis is very low (Baroni et al, 2012). However, the results in this chapter do not show the proportion of each type of ceramide present in the 3D

culture. Native human epidermis contains 12 major classes of ceramide in the stratum corneum, varying by sphingoid base and attached fatty acid chains (van Smeden et al, 2011). Some types of ceramide are more important to barrier function than others - for example, in mice the depletion of ELOVL4, which elongates fatty acids, results in a lack ω-hydroxy very long chain fatty acid ceramides. Mice with this knockout show a delayed epidermal maturity, an abnormally structured stratum corneum and die within 24 hours from dehydration caused by epidermal barrier failure (Li et al, 2007).

It is clear that the ratio of different epidermal ceramides is critical for barrier function. Therefore, in artificial epidermal equivalents, much effort has been devoted towards analysing the subtypes of ceramide present in the epidermis and stratum corneum. A study by Ponec et al, 2000 examined 8 epidermal ceramides in three commercial *in vitro* epidermal equivalents and found their percentage distribution to be inaccurate when compared to native epidermis (i.e. ceramide 2 comprised 42-55% of all ceramides in epidermal equivalents but only 25% of native epidermis, and ceramide 5 comprised 3-9% of equivalents but 21% of human epidermis).

Over time, improvements have been made to the ceramide profile of *in vitro* equivalents. In 2003, Ponec et al demonstrated that supplementation with linoleic acid, palmitic acid, arachadonic acid increased keratinocyte lipid production, and the physiological accuracy, of the proportions of each ceramide subtype produced by an *in vitro* equivalent. Therefore, this methodology was adopted for the "FFA" group shown in this chapter. Furthermore, Breiden et al, 2007 found that addition of 10µM linoleic acid to culture media, in combination with high calcium, resulted in a twofold increase in ceramide concentration, but also an increase in covalently bound ceramides and ω-hydroxylated fatty acids. Linoleic acid has dual functions as an agonist and transcription factor for PPAR-alpha and also as a substrate for ceramide biosynthesis in keratinocytes. PPAR-alpha regulates the synthesis of lipids including ceramides, FFAs, cholesterol and cholesterol esters, all of which play important roles in epidermal barrier function (Elias et al, 2012).

Pappinen et al, 2008 performed an in-depth comparison of ceramide subtypes from an *in vitro* model based on rat keratinocytes and compared them to human epidermis. They found that some ceramides were different or entirely absent from the *in vitro* cultures, in particular the important ω-linked acyl chains in hydroxyceramides

(acylCer) were altered. They showed that 10-20% of acylCer were in the linoleate form in the *in-vitro* model, compared to 80% in human epidermis. They hypothesised that this is likely due to the nature of *in vitro* models utilising serum as a nutrition source to supply essential fatty acids. For instance, calf serum contains only low levels of linoleic acid, hence part of the rationale behind supplementation of the culture media with free fatty acids, including 10µm linoleic acid.

All 3D cultures presented in this chapter showed a lower proportion of free fatty acid content (8% on average) compared to native epidermis (15-20%). Even those cultures with supplemented ascorbic acid or free fatty acids, which included linoleic acid, contained only 8% FFA. Interestingly, this pattern of low FFA content is found across many *in vitro* epidermis equivalents (Pappinen et al, 2012).

### 4.3.3 Future/potential Work into Lipid Analysis

As the 3D scaffold model does not form clear separation into distinctive epidermal layers, it would be interesting to assess the locations of various lipids throughout the 3D scaffold. For instance, precursor glucosylceramides are normally located inside lamellar bodies of the granular layer and are not found in the stratum corneum, whereas the end-product ceramides are located in extracellular spaces of the stratum corneum (Vielhaber et al, 2001). Similar analysis of the 3D scaffold cultures using immunogold labelled TEM would be interesting - namely to determine whether intercellular spaces are filled with ceramide and whether lamellar body packaging and secretion is fully functional in the 3D model.

As mentioned previously, the ceramide subtypes were not analysed in the previous experiments. As the data showed a high proportion of ceramide content (up to 43%) in the 3D cultures, it would be worth investigating the exact composition of these ceramides. This can be done by liquid chromatography combined with ESI-MS, as detailed in Pappinen et al, 2008.

The TLC protocol utilised in the previous chapter was chosen for clear separation of the essential barrier components of the epidermis - namely ceramides, FFA and cholesterol. However, not every epidermal lipid can be separated by the same solvent separation. For instance, lanosterol is a cholesterol precursor which is not detected by the TLC method used in this chapter. Lanosterol is present in low amounts in native human epidermis, and also in 3D cultures (Ponec et al, 2000) and high lanosterol

content can an immature barrier function due to anomalies in cholesterol processing. In the 3D cultures presented in this chapter, most showed a relatively normal proportion of cholesterol, suggesting that lanosterol is unlikely to be found in significant concentrations. However, if needed, different TLC development protocols could be used to determine the lanosterol to cholesterol ratio as a measure of lipid profile maturity.

There are a number of other cell culture additives and pharmaceutical agents which have been shown to affect epidermal lipid composition. In this project, most experiments were based on optimising the culture conditions for physiologically accurate results. However, purposefully disrupting keratinocyte differentiation or interfering with lipid production would be viable avenues for research. Researching the effects of exposure to irritants is a common use for *in vitro* epidermal equivalents. Surfactants such as SLS (found in most soaps and shampoos) have long been recognised as damaging to epidermal barrier function (Wilhelm et al, 1993) in terms of removing lipids, neutralising pH and changing stratum corneum hydration. Surfactants have been more recently found to induce changes to ceramide and FFA biosynthesis, as well as causing rearrangement of stratum corneum lipid lamellae (Torma and Berne, 2007). After damage by surfactants, the epidermal barrier undergoes repair (de Koning et al, 2012), and this response can be measured. These experiments could be carried out on 3D cultures and cultures analysed at various time points to assess barrier repair. Following on from this, cultures could be formed from cells with ablated proteins related to barrier repair such as transglutaminase, and the ability of cultures to re-form normal cornified envelopes after barrier disruption could be measured.

It is possible to measure the effect of a compound on lipid biosynthesis by provision of radiolabelled essential fatty acids or precursors, then measuring the radioisotope incorporation into each lipid fraction after a given amount of time (Uchida et al, 2010). This could be used to highlight the source of precursors involved in keratinocyte lipid synthesis.

Epidermal models have typically not been assessed for natural moisturising factor (NMF) production or the pH gradient found in native epidermis. This is due to the difficulties of creating and maintaining such a gradient under culture conditions - for instance, most culture media contains buffers so that cellular metabolism and $CO_2$

production will not create an acidic pH. The epidermis has a pH gradient which is contributed towards by many factors which are not replicable *in vitro*, such as sweat and the secretions of native microorganisms such as *Staphlococcus epidermidis* (Baroni et al, 2012). However, the acidity of the stratum corneum is a key factor in barrier permeability and is worth investigating.

### 4.3.4 Implications of Culture Media Supplementation

Shapiro et al, 1978 first understood X-linked Ichythosis caused by steroid sulphatase deficiency, showing that disorders in epidermal lipid metabolism are responsible for skin disorders and Elias, 1983 noted a disproportionate number of skin conditions associated with cholesterol metabolites. Culture experiments have shown that changing the conditions in which epidermal-equivalents are grown can alter their barrier properties. This has clear routes into potential therapeutic uses, particularly in disorders associated with a lack of certain lipid classes in the epidermis.

Therefore, researchers in the field have proposed lipids or pharmacological agents targeting lipid biosynthesis as a therapy for skin disorders - both in terms of dietary input (Belury et al, 2007, Duan et al, 2012) and the direct application of such agents to the skin surface. For instance, sphingolipids or their derivatives have also been shown experimentally to promote keratinocyte differentiation and may be used therapeutically to correct skin barrier defects in conditions such as psoriasis or atopic dermatitis (Paragh et al, 2008). Linoleic acid precursors have been applied to the epidermis in a cream to increase lipid metabolism and content of the epidermis (Raufast et al, 2010), and application of cholesterol directly to the skin surface has been used to restore barrier function in ichthyoses due to defects in lipid metabolism (Paller et al, 2011).

By better understanding the pathways of epidermal lipid metabolism, as well as feedback mechanisms, disorders can be targeted by providing raw materials for enzymatic conversion, using enzyme inhibitors to block degradation of target lipids, and to direct the lipid profile in the intended direction. Again, 3D models can aid in the understanding of the factors affecting lipid production and barrier formation, and may also be used as a substrate for testing the effect topical compounds. Ironically, one of the issues with topical treatment of skin disorders is the epidermal barrier itself which blocks many potentially therapeutic agents. 3D models can also aid in

this area by carrying out preliminary assessment of the permeability of pharmacological agents before moving onto animal or human studies.

### 4.3.5 Findings from 2D and 3D Culture Conditions

Results from 2D and 3D analysis did not always correlate. Figure 4.7 shows that HaCaT keratinocytes could not synthesise cornified envelopes under 2D culture conditions, even when differentiated with high calcium. In a comparison of lipid production, the differences between culture conditions were greater when cells were cultured in 3D vs 2D, for example, high calcium increased lipid production by 13% in 2D but by 28% in 3D. Conversely, the addition of 100µg/ml ascorbic acid increased lipid production by 63% in 3D but resulted in a slight decrease in 2D. In terms of lipid composition, 2D cultured and 3D cultured cells were completely different, likely because 2D cultured cells are always cultured submerged, rather than subjected to drying at the air-interface. However, even submerged 3D cultures produced a lipid profile which was different to 2D cultures (although different to those at the 3D air-liquid interface), suggesting that the 3D environment itself is a factor. It is known that cells cultured in 3D are more metabolically active and also more functional than their 2D-cultured counterparts. For instance, liver HepG2 cells produce more albumin (Bokhari et al, 2008) and more cP450 activity (Schutte et al, 2011) when cultured in 3D than in 2D. It is likely that keratinocytes follow a similar behaviour and modify their protein and lipid production in accordance with the 3D environment, particularly when combined with an air-liquid interface which induces differentiation. These results highlight the importance of the culture conditions and show that results achieved using 2D cell culture may benefit from further investigation in 3D.

### 4.3.6 The 3D Scaffold for Barrier Function Testing

Keratinocytes cultured in the 3D scaffold differentiated and produced barrier proteins and barrier lipids. Therefore the next step for investigation is to assess the barrier function of the 3D scaffold cultures. The results in this chapter have also shown that the 3D model could be used to test the effects of pharmaceutical agents. Therefore the following chapter will address these issues.

# 5 Chapter 5

# Functional Testing of the 3D Epidermal Model

# 5.1 Introduction

#### 5.1.1.1 Aims, Objectives and Overview

Results from the previous chapters have shown that keratinocytes form flattened cornified envelopes with covalently attached lipids, and synthesised lipids in a profile similar to native epidermis. Optimisation of the culture conditions by addition of ascorbic acid and a cocktail of free fatty acids was able to further modify the lipid profile to a more physiologically accurate composition.

This chapter will focus on assessing the permeability of the 3D scaffold epidermal model to a known permeant compound. Secondly, Inhibition of JNK signalling pathways by SP600125, a compound known to affect keratinocyte differentiation, will be tested in 3D conditions and compared against 2D findings. The 3D model will then be used to assess the permeability of cultures which have been treated with SP600125 and the lipid analysis will be correlated with these findings.

## 5.1.2 Barrier Permeability Assays

The next step for the development of this model is to test the permeability of the culture to relevant compounds. This is an important measurement in several industries - namely the medical, pharmaceutical and cosmetic fields. Researchers can use permeability measurements to understand how disorders (such as psoriasis and dermatitis) or disruption (by chemicals, burns or pathogens) affect barrier permeability. Transdermal medicines are a popular method of drug delivery, as they are non-invasive, can deliver a dosage of drug continuously and bypass first pass liver metabolism (Godin et al, 2007, Trovatti et al, 2012). For example, smoking replacement patches deliver nicotine continuously to stave off cravings over extended periods of time, and Fentanyl patches deliver continuous pain relief (BNF vol 63). Data concerning the permeability of these active agents through the epidermis is essential in order to calculate the formulation of the medicine, the concentration of active ingredients and patient dosage instructions. Some drugs or cosmetics such as moisturisers are designed to act directly on the epidermis itself, and so passage through into the dermis and systemic circulation is to be avoided. Whereas, other compounds are designed for systemic release and need to pass through the epidermal barrier and into the circulatory system in order to take effect. There are also factors affecting barrier function such as hydration and moisturisation, which have implications for therapeutics. For instance, application of a Fentanyl skin

patch is contraindicated following bathing, due to increased skin absorption (BNF, Vol 63). Therefore, understanding the permeability of compounds through the epidermis and mechanisms of barrier function which affect absorption are essential.

Commercial skin models and *in vitro* epidermal equivalents typically have barrier function which is inferior to *in vivo* epidermis. For instance, Suhonen et al, 2003 carried out extensive analysis of their rat epidermal keratinocyte (REK) model by analysing the permeation of 18 lipid soluble and water soluble compounds. Their model produced an artificial epidermis with morphological similarity to real human epidermis, including several layers of differentiated keratinocytes, expression of differentiation markers and a thick stratum corneum. However, in the analysis of permeability, their model was 0.3 - 5.2x more permeable than human cadaver epidermis. These results were actually favourable when compared to many other commercial models which displayed permeabilities of tens to hundreds of times higher than *in vivo* epidermis (Perkins et al, 1999, Schmook et al, 2001). This limits the usefulness of *in vitro* epidermal equivalents for permeability assessments.

There are two established standard methods for assessing epidermal barrier permeability. These are transepidermal water loss (TEWL) (Grubauer et al, 1987, Barel et al, 1995) and diffusion cell analysis (Larese et al, 2009, Trovatti et al, 2012).

#### 5.1.2.1 Transepithelial Water Loss (TEWL)

TEWL analysis is a non-invasive technique which measures the water retention capacity of the skin. Transepidermal evaporation occurs because a water concentration gradient exists from the deep layers of the epidermis, through the stratum corneum and into the air (Barel et al, 1995). Damaged or disrupted skin is less efficient in retaining water content than healthy skin, and so evaporation through the epidermis is increased (Grubauer et al, 1987). In contrast, skin treated with moisturisers displays decreased transepidermal evaporation (de Paépe et al 2001). TEWL is typically performed on the skin surface of live subjects, although it can be used with epidermal equivalents (Kuntsche et al, 2008). Evaporation is measured by placing an evaporimeter with a humidity sensor in a closed or ventilated capsule against the skin. In the closed system, vapour loss is collected into a capsule and continues until the humidity reaches 100% and evaporation ceases. A curve of evaporation is plotted and the epidermal permeability is calculated. In the ventilated system, the chamber against the skin is supplied with a gas of known humidity. The

gas is continuously ventilated as skin evaporation occurs to maintain a constant humidity. The rate of gas ventilation allows for continuous measurement of transepidermal evaporation over longer periods of time (Sotoodian et al, 2012).

The TEWL technique may be affected by ambient temperature, humidity, airflow of the room, and even the light sources in the room (Sotoodian et al, 2012) and requires the use of specialist evaporimeters such as the Tewameter (GmBH, Germany) or DermaLab (Cortex Technology, Denmark) systems.

#### 5.1.2.2 Diffusion Assays

Diffusion assays are used to directly measure the permeability of known compounds through a barrier. Samples of epidermis, stratum corneum, full thickness skin, epidermal-equivalents or any other form of barrier are tightly sandwiched between two glass or plastic chambers which are each filled with a solution. Permeability assays can be performed in a vertical Franz chamber (Gabbanini et al, 2009) or a side-by-side chamber with continuous stirring of both sides (Suhonen et al, 2003). The choice of chamber type does not make a difference to the final permeability curve generated (Schreiber et al, 2005). All reactions should be carried out at 34-37°C to maintain the living cells in the culture. One chamber is "spiked" with a permeant that can be measured as it diffuses across the barrier in accordance with the concentration gradient and the resistance posed by the sample. Samples are taken from both sides of the apparatus to preserve the volume gradient and the increasing concentration of the permeant in the recipient chamber is measured. The rate of diffusion and the time taken for equilibrium to be reached relate to the barrier permeability of the sample to that particular molecule. The diffusion cell is also an approved mechanism for testing the permeation of compounds through *in vitro* models according to the OECD (Series On Testing And Assessment, Number 28, ENV/JM/Mono,(2004)2).

Clearly, diffusion assays are invasive methods as the analysis requires the epidermis to be removed before it is placed into the chamber. Therefore permeability assays are usually performed on human cadaver skin, excised animal samples (commonly murine or porcine) or on *in vitro* equivalents. Diffusion assays have been used for testing the epidermal permeability of compounds such as cosmetic additives such as menthol, camphor etc (Gabbanini et al, 2009) or even solid nanoparticle penetration (Larese et al, 2009).

A diffusion assay reveals more about the properties of the sample epidermis because it directly tests particular compounds against the barrier. Increased TEWL may indicate a barrier defect in general, but a diffusion assay will show more information, such as whether the epidermis is more permeable to lipid-soluble or water-soluble compounds. With some permeants, for instance the silver nanoparticles mentioned previously (Larese et al, 2009), samples can then be fixed and stained or imaged by TEM to determine where the permeant was blocked by the barrier.

In this thesis, a permeability assay was established using a side-by-side diffusion cell (PermeGear, USA) shown in Figure 2.7. This assay was used to assess the barrier permeability of the 3D epidermal model which was described in detail during Chapter Four. The permeability co-efficient of each variation in the 3D model was calculated and these were compared to each other. Calculated permeability co-efficients were also compared to published literature for other epidermal models and measurements of human skin.

#### 5.1.2.3 Corticosterone Permeability Assay

Typically, permeability studies have used radiolabelled molecules as permeants, and measure diffusion into the recipient chamber by scintillation counters. However, for work in this thesis, radioactive isotopes were avoided for cost, safety and simplicity reasons. The assays presented in this chapter utilised corticosterone as a permeant molecule. Corticosterone is a steroid hormone produced in the adrenal glands, synthesised *in vivo* by conversion from cholesterol. Therefore it is lipid-soluble and structurally similar to other steroid hormones such as testosterone, progesterone and estradiol, which have therapeutic uses as transdermal treatments (Kuntsche et al, 2008). Corticosterone permeability has been used in several previous studies and is well established as a measurement of epidermal barrier function (Pasonen-Seppanen et al, 2001[2], Chantasart et al, 2007, Kuntsche et al, 2008, Ibrahim et al, 2009).

### 5.1.3 The Role of JNK Signalling Pathway in Epidermal Differentiation

One purpose for *in vitro* epidermal models is to carry out basic research on epidermal differentiation and to test the effect of novel compounds on epidermal cell biology and barrier function. One such compound is SP600125 (Calbiochem/Sigma, UK) a

selective Jun N-terminal Kinase (JNK) inhibitor compound (Bennett et al, 2001) which has been shown in 2D cultures (Gazel et al, 2006) to reduce proliferation and promote differentiation of keratinocytes.

JNK is normally inactive in healthy epidermis but shows constant low-level activity in cultured keratinocytes, whereas keratinocytes in tissue culture conditions have signalling pathways which more resemble an "activated" psoriatic or wound-healing state, rather than the basal epidermal keratinocytes under normal conditions (Freedburg et al, 2001). When exposed to stress via UV irradiation, JNK activity in cultured keratinocytes is further activated (Adachi et al, 2004). In mice, JNK inhibition by SP600125 has been used to reduce epidermal hyperplasia (Zhang et al, 2004) and JNK(-/-) mice showed a reduction in proliferative cells in the basal epidermis (Weston et al, 2004). It could be speculated that downregulation of stress-signalling pathways by JNK inhibition could be therapeutically applied in cases of hyperproliferation.

JNKs are responsible for serine phosphorylation of c-Jun and ATF-2, which participate in the AP-1 complex which subsequently induced expression of proteins such as involucrin, loricrin and transglutaminases (Bikle et al, 2004, Miodovnik et al, 2012). JNKs may also play a role in preventing the degradation of c-Jun ATF-2 and p53 by phosphorylating them (Sabapathy and Wagner, 2004). Phosphorylation of c-Jun is known to be important in inflammation and proliferation, as fibroblasts cultured from transgenic Jun(-/-) mice showed that c-Jun is essential for G1-S phase cell cycle transition (Behrens et al, 1999). There are three JNKs, with JNK1 and 2 expressed ubiquitously with four different splice isoforms each, and JNK3 mainly isolated to the brain. JNK1 is mostly involved with phosphorylation of c-Jun whereas JNK2 is primarily concerned with preventing c-Jun degradation and displays 25 times higher affinity for c-Jun, compared to JNK1 (Sabapathy and Wagner, 2004).

In the epidermis, evidence suggests that JNK is involved in the balance between proliferation and differentiation. JNK1 or JNK2-deficient mice display delayed epidermal development and deficiencies in both proliferation and differentiation. Epidermis of JNK(-/-) mice showed a lack of keratohyalin granules and reduced loricrin expression, and a reduction in the proliferating cells of the basal epidermis (Weston et al, 2004). JNK signalling is also implicated in transformation of epidermal cells in squamous cell carcinoma (Hengning et al, 2010).

Importantly, inhibition of the JNK pathway induces keratinocyte differentiation independently of calcium-initiated differentiation (Schmidt et al, 2000). High calcium concentration has been used throughout this thesis to induce keratinocyte differentiation and will be combined with SP600125 in this chapter.

Gazel et al, 2006 found that SP600125 reduced proliferation of cultured keratinocytes, induced stratification, and caused the production of cornified envelopes in 2D culture. Microarray analysis found that enzymes involved in lipid and steroid metabolism were activated as well as proteins associated with desmosome and tight junction formation.

Firstly, these effects will be verified in 2D and 3D with the current HaCaT and WTK cell lines. Various concentrations of SP600125 will be used and examined for their effect on cell viability and proliferation in accordance with the literature presented. Using an optimal concentration, 3D cultures will be grown with the SP600125 compound and compared to controls on the basis of morphology, cornified envelope production, lipid production and barrier permeability to corticosterone. Both calcium and SP600125-induced differentiation will be compared and conclusions about the activity of both will be made.

Previous results have shown that keratinocyte differentiation occurs within the 3D scaffold - evidenced by cornified envelope production, a mature lipid profile and expression of proteins such as involucrin. However, there were also some deficiences observed - cornified envelopes were more fragile and immature than native epidermis counterparts, involucrin expression was disorganised throughout the scaffold and no stratified layers were formed, likely due to the confines of the 3D scaffold polystyrene. Therefore SP600125, shown to increase differentiation and promote cornified envelope formation, was used with the goal of increasing the level of differentiation of keratinocytes inside the 3D scaffold. This was hypothesised to improve the barrier function of the 3D cultures through increased production of barrier lipids and cornified envelopes. These experiments also investigate the role of JNK pathway inhibition in 3D culture, which had not been examined previously.

These results also demonstrate the 3D scaffold epidermal model as a tool for studying the activity of a compound and its effect on keratinocyte differentiation and barrier function.

## 5.2 Results

### 5.2.1 Barrier Permeability of 3D Cultures to Corticosterone

Firstly, the permeability of the 3D scaffold epidermal model to corticosterone was measured. An enzyme immunoassay (EIA) for corticosterone was used and a standard curve was generated from corticosterone diluted in DMEM culture media at 37°C. The standard curve used corticosterone concentrations between 20,000 and 32pg/ml and is shown in Figure 5.1. The plot from the standard curve was analysed and a starting concentration of 15,000pg/ml corticosterone was selected for the permeability assessments, based on the sensitivity of the assay. The assay allowed a minimum concentration of 32pg/ml to be detected, which represents 0.2% of corticosterone diffused from the donor to recipient side. The assay was tested against the permeant corticosterone by diluting various concentrations of corticosterone in DMEM and was found to be accurate.

In order to establish a baseline control level of diffusion across the 3D scaffold, 3T3 cells were grown submerged inside the 3D scaffold for 7 days. 3T3 cells proliferate and fill the 3D scaffold, providing passive resistance but not a specialised keratinocyte barrier formed by cornified envelopes, barrier lipids and junctional proteins. It was not possible to use an empty 3D scaffold as a baseline control, due to excessive leaking from the diffusion chamber. Cultures were placed in the side-by-side diffusion cell for 3 hours at 37°C and 15,000pg/ml corticosterone in DMEM was used as the permeant. The experiment was run for four hours at 37°C and results were discarded if any leaking was detected from the diffusion chamber. A graph showing the accumulating percentage of corticosterone diffused into the recipient chamber against time is shown in Figure 5.2.

HaCaT cells were grown for 14 days at the air-liquid interface following protocols from the previous two chapters. These cultures were then placed into the diffusion apparatus with the air-exposed surface facing the donor chamber and the experiment was run for 3 hours at 37°C. Results of the diffusion assay compared to 3T3 cells as a control are shown in Figure 5.3 as the % of corticosterone diffused (up to a maximum of 50%) versus time in minutes for clear representation of the data. For permeability co-efficient calculations, graphs of cumulative amount of corticosterone (μg) versus time in seconds were made.

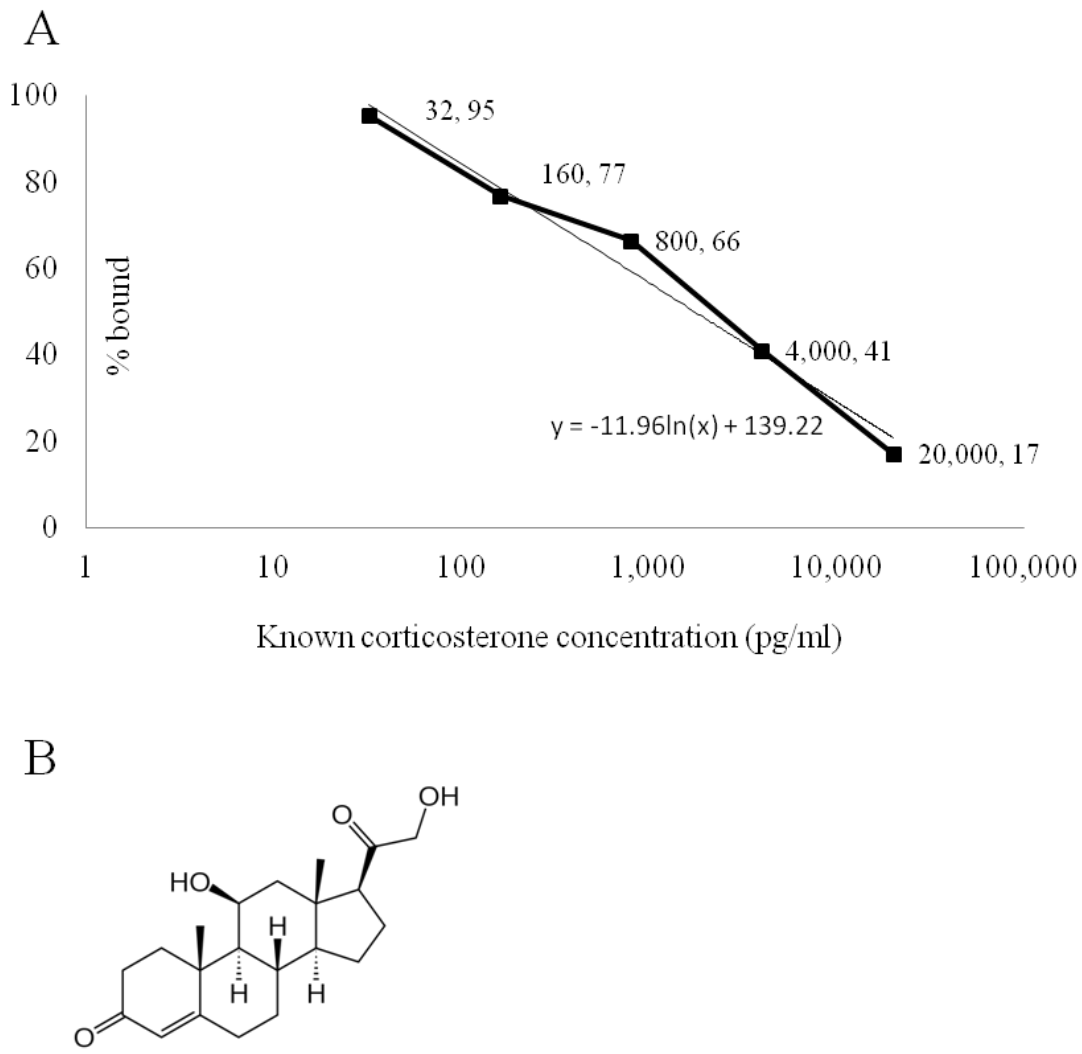


**Figure 5.1. Standard Curve for the Corticosterone Assay**

A) Graph showing standard curve of corticosterone concentration vs % bound in assay. This was used to calculate the concentration of corticosterone, and subsequently the percentage which had diffused across the 3D scaffold; B) Structure of corticosterone molecule. Corticosterone is a steroid hormone synthesis from dietary cholesterol and secreted from the adrenal glands and is structurally similar to testosterone or estradiol.

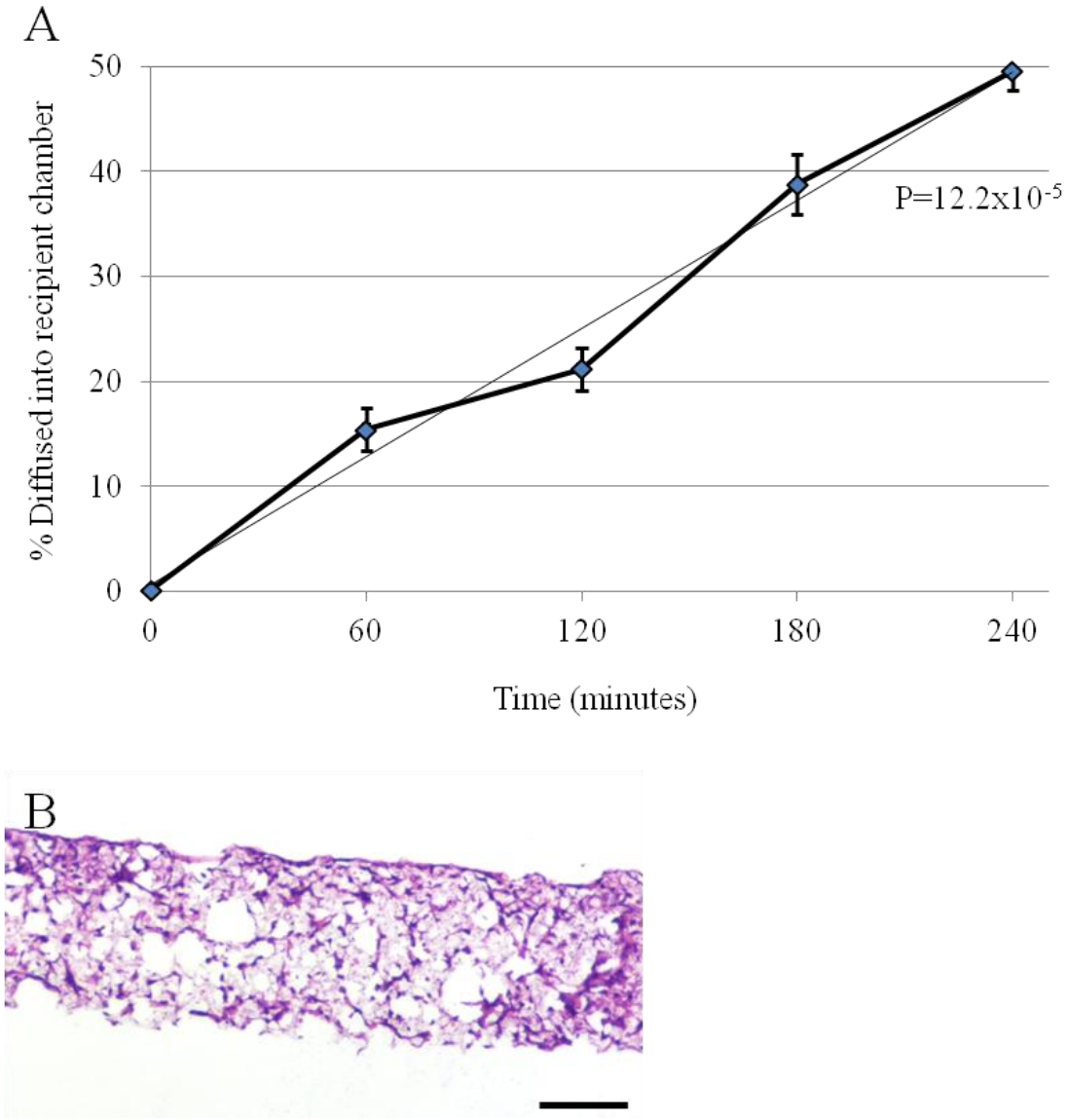


**Figure 5.2. Corticosterone Diffusion Assay of 3D Cultured Fibroblasts**

A) Graph showing % of corticosterone diffused into the recipient chamber against time through 3T3-NIH mouse fibroblasts grown submerged in the 3D scaffold for 7 days. After 4 hours, an average of 49.56% of the corticosterone has diffused across the scaffold, indicating that equilibrium had been reached. Permeability coefficient was calculated as $12.2 \times 10^{-5}$. The 3T3 cells display little barrier function, as expected; B) H&E stained image of 3T3 cells cultured in the 3D scaffold for 7 days. Scale bar 100µm.

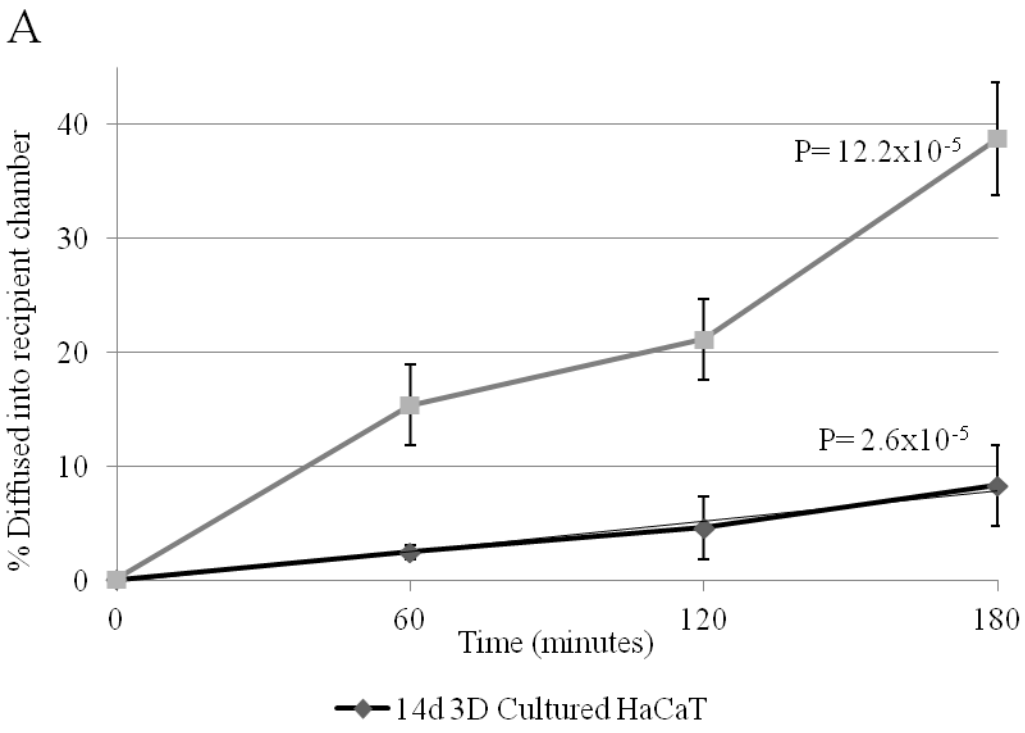


**Figure 5.3. Corticosterone Assay of 3D Cultured HaCaT Cells**

Graph showing % of corticosterone diffused into the recipient chamber against time through HaCaT cells cultured for 2 days submerged, then 14 days at the air-liquid interface under standard conditions as previously described. Diffusion curve of the 3T3 fibroblasts from Figure 5.2 is repeated here for comparison. After 180 minutes of diffusion through cultures containing fibroblasts or HaCaTs, 38.8% ($P= 12.2x10^{-5}$) and 8.4% ($P= 2.6x10^{-5}$) of corticosterone had diffused through each culture respectively. This shows that the differentiated HaCaT cells have formed an epidermal barrier which is 4.7x more resistant than fibroblasts.

The permeability coefficient was calculated, as described in the Materials and Methods Chapter. After 4 hours, an average of 49.56% of the corticosterone has diffused across the scaffold containing 3T3 cells (Figure 5.2), indicating that equilibrium (50%) has been reached. The permeability co-efficient was calculated as $P=12.2x10^{-5}$, showing that 3T3 cells form a poor permeability barrier, as expected. This is in line with published literature (Oshizaka et al, 2012) which shows that the dermis contributes very little towards skin barrier properties. Figure 5.2B shows that 3T3 cells proliferate throughout the full thickness 3D scaffold. However, they do not form a specialised epidermal barrier.

A comparison of 3D-cultured HaCaT cells against 3T3 cells over three hours of corticosterone diffusion is shown in Figure 5.3. After 3 hours, 8.36% of corticosterone added to the donor chamber has diffused across the HaCaT culture, compared to 38.8% through the 3T3-filled scaffold. This shows that HaCaT cells have produced an epidermal barrier ($P=2.6x10^{-5}$) which is 4.7x more resistant to corticosterone diffusion than fibroblast cultures ($P=12.2x10^{-2}$).

WTK mouse keratinocytes were tested for their permeability to corticosterone after culture in low (0.06mM) and high (1.5mM) calcium conditions and compared to HaCaT keratinocytes. Results are shown in Figure 5.4.

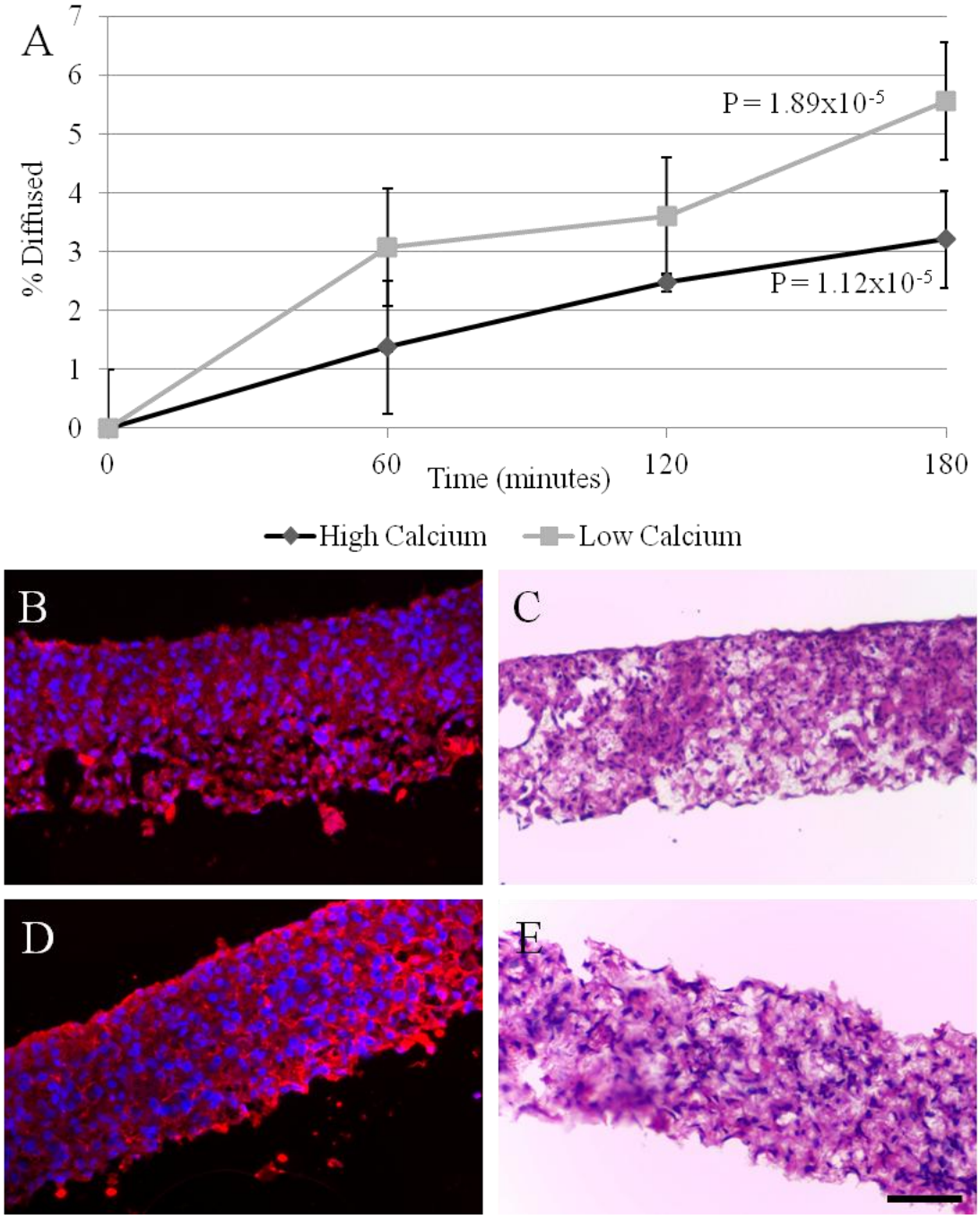


**Figure 5.4. Permeability of WTK Cells Cultured in 3D Scaffold**

A) Diffusion analysis over 3 hours of WTK cells grown at the air-liquid interface for 14 days showing that after 180 minutes, 5.6% ($P= 1.89x10^{-5}$) and 3.2% ($P= 1.12x10^{-5}$) of corticosterone had diffused for low and high calcium cultures respectively. This difference was significantly different; B, C) Involucrin and H&E staining from low calcium cultures; D, E) Involucrin and H&E staining from high calcium cultures. High calcium cultures show slightly more intense involucrin staining and flattened nuclei visible in the H&E image.

The experimental results (Figure 5.4) show that WTK cells form a functional barrier in the 3D scaffold when cultured at the air-liquid interface for 14 days in either low or high calcium conditions. All cultures show growth through the full thickness of the scaffold. Panel B shows that the low calcium culture is differentiated, although the high calcium culture (D) shows more differentiation as expected. H&E staining of the high calcium culture (E) shows some flattened cell nuclei but overall these cultures are similar in appearance and would both be expected to show similar barrier function.

The graph in Panel A shows that the cultures have good barrier function. After three hours of corticosterone diffusion, 3.2% and 5.6% of the donor corticosterone has diffused through the high and low calcium cultures respectively. The high calcium cultured WTK cells have a more resistant barrier than those cultured in low calcium. This is most likely because, as shown in the previous chapter, high calcium induces more differentiation including barrier proteins, increased lipid production and a more mature lipid profile. For low calcium cultures, $P = 1.89x10^{-5}$ and for high calcium cultures $P = 1.12x10^{-5}$.

**Table 5.1. Summary of Permeability Coefficients**

| **Culture** | **$Px10^{-5}$** | **180 min $\%_{diff}$** | **n** |
|---|---|---|---|
| 3T3 Cells | 12.2 | 49.56 ± 3.03 | 3 |
| HaCaT | 2.60 | 8.36 ± 3.58 | 7 |
| WTK low calcium | 1.89 | 3.21 ± 0.81 | 4 |
| WTK high calcium | 1.12 | 5.57 ± 0.94 | 5 |
| *Human epidermis* | $0.87x10^{-7}$ to $3.4\pm 0.9x10^{-7}$ | - | *Kuntsche et al, 2008. Chantasart et al, 2009* |

*$Px10^{-5}$ = permeability coefficient (cm/s). A lower number indicates lower permeability to corticosterone; 180 min $\%_{diff}$ = percentage of permeant diffused to recipient chamber after 180 minutes; n = number of individual samples analysed.*

### 5.2.2 Investigation of the JNK Inhibitor Compound SP600125 on Keratinocyte Differentiation

Published data (Zhang et al, 2003, Sabapathy et al, 2004, Gazel et al, 2006) suggests that the JNK pathway may be a suitable target for therapeutic intervention in cases of hyperproliferation. As described earlier, the JNK inhibitor compound SP600125 has been shown to increase the rate of keratinocyte differentiation (Gazel et al, 2006) and rapidly reduce epidermal proliferation (Sabapathy et al, 2004).

Therefore, the scaffold-based 3D epidermal model was used as part of a series of investigations to test a compound for its effect on keratinocyte differentiation and epidermal permeability. The compound was first tested on cells cultured in 2D, before being tested in 3D cultures. This will show whether the epidermal model using the 3D scaffold can act as a suitable predictor of how a compound will affect epidermal barrier function.

To assess the morphology of keratinocytes with SP600125 treatment, four culture conditions were used in this study. Based on results in the previous chapter, all culture media were supplemented with 100µg/ml ascorbic acid to optimise epidermal lipid synthesis.

**Table 5.2. Culture Media Containing SP600125**

| Culture Media | Calcium | Ascorbic Acid | SP600125 | cFBS |
|---|---|---|---|---|
| High | 0.06mM | 100µg/ml | - | 10% |
| Low | 1.50mM | 100µg/ml | - | 10% |
| High SP AA | 1.50mM | 100µg/ml | 50µM | 10% |
| Low SP AA | 0.06mM | 100µg/ml | 50µM | 10% |

As WTK mouse keratinocytes showed greater sensitivity to calcium concentration, WTK cells were cultured under standard conditions for 48 hours, then switched into the four culture conditions in Table 5.2 for 72 hours. Light microscopy images showing changes in cell morphology are shown in Figure 5.5.

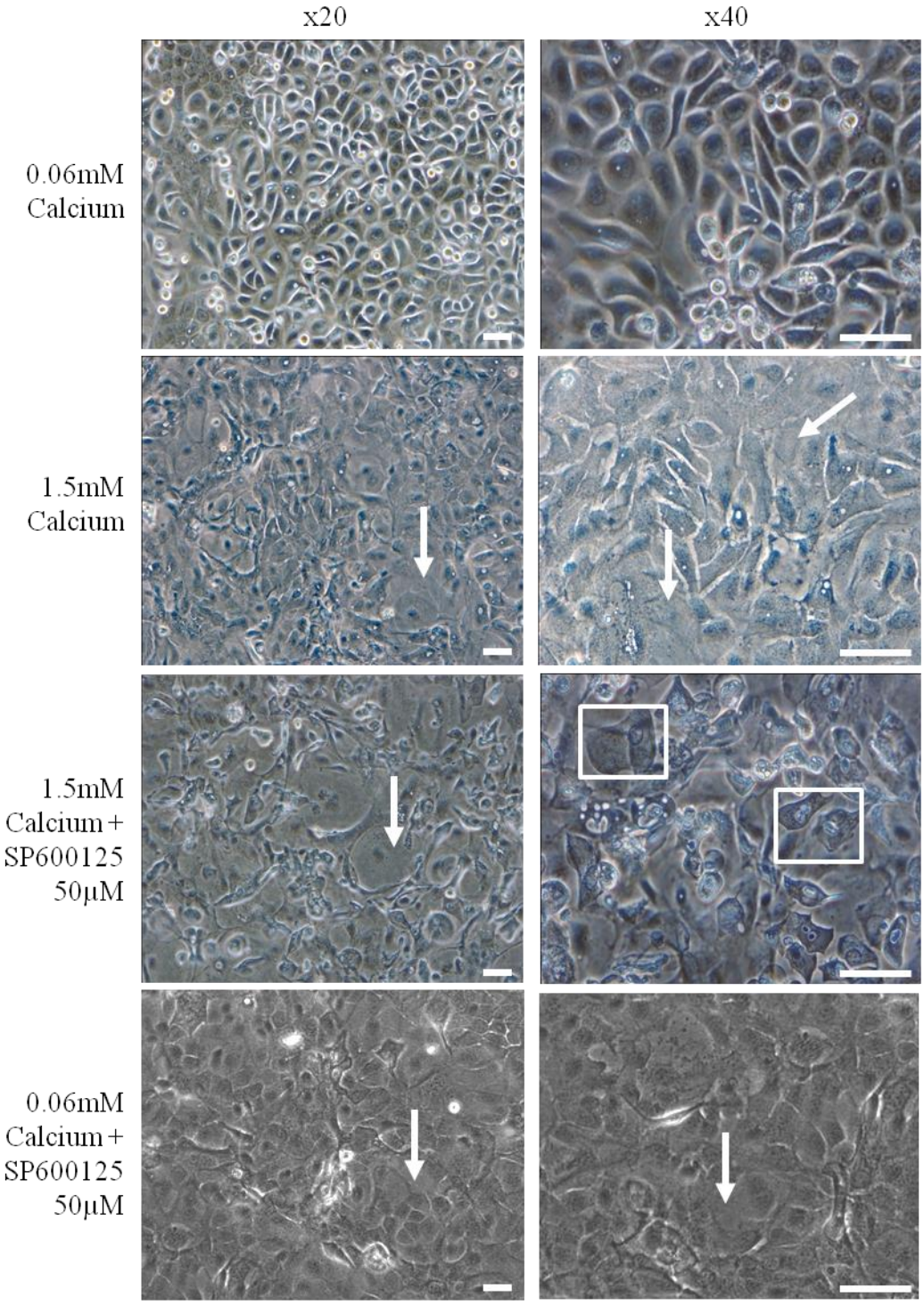


**Figure 5.5. SP600125 Differentiates WTK Mouse Keratinocytes**

Samples were cultured for 48 hours in low (0.06mM) calcium before being switched into low (0.06mM) or high (1.5mM) calcium in the presence or absence of 50µM SP600125 for 72 hours. Floating cornified envelopes are indicated by white boxes and examples of flattened cells are indicated by white arrows. Scale bars = 50µm.

Cells grown in low calcium culture media showed a standard cobblestone appearance with sparse floating cells. This is typical of proliferative, non-differentiated keratinocytes. Cells grown in high calcium media show flattening, closer cell-cell contacts and some cells (indicated with white arrows) are flattened to occupy a larger surface area of the culture flask, forming a sheet-like layer of cells. Keratinocytes cultured in the presence of SP600125 and high calcium are visibly very different to previous conditions, showing flattened cells in a much more "loose" arrangement in the flask with a large number of floating flattened objects which appear to be cornified envelopes. Keratinocytes cultured with SP600125 and low calcium show some morphological changes and appear similar to those cultured in high calcium alone, forming a sheet of flattened cells on the surface of the flask.

This experiment was then repeated with HaCaT cells grown on glass cover slips for immunofluorescence staining of differentiation markers, as the WTK cell line does not adhere or proliferate well on glass. Cells were cultured under standard conditions for 24 hours before being switched into experimental culture media for 48 hours. Representative images are shown in Figure 5.6.

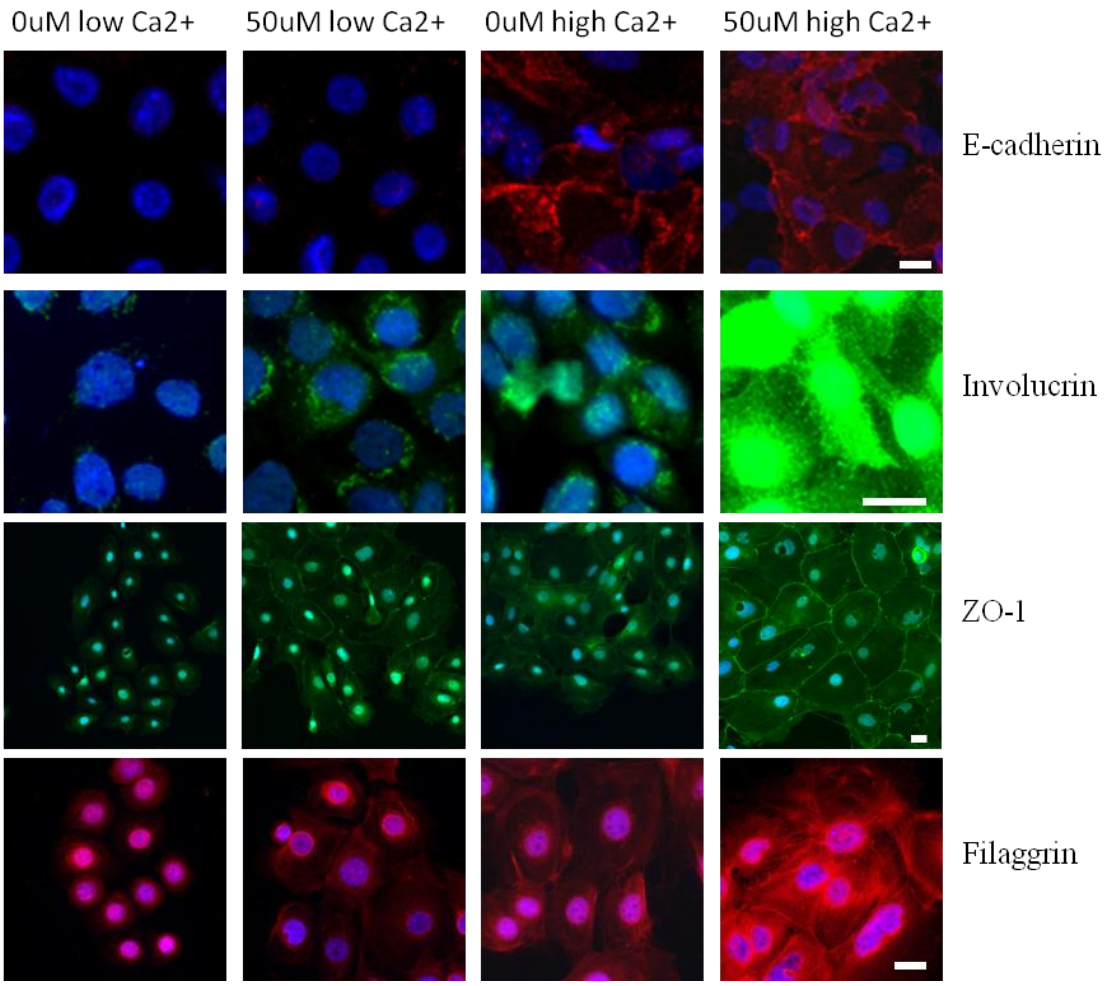


**Figure 5.6. 2D Immunofluorescence of SP600125-treated HaCaT Cells**

2D Immunofluorescence staining of HaCaT cells grown in the presence of low or high calcium concentration and treated with either 0µM or 50µM SP600125. Scale bars 10µm.

Immunofluorescence staining shows that SP600125 accelerates HaCaT cell differentiation and these effects appear to be enhanced by high calcium concentration (Figure 5.6). For example, E-cadherin staining is negative when cells are cultured in low calcium, as expected, but is also negative when cells are cultured in low calcium with SP600125, indicating that JNK pathway inhibition is not sufficient to induce E-cadherin expression or relocation to the cell membrane. As the formation of adherens junctions is calcium dependent (Delva et al, 2009), this is predictable as JNK inhibition and high calcium concentration induce differentiation by different mechanisms (Schmidt et al, 2000). However when cells are cultured with both SP600125 and high calcium, E-cadherin appears to be expressed more strongly along more cell-cell boundaries than with high calcium alone.

With both involucrin and filaggrin staining, it appears that SP600125 alone is able to induce expression and subcellular distribution similar to high calcium conditions. However, when high calcium and SP600125 are combined, involucrin and filaggrin expression is very strong. The exposure for all images was equal to show the relative intensity of staining, hence overexposure in involucrin staining for the high calcium and SP600125 treatment panel. ZO-1, a tight junction component, is only slightly increased by SP600125 or by high calcium alone, but is strongly expressed at cell-cell borders when SP600125 and high calcium are used in combination. Tight junctions are an important aspect of epidermal barrier function (Furuse et al, 2001, Kuroda et al, 2010), and so 3D cultures with SP600125 might be expected to form a more impermeable epidermal barrier.

The results clearly show that SP600125 treatment accelerates keratinocyte differentiation, but it is not known how quickly these effects take place or how much impact SP600125 has on proliferation. This is important, as when culturing keratinocytes for 14 days at the air-liquid interface, there needs to be a sufficient number of cells proliferating inside the scaffold before being induced to differentiate. It also means that it may be optimal to introduce the SP600125 into the culture at a later stage of the 3D culture.

Therefore, HaCaT cells grown on 2D glass coverslips were also stained for the proliferation marker Ki67. Five fields of cells were counted for each coverslip and cells were categorised as either totally absent from staining, intermediate staining or strong staining of mitotic chromosomes. Several concentrations of SP600125 were

used and experiments were carried out at several time points. The resulting graphs are shown in Figure 5.7. In addition, ViaCount analysis was performed on HaCaT cells cultured in 12 well plates for 24 hours to measure proliferative and apoptotic cells. Results are presented in Figure 5.7.

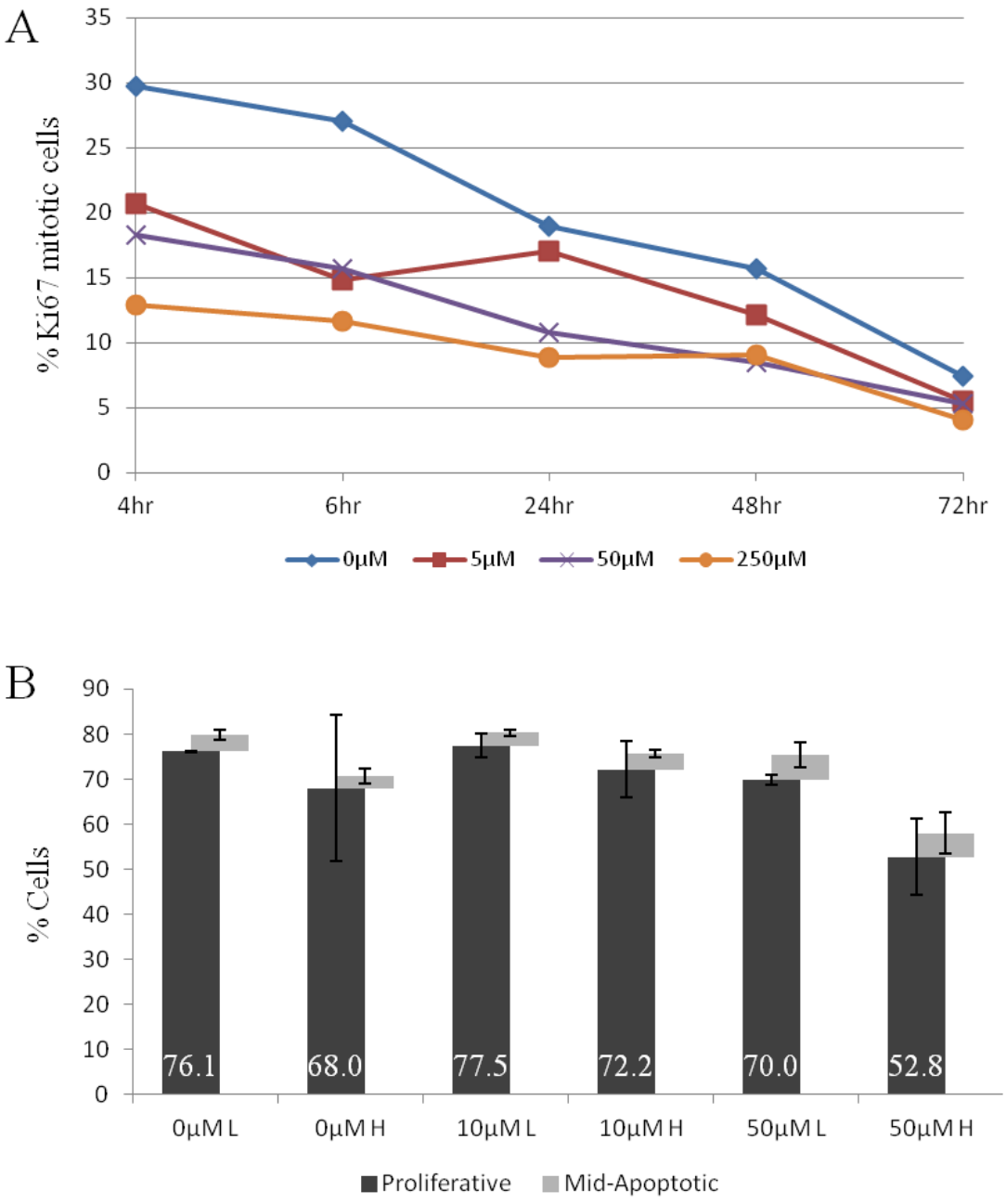


**Figure 5.7. Ki67 and ViaCount Analysis of SP600125-treated HaCaT Cells**

A) Percentage of mitotic cells over time with 0μM, 5μM, 25μM or 250μM SP600125; B) ViaCount analysis showing proliferative and apoptotic cells after 24 hours in various concentrations of SP600125. L/H = 0.06mM/1.5mM $Ca^{2+}$.

HaCaT cells treated with SP600125 quickly become less proliferative in accordance with the concentration used, as shown in Figure 5.7A. Even with the lowest concentration of SP600125 (5μM), there is a rapid reduction in the percentage of mitotic cells in the culture after 4 hours compared to un-supplemented culture media. This decrease in proliferation is correlated with dosage. However, after 72 hours all cultures are similarly proliferative.

Cultured media was replaced after 24 hours and these data suggest that lower concentrations of SP600125 such as 5μM "wear off" in the culture media. The number of mitotic cells in untreated cells continues to decrease as the confluence of the culture increases, as expected. From these data, two things can be determined - SP600125 acts quickly and shows effects on cell proliferation within 24 hours of being added to the culture media, and the effect of SP600125 reduces over time.

In order to assess cell viability with SP600125, ViaCount analysis (Figure 5.7B) was used. ViaCount analysis counts cells by flow cytometry and classifies them as viable, mid-apoptotic or dead depending on their ability to uptake two dyes. The results show that the majority of cells remain proliferative after 24 hours, which appears contrary to Ki67 results. However, ViaCount includes all viable cells, and not only mitotic cells, whereas only mitotic cells were included in Ki67 analysis. The addition of 1.5mM calcium to the culture media slightly decreased the percentage of viable cells compared to low calcium conditions, possibly due to differentiation or growth arrest. Interestingly, the addition of SP600125 alone did not reduce the percentage of viable cells in the culture but when SP600125 was added in conjunction with high calcium, the proportion of viable cells decreases in a concentration-dependent manner. No significant differences in the proportion of apoptotic cells were noted, showing that 50μM SP600125 does not induce apoptosis. The remaining 40% of cells in the culture were as classed as "dead", although the ViaCount assay is likely mislead by differentiated, anucleate cells.

### 5.2.3 Assessment of SP600125 JNK Inhibition in 3D Cultures

#### 5.2.3.1 Cell Proliferation and Morphology

To assess the affect of SP600125 in 3D conditions, HaCaT cells were cultured in 3D scaffolds, following the protocols established earlier. As previous experiments have shown that SP600125 acts quickly, 50µM SP600125 was introduced after the cultures were raised to the air-liquid interface. After seven days at the air-liquid interface an MTS assay was carried out. ViaCount is not compatible with the 3D scaffold as the cells cannot be reliably trypsinised out of the scaffold for analysis. Results of the MTS assay, showing a large and significant reduction in the conversion of MTS reagent, are shown in Figure 5.8. Cultures grown to 14 days were fixed and stained with H&E and for involucrin and these images are shown in Figure 5.9 to observe changes in morphology and differentiation.

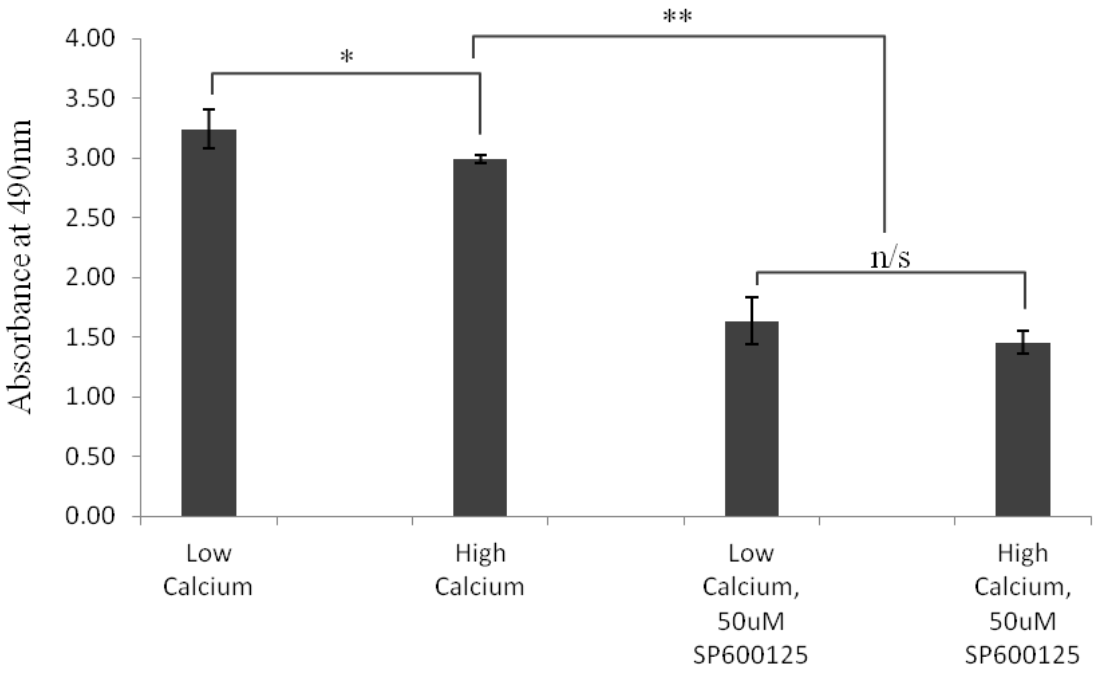


**Figure 5.8. MTS Assay of 3D Cultured HaCaT Cells with SP600125**

MTS assay showing HaCaT cell viability of 3D cultures grown for 7 days in the presence or absence of low/high (0.06/1.5mM) calcium and/or 50µM SP600125. Error bars show SEM. * = P<0.05, n/s = not significant.

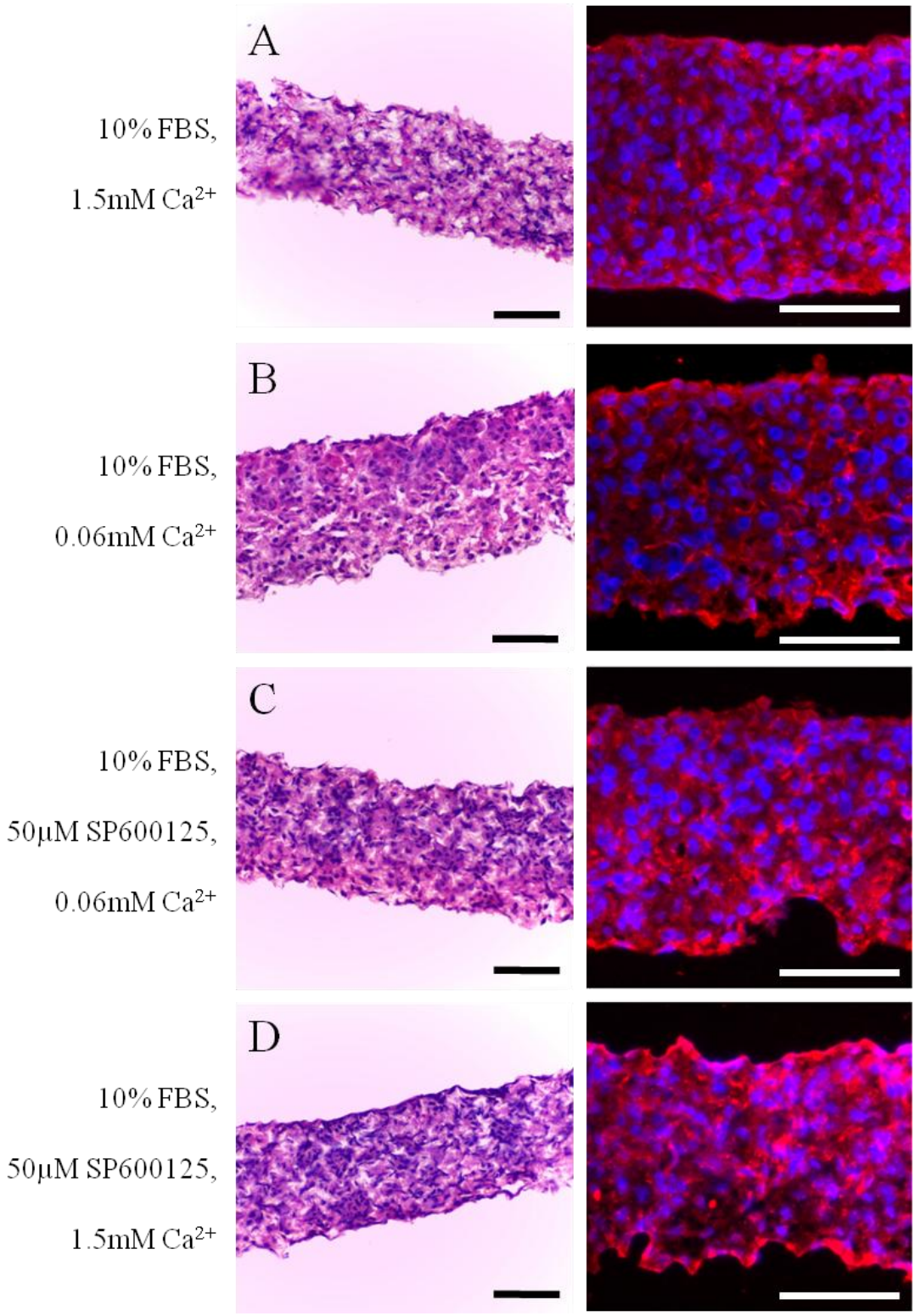


**Figure 5.9. 3D Cultured HaCaT Cells with SP600125**

H&E and Involucrin staining of HaCaT cells cultured at the air-liquid interface for 14 days in culture media containing. All scale bars 100µm.

The MTS assay shown in Figure 5.8 shows a significant and large reduction in metabolic activity when 50µM SP600125 is present. This may be due to the increased terminal differentiation present within the culture. This corresponds with the findings in 2D cultures where the population of proliferating cells significantly decreased with SP600125 treatment (Figure 5.7), although the difference is more pronounced in the 3D environment. Interestingly, SP600125 alone was enough to significantly reduce the metabolic activity of the entire culture, even with low calcium concentration. While high calcium induced a small decrease in MTS viability without SP600125, there was no significant difference in MTS viability observed between the low or high calcium SP600125 cultures.

H&E and involucrin-stained sections from 3D cultures are shown in Figure 5.9. H&E stained sections show some slight differences between each culture condition, although all cultures have fully filled the depth of the 3D scaffold. Cells grown in high calcium show flatter nuclei than those grown in low calcium. Similar to 2D culture experiments, low calcium with 50µM SP600125 shows a morphology more differentiated than low calcium alone but less differentiated than high calcium alone. Cultures grown in 50µM SP600125 and high calcium show the most involucrin staining, in line with previous findings that SP600125 and raised calcium concentration increases differentiation. As shown in Chapter Three, the air-liquid interface influences differentiation of keratinocytes - therefore there are three major contributing factors to the differentiation seen in the cultures - the air-liquid interface, calcium concentration and the presence or absence of SP600125.

#### 5.2.3.2 Cornified Envlope Formation in SP600125-treated 3D Cultures

As SP600125 clearly accelerates keratinocyte differentiation, and structures appearing to be cornified envelopes were observed in 2D culture, cornified envelope extractions were performed on 3D cultures and stained with 0.5mg/ml Nile Red. Results of the extraction showing isolated cornified envelopes are presented in Figure 5.10.

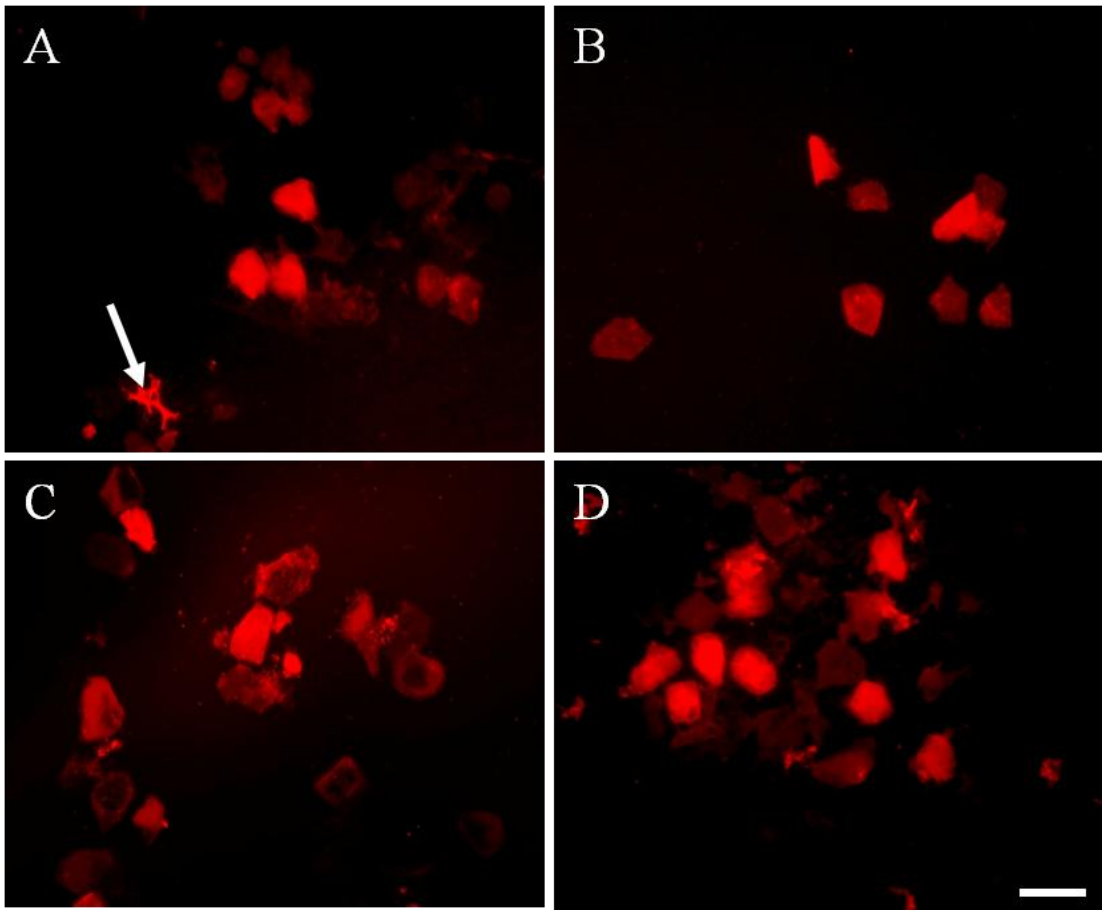


**Figure 5.10. Cornified Envelopes Isolated From SP6001250-treated Keratinocytes**

Nile Red-stained cornified envelopes extracted from HaCaT cells grown in the 3D scaffold for 2d submerged, then 14d at the air-liquid interface in A) 0.06mM $Ca^{2+}$; B) 1.5mM $Ca^{2+}$ ;C) 0.06mM $Ca^{2+}$ and 50µM SP600125; D) 1.5mM $Ca^{2+}$ and 50µM SP600125. Contamination by pieces of 3D scaffold marked with white arrow. Scale bar 50µm.

Cornified envelope extraction and Nile Red staining shows that cornified envelopes can be isolated from all culture conditions. Similar to results presented in the previous chapter, a mixture of mature and immature cornified envelopes are observed in all culture conditions. There were more cornified envelopes isolated from SP600125-treated cultures, although interestingly they do not show more intense staining with Nile Red than those from standard high calcium conditions. This suggests that while SP600125 may increase cornified envelope formation, it does not necessarily increase their maturity in terms of structure and covalently attached lipids. To support this, there was no difference observed in cornified envelopes from low or high calcium with SP600125. Staining in Figure 5.9 showed more intense involucrin staining (panel D), which is a component of the cornified envelope (Ishida-Yamamoto et al, 1995) and there are more cornified envelope isolated from the same culture conditions (i.e. high calcium with 50μM SP600125). However, this does not necessarily mean that the attachment of ceramides onto the protein structure is also increased, hence no changes in Nile Red staining. In microarray analysis of keratinocytes treated with SP600125 Gazel et al, 2006 showed that transglutaminase 1 (TGase1) was upregulated two-fold. However, those analyses were performed in 2D where TGase1 activity is normally very low compared to work in this chapter where the air-liquid interface differentiates the cells and likely increases TGase activity.

#### 5.2.3.3 Effect of SP600125 on 3D Cultured Keratinocyte Lipid Profile

In order to examine the effect of SP600125 on the lipid profile of 3D cultured keratinocytes, lipid extractions, separation on TLC plates and quantitation using ImageJ were performed. HaCaT cells were cultured in 3D and the total lipid extracted from 3D cultures, standardised against protein extracts, and a summary of the lipid profiles are shown in Figure 5.11.

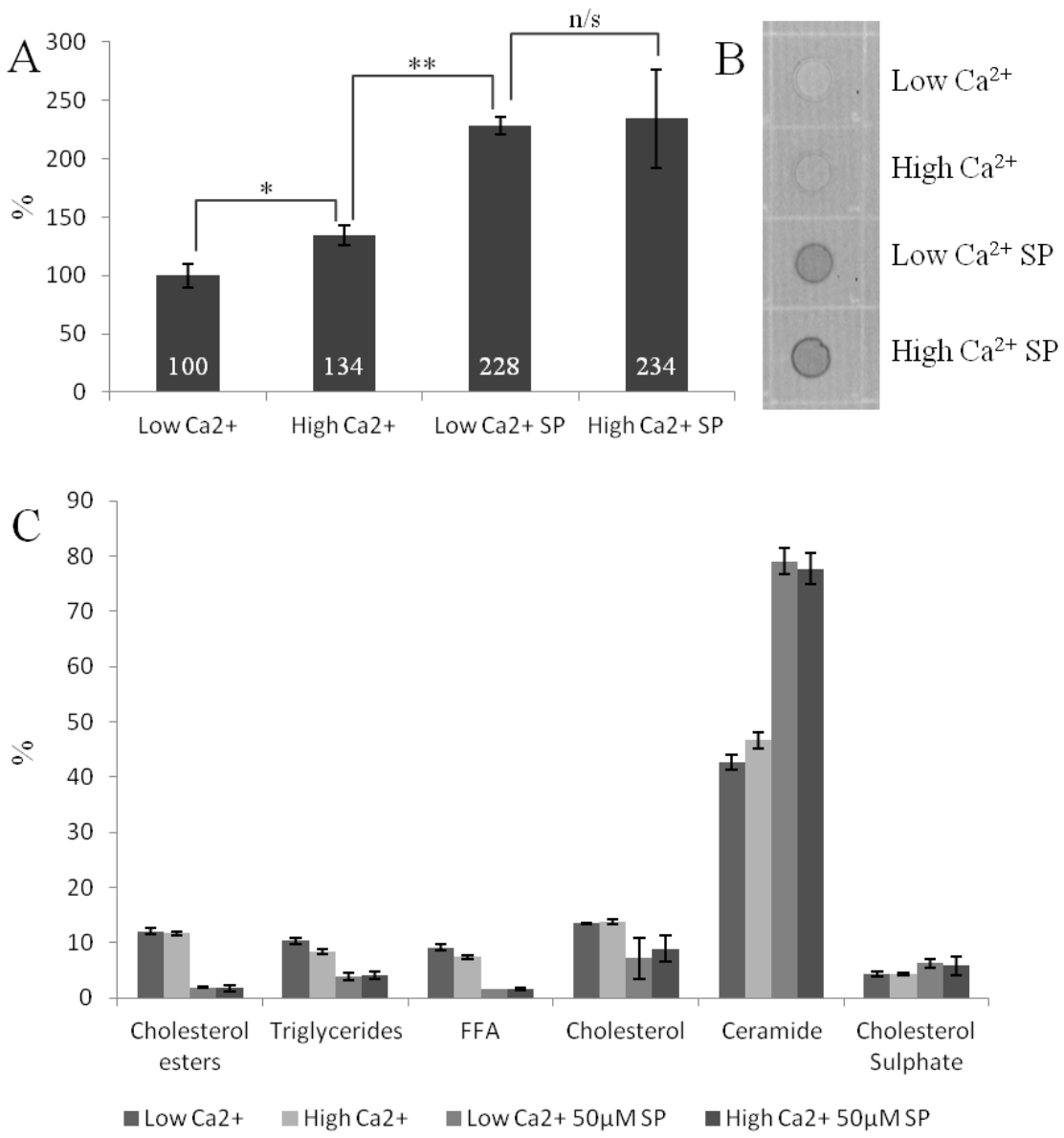


**Figure 5.11. Lipid Composition of 3D Cultures with SP600125**

A) Total lipids extracted from HaCaT cells grown in 3D culture in low/high calcium concentration and the presence or absence of 50µm SP600125. Lipid concentration expressed as a % against control; B) Spots of lipid extracts from each culture condition showing increased concentration from SP600125-treated cultures; C) Summary graph showing overall lipid composition of 3D cultured keratinocytes in low/high calcium in the presence/absence of SP600125. * = $p<0.05$, ** = $P<0.01$, n/s = not significant. Error bars show SEM.

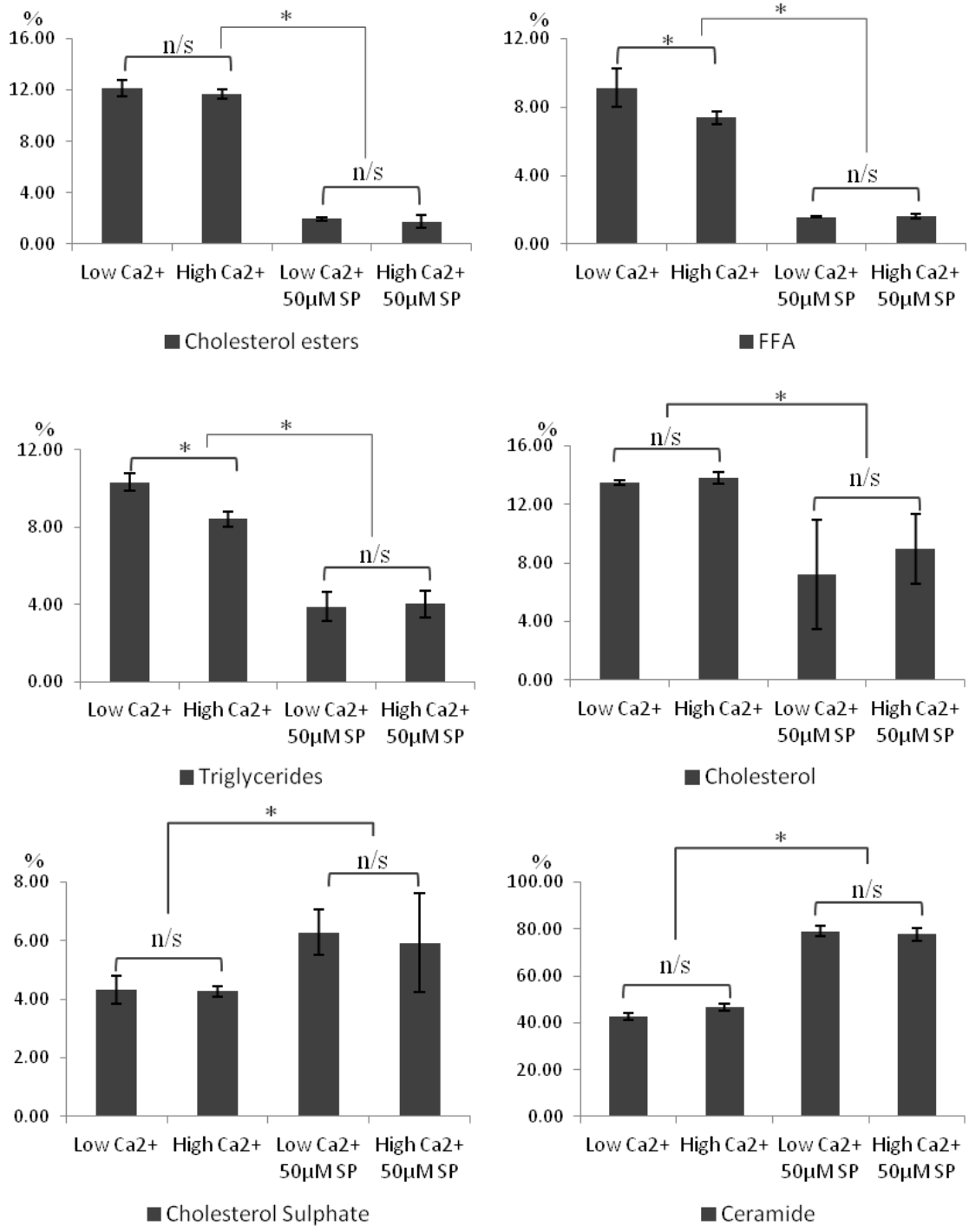


**Figure 5.12. Lipid Composition of 3D Cultures After 14 Days with SP600125**

Low $Ca^{2+}$ = 0.06mM calcium, High $Ca^{2+}$ = 1.5mM calcium, SP = SP600125. Error bars show SEM.

Quantitation of the average lipid content from each culture condition (Figure 5.11) shows that SP600125 dramatically increases lipid production. The presence of high calcium in the culture media moderately increased lipid production, but SP600125 was a far larger variable in increasing lipid production.

The overview in Figure 5.11 and detailed analysis shown in Figure 5.12 shows that SP600125 is the largest determinant in the lipid composition of the cultures. Aside from triglyceride and FFA which were moderately reduced by high calcium, calcium concentration did not alter the lipid composition of the cultures whereas with SP600125 treatment, every lipid was significantly different to untreated counterparts. Again, the presence of both high calcium and SP600125 did not significantly change lipid composition compared to low calcium and SP600125. However, high calcium did increase the total amount of lipid isolated from 3D cultures (Figure 5.11).

Ceramide production has significantly increased due to SP600125 treatment. Yet, the whole lipid content appears to show a more immature profile if compared to native human epidermis or to the samples cultured without SP600125. For instance, cholesterol ester content, which is highly hydrophobic and essential in barrier function (Masahiro and Masao, 2007), has significantly decreased in both SP600125 treatment groups, as well as free fatty acids. In native human epidermis, cholesterol ester comprises 6-10% of epidermal lipids (Elias et al, 2012). All 3D cultures show FFA content which is significantly lower than native epidermis (~15%), but those treated with SP600125 contain almost no FFA. Cholesterol content has also fallen in cultures treated with SP600125, and correspondingly, the immature precursor cholesterol sulphate has increased in proportion. Overall, SP600125-treated cultures show a more immature lipid profile, even though lipid production as a whole is dramatically increased.

#### 5.2.3.4 Effect of SP600125 on Barrier Function of 3D Cultured Keratinocytes

The results suggest that SP600125 inhibition of the JNK pathway increases ceramide synthesis as part of keratinocyte differentiation. To determine the effect of these changes in lipid composition on barrier function, samples were assessed for their permeability to corticosterone and are shown in Figure 5.13.

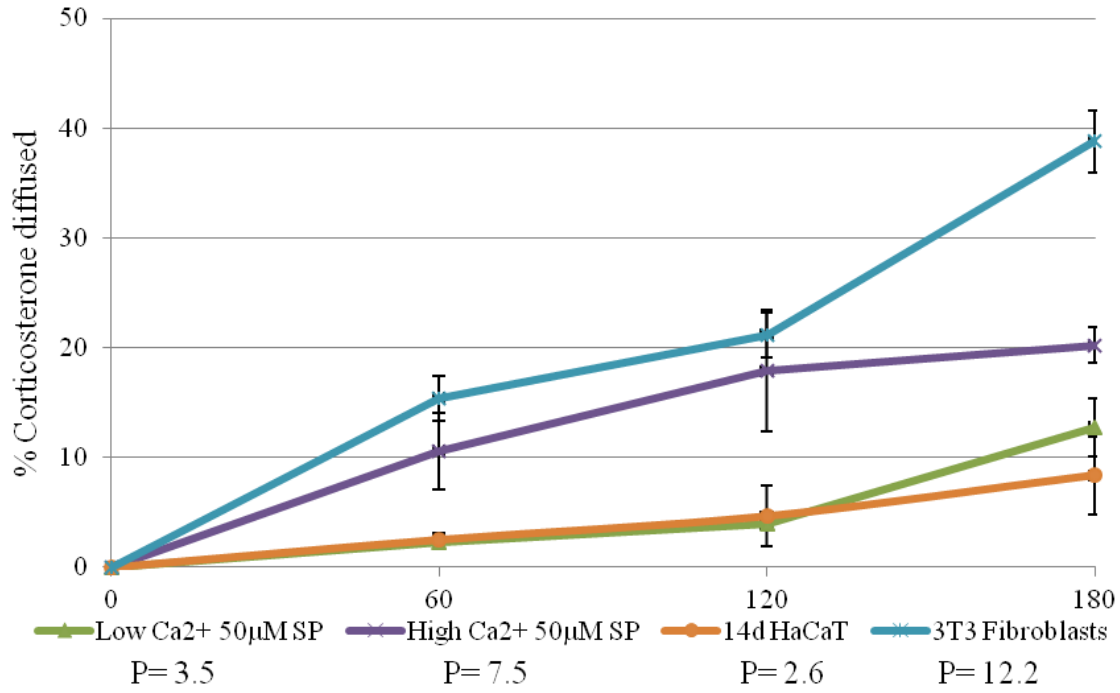


**Figure 5.13. Corticosterone Permeability of SP600125-treated 3D Cultures**

Graph showing % of corticosterone diffused into the recipient chamber against time through HaCaT keratinocytes or 3T3-NIH fibroblast cells cultured in the 3D scaffold. HaCaT cells were cultured for 2d submerged in standard culture media, then lifted to the air-liquid interface for 14 days in the presence of absence of SP600125. Fibroblast cultures were grown submerged for 7 days and are shown for comparison. The results show that after 180 minutes, the addition of SP600125 made the barrier more permeable to corticosterone diffusion. Permeability coefficients as $Px10^{-5}$ are noted in the legend. Error bars show SEM.

The permeability assays shown in Figure 5.13 show that the JNK pathway inhibition by SP600125 in combination with high calcium reduced the barrier function of 3D cultured HaCaT keratinocytes. A summary of the findings from all permeability experiments, including SP600125-treated cultures and comparitive data from published literature, is shown in Table 5.3 below.

**Table 5.3. Summary of All Permeability Coefficients**

| **Culture** | **Px10$^{-5}$** | **180 min %$_{diff}$** | **n** |
|---|---|---|---|
| 3T3-NIH Fibroblasts | 12.2 | 49.56 ± 3.03 | 3 |
| HaCaT DMEM | 2.60 | 8.36 ± 3.58 | 7 |
| WTK Low Calcium | 1.89 | 3.21 ± 0.81 | 4 |
| WTK High Calcium | 1.12 | 5.57 ± 0.94 | 5 |
| HaCaT 50µM SP600125 Low Calcium | 3.40 | 12.75 ± 2.65 | 6 |
| HaCaT 50µM SP600125 High Calcium | 7.50 | 20.21 ± 1.61 | 6 |
| **Published Data** | | | |
| **Name** | **Px10$^{-7}$** | **Reference** | |
| Human cadaver epidermal membrane | 2.1 | Ibrahim et al, 2009 | |
| Human cadaver epidermis | 1.62 ± 0.84 | Suhonen et al, 2003 | |
| Human epidermis | 0.89 | Buchwald et al, 2001 | |
| Human epidermis | 0.80 | Kuntsche et al, 2008 | |
| Human epidermis | 3.4 ± 0.9 | Chantasart et al, 2009 | |
| ROC (Rat Organotypic Culture) | 1.75[a]<br>2.72 ± 1.08[b] | [a]Kuntsche et al, 2008<br>[b]Suhonen et al, 2003 | |

*All keratinocytes cultured for 14 days at the air-liquid interface. 3T3-NIH fibroblasts cultured subermerged for 7 days. Permeability coefficients from published literatire are based on corticosterone permeability in either side-by-side or Franz type diffusion chambers at 37°C. The solvent for corticosterone was PBS or culture media, and no permeation enhancers were present. The corticosterone concentration was determined by ELISA or radioactive scintillation and permeability coefficients calculated.*

These findings are in line with previous data which showed that SP600125 caused abnormalities in the lipid profile and a reduction in many barrier-forming lipids such as cholesterol ester and free fatty acids. Interestingly, SP600125 in combination with high calcium showed a significantly greater barrier permeability than in combination with low calcium ($P=7.5 \times 10^{-5}$ vs $P= 3.5 \times 10^{-5}$), even though the lipid profile, extracted cornified envelopes and involucrin expression of those cultures were very similar. There was also no difference in the viability of the cultures (Figure 5.8) which may have explained the increased permeability of the high calcium cultures. The results show that while SP600125 undoubtedly accelerates keratinocyte differentiation, the resulting phenotype does not display better barrier function than other samples. This is potentially due to the rapidly accelerated differentiation of keratinocytes not allowing a sufficient barrier to form within the 14 day time period. With hindsight it may have been beneficial to culture the epidermal equivalents for a longer time, then added SP600125 at a later timepoint.

## 5.3 Discussion

### 5.3.1 Summary of Results

Results have shown that keratinocytes cultured in the 3D scaffold form an epidermal barrier with resistance to the diffusion of the lipid-soluble compound corticosterone. The level of permeability is correlated with characteristics of the cells in the 3D scaffold, including the profile of lipids produced by the cultured cells. However, the overall barrier permeability is considerably more permeable than human skin.

The 3D scaffold model developed over the previous chapters was used to assess the action of a JNK pathway inhibitor. Previous results shown in Chapter Four showed that 3D cultures did not form several layers of flattened cells or a stratum corneum, and some corneocytes still appeared to contain nuclei, indicating a deficiency in differentiation. SP600126 has been shown to induce keratinocyte differentiation in 2D conditions (Gazel et al, 2006) and was therefore chosen as a potential method to accelerate differentiation within the 3D scaffold cultures, with the aim of improving the barrier function of the cultures. SP600125 had also not been tested in 3D culture conditions, or tested for its impact on barrier permeability.

Firstly, the compound was analysed in 2D and confirmed to rapidly reduce proliferation and increase differentiation of keratinocytes. When keratinocytes were

cultured with SP600125 in 2D conditions, cells showed differentiation as visualised by changes in cell morphology and increased involucrin, desmoplakin and filaggrin expression. SP600125 also induced tight junction formation, visualised by ZO-1 staining. In 3D, SP600125 was found to increase the number of cornified envelopes isolated from the culture although these cornified envelopes were not necessarily more mature, as visualised by Nile Red staining for covalently attached lipids. These findings indicated that keratinocytes cultured in the presence of SP600125 would be expected to form a more hydrophobic and more resistant epidermal barrier.

However, lipid extractions showed that SP600125 significantly increased the proportion of ceramides produced by 3D cultured keratinocytes. A high percentage (~35-50%) of ceramides is physiologically normal and associated with mature barrier function (Stahl et al, 2009) but SP600125-treated cultures contained almost 80% ceramides, which is abnormally high. Perhaps more significantly, the proportion of hydrophobic cholesterol esters, cholesterol and free fatty acids were significantly lower, and the precursor lipid cholesterol sulphate was also elevated with SP600125 treatment. These lipid precursors have been shown to have their own effect on epidermal differentiation. For example, cholesterol sulphate has been recently found to induce differentiation markers such as filaggrin through the retinoic acid receptor-related orphan receptor alpha (RORα) (Hanyu et al, 2012). Cholesterol and ceramides have also been found to have co-ordinated signalling roles in the epidermis, where their release from lamellar bodies and subsequent conversion into active molecules which regulate the development of the stratum corneum (Feingold and Jiang, 2011). Therefore it is possible that the disturbances in the 3D cultured epidermis caused by SP600125 not only affected the profile of lipids important in the barrier function, but also affected the signalling involved in maturation of the stratum corneum. These factors combined to cause a decreased barrier function in cultures supplemented with SP600125.

Gazel et al, 2006 showed that several genes coding enzymes associated with lipid production and conversion were upregulated with SP600125 treatment, supporting this theory. These included ACAT2 (cytosolic acetoacetyl-CoA thiolase, responsible for cholesterol ester synthesis) and FABP2 (epidermal fatty acid binding protein 2, involved with fatty acid metabolism and upregulated in psoriasis). A number of lipodolytic enzymes were also regulated, although none of those mentioned in the

published data are associated with epidermal lipid lipodolysis. Lipid extraction from the 3D epidermal cultures in this chapter showed that cholesterol ester content decreased, which would be unexpected if ACAT2 is upregulated. However, Gazel and colleagues' microarray analysis was performed on 2D-cultured cells which are normally maintained in a basal, non-differentiated state, compared to the 3D scaffold where keratinocytes will differentiate at the air-liquid interface without the need for further external stimulus such as raised calcium or SP600125. The 3D environment has been shown to change cellular behaviour throughout this thesis, and so results from 2D and 3D cultures can not necessarily be compared like for like. It is probable that gene expression of keratinocytes cultured in the 3D scaffold would be different to keratinocytes cultured in 2D dishes and therefore the whole basis for comparing the action of SP600125 would be different.

The SP600125-treated cultures with altered lipid composition showed increased permeability to corticosterone compared to other cultures, highlighting the importance of lipids in the barrier permeability of epidermal cultures. However, cultures grown in high/low calcium with SP600125 showed differing permeabilities, even though their lipid profiles, extracted cornified envelopes and viabilities were similar, showing that there may be other factors affecting permeability that remain unaccounted for. In this case, it is likely that SP600125 accelerated differentiation to the point where the cells differentiated prematurely before being able to form a mature barrier. This highlights the importance of ordered differentiation, and with hindsight, a lower concentration of SP600125 introduced at a later stage of the culture period may have been beneficial.

These results showed that the 3D scaffold model developed in the previous two chapters could be used to measure the effect of a compound on keratinocyte behaviour and barrier function. These results also highlight the importance of functional testing such as direct barrier assessment and show that findings in 2D and 3D environments can differ substantially. Zhang et al, 2003 demonstrated that inhibition of the JNK pathway by SP600125 was able to reverse epidermal hyperplasia in mice. However they did not assess the barrier function or lipid production of the resulting epidermis. The observations in this Chapter indicate that accelerating differentiation or reducing proliferation by inhibition of the JNK pathway may not be a suitable therapeutic approach for treatment of skin disorders

due to profound changes in the lipid profile and barrier permeability of the epidermis. However, this would need to be investigated further. One key difference is that the 3D scaffold model represents a somewhat "normal" epidermis which already forms a normal lipid profile and barrier function and so SP600125 disrupts that behaviour. However, disordered skin may still be corrected by SP600125.

### 5.3.2 Future Work

Testing the 3D scaffold model permeability with more compounds would be beneficial as the corticosterone compound used in this chapter is a lipid-soluble steroid molecule and permeates through the barrier of corneocytes, extracellular lipids and viable cell membranes more readily than water-soluble substances. The OECD guidelines mentioned previously recommend use of both lipid and water soluble permeants in assessing an epidermal permeability model. Water soluble substances used for permeability testing include caffeine, mannitol or glucose (Buchwald and Bodor, 2001, Suhonen et al, 2003, Pappinen et al, 2012). Caffeine is also the OECD Guidance 28 (OECD, 2004) approved standard for permeability testing of *in vitro* equivalents designed for replacing *in vivo* testing. A low molecular weight tracer, colloidal lanthanum nitrate has been used previously (Gruber et al, 2011) to visualise paracellular transport through the epidermis. Use of a tracer, as well as water-soluble compounds will give insight as to the diffusion pathway taken by molecules through the 3D cultures (i.e. transcellular or intercellular) and show possible areas of improvement for the model.

One important factor for an *in vitro* model is not necessarily to match the permeability of human skin exactly, but rather to accurately predict the penetration of a compound through human skin. This so-called "permeability ratio" of $P_{model}/P_{human}$ can be used to predict the permeability of a compound through human skin based on the permeation through an epidermal model (Pappinen et al, 2012). In order to further assess the usefulness of the 3D scaffold model for predicting the effect of compounds on epidermis, animal epidermal samples could be used to formulate a more complete permeability ratio for multiple compounds.

It is important to note that *in vitro* epidermal equivalents can vary considerably in their permeabilities to different compounds relative to human epidermis. For instance, Suhonen et al, 2003 compared a well-developed epidermal model to human epidermis. While their model was very accurate for some compounds such as Nadolol and Pindolol ($P_{model}/P_{human}$ 1.0 and 1.2 respectively), it was far less permeable to water soluble salicylic acid (0.3) but much more permeable to lipid soluble beta-estradiol (5.2). This is likely due to the preferred permeability pathways of each molecule and lack of hair follicles in *in vitro* models. *In vitro* epidermal equivalents can still be useful even with varying permeabilites compared to real

epidermis - as long as the permeability rating for a particular compound is consistent. Therefore, in order to fully characterise the 3D scaffold model, a greater number of permeants need to be tested and larger numbers of repeats performed. In addition, organotypic models typically overestimate the permeation enhancing effect of compounds such as ethanol or SDS, but if these results are predictable then they are still useful (Pappinen et al, 2007).

For reference, published corticosterone permeability coefficients of human epidermis are $Px10^{-7}$ = 1.62±0.84 (Suhonen et al, 2003) or 0.87 (Kuntsche et al, 2008), which are significantly lower than the coefficients derived for the 3D scaffold model in this chapter. However, it is difficult to directly compare these figures as the calculated permeability coefficient will depend on which part of the slope of increasing permeant concentration is used for the calculation. Clearly, the most rapid diffusion into the recipient chamber is at the start of the experiment where the concentration gradient between the two chambers is largest. Over time, the rate of diffusion will fall and would provide a much smaller permeability coefficient. Alternatively, some permeants display a lag time before any of the substance diffuses through. Therefore, the figures provided above are for reference and not direct comparison as it is not known which area of the graph was used for calculation in the published literature.

As mentioned previously, low and high calcium SP600125-treated cultures in 3D showed increased involucrin staining and increased cornified envelope formation and very similar lipid profiles. However, low and high calcium SP600125 cultures significantly differed in terms of barrier permeability. One reason may be that cells are being differentiated too quickly, rather than undergoing the controlled and ordered process which normally occurs. For instance, Ishida-Yamamoto et al, 1995 found that cornified envelope formation occurs too early within the differentiation process of psoriatic skin, resulting in reduced epidermal barrier function. The cornified envelopes isolated from these patients were also determined to be more fragile than those from normal skin. Staining shown in Figure 5.10D shows that while SP600125 induced more cornified envelope production, they were not necessarily more mature in terms of covalently attached lipids. Adding earlier time points to the work in this chapter would show whether this is the case for SP600125 treatment. Future work could also alter the timing of SP600125 addition so that it could potentially be used to enhance terminal differentiation after keratinocytes have

already begun to differentiate at the air-liquid interface. Future work could also assess the structural stability of cornified envelopes by use of sonication as a measure of their maturity (as in Sevilla et al, 2007). Analysing the ceramides produced by SP600125-treated cultures would also be worthy of investigation, as the bands on the TLC plate suggested that two particular ceramides are increased in comparison to the other cultures (data not shown).

Mouse keratinocytes formed a more effective barrier to corticosterone penetration than HaCaT cells and ideally future work would be carried out utilising this cell line, although their much slower proliferation makes this significantly more time consuming.

#### 5.3.2.1 Evaluation of SP600125 and JNK Pathway Function

To date, the effect of SP600125 on epidermal barrier function had not been tested. Data presented in this chapter suggests that SP600125 induces premature differentiation of keratinocytes and reduces overall barrier function under *in vitro* conditions where the cells differentiate normally. This hypothesis could be tested using animal studies and cornified envelope extractions, lipid extractions and barrier permeability analysis could be compared between the 3D scaffold model and samples of the animal epidermis.

The results in this chapter show that SP600125 induced differentiation in keratinocytes and dramatically increased ceramide content, but these changes did not translate to improved barrier resistance to corticosterone. However, the 3D scaffold model is based on healthy epidermis with a physiologically accurate lipid profile and mature cornified envelope production. Inhibition of the JNK pathway with SP600125 and corresponding changes in keratinocyte behaviour may have potential therapeutic uses in cases where the target skin is not physiologically normal. For instance, hyperproliferation and incomplete terminal differentiation (lack of cornified envelopes, or immature envelopes) are both features of psoriasis (Kawashima et al, 2004). Psoriatic skin also shows larger intercellular spaces (Kawashima et al, 2004), reduced barrier function (Wolf et al, 2012) and reduced ceramide synthesis correlated with clinical severity (Cho et al, 2004).

In data presented in this chapter, SP600125 increased cell-cell tight junctions and increased ceramide content, as well as reduced the rate of keratinocyte proliferation,

all of which may be beneficial when applied to psoriatic skin. Although SP600125 has not been directly tested against psoriatic skin, published data and the data shown in this chapter suggest that compounds altering keratinocyte proliferation and differentiation may have therapeutic uses in some cases of psoriasis. Zhang et al, 2004 applied topical SP600125 to mice with hyperproliferative epidermis and found that keratinocyte proliferation was reduced to normal levels. Clearly, psoriasis is a complex disorder which may caused by several deficiencies in keratinocyte behaviour (such as genetic transglutaminase deficiency, pathogenic T-cells and drug side effects (Cho et al, 2004, Wolf et al, 2012)), but based on findings utilising the 3D scaffold model, application of SP600125 to a psoriatic mouse model (such as Zenz et al, 2004) or psoriatic *in vitro* model (such as Barker et al, 2004) would be an interesting line of investigation.

Findings from the 3D culture model could be confirmed by further experiments using siRNAs. Keratinocyte JNK expression (both isoforms of JNK, either separately or together) could be ablated with a lentiviral vector (for stability, due to the long growth period required in the 3D scaffold) and those cells could be cultured in the 3D scaffold. If there was an effect on differentiation and barrier permeability, this would show that the normal activity of the JNK pathway is important for suppressing differentiation. Carrying on from this, target proteins such as c-Jun and ATF-2 could be independently knocked down which would give insight as to which activator is most important in suppressing keratinocyte differentiation. Analysing the keratinocytes at multiple time points would also give insight as to the process of how JNK regulates differentiation.

In Chapter Three, MET4 squamous carcinoma cells were successfully cultured in the 3D scaffold. These cells are known to show cell cycle disorders and the inability to differentiate (Proby et al, 2000). Studies have shown overactive JNK in over 75% of squamous cell carcinoma patients, and JNK inhibitor drugs and compounds are under investigation as potential therapeutics (Hengning et al, 2010). MET cell lines could be cultured in the 3D scaffold with and without SP600125, and assessed for JNK activity as well as proliferation and viability.

#### 5.3.2.2 Other Types of Epidermal Permeability Assessment

Diffusion analysis is an effective method for measuring barrier function, although it has several negative aspects. Firstly, cultures which have been subjected to diffusion cell analysis lose integrity over time and will absorb some of the permeant molecule (or radioactivity if radiolabelled compounds are used), meaning that they cannot be re-tested in the future. Also, to reach equilibrium on both sides of the diffusion apparatus may take several days, during which time the integrity of the cultured epidermis reduces. The upper surface of *in vitro* cultures or real epidermis is normally air-exposed and dry, but during diffusion analysis the sample is fully submerged. As discussed in the previous chapter, over-hydration of the epidermis has a profound effect on barrier permeability (Warner et al, 2003). During investigations in this chapter, some cultures were subjected to corticosterone diffusion for up to 48 hours, during which results became more variable as the integrity of the culture lessened. Therefore, samples were measured over the first three hours to measure barrier permeability without adverse effect on the cultures themselves and a permeability curve was generated. Schreiber et al, 2005, showed that *in vitro* substitutes are more susceptible to the effect of the experimental environment than human epidermis samples during diffusion-based permeability assessment. For instance, when Igepal was used as a solubiliser in the permeant solution, it increased permeability of the *in vitro* epidermis models SkinEthic and EpiDerm by five to seven-fold but did not affect human or porcine epidermal samples. Therefore, long-term diffusion assays of *in vitro* equivalents are not ideal.

Other techniques have been used to act as a proxy for epidermal barrier function. For instance, the water content of the stratum corneum is a key indicator of barrier function which can be measured directly by NMR (Sotoodian et al, 2012). Transient thermal transfer (TTT) uses a heated probe (Hydrascan by Dermascan labs, France) applied to the surface of the skin. A thermometer measures the temperature increase at a distal site, and the rate of temperature increase with relation to distance is correlated with barrier function (Girard et al, 2000). As TTT is a non-destructive technique, cultures differentiating at the air-liquid interface could be measured repeatedly over time as a quick assessment of barrier function until an optimal barrier function is reached. Diffusion analysis could then be carried out on optimised cultures which reached a pre-determined TTT score, thus improving reliability of data. Transepithelial electrical resistance (TEER) is a similar non-destructive method

which passes a small electrical current across the culture without affecting viability. Higher electrical resistance is caused by drying and high lipid content and is therefore correlated with barrier function (Girard et al, 2000). Either of these methods could be used to assess barrier permeability in the 3D scaffold model before, during or after diffusion testing as a means of quality control. This would improve the reliability of the gathered data by standardising the cultures selected for permeability testing i.e. cultures could be selected for permeability testing once a certain TEER score has been achieved. The TEER of the cultures could be measured continuously during permeability testing, showing if any degradation in the barrier occurs. TEER could also be used to determine the optimal time for addition of compounds such as SP600125 by monitoring the formation of the barrier and adding the compound when "normal" barrier maturity is reached.

# 6 General Discussion

## 6.1 Summary of Results

The results presented in this thesis have shown that a porous polystyrene 3D scaffold can be used to culture keratinocytes without a dermal equivalent. When raised to the air-liquid interface, these cultures of keratinocytes are induced to terminally differentiate, expressing proteins such as keratin 1, involucrin and filaggrin. Further examination showed that keratinocytes displayed features such as lamellar bodies, keratin bundling, desmosomes and keratohyalin granules, all of which are essential for epidermal barrier function. However, cells appeared to be disordered and only 2-3 layers of flattened cells were observed. Nevertheless, cornified envelopes were isolated from the cultures, indicating that keratinocytes had reached terminal differentiation.

These cultures were found to synthesise lipids associated with barrier function (ceramide, free fatty acids and cholesterol), and modifying the culture conditions with supplements such as ascorbic acid increased the level of keratinocyte differentiatin and optimised the lipid synthesis with a resulting lipid profile similar to native epidermis. However, these cultures still did not display a normal organisation of differentiation markers or the formation of several stratified layers of flattened corneocytes. The 3D scaffold epidermal model was subsequently characterised in terms of barrier resistance to corticosterone diffusion and was used to investigate the effect of a compound, SP600125, which had been shown to induce differentiation under 2D conditions but had not been previously studied in a 3D environment. Inhibition of the JNK pathway by SP600125 appeared to rapidly induce differentiation in 2D and 3D culture conditions and altered the lipid synthesis of the cells. The effect of this compound on 3D cultured cells was different in comparison to cells cultured in 2D, highlighting the importance of the 3D culture environment on behaviour of cells. In spite of increased cell differentiation, the barrier formed by SP600125-treated keratinocytes was more permeable, likely due to the disturbance in normal lipid synthesis and accelerated differentiation. This was counter to the original hypothesis stated in Chapter One (1.5). This demonstrates that 2D culture does not necessarily give predictable results and emphasises the importance of functional testing in addition to analysing barrier components.

Overall, the results showed that complete terminal differentiation was able to take place even when keratinocytes were constrained within the porous 3D material. This shows that horizontal, flat stratification observed *in vivo* is not a requirement for keratinocyte terminal differentiation and cornified envelope formation, nor is it required for epidermal lipid synthesis. This was observed with both HaCaT cells and mouse keratinocytes and could be further validated by cell culture in alternative 3D materials with altered physical properties and use of human primary cells.

### 6.1.1 Potential Uses of the 3D Scaffold and Future Work

As well as culturing keratinocytes at the air-liquid interface directly, there are many other uses for the 3D scaffold. Preliminary investigation in this chapter showed that fibroblasts can be cultured in the 3D scaffold. Therefore a multi-layered co-culture may be possible, where fibroblasts are cultured to confluence inside the scaffold and keratinocytes seeded onto the surface, then raised to the air-liquid interface. Initially, attempts were made to create this model (data not shown) but the fibroblast cultures were not confluent enough to prevent keratinocytes from falling inside the scaffold. When cultures were stained for markers of fibroblasts or keratinocytes, only keratinocytes were detected, located throughout the 3D material. This shows that the keratinocytes had most likely fallen into the 3D scaffold and outcompeted the fibroblasts. Separating the fibroblasts culture with a thin layer of Matrigel or collagen and then seeding a keratinocyte culture on the surface may produce the desired results.

Other co-cultures would also be possible with the 3D scaffold, utilising the well-inserts to bind multiple scaffolds containing different cell types. This may be used for culture of dependent cell types such as keratinocytes and feeder fibroblasts, or astrocytes and neuronal cells. This system would allow two cell types to be cultured in 3D while sharing the same culture media.

#### 6.1.1.1 Cell Motility and Invasion Studies

The 3D scaffold may be used for cancer cell invasion studies. Collagen gels or collagen-coated matrices have been used previously (McInroy et al, 2007, 2011) to monitor carcinoma cell invasion behaviour. Typically this is achieved by seeding carcinoma cells onto the surface of a gel which represents healthy tissue, and encouraging carcinoma cells to invade. The 3D scaffold could be used to culture an *in vitro* "tissue" that can then be subjected to cell invasion. For instance, the

epidermal model developed in this chapter could be subjected to invasion by carcinoma cell line such as MET4 cells, or the HBL human melanoma cell line (Eves et al, 2003).

#### 6.1.1.2 Perfusion Chamber System

Experiments in Chapter One showed that a larger amount of cell culture media available to cells growing in 3D improved their viability. This could be taken a step further by use of a perfusion chamber system, where 3D scaffolds are subject to constant culture media turnover and infusion of oxygen, allowing for optimal cell nutrition, waste clearance and buffering of the culture media. This system could be utilised for submerged cell culture of other cell types. This method was recently used with a biodegradable poly(lactic acid)-based scaffold to culture liver cells and measure their cytochrome P450 activity in response to cytotoxic anticancer drugs (Ma et al, 2012). Such systems have been used previously (Sun et al, 2005) to culture keratinocytes at an air-liquid interface with constant media turnover, resulting in improved cell viability. The 3D scaffold used in this study could be similarly used and may be advantageous due to its inherent stability for long culture periods.

#### 6.1.1.3 Routine Cell Culture

The 3D scaffold could be for routine 3D cell culture. Increasingly, cell biologists are becoming aware of limitations in 2D cell culture (Schmeichel, 2003, Baker et al, 2012). 2D cell culture has many deficiencies, and even alters long-term cell behaviour of cell lines after prolonged culture, further removing cells from their *in vivo* behaviour. This is outlined in greater detail during Chapter One. As the 3D scaffold is stable and non-biodegradable it should be possible to remove cultured, semi-confluent cells from the scaffold for sub-culture into new scaffolds. It would therefore be possible to routinely maintain cultured cells in 3D rather than 2D, potentially improving their usefulness for studying cell biology and modelling disease by reducing the adaptations cells undergo in prolonged 2D culture. Preliminary investigations showed that it was difficult to trypsinise cultured HaCaT cells out of the 3D scaffold used in this thesis, however HaCaT cells which strongly adhere to surfaces are also not an ideal cell line for this type of routine 3D culture. HaCaT cultures subjected to 40+ minutes of trypsinisation at 37°C still showed considerable numbers of keratinocytes inside the 3D scaffold after fixation and H&E staining. However, work undertaken by a project student in our lab showed that a

SW480 colon cancer cell line could be successfully grown in the 3D scaffold, separated from the material and then re-seeded into a new 3D scaffold, allowing for full long-term 3D culture cell maintenance. A new version of the 3D scaffold and improved protocols using non-enzymatic cell detachment methods are also under development in our lab with this routine cell culture purpose in mind. Keratinocytes could then be cultured long-term in low calcium, submerged conditions which have been shown in Chapter Three to prevent differentiation. Cultures can then be raised to the air liquid interface for experimentation purposes.

#### 6.1.1.4 Isolation of Primary Cells

Current methods of primary keratinocytes isolation rely on separating the epidermis from the dermis, and then isolating keratinocytes by trypsinisation, centrifugation, physical agitation or heat. The isolated cells are then seeded directly onto 2D Petri dishes or glass plates (Turksen et al, 2006). This forces selective pressure onto cells, where only those capable of quickly adhering to the surface and adapting to the submerged 2D cultured conditions are able to survive and proliferate. As a result, these primary cells do not necessarily represent their *in vivo* counterparts closely. Assuming that current issues around cell trypsinisation are resolved, a stable, relatively rigid material such as the 3D scaffold could potentially be used for isolation and initial culture of primary keratinocytes from epidermal samples. This allows for more cell-cell contact and communication and long-term, this may preserve more of the cells' *in vivo* proliferative characteristics, allowing for more representative results *in vitro*. The use of the 3D scaffold for tissue explants is currently under investigation in our lab.

#### 6.1.1.5 Further Development of the 3D Scaffold Material

The scaffold itself is under further development in our lab. Steps have been taken towards functionalisation of the polymer surface, such as covalent attachment of ligands, including collagen coating discussed in this chapter. Incorporation of soluble signalling molecules and growth factors into the 3D scaffold is also under investigation, for the production of "smart materials" which direct cell fate (Zeyfert et al, 2009). Other labs have shown that multiple growth factors can be released from materials over time due to differing release kinetics, and staggered to create optimal culture conditions with multi-stage proliferation or differentiation signals (Richardson et al, 2001).

Improvements to lab techniques and adjustments to standard protocols are being developed so that more techniques such as live cell imaging, cell transfections and protein extractions can be used in combination with cells cultured in the 3D scaffold.

### 6.1.2 Further Investigation into the 3D Scaffold Epidermal Model

Clearly no *in vitro* epidermal equivalent can yet replace native epidermis for final stage testing before a novel compound is approved for human use. This is for several reasons, but primarily because these models, including the 3D scaffold model, are still simple cultures utilising only keratinocytes or keratinocytes with a simple dermal equivalent. Although most models show several stratified layers of epidermal cells, differentiation markers and representative lipid profiles, these epidermal models have lack of vascularisation (and therefore only viable for short-term experiments), absence of Langerhans cells or melanocytes, lack of hair follicles, sebaceous glands or native floral microorganisms (Baroni et al, 2012). Several factors such as the presence/absence of hair follicles, lipid composition and morphology have been shown to be important in barrier permeability (Lademann et al, 2001) and therefore the current generation of epidermal models can not completely represent *in vivo* epidermis.

Therefore all *in vitro* equivalents using current technology are limited and generally have permeabilities exceeding those of native epidermis (Schmook et al, 2001, Suhonen et al, 2003, Pappinen et al, 2012). However, 3D models are useful for preliminary testing the permeability of novel compounds and also for assessing the effect of compounds on epidermal differentiation, as SP600125 was assessed during the previous chapter. Understanding the actions of such compounds will uncover more understanding of signalling pathways involved in proliferation, differentiation and barrier function and how they may be manipulated for therapeutic benefit. For instance, some epidermal disorders may be treated by topical application of compounds affecting lipid metabolism (Elias et al, 2012).

As mentioned in Chapter One, the epidermal barrier, in particular the stratum corneum, is the principle site of resistance to topical drug treatments. Therefore considerable research effort has been focused on increasing the permeability of molecules through the epidermis in order to improve drug delivery and the

effectiveness of topical treaments including delivery of hormones (testosterone replacement, hormonal contraception), nicotine replacement and painkillers in the form of creams or patches. These topical treatments are attractive therapeutically as they are painless, non-invasive and can be administered at home by the patient, making them preferable to injections. They also bypass first pass liver metabolism which represents an advantage over oral medications in terms of ease of drug design and avoiding complications due to metabolic byproducts. As described in Chapter One, these techniques for improving epidermal permeability have included using lipophilic permeation enhancers (Ochalek et al, 2012), microneedles (Wu et al, 2006) or encasing drugs inside lipid nanoparticles (Kuntsche et al, 2008), as well as mixing target compounds with oils, alcohols and other lipid soluble diluents to aid their passage through the epidermis. Testing of these compounds is one potential use for *in vitro* epidermal models, as they are reproducible and can cultured in large numbers for high volume testing. The 3D epidermal model established in this thesis could be treated with a chemical permeation enhancer and the effect on permeant diffusion measured. This is a common area of research where models generally exaggerate the permeation enhancing effect of compounds (Pappinen et al, 2007).

The 3D scaffold model was generally reliable and reproducible, with only a few cultures being discarded because of leaking during diffusion experiments. In terms of morphology and lipid composition, 3D scaffold cultures were repeatable and reproducible because the 3D scaffold material itself is synthetic and stable, and the use of a stable cell line further increased reproducibility. As mentioned previously, native human epidermis shows considerable variation depending on the age, gender, race and genetics of individual donors, as well as body site, skin moisturisation and many other factors (Darlenski and Fluhr, 2012). This variation has also been found in commercial *in vitro* models using human NEK cells (Ponec et al, 2000, Schreiber et al, 2005) and variation in human epidermis permeability can be observed in data presented in Table 5.3. This makes preliminary testing of compounds more difficult and time-consuming due to increased variability in human samples.

Interestingly, the direction of diffusion (i.e. dermis to epidermis or epidermis to dermis) shows equal resistance in human full thickness skin for most permeants, but is observed to be different for some large molecular weight compounds using *in vitro* skin equivalents (Oshizaka et al, 2012). The reason for this is likely due to the lack of

hair follicles in the *in vitro* model, which provide a route of passage for some hydrophilic compounds, whereas these compounds diffuse very slowly through paracellular pathways of the mature stratum corneum. Similar to findings in this chapter modelled by a 3D culture of 3T3 fibroblasts, Oshizaka and colleagues noted that the dermis alone provides very little barrier function (supported by further evidence in Schreiber et al, 2005) and proposed a "conical pore" model for the passage of hydrophilic and lipophilic in both directions of diffusion. Although the epidermal to dermal permeation of compounds is the most frequently studied, clearly dermal to epidermal diffusion is also important to maintain the homeostasis of the body. This could be tested using the 3D scaffold epidermal model by reversing the orientation of the culture in the diffusion apparatus.

### 6.1.3 Future Work for 3D Materials

Although promising, three dimensional cell culture is still a developing technique used by a minority of laboratories, even though the benefits are relatively well described. In order to achieve more widespread use, 3D cell culture needs to become more standardised, with routine protocols for cell seeding, analysis and experimentation widely available and economically viable. It is likely that in the intermediate future 3D cell culture may be used for validating discoveries made in 2D, rather than replacing 2D culture outright for initial experimentation.

Commercially, there is a growing demand for alternatives to animal models. Epidermal equivalents are one such area, which will be discussed in the following subsection. Liver biology is also an emerging 3D culture niche (Xu et al, 2003), as most pharmaceutical drugs are metabolised by the liver and many drugs display a level of hepatotoxicity (Bokhari et al, 2008, Skardal et al, 2012). An *in vitro* model of liver which can accurately predict drug toxicity and/or metabolism will be commercially successful, and so considerable efforts are being directed towards 3D hepatocyte culture.

Regulatory steps also need to be taken by lawmakers in order to recognise future *in vitro* models as suitably verified alternatives to animal testing, which is often itself required by law before a drug, pharmaceutical or cosmetic can be used on humans. The European Centre for Validation of Alternate Methods (ECVAM) and the US

Food and Drug Administration (FDA) have approved some *in vitro* models for skin irritancy, corneal irritancy and epidermal permeability testing, but these review and approval processes are very slow and often lag far behind scientific developments (Wagner et al, 2012).

In terms of the 3D culture materials themselves, there are currently no clear "winners", as different cell types each benefit from different materials and different culture conditions. However, there are interesting developments such integrating more extracellular matrix features, customising material surfaces to release growth factors, or altering micro-scale surface features and patterns to influence cell alignment and behaviour (Lee et al, 2008). Carbon nanotubes are an emerging material which can be precisely manufactured into highly specialised nanoscale surfaces. These surfaces are multi-purpose and can be used to control cell behaviour, track cells through embedded electrochemical resistance sensors or to provide structural support for synthetic polymer matrices (Harrison et al, 2007).

Future developments in cell culture materials, culture techniques and analytical technology will help to make *in vitro* analyses more relevant and representative of *in vivo* behaviour, reducing animal testing as well as improving the safety of commercial products and acclerating research in the area.

# 7 References

Adachi M, Gazel A, Pintucci G, Shuck A, Shifteh S, Ginsburg D, S. Rao L, Kaneko T, Freedberg IM, Tamaki K and Blumenberg M, 2003. Specificity in Stress Response: Epidermal Keratinocytes Exhibit Specialized UV-Responsive Signal Transduction Pathways. DNA and Cell Biology. October 2003, 22(10): 665-677.

Adams MP, Mallet DG and Pettet GJ, 2012. Active regulation of the epidermal calcium profile. Journal of Theoretical Biology Volume 301, 21 May 2012, Pages 112‑121

Aho S, Li KY, McGee RC, Ishida-Yamamoto A, Uitto J, and Klement JF, 2004. Periplakin gene targeting reveals a constituent of the cornified cell envelope dispensable for normal mouse development. Mol. Cell. Biol. 24:6410–6418

Ambler CA and Määttä A, 2008. Epidermal stem cells: location, potential and contribution to cancer. J Pathol 2009; 217: 206–216

Ambler CA and Watt FM, 2010. Adult epidermal Notch activity induces dermal accumulation of T cells and neural crest derivatives through upregulation of jagged 1. Development 137, 3569-3579 (2010)

Amjad SB, Carachi R and Edward M, 2007. Keratinocyte regulation of TGF-β and connective tissue growth factor expression: A role in suppression of scar tissue formation. Wound Repair and Regeneration Volume 15, Issue 5, pages 748–755,

Astarita G, Jung K-M, Vasilevko V, DiPatrizio NV, Martin SK, Cribbs DH, Head E, Cotman CW and Piomelli D, 2011. Elevated Stearoyl-CoA Desaturase in Brains of Patients with Alzheimer's Disease. PLoS ONE 6(10)

Atala A, Bauer SB, Soker S, Yoo JJ and Retik AB, 2006. Tissue-engineered autologous bladders for patients needing cystoplasty. LANCET Volume: 367 Issue 9518 Pages: 1241-1246

Batheja P, Song Y, Wertz P and Michniak-Kohn B, 2009. Effects of growth conditions on the barrier properties of a human skin equivalent. Pharm Res. 2009 Jul;26(7):1689-700

Batout S and Cheta N, 1996. Matrigel: a useful tool to study endothelial differentiation. Rom J Intern Med. 1996 Jul-Dec;34(3-4):263-9.

Baker BM and Chen CS, 2012. Deconstructing the third dimension - how 3D culture microenvironments alter cellular cues. J Cell Sci. 2012 Jul 13.

Barel AO and Clarys P, 1995. Study of the stratum corneum barrier function by transepidermal water loss measurements: comparison between two commercial instruments: Evaporimeter and Tewameter. Skin Pharmacol 1995;8:186-95.

Barker CL, McHale MT, Gillies AK, Waller J, Pearce DM, Osborne J, Hutchinson PE, Smith GM and Pringle JH, 2004. The Development and Characterization of an In Vitro Model of Psoriasis. Journal of Investigative Dermatology (2004) 123, 892–901

Barnard JH, Collings JC, Whiting A, Przyborski SA and Marder TB, 2009. Synthetic Retinoids: Structure-Activity Relationships. Chemistry-A European Journal Volume: 15 Issue: 43 Pages: 11430-11442

Baroni A, Buommino E, De Gregorio V, Ruocco E, Ruocco V and Wolf R, 2012. Structure and function of the epidermis related to barrier properties. Clinics in Dermatology (2012) 30, 257–262

Beck B and Blanpain C, 2012. Mechanisms regulating epidermal stem cells. The EMBO Journal (2012) 31, 2067–2075

Behrens A, Sibilia M and Wagner EF. Amino-terminal phosphorylation of c-Jun regulated stress-induced apoptosis and cellular proliferation. Nature Genetics 1999; 21:p326-329

Bell E, Sher S, Hull B, Merrill C, Rosen S, Chamson A, Asselineau D, Dubertret L, Coulomb B, Lapiere C, Nusgens B and Neveux Y, 1983. The Reconstitution of Living Skin. Journal of Investigative Dermatology, 81:2a-10e, 1983.

Belury MA, Kavanaugh CJ and Liu K, 2007. Conjugated linoleic acid modulates phorbol ester–induced PPAR-δ and K-FABP mRNA expression in mouse skin. Nutrition Research Volume 27, Issue 1, January 2007, Pages 48–55

Bennett BL, Sasaki DT, Murray BW, O'Leary EC, Sakata ST, Xu W, Leisten JC, Motiwala A, Pierce S, Satoh Y, Bhagwat SS, Manning AM and Anderson DW, 2001.

SP600125, an anthrapyrazolone inhibitor of Jun N-terminal kinase. Proc Natl Acad Sci U S A. 2001 Nov 20;98(24):13681-6.

Bickenbach JR, 1981. Identification and behavior of label-retaining cells in oral mucosa and skin. J Dent Res 1981;60:1611–1620.

Biedermann T, Pontiggia L, Bottcher-Haberzeth S, Tharakan S, Braziulis E, Schiestl C, Meuli M and Reichmann E, 2010. Human Eccrine Sweat Gland Cells Can Reconstitute a Stratified Epidermis. Journal of Investigative Dermatology (2010), Volume 130, p1996-2009

Bikle DD, Nemanic MK, Gee E, Elias P, 1986. 1,25-Dihydroxyvitamin D3 production by human keratinocytes. Kinetics and regulation. J Clin Invest 78:557–566.

Bikle DD, 2004. Vitamin D regulated keratinocyte differentiation. Journal of Cellular Biochemistry Volume 92, Issue 3, pages 436–444, 1 June 2004

Blackwood KA, McKean R, Canton I, Freeman CO, Franklin KL, Cole D, Brook I, Farthing P, Rimmer S and Haycock JW, 2008. Development of biodegradable electrospun scaffolds for dermal replacement. Biomaterials 29, 3091-3104.

Blanpain C and Fuchs E, 2006. Epidermal stem cells of the skin. Annu Rev Cell Dev Biol 2006;22:339-73.

Blanpain C, Horsley V and Fuchs E, 2007. Epithelial stem cells: turning over new leaves. Cell 128: 445–458

Bohme M, Soderhall C, Kull I, Bergstrom A, van Hage M and Wahlgren CF, 2012. Filaggrin mutations increase the risk for persistent dry skin and eczema independent of sensitization. Journal of Allergy and Clinical Immunology Volume 129, Issue 4, April 2012, Pages 1153‑1155

Bokhari M, Carnachan RJ, Cameron NR and Przyborski SA, 2007. Culture of HepG2 liver cells on three dimensional polystyrene scaffolds enhances cell structure and function during toxicological challenge. J Anat. 2007 October; 211(4): 567–576.

Bokhari M, Carnachan RJ, Cameron NR and Przyborski SA, 2007b. Novel cell culture device enabling three-dimensional cell growth and improved cell function. Biochemical and Biophysical Research Communication 354 1095-1100 (2007)

Bokhari M, Carnachan RJ, Przyborski SA and Cameron NR, 2007c. Emulsion-templated porous polymers as scaffolds for three dimensional cell culture: effect of synthesis parameters on scaffold formation and homogeneity. J. Mater. Chem., 2007,17, 4088-4094

Bokhari M, Carnachan RJ, Cameron NR, Przyborski SA, 2008. Culture of HepG2 liver cells on three dimensional polystyrene scaffolds enhances cell structure and function during toxicological challenge. Journal of Anatomy Volume: 211. Issue: 4

Boelsma E, Verhoeven MC and Ponec M., 1999. Reconstruction of a Human Skin Equivalent Using a Spontaneously Transformed Keratinocyte Cell Line (HaCaT). J Invest Dermatol. 1999 Apr;112(4):489-98.

Boukamp P, Petrussevska RT, Breitkreutz D, Hornung J, Markham A and Fusenig NE, 1988. Normal Keratinization in a Spontaneously Immortalized Aneuploid Human Keratinocyte Cell Line. The Journal of Cell Biology, Volume 106, March 1988 761-771

Boukamp P, Popp S, Altmeyer S, Hülsen A, Fasching C, Cremer T and Fusenig NE., 1997. Sustained nontumorigenic phenotype correlates with a largely stable chromosome content during long-term culture of the human keratinocyte line HaCaT. Genes Chromosomes Cancer. 1997 Aug;19(4):201-14.

Bouwstra JA, De Graaff A, Gooris GS, Nijsse J, Wiechers J and Van Aelst AC, 2003. Water distribution and related morphology in human stratum corneum at different hydration levels. J Invest Dermatol 2003: 120: 750–758.

Bouwstra JA, Wouter, H, Groenink W, Kempenaar JA, Romeijn SG and Ponec M, 2008. Water distribution and natural moisturizer factor content in human skin equivalents are regulated by environmental relative humidity. Journal Of Investigative Dermatology Volume: 128 Issue: 2 Pages: 378-388

Boyce ST, Kagan RJ, Meyer NA, Yakuboff KP and Warden GD, 1999. The 1999 clinical research award. Cultured skin substitutes combined with Integra Artificial

Skin to replace native skin autograft and allograft for the closure of excised full-thickness burns. J Burn Care Rehabil. 1999 Nov-Dec;20(6):453-61

Boyce ST, Supp AP, Swope VB and Warden GD, 2002. Vitamin C regulates keratinocyte viability, epidermal barrier, and basement membrane in vitro, and reduces wound contraction after grafting of cultured skin substitutes. J Invest Dermatol. 2002 Apr;118(4):565-72

Brattsand M, Stefansson K, Hubiche T, Nilsson SK and Egelrud T, 2009. SPINK9: a selective, skin-specific Kazal-type serine protease inhibitor. J Invest Dermatol 129:1656–1665

Breiden B, Gallala H, Doering T and Sandhoff K., 2007. Optimization of submerged keratinocyte cultures for the synthesis of barrier ceramides. European Journal of Cell Biology 86 (2007) 657–673

Breitkreutz D, Mirancea N and Nischt R, 2009. Basement membranes in skin: unique matrix structures with diverse functions? Histochem Cell Biol. 2009 Jul;132(1):1-10.

Brennan D, Hu Y, Joubeh S, Choi YW, Whitaker-Menezes D, O'Brien T, Uitto J, Rodeck U and Mahoney MG, 2007. Suprabasal Dsg2 expression in transgenic mouse skin confers a hyperproliferative and apoptosis-resistant phenotype to keratinocytes. J Cell Sci 120: 758–771.

British National Formulary (BNF) vol 63, 2012. Pharmaceutical Press; 63rd Revised edition edition (9 Mar 2012). ISBN-10: 0857110233

Brody I, 1957. An Ultrastructural Study on the Ro1e of the Keratohyalin Granules in the Keratinization Process J. Ultrastructure Research 3, 84-104 (1959)

Brooke MA, Nitoiu D and Kelsell DP, 2012. Cell-cell connectivity: desmosomes and disease. J. Pathol. 226, 158-171.

Brown SJ, McLean WHI, 2012. One Remarkable Molecule: Filaggrin. Journal of Investigative Dermatology 132, 751-762 (March 2012)

Cabral RM, Wan H, Cole CL, Abrams DJ, Kelsell DP and South AP, 2010. Identification and characterization of DSPIa, a novel isoform of human desmoplakin. Cell Tissue Res. 341, 121-129.

Cabral RM, Tattersall D, Patel V, McPhail GD, Hatzimasoura E, Abrams DJ, South AP and Kelsell DP, 2012. The DSPII splice variant is crucial for desmosome-mediated adhesion in HaCaT keratinocytes. Journal of Cell Science 125 (12). 2853-2861

Candi E, Schmidt R and Melino G, 2005. The cornified envelope: A model of cell death in the skin. Nature Reviews Molecular Cell Biology Volume: 6 Issue: 4 Pages: 328-340

Carnachan, R.J., Bokhari, M., Määttä, A., Cameron, N.R., Przyborski, S.A, 2008. Emulsion-templated porous scaffolds enabling three dimensional cell culture. Polymer Preprints. American Chemical Society, Division of Polymer Chemistry, 49, 418-419.

Caspers PJ, Lucassen GW, Carter EA, Bruining HA and Puppels GJ, 2001. In vivo confocal Raman microspectroscopy of the skin: noninvasive determination of molecular concentration profiles. J Invest Dermatol 2001: 116: 434–442.

Caspers PJ, Lucassen GW and Puppels GJ, 2003. Combined In Vivo Confocal Raman Spectroscopy and Confocal Microscopy of Human Skin. Biophysical Journal Volume 85, Issue 1, July 2003, Pages 572–580

Celli A, Sanchez S, Behne M, Hazlett T, Gratton E and Mauro T, 2010. The Epidermal $Ca2^{+}$ Gradient: Measurement Using the Phasor Representation of Fluorescent Lifetime Imaging. Biophysical Journal Volume 98 March 2010 911–921

Chantasart D, Pongjangkul T, Higuchi WI and Li KS, 2009. Effects of oxygen-containing terpenes as skin permeation enhancers on the lipoidal pathways of human epidermal membrane. Journal of Pharmaceutical Sciences Volume 98, Issue 10, pages 3617–3632

Cho Y, Lew BL, Seong K, et al. An inverse relationship between ceramide synthesis and clinical severity in patients with psoriasis. J Korean Med Sci 2004;19:859-63.

Cumpstone MB, Kennedy AH, Harmon CS, Potts RO, 1989. The water permeability of primary mouse keratinocyte cultures grown at the air-liquid interface. Journal of Investigative Dermatology. Vol. 92 598-600.

Chan A, Holleran WM, Ferguson T, Crumrine D, Goker-Alpan O, Schiffmann R, Tayebi N, Ginns EI, Elias PM and Sidransky E, 2011. Skin ultrastructural findings in type 2 Gaucher disease: Diagnostic implications. Molecular Genetics and Metabolism. Volume 104, Issue 4, December 2011, Pages 631–636

Chantasart D, Sa-Nguandeekul P, Prakongpan S, Li SK and Higuchi WI, 2007. Comparison of the effects of chemical permeation enhancers on the lipoidal pathways of human epidermal membrane and hairless mouse skin and the mechanism of enhancer action. Journal Of Pharmaceutical Sciences Volume: 96 Issue: 9 Pages: 2310-2326

Chaturvedi V, Sitailo LA, Bodner B, Denning MF and Nickoloff BJ, 2006. Defining the caspase-containing apoptotic machinery contributing to cornification in human epidermal equivalents. Exp Dermatol. 2006 Jan;15(1):14-22.

Chen HY, Elkasabi Y and Lahann J, 2006. Surface modification of confined microgeometries via vapor-deposited polymer coatings. J. Am. Chem. Soc 128, 374.

Cheng J, Syder AJ, Yu QC, Letai A, Paller AS and Fuchs E, 1992. The genetic basis of epidermolytic hyperkeratosis: a disorder of differentiation-specific epidermal keratin genes. Cell.1992 Sep 4;70(5):811-9.

Chhatriwala MK, Cipolat S, Sevilla LM, Nachat R and Watt FM, 2012. Exons 5-15 of Kazrin Are Dispensable for Murine Epidermal Morphogenesis and Homeostasis. Journal Of Investigative Dermatology Volume: 132 Issue: 8 Pages: 1977-1987

Choi JS, Lee SJ, Christ GJ, Atala A, Yoo JJ and James J, 2008. The influence of electrospun aligned poly(epsilon-caprolactone)/collagen nanofiber meshes on the formation of self-aligned skeletal muscle myotubes. Biomaterials Volume: 29 Issue: 19 Pages: 2899-2906

Clark RA, Ghosh K and Tonneson MG, 2007. Tissue Engineering for Cutaneous Wounds. Journal of Investigative Dermatology (2007) 127, 1018–1029. doi:10.1038/sj.jid.5700715

Clayton E, Doupe DP, Klein AM, Winton DJ, Simons BD and Jones PH. A single type of progenitor cell maintains normal epidermis. Nature 2007;446(7132):185–189

Cook JR, Patrone LM, Rhoads LS and van Buskirk RG, 1993. A human epidermal model grown on an acellular gel. Journal of Toxicology - Cutaneous and Ocular Toxicology Volume: 12 Issue: 2 Pages: 109-128 Published: 1993

Cooke MJ, Phillips SR, Shah DSH, Athey D, Lakey JH and Przyborski SA, 2008. Enhanced cell attachment using a novel cell culture surface presenting functional domains from extracellular matrix proteins. Cytotechnology. 2008 Feb;56(2):71-9.

Cornelissen LH, Oomens CWJ, Huyghe JM and Baaijens FPT, 2007. Mechanisms that play a role in the maintenance of the calcium gradient in the epidermis. Skin Research and Technology Volume 13, Issue 4, pages 369–376, November 2007

Coulombe PA, Hutton ME, Letai A, Hebert A, Paller AS and Fuchs E, 1991. Point Mutations In Human Keratin-14 Genes Of Epidermolysis-Bullosa Simplex Patients - Genetic And Functional Analyses. CELL Volume: 66 Issue: 6 Pages: 1301-1311

Coulombe PA and Lee CH, 2012. Defining Keratin Protein Function in Skin Epithelia: Epidermolysis Bullosa Simplex and Its Aftermath. Journal Of Investigative Dermatology Volume: 132 Issue: 3 Pages: 763-775

Covaciu C, Castori M, De Luca N, Ghirri P, Nannipieri A, Ragone G, Zambruno G and Castiglia D, 2010. Lethal autosomal recessive epidermolytic ichthyosis due to a novel donor splice-site mutation in KRT10. British Journal of Dermatology Volume 162, Issue 6, pages 1384–1387, June 2010

Csizmazia E, Eros G, Berkesi O, Berko S, Szabo-Revesz P and Csanyi E, 2011. Penetration enhancer effect of sucrose laurate and Transcutol on ibuprofen. Journal Of Drug Delivery Science And Technology Volume: 21 Issue: 5 Pages: 411-415

Cukierman E, Pankov R, Stevens DR, Yamada KM. Taking cell-matrix adhesions to the third dimension. Science. 2001 Nov 23;294(5547):1708-12.

Darlenski and Fluhr, 2012. Influence of skin type, race, sex, and anatomic location on epidermal barrier function. Clinics in Dermatology Volume 30, Issue 3, May–June 2012, Pages 269–273

de Breij A, Haisma EM, Rietveld M, El Ghalbzouri A, van den Broek PJ, Dijkshoorn L and Nibbering PH, 2012. Three-Dimensional Human Skin Equivalent as a Tool To Study Acinetobacter baumannii Colonization. Antimicrobial Agents And Chemotherapy Volume: 56 Issue: 5 Pages: 2459-2464

de Koning HD, van den Bogaard EH, Bergboer JG, Kamsteeg M, van Vlijmen-Willems IM, Hitomi K, Henry J, Simon M, Takashita N, Ishida-Yamamoto A,Schalkwijk J and Zeeuwen PL, 2012. Expression profile of cornified envelope structural proteins and keratinocyte differentiation-regulating proteins during skin barrier repair. British Journal of Dermatology Volume 166, Issue 6, pages 1245–1254, June 2012

De Paépe K, Hachem JP, Vanpee E, Goossens A, Germaux MA, Lachapelle JM, Lambert J, Matthieu L, Roseeuw D, Suys E, Van Hecke E and Rogiers V, 2001. Beneficial effects of a skin tolerance-tested moisturizing cream on the barrier function in experimentally-elicited irritant and allergic contact dermatitis. Contact Dermatitis 2001;44:337-43.

Decher G, 1997. Fuzzy nanoassemblies: toward layered polynumeric multicomposites. Science 277, 1232.

Delva E, Tucker DK and Kowalczyk AP, 2009. The Desmosome. Cold Spring Harb Perspect Biol 2009, 1:a002543

Demerjian M, Crumrine DA, Milstone LM, Williams ML and Elias PM, 2006. Barrier dysfunction and pathogenesis of neutral lipid storage disease with ichthyosis (Chanarin Dorfman syndrome). J Invest Dermatol, 126 (2006), pp. 2032–2038

Denecker G, Ovaere P, Vandenabeele P and Declercq W, 2008. Caspase-14 reveals its secrets. JCB vol. 180 no. 3 451-458

Di Colandrea T, Karashima T, Maätta Ä and Watt FM, 2000: Subcellular distribution of envoplakin and periplakin: Insights into their role as precursors of the epidermal cornified envelope. J Cell Biol 151:573–585, 2000

Doupe DP, Klein AM, Simons BD and Jones PH, 2010. The ordered architecture of murine ear epidermis is maintained by progenitor cells with random fate. Dev Cell 18: 317–323

Doupe DP and Jones PH, 2012. Interfollicular epidermal homeostasis: dicing with differentiation. Experimental Dermatology Volume: 21 Issue: 4 Pages: 249-253

Duan J, Sugawara T, Hirose M, Aida K, Sakai S, Fujii A and Hirata T, 2012. Dietary sphingolipids improve skin barrier functions via the upregulation of ceramide synthases in the epidermis. Experimental Dermatology Volume 21, Issue 6, pages 448–452, June 2012

Duh JS and Her GR, 1992. Analysis of Permethylated Glycosphingolipids by Desorption Chemical Ionization/Triple-Quadrupole Tandem Mass Spectrometry. Biological Mass Spectrometry, Vol. 21, 391-396 (1992)

Dvir-Ginzberg M, Elkayam T, Aflalo ED, Agbaria R, Cohen S, 2004. Ultrastructural and functional investigations of adult hepatocyte spheroids during in vitro cultivation. Tissue Eng. 2004 Nov-Dec;10(11-12):1806-17.

Eckert RL, Yaffe MB, Crish JF, Murthy S, Rorke EA and Welter JF, 1993. Involucrin - Structure and Role in Cell Assembly. The Journal of Investigative Dermatology Vol. 100, No.5, May 1993.

El-Ayoubi R, Degrandpre C, DiRaddi R, Yousefi AM and Lavigne P, 2011. Design and Dynamic Culture of 3D-Scaffolds for Cartilage Tissue Engineering. Journal of Biomaterials Applications, Volume 25, Issue 5, p429-444

El-Ghalbzouri A, Lamme EN, van Blitterswijk C, Koopman J and Ponec M, 2004. The use of PEGT/PBT as a dermal scaffold for skin tissue engineering. Biomaterials. 2004 Jul;25(15):2987-96

Elias PM, 1981. Epidermal Lipids, Barrier Function, and Desquamation.

Elias PM, Cooper ER, Korc A and Brown BE, 1981. Percutaneous transport in relation to stratum corneum structure and lipid composition. J Invest Dermatol. 1981 Apr;76(4):297-301.

Elias PM, 1983. Epidermal lipids, barrier function, and desquamation. J Invest Dermatol 80(suppl):44s–49s

Elias PM, Williams ML, Maloney ME, Bonifas JA, Brown BE, Grayson S, Epstein EH Jr, 1984. Stratum corneum lipids in disorders of cornification. Steroid sulfatase

and cholesterol sulfate in normal desquamation and the pathogenesis of recessive X-linked ichthyosis. J Clin Invest 1984;74:1414-21.

Elias PM, Ahn S, Brown B, Crumrine D and Feingold KR, 2002. Origin of the epidermal calcium gradient: regulation by barrier status and role of active vs passive mechanisms. J. Invest. Dermatol. 119:1269–1274.

Elias PM, 2006. Stratum corneum ceramides: function, origins, and therapeutic implications. In: Elias P M, Feingold K R, eds. Skin Barrier. New York: Taylor and Francis, 2006: 43–64. Accessed via Google Books.

Elias PM, Williams ML and Feingold KR. 2012. Abnormal barrier function in the pathogenesis of ichthyosis: Therapeutic implications for lipid metabolic disorders. Clinics In Dermatology Volume: 30 Issue: 3 Pages: 311-322

Engler AJ, Sen S, Sweeney HL and Discher DE, 2006. Matrix elasticity directs stem cell lineage specification. Cell 126, 677.

ESAC Peer Review - European Commission Statement on the Application of the SkinEthic human skin model for skin corrosivity testing. Summary and conclusions of the peer review panel, 6pp, October 2006.

Estrach S, Ambler CA, Lo Celso C, Hozumi K and Watt FM, 2006. Jagged 1 is a beta-catenin target gene required for ectopic hair follicle formation in adult epidermis. Development 133, 4427-4438.

Eves P, Layton C, Hedley S, Dawson RA, Wagner M, Morandini R, Ghanem G, MacNeil S, 2003. Characterization of an in vitro model of human melanoma invasion based on reconstructed human skin. Br. J. Dermatol. 142, 210–222 (2003).

Feingold KR and Jiang YJ, 2011. The mechanisms by which lipids coordinately regulate the formation of the protein and lipid domains of the stratum corneum: Role of fatty acids, oxysterols, cholesterol sulfate and ceramides as signaling molecules. Dermatoendocrinol. 2011 Apr;3(2):113-8

Fernandez TL, Dawson RA, Van Lonkhuyzen DR, Kimlin MG and Upton Z., 2012. A tan in a test tube –in vitro models for investigating ultraviolet radiation–induced damage in skin. Experimental Dermatology Volume 21, Issue 6, pages 404–410, June 2012

Fleckman P and Brumbaugh S, 2002. Absence of the granular layer and keratohyalin define a morphologically distinct subset of individuals with ichthyosis vulgaris. Experimental Dermatology Volume 11, Issue 4, pages 327–336, August 2002

Fluhr JW, Kao J, Jain M, Ahn SK, Feingold KR and Elias PM, 2001. Generation of free fatty acids from phospholipids regulates stratum corneum acidification and integrity. J Invest Dermatol. 2001;117:44–51

Fluhr JW and Elias PM, 2002. Stratum corneum pH: formation and function of the acid mantle. Exog Dermatol 2002: 1: 163–175.

Fortugno P, Bresciani A, Paolini C, Pazzagli C, El Hachem M, D'Alessio M and Zambruno G, 2011. Proteolytic activation cascade of the Netherton syndrome-defective protein, LEKTI, in the epidermis: implications for skin homeostasis. J Invest Dermatol. 2011 Nov;131(11):2223-32

Freedberg IM, Tomic-Canic M, Komine M and Blumenberg M. Keratins and the Keratinocyte Activation Cycle. Journal of Investigative Dermatology (2001) 116, 633–640

Fuchs E and Green H. 1981. Regulation of terminal differentiation of cultured human keratinocytes by vitamin A. Cell 25:617–625.

Fuchs E and Horsley V, 2008. More than one way to skin. Genes Dev 2008;22(8):976–985

Fuchs E, 2012 in "Lander et al - What does the concept of the stem cell niche really mean today?" BMC Biology 2012, 10:19

Furuse, M. Hata, M and Furuse K, 2002. Claudin-based tight junctions are crucial for the mammalian epidermal barrier: a lesson from claudin-1-deficient mice. J Cell Biol, 156 (2002), pp. 1099–1111

Fusenig NE, Amer SM, Boukamp P and Worst PK, 1978. Characteristics of chemically transformed mouse epidermal cells in vitro and in vivo. Bulletin du Cancer. 1978;65(3):271-9

Gabbanini, Lucchi, Berlini, Minghetti and Valgimigli, 2009. In vitro evaluation of the permeation through reconstructed human epidermis of essentials oils from

cosmetic formulations. Journal of Pharmaceutical and Biomedical Analysis Volume 50, Issue 3, 15 October 2009, Pages 370–376

Gazel A, Banno T, Walsh R and Blumenberg M, 2006. Inhibition of JNK promotes differentiation of epidermal keratinocytes. Journal Of Biological Chemistry Volume: 281 Issue: 29 Pages: 20530-20541

Getsios S, Amargo EV, Dusek RL, Ishii K, Sheu L, Godsel LM and Green KJ, 2004. Coordinated expression of desmoglein 1 and desmocollin 1 regulates intercellular adhesion. Differentiation 72: 419–433.

Girard P, Beraud A, Sirvent A, 2000. Study of three complementary techniques for measuring cutaneous hydration in vivo in human subjects: NMR spectroscopy, transient thermal transfer and corneometry—application to xerotic skin and cosmetics. Skin Res Technol 2000;6:205-13.

Godin B and Touitou E, 2007. Transdermal skin delivery: Predictions for humans from in vivo, ex vivo and animal models. Advanced Drug Delivery Reviews 59 (2007) 1152–1161.

Grant I, Warwick K, Marshall J, Green C and Martin R, 2002. The co-application of sprayed cultured autologous keratinocytes and autologous fibrin sealant in a porcine wound model. Br J Plast Surg 55(3):219–227

Green H, 1977. Terminal Differentiation of Cultured Human Epithelial Cells. Cell 1977, 11 (2), 405-416.

Greenspan P, Mayer EP and Fowler SD, 1985. Nile Red: a selective fluorescent stain for intracellular lipid droplets. Journal Cell Biology: 100: 965-973

Groot KR, Sevilla LM, Nishi K, DiColandrea T and Watt FM, 2004. Kazrin, a novel periplakin-interacting protein associated with desmosomes and the keratinocyte plasma membrane. Journal Of Cell Biology Volume: 166 Issue: 5 Pages: 653-659

Grubauer G, Feingold KR and Elias PM, 1987. Relationship of epidermal lipogenesis to cutaneous barrier function. J Lipid Res 1987;28:746-52.

Gruber R, Elias PM, Crumrine D, Lin T, Brandner JM, Hachem J, Presland RB, Fleckman P, Janecke AR, Sandilands A, McLean WHI, Fritsch PO, Mildner M, Tschachler E and Schmuth M, 2011. Filaggrin Genotype in Ichthyosis Vulgaris

Predicts Abnormalities in Epidermal Structure and Function. The American Journal of Pathology Volume 178, Issue 5, May 2011, Pages 2252–2263

Grzesiak JJ, Pierschbacher MD, Amodeo MF, Malaney TI and Glass JR, 1997. Enhancement of cell interactions with collagen/ glycosaminoglycan matrices by RGB derivatization. Biomaterials 1997, Vol. 18 No. 24.

Hadgraft J, 2001. Modulation of the barrier function of the skin. Skin Pharmacol Appl Skin Physiol. 14(1): 72-81

Haftek M, Callejon S, Sandjeu Y, Padois K, Falson F, Pirot F, Portes P, Demarne F and Jannin V, 2011. Compartmentalization of the human stratum corneum by persistent tight junction-like structures. Experimental Dermatology, 20, 617–621

Hanyu O, Nakae H, Miida T, Higashi Y, Fuda H, Endo M, Kohjitani A, Sone H and Strott CA, 2012. Cholesterol sulfate induces expression of the skin barrier protein filaggrin in normal human epidermal keratinocytes through induction of RORα. Biochem Biophys Res Commun. 2012 Nov 9;428(1):99-104

Hara-Chikuma M and Verkman AS, 2005. Aquaporin-3 functions as a glycerol transporter in mammalian skin. Biol Cell 2005;97:479-486.

Hara-Chikuma M and Verkman AS, 2008. Aquaporin-3 facilitates epidermal cell migration and proliferation during wound healing. J Mol Med (Berl) 2008;86:221-231

Harris IR, Höppner H, Siefken W, Farrell AM and Wittern KP, 2000. Regulation of HMG-CoA Synthase and HMG-CoA Reductase by Insulin and Epidermal Growth Factor in HaCaT Keratinocytes. Journal of Investigative Dermatology (2000) 114, 83–87

Hartung T, 2010. Comparative analysis of the revised Directive 2010/63/EU for the protection of laboratory animals with its predecessor 86/609/EEC - a t4 report. ALTEX. 2010;27(4):285-303.

Haugh MH, Meyer EG, Thorpe SD, Vinardell T, Duffy GP and Kelly DJ, 2011. Temporal and Spatial Changes in Cartilage-Matrix-Specific Gene Expression in Mesenchymal Stem Cells in Response to Dynamic Compression. Tissue Engineering Part A Volume: 17 Issue: 23-24 Pages: 3085-3093

Hayden PJ, Petrali JP, Hamilton TA, Kubilus J, Smith WJ and Kalusner M, 2005. Development of a full thickness in vitro human skin equivalent (Epiderm-FT) for sulfur mustard research. Proceedings of the Soc. of Investigative Dermatology, May 2005.

Hayman MW, Smith KH, Cameron NR and Przyborski SA, 2005. Growth of human stem cell-derived neurons on solid three-dimensional polymers. Journal of Biochemical and Biophysical Methods Volume 62, Issue 3, 31 March 2005, Pages 231–240

Hayman MW, Smith KH, Cameron NR and Przyborski SA, 2004. Enhanced neurite outgrowth by human neurons grown on solid three-dimensional scaffolds. Biochem Biophys Res Commun. 2004 Feb 6;314(2):483-8.

Hengning K, Harris R, Coloff J, Jin JY, Leshin B, Miliani de Marval P, Tao S, Rathmell JC, Hall RP, Zhang JY, 2010. Cancer Res. 2010 April 15; 70(8): 3080–3088

Hennings H, Michael D, Cheng C, Steinert P, Holbrook K and Yuspa S, 1980. Calcium Regulation of Growth and Differentiation of Mouse Epidermal Cells in Culture. Cell, Vol. 19, 245-254, January 1980

Hernon CA, Dawson RA, Freedlander E, Short R, Haddow DB, Brotherston M and MacNeil S, 2006. Clinical experience using cultured epithelial autografts leads to an alternative methodology for transferring skin cells from the laboratory to the patient. Regen Med. 2006 Nov;1(6):809-21.

Hershkovitz D, Mandel H, Ishida-Yamamoto A, Chefetz I, Hino B, Luder A, Indelman M, Bergman R and Sprecher E, 2008. Defective lamellar granule secretion in arthrogryposis, renal dysfunction, and cholestasis syndrome caused by a mutation in VPS33B. Arch Dermatol 144:334–340

Hesse M, Magin TM and Weber K, 2001. Genes for intermediate filament proteins and the draft sequence of the human genome: novel keratin genes and a surprisingly high number of pseudogenes related to keratin genes 8 and 18. Journal Of Cell Science Volume: 114 Issue: 14 Pages: 2569-2575

Hicks K.O, Pruijn FB, Secomb TW, Hay MP, Hsu R, Brown JM, Denny WA, Dewhirst MW and Wilson WR, 2006. Use of three-dimensional tissue cultures to model extravascular transport and predict in vivo activity of hypoxia-targeted anticancer drugs. J. Natl. Cancer Inst. 98, 1118–1128.

Higashi Y, Fuda H, Yanai H, Lee Y, Fukushige T, Kanzaki T and Strott CA, 2004. Expression of cholesterol sulfotransferase (SULT2B1b) in human skin and primary cultures of human epidermal keratinocytes. J Invest Dermatol. 2004 May;122(5):1207-13.

Hirao T, Denda M and Takahashi M, 2001. Identification of immature cornified envelopes in the barrier-impaired epidermis by characterization of their hydrophobicity and antigenicities of the components. Experimental Dermatology 2001: 10: 35-44

Hitomi K, 2005. Transglutaminases in skin epidermis. Eur J Dermatol 2005;15:313-9

Hoffmann J, Heisler E, Karpinski S, Losse J, Thomas D, Siefken W, Ahr HJ, Vohr HW and Fuchs HW, 2005. Epidermal-skin-test 1,000 (EST-1,000)--a new reconstructed epidermis for in vitro skin corrosivity testing. Toxicol In Vitro. 2005 Oct;19(7):925-9

Holleran WM, Ginns EI, Menon GK, Grundmann JU, Fartasch M, McKinney CE, Elias PM and Sidransky E, 1994. Consequences of beta-glucocerebrosidase deficiency in epidermis. Ultrastructure and permeability barrier alterations in Gaucher disease. J Clin Invest 1994;93:1756-64.

Holleran WM, Ziegler SG, Goker-Alpan O, Eblan MJ, Elias PM, Schiffmann R and Sidransky E, 2006. Skin abnormalities as an early predictor of neurologic outcome in Gaucher disease. Clin Genet 2006;69:355-7.

Holleran WM, Takagi Y and Uchida Y, 2006b. Epidermal sphingolipids: metabolism, function, and role(s) in skin disorders. FEBS Lett 2006;23:5456—66.

Hollister SJ, 2006. Porous scaffold design for tissue engineering. Nature Materials 5, 590, 2006.

Hoogstraate AJ, Verhoef J, Brussee J, IJzerman AP, Spies F and Boddé HE, 1991. Kinetics, ultrastructural aspects and molecular modelling of transdermal peptide flux enhancement by N-alkylazacycloheptanones. Int J Pharm. 1991;76(1–2):37–47

Hoppe T, Winge MCG, Bradley M, Nordenskjold M, Vahlquist A, Berne B and Torma H, 2012. X-linked recessive ichthyosis: an impaired barrier function evokes limited gene responses before and after moisturizing treatments. British Journal Of Dermatology Volume: 167 Issue: 3 Pages: 514-522

Hotary KB, Allen ED, Brooks PC, Datta NS, Long MW and Weiss SJ, 2003. Membrane type I metalloproteinase usurps tumor growth control imposed by the three-dimensional extracellular matrix. Cell 114, 33.

Huang YC, Wang TW, Sun JS and Lin FH, 2005. Epidermal morphogenesis in an *in vitro* model using a fibroblasts-embedded collagen scaffold. Journal of Biomedical Science (2005) 12:855–867. 855. DOI 10.1007/s11373-005-9018-x

Hughes CS, Postovit LM and Lajoie GA 2010. Matrigel: a complex protein mixture required for optimal growth of cell culture. Proteomics. 2010 May;10(9):1886-90.

Ibrahim SA and Li SK, 2009. Effects of solvent deposited enhancers on transdermal permeation and their relationship with Emax. Journal Of Controlled Release Volume: 136 Issue: 2 Pages: 117-124

Ikuta S, Sekino N, Hara T, Saito Y and Chida K, 2006. Mouse Epidermal Keratinocytes in Three-Dimensional Organotypic Coculture with Dermal Fibroblasts Form a Stratified Sheet Resembling Skin/ Biosci. Biotechnol. Biochem 70 (11) 2669-2675, 2006

Ishida-Yamamoto A and Iizuka H, 1995. Differences in Involucrin Immunolabeling Within Cornified Cell Envelopes in Normal and Psoriatic Epidermis. The Journal of Investigative Dermatology Vol. 104, No. 3, March 1995.

Ishida-Yamamoto A, Deraison C, Bonnart C, Bitoun E, Robinson R, O'Brien TJ, et al, 2005. LEKTI is localized in lamellar granules, separated from KLK5 and KLK7, and is secreted in the extracellular spaces of the superficial stratum granulosum. J Invest Dermatol. 2005;124:360–366

Ishida-Yamamoto A and Kishibe M, 2011. Involvement of corneodesmosome degradation and lamellar granule transportation in the desquamation process. Med Mol Morphol (2011) 44:1–6

Ishida-Yamamoto A, Kishibe M, Murakami M, Honma M and Takahashi H, 2012. Lamellar Granule Secretion Starts before the Establishment of Tight Junction Barrier for Paracellular Tracers in Mammalian Epidermis. PLoS ONE 7(2): e31641. 2012

Jacks T and Weinberg RA, 2002. Taking the study of cancer cell survival to a new dimension. Cell Volume: 111 Issue: 7 Pages: 923-925

Jampilek J and Brychtova K, 2010. Azone analogues: classification, design, and transdermal penetration principles. Medicinal Research Reviews Volume 32, Issue 5, pages 907–947, September 2012

Jayapal KP, Wlaschin KF, Hu W and Yap MGS, 2007. Recombinant Protein Therapeutics from CHO Cells - 20 years and counting. CHO Consortium. SBE Special Section, Page 40

Jean J, Soucy J and Pouliot R, 2011. Effects of Retinoic Acid on Keratinocyte Proliferation and Differentiation in a Psoriatic Skin Model. Tissue Engineering Part A Volume: 17 Issue: 13-14 Pages: 1859-1868

Jonca N, Guerrin M, Hadjiolova K, Caubet C, Gallinaro H, Simon M and Serre G, 2002. Corneodesmosin, a component of epidermal corneocyte desmosomes, displays homophilic adhesive properties. J Biol Chem 277:5024–5029

Judah D, Rudkouskaya A, Wilson R, Carter DE and Dagnino L, 2012. Multiple Roles of Integrin-Linked Kinase in Epidermal Development, Maturation and Pigmentation Revealed by Molecular Profiling. PloS One 2012:7(5) e36704

Kamata Y, Taniguchi A, Yamamoto, M, Nomura J, Ishihara K, Takahara H, Hibino T and Takeda A, 2009. Neutral Cysteine Protease Bleomycin Hydrolase Is Essential for the Breakdown of Deiminated Filaggrin into Amino Acids. Journal Of Biological Chemistry Volume: 284 Issue: 19 Pages: 12829-12836

Kartasova T, Roop DR, Holbrook KA and Yuspa SH, 1993. Mouse Differentiation-specific Keratins 1 and 10 Require a Preexisting Keratin Scaffold to Form a

Filament Network. The Journal of Cell Biology, Volume 120, Number 5, March 1993 1251 - 1261

Katsuta Y, Iida T, Hasegawa K, Inomata S and Denda M, 2008. Function of oleic acid on epidermal barrier and calcium influx into keratinocytes is associated with N-methyl D-aspartate-type glutamate receptors. British Journal of DermatologyVolume 160, Issue 1

Kawashima K, Doi H, Ito Y, Shibata M, Yoshinaka R and Otsuki Y, 2004. Evaluation of cell death and proliferation in psoriatic epidermis. Journal of Dermatological Science Volume 35, Issue 3, September 2004, Pages 207‑214

Keith B and Simon MC, 2007. Hypoxia-Inducible Factors, Stem Cells, and Cancer. Cell, Volume 129, Issue 3, 465-472, 4 May 2007

Kezic S, Kemperman PM, Koster ES, de Jongh CM, Thio HB and Campbell LE, 2008. Loss-of-function mutations in the filaggrin gene lead to reduced level of natural moisturizing factor in the stratum corneum. J Invest Dermatol 2008;128:2117–2119

Kezic S, O'Regan GM, Yau N, Sandilands A, Chen H, Campbell LE, Broboth K, Watson R, Rowland M, McLead WHI and Irvine AD, 2011. Levels of filaggrin degradation products are influenced by both filaggrin genotype and atopic dermatitis severity. Allergy Volume 66, Issue 7, pages 934–940

Kezic S, O'Regan GM, Lutter R, Jakasa I, Koster ES, Saunders S, Caspers P, Kemperman PMJH, Patrick MJH, Puppels GJ, Sandilands A, Chen HJ, Campbell LE, Kroboth K, Watson R, Fallon PG, McLead WHI and Irvine AD, 2012. Filaggrin loss-of-function mutations are associated with enhanced expression of IL-1 cytokines in the stratum corneum of patients with atopic dermatitis and in a murine model of filaggrin deficiency. Journal Of Allergy And Clinical Immunology Volume: 129 Issue: 4 Pages: 1031-U542

Kim MY, Lee SE, Chang JY and Kim SC, 2011. Retinoid Induces the Degradation of Corneodesmosomes and Downregulation of Corneodesmosomal Cadherins: Implications on the Mechanism of Retinoid-induced Desquamation. Annals Of Dermatology. Volume: 23 Issue: 4 Pages: 439-447

Kirschner N, Rosenthal R, Günzel D, Moll I and Brandne JM, 2012. Tight junctions and differentiation – a chicken or the egg question? Experimental Dermatology Volume 21, Issue 3, pages 171–175, March 2012

Klinkner AM, Bugelski PJ, Waites CR, Louden C, Hart TK and Kerns WD, 1997. A Novel Technique For Mapping the Lipid Composition of Atherosclerotic Fatty Streaks by En Face Fluorescence Microscopy. The Journal of Histochemistry & Cytochemistry. Volume 45(5): 743–753, 1997

Knies Y, Bernd A, Kaufmann R, Bereiter-Hahn J and Kippenberger S, 2006. Mechanical stretch induces clustering of beta1-integrins and facilitates adhesion. Exp. Dermatol. 15, 347–355.

Knight E, Murray B, Carnachan R, Przyborski S.A, 2011. Alvetex : Polystyrene scaffold technology for routine three dimensional cell culture. Methods in Molecular Biology, 695, 323-40.

Koch PJ, de Viragh PA, Scharer E, Bundman D, Longley MA, Bickenbach J, Kawachi Y, Suga Y, Zhou Z, Huber M, Hohl D, Kartasova T, Jarnik M, Steven AC and Roop DR, 2000. Compensatory Mechanisms Maintaining Skin Barrier Function in the Absence of a Major Cornified Envelope Protein. JCB vol. 151 no. 2 389-400

Koch PJ and Roop DR, 2004. The Role of Keratins in Epidermal Development and Homeostasis—Going Beyond the Obvious. Journal of Investigative Dermatology (2004) 123, x–xi; doi:10.1111/j.0022-202X.2004.23495.x

Komatsu N, Tsai B, Sidiropoulos M, Saijoh K, Levesque MA, Takehara K and Diamandis EP, 2006. Quantification of eight tissue kallikreins in the stratum corneum and sweat. J Invest Dermatol 126:925–929

Komatsu N, Saijoh K, Jayakumar A, Clayman GL, Tohyama M, Suga Y, Mizuno Y, Tsukamoto K, Taniuchi K, Takehara K, Diamandis EP, 2008. Correlation between SPINK5 gene mutations and clinical manifestations in Netherton syndrome patients. J Invest Dermatol 128:1148–1159

Komuves L, Oda Y, Tu CL, Chang WH, Ho-Pao CL, Mauro T and Bikle DD, 2002. Epidermal expression of the full-length extracellular calcium-sensing receptor is

required for normal keratinocyte differentiation. Journal of Cellular Physiology Volume 192, Issue 1, pages 45–54, July 2002

Koria P and Andreadis ST, 2006. Epidermal Morphogenesis: The Transcriptional Program of Human Keratinocytes during Stratification. Journal of Investigative Dermatology (2006) 126, 1834–1841

Kubo A, Nagao K, Yokouchi M, Sasaki H and Amagai M, 2009. External antigen uptake by Langerhans cells with reorganization of epidermal tight junction barriers. J Exp Med 206: 2937–2946.

Kunii T, Hirao T, Kikuchi K and Tagami H, 2003. Stratum Corneum lipid profile and maturation pattern of corneocytes in the outermost layer of fresh scars: the presence of immature corneocytes plays a much more important role in the barrier dysfunction than do changes in intercellular lipids. British Journal of Dermatology 2003: 149: 749-756

Kuntsche J, Bunjes H, Fahr A, Pappinen A, Ronkko, S, Suhonen, MU, Urtti, A, 2008. International Journal Of Pharmaceutics Volume: 354 Issue: 1-2 Pages: 180-195

Kurasawa M, Maeda T, Oba A, Yamamoto T and Sasaki H, 2011. Tight junction regulates epidermal calcium ion gradient and differentiation. Biochemical And Biophysical Research Communications Volume: 406 Issue: 4 Pages: 506-511

Kuroda S, Kurasawa M, Mizukoshi K, Maeda T and Yamamoto T, 2010. Perturbation of lamellar granule secretion by sodium caprate implicates epidermal tight junctions in lamellar granule function. J Dermatol Sci 59:107–114.

Kwak S, Brief E, Langlais D, Kitson N, Lafleur M and Thewalt J, 2012. Ethanol perturbs lipid organization in models of stratum corneum membranes: An investigation combining differential scanning calorimetry, infrared and H-2 NMR spectroscopy. Biochimica Et Biophysica Acta. Biomembranes Volume: 1818 Issue: 5 Pages: 1410-1419

Kypriotou M, Huber M, Hohl D, 2012. The human epidermal differentiation complex: cornified envelope precursors, S100 proteins and the 'fused genes' family. Experimental dermatology Volume: 21 Issue: 9 Pages: 643-9

Lademann J, Otberg N, Richter H, Weigmann HJ, Lindemann U, Schaefer H and Sterry W, 2001. Investigation of follicular penetration of topically applied substances, Skin Pharmacol. Appl. Skin Physiol. 14 (Suppl. 1) (2001) 17–22.

Laemmli UK, 1970. Cleavage of Structural Proteins during the Assembly of the Head of Bacteriophage T4. Nature 227, 680 - 685

Lai Cheong JE, Wessagowit V and McGrath JA, 2005. Molecular abnormalities of the desmosomal protein desmoplakin in human disease. Clin Exp Dermatol 30: 261–266

Lampe MA, Williams ML and Elias PM, 1983. Human epidermal lipids: characterization and modulations during differentiation. J Lipid Res. 1983 Feb;24(2):131-40.

Larese FF, D'Agostin F, Crosera M, Adami G, Renzi N, Bovenzi M and Maina G, 2009. Human skin penetration of silver nanoparticles through intact and damaged skin. Toxicology. Volume: 255 Issue: 1-2 Pages: 33-37

Lee & Cho, 2005. The effects of epidermal keratinocytes and dermal fibroblasts on the formation of cutaneous basement membrane in three-dimensional culture systems. Archives Of Dermatological Research Volume: 296 Issue: 7 Pages: 296-302

Lee DD, Stojadinovic O, Krzyzanowska A, Vouthounis C, Blumenberg M and Tomic-Canic M, 2009. Retinoid-Responsive Transcriptional Changes in Epidermal Keratinocytes. Journal Of Cellular Physiology Volume: 220 Issue: 2 Pages: 427-439

Lee J, Cuddihy MJ and Kotov NA, 2008. Three-Dimensional Cell Culture Matrices: State of the Art. Tissue Engineering, Part B. Volume 14, Number 1, p68

Lee Y, Je YJ, Lee SS, Li ZJ, Choi DK, Kwon YB, Sohn KC, Im M, Seo YJ and Lee JK, 2012. Changes in Transepidermal Water Loss and Skin Hydration according to Expression of Aquaporin-3 in Psoriasis. Annals Of Dermatology Volume: 24 Issue: 2 Pages: 168-174

Le Fur I, Reinberg A, Lopez S, Morizot F, Mechkouri M, Tschachler E, 2001. Analysis of circadian and ultradian rhythms of skin surface properties of face and forearm of healthy women. J Invest Dermatol 2001;117:718-24.

Levy L, Broad S, Diekmann D, Evans RD and Watt FM, 2000. beta1 integrins regulate keratinocyte adhesion and differentiation by distinct mechanisms. Mol Biol Cell. 2000 Feb;11(2):453-66.

Li W, Sandhoff R, Kono M, Zerfas P, Hoffmann V, Ding BC, Proia RL, Deng CX, 2007. Depletion of ceramides with very long chain fatty acids causes defective skin permeability barrier function, and neonatal lethality in ELOVL4 deficient mice. Int J Biol Sci 2007; 3(2):120-128. doi:10.7150/ijbs.3.120

Li N, Wu XH, Jia WB, Zhang MC, Tan FP and Zhang J, 2012. Effect of ionization and vehicle on skin absorption and penetration of azelaic acid. Drug Development And Industrial Pharmacy Volume: 38 Issue: 8 Pages: 985-994

Liang Y, Xia L, Du Z, Sheng L, Chen H, Chen G and Li Q, 2012. HOXA5 inhibits keratinocytes growth and epidermal formation in organotypic cultures in vitro and in vivo. Journal of Dermatological Science, Volume 66, Issue 3, June 2012, Pages 197–206

Livshits G, Kobielak A and Fuchs E, 2012. Governing epidermal homeostasis by coupling cell–cell adhesion to integrin and growth factor signaling, proliferation, and apoptosis. PNAS vol. 109 no. 13 4886-4891

Lowell S, Jones P, Le Roux I, Dunne J and Watt FM, 2000. Stimulation of human epidermal differentiation by delta-notch signalling at the boundaries of stem-cell clusters. Curr Biol. 2000 May 4;10(9):491-500.

Lowry WE, Blanpain C, Nowak JA, Guasch G, Lewis L and Fuchs E, 2005. Defining the impact of β-catenin/Tcf transactivation on epithelial stem cells. Genes Dev 2005;19(13):1596–1611

Lulevich V, Yang H, Isseroff RR and Liu G, 2010. Single cell mechanics of keratinocyte cells. Ultramicroscopy, 110 (2010) 1435-1442

Ma L, Barker J, Zhou C, Li W, Zhang J, Lin B, Foltz G, Küblbeck J and Honkakoski P, 2012. Towards personalized medicine with a three-dimensional micro-scale perfusion-based two-chamber tissue model system. Biomaterials Volume 33, Issue 17, June 2012, Pages 4353–4361

Määttä A, DiColandrea T, Groot K and Watt FM, 2001. Gene Targeting of Envoplakin, a Cytoskeletal Linker Protein and Precursor of the Epidermal Cornified Envelope. Mol. Cell. Biol. October 2001 vol. 21 no. 20 7047-7053

Määttä A, 2004. Roads to the edge of the cell: Intracellular transport of cornified envelope precursors. Journal Of Investigative. Dermatology Volume: 122 Issue: 1 Pages: XII-XIII

Maas-Szabowski N, Stärker A and Fusenig NE, 2003. Epidermal tissue regeneration and stromal interaction in HaCaT cells is initiated by TGF-α. Journal of Cell Science 116 (14)

Maas-Szabowski N, Szabowski A, Stark HJ, Andrecht S, Kolbus A, Schorpp-Kistner M, Angel P and Fusenig NE, 2001. Organotypic Cocultures with Genetically Modified Mouse Fibroblasts as a Tool to Dissect Molecular Mechanisms Regulating Keratinocyte Growth and Differentiation. Journal of Investigative Dermatology. Vol. 116, No. 5 May 2001.

Macneil S, 2007. Progress and opportunities for tissue-engineered skin. Nature Vol 445. 22 February 2007

Mak VH, Cumpstone MB, Kennedy AH, Harmon CS, Guy RH and Potts RO, 1991. Barrier Function of Human Keratinocyte Air-liquid Cultures. Journal of Investigative Dermatology. Vol. 96 No. 3 March 1991

Margulis A, Zhang W, Alt-Holland A, Pawagi S, Prabhu P, Cao J, Zucker S, Pfeiffer L, Garfield J, Fusenig NE and Garlick JA, 2006. Loss of intercellular adhesion activates a transition from low- to high-grade human squamous cell carcinoma. International Journal Of Cancer Volume: 118 Issue: 4 Pages: 821-831

Masahiro and Masao, 2007. Mass spectrometric characterization of cholesterol esters and wax esters in epidermis of fetal, adult and keloidal human skin. Experimental Dermatology Volume 17, Issue 4, pages 318–323, April 2008

Mazar J, Sinha S, Dinger ME, Mattick JS and Perera RJ, 2010. Protein-coding and non-coding gene expression analysis in differentiating human keratinocytes using a three-dimensional epidermal equivalent. Molecular Genetics And Genomics Volume: 284 Issue: 1 Pages: 1-9

McInroy L and Määttä A, 2007. Down-regulation of vimentin expression inhibits carcinoma cell migration and adhesion. Biochemical And Biophysical Research Communications Volume: 360 Issue: 1

McInroy L and Määttä A, 2011. Plectin regulates invasiveness of SW480 colon carcinoma cells and is targeted to podosome-like adhesions in an isoform-specific manner. Experimental Cell Research Volume: 317 Issue: 17

Menon GK and Elias PM, 1991. Ultrastructural localization of calcium in psoriatic and normal human epidermis. Arch Dermatol 1991; 127: 57–63.

Menon, GK, Elias, P, Lee, S and Feingold, K, 1992. Localization of calcium in murine epidermis following disruption and repair of the permeability barrier. Cell Tissue Res. 270, 503–512.

Micallef L, Belaubre F, Pinon A, Jayat-Vignoles C, Delage C, Charveron M and Simon A, 2008. Effects of extracellular calcium on the growth-differentiation switch in immortalized keratinocyte HaCaT cells compared with normal human keratinocytes. Experimental Dermatology 2009 Feb;18(2):143-51. Epub 2008 Jul 9.

Michel S and Juhlin L, 1990. Cornified Envelopes in congenital disorders of keratinization. British Journal of Dermatology: 122, 15-21.

Mihara, 1988. Scanning electron microscopy of skin surface and the internal structure of corneocyte in normal human skin. An application of the osmium-dimethyl sulfoxide-osmium method. Arch Dermatol Res (1988) 280:293-299

Mildner M, Jin J, Eckhart L, Kezic S, Gruber F, Barresi C, Stremnitzer C, Buchberger M, Mlitz V, Ballaun C, Sterniczky B, Födinger D and Tschachler E, 2010. Knockdown of Filaggrin Impairs Diffusion Barrier Function and Increases UV Sensitivity in a Human Skin Model. Journal Of Investigative Dermatology Volume: 130 Issue: 9 Pages: 2286-2294

Millipore Website - http://www.millipore.com/catalogue/module/c10504. Accessed 25/03/2012

Mikos AG, Sarakinos G, Leite SM, Vacanti JP and Langer R, 1993. Laminated three-dimensional biodegradable foams for use in tissue engineering. Biomaterials Volume 14, Issue 5, April 1993, Pages 323–330

Mikos AG, Thorsen AJ, Czerwonka LA, Bao Y, Langer R, Winslow DN and Vacanti JP, 1994. Preparation and characterisation of poly(lactic acid) foams. Polymer 35, 1068.

Miodovnik M, Koren R, Ziv E and Ravid A, 2012. The inflammatory response of keratinocytes and its modulation by vitamin D: The role of MAPK signaling pathways. Journal of Cellular Physiology Volume 227, Issue 5, pages 2175–2183, May 2012

Mitragotri, 2002. Modeling skin permeability to hydrophilic and hydrophobic solutes based on four permeation pathways. Journal of Controlled Release 86 (2003) 69–92

Miyai E, Yanagida M, Akiyama J and Yamamoto I, 1996. Ascorbic acid 2-O-alpha-glucoside, a stable form of ascorbic acid, rescues human keratinocyte cell line, SCC, from cytotoxicity of ultraviolet light B. Biological & Pharmaceutical Bulletin Volume: 19 Issue: 7 Pages: 984-987

Mizutani Y, Kihara A and Igarashi Y, 2006. LASS3 is a mainly testis-specific (dihydro)ceramide synthase with relatively broad substrate specificity, Biochem. J. 398 (2006) 531–538.

Mizutani Y, Kihara A, Chiba H, Tojo H and, Igarashi Y, 2008. 2-Hydroxy-ceramide synthesis by ceramide synthase family: enzymatic basis for the preference of FA chain length, J. Lipid Res. 49 (2008) 2356–2364.

Mizutani Y, Mitsutake S, Tjusi K, Kihara A and Igarashi Y, 2009. Ceramide biosynthesis in keratinocyte and its role in skin function. Biochimie 91 (2009) 784–790

Moghimi HR, Williams AC and Barry BW, 1996. A lamellar matrix model for the stratum corneum intercellular lipids. Characterization and comparison with stratum corneum intercellular structure. Int J Pharm 1996;131:103–115.

Rowley JA, Madlambayan G, Mooney DJ, 1999. Alginate hydrogels as synthetic extracellular matrix materials. Biomaterials. 1999 Jan;20(1):45-53.

Mooney DJ, Baldwin DF, Suh NP, Vacanti JP and Langer R, 1996. Novel approach to fabricate porous sponges of poly(lactic-coglycolic acid) without the use of organic solvents. Biomaterials 17, 1417.

Morar N, Cookson WOCM, Harper JI and Moffatt MF, 2007. Filaggrin Mutations in Children with Severe Atopic Dermatitis. Journal of Investigative Dermatology (2007) 127, 1667–1672

Naoe Y, Hata T, Tanigawa K, Kimura H, Masunaga T, 2009. Bidimensional analysis of desmoglein1 distribution on the outermost corneocytes provides the structural and functional information of the stratum corneum. Journal of Dermatological Science. Volume 57, Issue 3, March 2010, Pages 192–198

Nemes and Steinert, 1999. Bricks and Mortar of the Epidermal Barrier. Exp Mol Med 1999; 31:5-19.

Neofytou EA, Chang E, Patlola B, Joubert L-M, Rajadas J, Gambhir SS, Cheng Z, Robbins RC, Beygui RE. 2011. Adipose tissue-derived stem cells display a proangiogenic phenotype on 3D scaffolds. J Biomed Mater Res Part A 2011:98A:383–393.

Netzlaff F, Lehr CM, Wertz PW and Schaefer UF, 2005. The human epidermis models EpiSkin, SkinEthic and EpiDerm: An evaluation of morphology and their suitability for testing phototoxicity, irritancy, corrosivity, and substance transport. European Journal of Pharmaceutics and Biopharmaceutics 60 (2005) 167–178

Nin M, Katoh N, Kokura S, Handa O, Yoshikawa T and Kishimoto S, 2009. Dichotomous effect of ultraviolet B on the expression of corneodesmosomal enzymes in human epidermal keratinocytes. Journal of Dermatological Science. Volume 54, Issue 1, April 2009, Pages 17–24

Norgett EE, Hatsell SJ, Carvajal-Huerta L, Cabezas JC, Common J, Purkis PE, Whittock N, Leigh IM, Stevens HP and Kelsell DP, 2000. Recessive mutation in desmoplakin disrupts desmoplakin-intermediate filament interactions and causes dilated cardiomyopathy, woolly hair and keratoderma. Hum Mol Genet. 2000 Nov 1;9(18):2761-6.

Nolte CJM, Oleson MA, Bilbo PR and Parenteau NL, 1993. Development of a stratum corneum and barrier function in an organotypic skin culture. Arch Dermatol Res (1993) 285:466-474

Nova D, Le Griel C, Holvoet S, Gentilhomme E, Vincent C, Staquet MJ, Schmitt D and Serres M, 2003. Comparative studies on the secretion and activation of MMPs in two reconstructed human skin models using HaCaT- and HaCaT-ras-transfected cell lines. Clinical & Experimental Metastasis Volume: 20 Issue: 8 Pages: 675-683

Novotný M, Klimentová J, Janůšová B, Palát K, Hrabálek A and Vávrová K, 2011. Ammonium carbamates as highly active transdermal permeation enhancers with a dual mechanism of action. Journal of Controlled Release Volume 150, Issue 2, 10 March 2011, Pages 164–170

Nowak JA, Polak L, Pasolli HA and Fuchs E, 2008. Hair follicle stem cells are specified and function in early skin morphogenesis. Cell Stem Cell 3: 33–43

Ng W and Ikeda S, 2011. Standardized, Defined Serum-free Culture of a Human Skin Equivalent on Fibroblast-populated Collagen Scaffold. Acta Derm Venereol 2011

O'connell MB, 1995. Pharmacokinetic And Pharmacological Variation Between Different Estrogen Products. Journal Of Clinical Pharmacology Volume 35, Issue: 9, Pages: S18-S24, Sept 1995

O'Regan GM, Sandilands A, McLean WHI and Irvine AD, 2009. Filaggrin in atopic dermatitis. Journal of Allergy and Clinical Immunology Volume 124, Issue 3, Supplement 2, September 2009, Pages R2–R6

Ochalek, Podhaisky, Ruettinger and Neubert, 2012. SC lipid model membranes designed for studying impact of ceramide species on drug diffusion and permeation, Part III: Influence of penetration enhancer on diffusion and permeation of model drugs. International Journal of Pharmaceutics Volume 436, Issues 1‑2, 15 October 2012, Pages 206–213

Odorisio T, De Luca N, Vesci L, Luisi PL, Stano P, Zambruno G and Pisano C, 2012. The atypical retinoid E-3-(3'-Adamantan-1-yl-4'-methoxybiphenyl-4-yl)-2-propenoic acid (ST1898) displays comedolytic activity in the rhino mouse model. European journal of dermatology : EJD Volume: 22 Issue: 4 Pages: 505-11

OECD Guidance Document For The Conduct Of Skin Absorption Studies. OECD Series On Testing And Assessment Number 28, 5th March 2004. ENV/JM/Mono(2004)2

Ojeh N, Pekovic V, Jahoda C and Määttä A, 2008. The MAGUK-family protein CASK is targeted to nuclei of the basal epidermis and controls keratinocyte proliferation. August 15, 2008 J Cell Sci121, 2705-2717.

Onorato JM, Langish R, Hellings S, Shipkova P and Gargalovic PS, 2012. Characterizing the Lipid-loading Properties of Macrophages Using LC/MS for the Detection of Cholesterol and Cholesteryl-Esters. American Pharmaceutical Review 2012.

Osborne CS, Reid WH, Grant MH, 1997. Investigation into cell growth on collagen/chondroitin-6-sulphate gels: the effect of crosslinking agents and diamines. Journal Of Materials Science: Materials In Medicine 8 (1997) 179—184

Osborne CS, Reid WH and Grant MH, 1998. Investigation into the biological stability of collagen/chondroitin-6-sulphate gels and their contraction by fibroblasts and keratinocytes: the effect of crosslinking agents and diamines. Biomaterials 20 (1999) 283-290.

Paller AS, van Steensel MA, Rodriguez-Martin M, Sorrell J, Heath C and Crumrine D, 2011. Pathogenesis-based therapy reverses cutaneous abnormalities in an inherited disorder of distal cholesterol metabolism. J Invest Dermatol 2011;131:2242-8.

Pappinen, Tikkinen, Pasonen-Seppänen, Murtomäki, Suhonen, Urtti A, 2007. Rat epidermal keratinocyte organotypic culture (ROC) compared to human cadaver skin: the effect of skin permeation enhancers, Eur. J. Pharm. Sci. 30 (2007) 240–250.

Pappinen S, Hermansson M, Kuntsche J, Somerharju P, Wertz P, Urtti A and Suhonen M, 2008. Comparison of rat epidermal keratinocyte organotypic culture (ROC) with intact human skin: Lipid composition and thermal phase behavior of the stratum corneum. Biochimica et Biophysica Acta 1778 (2008) 824–834

Pappinen S, Pryazhnikov E, Khiroug L, Ericson MB, Yliperttula M and Urtti A, 2012. Organotypic cell cultures and two-photon imaging: Tools for in vitro and in

vivo assessment of percutaneous drug delivery and skin toxicity. Journal of Controlled Release. Volume 161, Issue 2, 20 July 2012, Pages 656–667

Paragh G, Schling P, Ugocsai P, Kel AE, Liebisch G, Heimerl S, Moehle C, Schiemann Y, Wegmann M, Farwick M, Wikonkál NM, Mandl J, Langmann T and Schmitz G, 2008. Novel sphingolipid derivatives promote keratinocyte differentiation. Experimental Dermatology Volume 17, Issue 12, pages 1004–1016, December 2008

Pasonen-Seppänen S, Suhonen TM, Kirjavainen M, Suihko E, Urtti A, Miettinen M, Hyttinen M, Tammi M and Tammi R, 2001. Vitamin C enhances differentiation of a continuous keratinocyte cell line (REK) into epidermis with normal stratum corneum ultrastructure and functional permeability barrier. Histochemistry And Cell Biology Volume: 116 Issue: 4

Pasonen-Seppänen S, Suhonen TM, Kirjavainen M, Miettinen M, Urtti A, Tammi M and Tammi R, 20012. Formation of Permeability Barrier in Epidermal Organotypic Culture for Studies on Drug Transport. Journal of Investigative Dermatology (2001) 117, 1322–1324

Peltonen S, Riehokainen J, Pummi K and Peltonen J, 2006. Tight junction components occludin, ZO-1, and claudin-1,-4 and -5 in active and healing psoriasis. British Journal of Dermatology 2007 156, pp466–472

Perkins, Osborne, Rana, Ghassemi and Robinson, 1999. Comparison of *in vitro* and *in vivo* human skin response to consumer products and ingredients with a range of irritancy potential. Toxicol. Sci., 48 (1999), pp. 218–229

Piehowski PD, Carado AJ, Kurczy ME, Ostrowski SG, Heien ML, Winograd N and Ewing AG, 2008. MS/MS Methodology To Improve Subcellular Mapping of Cholesterol Using TOF-SIMS. Anal. Chem. 2008, 80, 8662–8667

Pillai S and Bikle DD, 1991. Role of intracellular-free calcium in the cornified envelope formation of keratinocytes: Differences in the mode of action of extracellular calcium and 1,25 dihydroxyvitamin D3. Journal of cellular physiology 146 (1): 94–100

Ponec M, Boelsma E, Weerheim A, Mulder A, Bouwstra J and Mommaas M, 2000. Lipid and ultrastructural characterization of reconstructed skin models. International Journal of Pharmaceutics Volume 203, Issues 1–2, 1 August 2000, Pages 211–225

Ponec, Weerheim, Pankhorst and Wertz, 2003. New Acylceramide in Native and Reconstructed Epidermis. Journal of Investigative Dermatology (2003) 120, 581–588

Ponec M, Weerheim A, Kempenaar J, Mulder A, Gooris GS, Bouwstra J and Mommaas AM, 1997, The formation of competent barrier lipids in reconstructed human epidermis requires the presence of vitamin C. J. Invest. Dermatol. 109 (1997) 348–355

Poumay Y and Coquette A, 2007. Modelling the human epidermis in vitro: tools for basic and applied research. Arch Dermatol Res (2007) 298:361–369

Poumay Y, Dupont F, Marcoux S, Leclercq-Smekens M, Hérin M and Coquette A, 2004. A simple reconstructed human epidermis: preparation of the culture model and utilization in in vitro studies. Arch Dermatol Res. 2004 Oct;296(5):203-11

Poumay and Pittelkow et al, 1994. Cell Density and Culture Factors Regulate Keratinocyte Commitment to Differentiation and Expression of Suprabasal K1/K10 Keratins. Journal of Investigative Dermatology (1995) 104, 271–276

Powell HM, Supp DM and Boyce ST, 2008. Influence of electrospun collagen on wound contraction of engineered skin substitutes. Biomaterials. 2008 Mar;29(7):834-43

Powell HM and Boyce ST, 2009. Engineered human skin fabricated using electrospun collagen-PCL blends: morphogenesis and mechanical properties. Tissue Eng Part A. 2009 Aug;15(8):2177-87

Price And Gregory 1982, Relationship Between In Vitro Growth Promotion And Biophysical And Biochemical Properties Of The Serum Supplement. In Vitro Vol. 18, No. 6, June 1982

Proby CM, Purdie KJ, Sexton CJ, Purkis P, Navsaria HA, Stables JN and Leigh IM, 2000. Spontaneous keratinocyte cell lines representing early and advanced stages of malignant transformation of the epidermis. Exp Dermatol 2000: 9: 104–117

Proksch E, Brandner JM and Jensen JM, 2008. The skin: an indispensable barrier. Experimental Dermatology, 17, 1063–1072.

Prunieras M, Regnier M and Woodley D et al, 1983. Methods for cultivation of keratinocytes with an air-liquid interface. J Invest Dermatol. 1983 Jul;81(1 Suppl):28s-33s

Rasmussen C, Gratz K, Liebel F, Southall M, Garay M, Bhattacharyya S, Simon N, Vander Zanden M, Van Winkle K, Pirnstill J, Pirnstill S, Comer A and Allen-Hoffmann BL, 2010. The StrataTest human skin model, a consistent in vitro alternative for toxicological testing. Toxicol In Vitro. 2010 Oct;24(7):2021-9

Raufast, 2010. The use of a precursor as a source of exogenous bio-available linoleic acid: assessment of the skin metabolism and of the nourishing effect of a cream containing it. Journal Of Investigative Dermatology. Volume: 130 Supplement: 2 Pages: S31-S31 Published: SEP 2010

Rawlings AV, Harding CR, Watkinson A, Banks J, Ackerman C, Sabin R, 1995. The effect of glycerol and humidity on desmosome degradation in stratum corneum. Arch Dermatol Res 287:457-464,1995

Rawlings AV, 2003. Trends in stratum corneum research and the management of dry skin conditions. International Journal of Cosmetic Science, 2003, 25, 63-95

Rawlings AV and Harding CR, 2004. Moisturisation and Skin Barrier Function. Dermatologic Therapy Volume 17, Issue Supplement s1, pages 43–48

Regnier M, Prunieras M and Woodley D, 1981. Growth and differentiation of adult human epidermal cells on dermal substrates. Frontiers Matrix Biol. 9, 4-35.

Reichelt J, Bussow H, Grund C and Magin TM, 2001. Formation of a normal epidermis supported by increased stability of keratins 5 and 14 in keratin 10 null mice. Mol. Biol. Cell 12, 1557-1568.

Rheins LA, Edwards SM, Miao O and Donnelly TA, 1994. Skin(2TM): An in vitro model to assess cutaneous immunotoxicity. Toxicol In Vitro. 1994 Oct;8(5):1007-14.

Rheinwald JG and Green H, 1975. Serial Cultivation of Strains of Human Epidermal Keratinocytes: the Formation of Keratinizing Colonies from Single Cells. Cell, Vol 6, 331-344, November 1975.

Rheinwald JG and Green H, 1977. Epidermal growth factor and the multiplication of cultured human epidermal keratinocytes. Nature 265, 421 - 424

Rice RH and Green H, 1979. The Cornified Envelope of Terminally Differentiated Human Epidermal Keratinocytes Consists of Cross-linked Protein. Cell 11:417-422.

Richardson TP, Peters MC, Ennett AB and Mooney DJ, 2001. Polymeric system for dual growth factor delivery. Nat Biotech 19, 1029.

Rickelt S, Moll I and Franke WW, 2012. Intercellular adhering junctions with an asymmetric molecular composition: desmosomes connecting Merkel cells and keratinocytes. Cell And Tissue Research Volume: 346 Issue: 1Pages: 65-77

Roelandt T, Hillary T, Giddelo C, Baudouin C, Msika P, Mangelings D, Vander Heyden Y, Fluhr J, Schmuth M and Hachem J, 2011. Filaggrin buffering capacity participates in the stratum corneum acid mantle. Journal Of Investigative Dermatology, Volume: 132, Supplement: 1

Ronfard V, Rives JM, Neveux Y, Carsin H and Barrandon Y, 2000. Long-term regeneration of human epidermis on third degree burns transplanted with autologous cultured epithelium grown on a fibrin matrix. Transplantation 70:1588–1598

Rosdy M and Clauss LC, 1990. Terminal Epidermal Differentiation of Human Keratinocytes Grown in Chemically Defined Medium on Inert Filter Substrates at the Air-Liquid Interface. Journal of Investigative Dermatology. Vol 95. No.4 Oct 1990.

Rugg EL, McLean WHI, Lane EB, Pitera R, McMillan JR, Dopping-Hepenstal PJC, Navsaria HA, Leigh IM and Eady RAJ, 1994. A functional "knockout" of human keratin 14. Genes Dev. 1994 8: 2563-2573

Sabapathy K and Wagner EF (2004) JNK2: a negative regulator of cellular proliferation. Cell Cycle 3:1520–3

Sakaguchi M, Miyazaki M, Takaishi M, Sakaguchi Y, Makino E, Kataoka N, Yamada H, Namba M and Huh NH, 2003. S100C/A11 is a key mediator of Ca2+-induced growth inhibition of human epidermal keratinocytes. J Cell Biol. 2003 November 24; 163(4): 825–835.

Sandilands E, Sutherland C, Irvine AD and McLean WHI, 2009. Filaggrin in the frontline: role in skin barrier function and disease. Journal of Cell Science 122, 1285-1294

Santos M, Paramio JM, Bravo A, Ramirez A and Jorcano JL, 2002. The expression of keratin k10 in the basal layer of the epidermis inhibits cell proliferation and prevents skin tumorigenesis. J Biol Chem 277: 19122–19130

Schäfer-Korting, M, Bock U, Diembeck W, Düsing HJ, Gamer A, Haltner-Ukomadu E, Hoffmann C, Kaca M, Kamp H, Kersen S, Kietzmann M, Korting HC,Krächter HU, Lehr CM, Liebsch M, Mehling A, Müller-Goymann C, Netzlaff F, Niedorf F, Rübbelke MK, Schäfer U, Schmidt E, Schreiber S, Spielmann H, Vuia A and Weimer M.The use of reconstructed human epidermis for skin absorption testing: Results of the validation study. Altern Lab Anim. 2008 May;36(2):161-87.

Schmeichel KL and Bissell MJ, 2003. Modeling tissue-specific signaling and organ function in three dimensions. J. Cell Sci., 116 (2003), pp. 2377–2388

Schmidt M, Goebeler M, Posern G, Feller SM, Seitz CS, Bröcker E, Rapp UR and Ludwig S, 2000. Ras-independent Activation of the Raf/MEK/ERK Pathway upon Calcium-induced Differentiation of Keratinocytes. J. Biol. Chem., Vol. 275, Issue 52, 41011-41017

Schmook FP, Meingassner JG and Billich A, 2001. Comparison of Human Skin of Epidermis models with human and animal skin in in-vitro percutaneous absorbtion. International Journal of Pharmaceutics. Vol 215, 1-2, p51-56

Schoop VM, Mirancea N and Fusenig NE, 1999. Epidermal Organization and Differentiation of HaCat Keratinocytes in Organotypic Coculture with Human Dermal Fibroblasts. J. Invest Dermatol 112:343-353, 1999.

Schreiber S, Mahmoud A, Vuia A, Rübbelke MK, Schmidt E, Schaller M, Kandarova H, Haberland A, Schafer UF, Bock U, Korting HC, Liebsch M and Schafer-Korting, 2005. Reconstructed epidermis versus human and animal skin in skin absorption studies. Toxicology in Vitro Volume 19, Issue 6, September 2005, Pages 813‑822

Schutte M, Fox B, Baradez M, Devonshire A, Minguez J, Bokhari M and Przyborski S, 2011. Rat primary hepatocytes show enhanced performance and sensitivity to acetaminophen during three-dimensional culture on a polystyrene scaffold designed for routine use. Assay and Drug Development Technologies DOI: 10.1089/adt.2011.0371

Schweizer J, Bowden PE, Coulombe PA, Langbein L, Lane EB, Magin TM, Maltais L, Omary MB, Parry DA, Rogers MA and Wright MW, 2006. New consensus nomenclature for mammalian keratins. J Cell Biol. 2006 July 17; 174(2): 169–174.

Semlin L, Schäfer-Korting M, Borelli C and Korting HC, 2010. In vitro models for human skin disease. Drug Discovery Today Volume 16, Issues 3–4, February 2011, Pages 132–139

Seto JE, Polat BE, VanVeller B, Lopez RFV, Langer R and Blankschtein D, 2012. Fluorescent penetration enhancers for transdermal applications. Journal Of Controlled Release Volume: 158 Issue: 1 Pages: 85-92

Sevilla LM, Nachat R, Groot KR, Klement JF, Uitto J, Djian P, Määttä A, Watt FM, 2007. Mice deficient in involucrin, envoplakin, and periplakin have a defective epidermal barrier. JCB vol. 179 no. 7 1599-1612

Sevilla LM, Nachat R, Groot KR and Watt FM, 2008. Kazrin regulates keratinocyte cytoskeletal networks, intercellular junctions and differentiation. November 1, 2008 J Cell Sci 121, 3561-3569.

Shapiro LJ, Weiss R, Webster D, France JT: X-linked ichthyosis due to steroid sulfatase deficiency. Lancet 1:70–72, 1978

Shapiro L and Cohen S, 1997. Novel alginate sponges for cell culture and transplantation. Biomaterials. 1997 Apr;18(8):583-90

Skardal A, Smith L, Bharadwaj S, Atala A, Soker S and Zhang YY, 2012. Tissue specific synthetic ECM hydrogels for 3-D in vitro maintenance of hepatocyte function. Biomaterials Volume: 33 Issue: 18 Pages: 4565-4575

Slavik MA, Allen-Hoffman BL, Liu BY and Alexander CM, 2007. Wnt signaling induces differentiation of progenitor cells in organotypic keratinocyte cultures. BMC Developmental Biology 2007, 7:9

Smith LE, Smallwood R and MacNeil S, 2010. A Comparison of Imaging Methodologies for 3D Tissue Engineering. Microscopy Research And Technique 73:1123–1133 (2010)

Smola H, Thiekötter G and Fusenig NE, 1993. Mutual induction of growth factor gene expression by epidermal-dermal cell interaction. JCB vol. 122 no. 2 417-429

Smola H, Stark HJ, Thiekötter G, Mirancea N, Krieg T and Fusenig NE, 1998. Dynamics of Basement Membrane Formation by Keratinocyte-Fibroblast Interactions in Organotypic Skin Culture. Experimental Cell Research 239, 399-410 (1998)

Sobral CS, Gragnani A, Cao X, Morgan JR and Ferreira LM, 2007. Human keratinocytes cultured on collagen matrix used as an experimental burn model. Journal Of Burns And Wounds Volume: 7 Pages: e6 Published: 2007 Oct 30

Sotoodian B and Maibach HI, 2012. Non-invasive test methods for epidermal barrier function. Clinics in Dermatology (2012) 30, 301–310

Specht C, Stoye I and Muller-Goymann CC, 1998. Comparative investigations to evaluate the use of organotypic cultures of transformed and native dermal and epidermal cells for permeation studies. European Journal of Pharmaceutics and Biopharmaceutics Volume 46, Issue 3, 1 November 1998, Pages 273–278

Stahl J, Niedorf F and Kietzmann M, 2009. Characterisation of epidermal lipid composition and skin morphology of animal skin ex vivo. European Journal of Pharmaceutics and Biopharmaceutics 72 (2009) 310–316

Stahl J, Wohlert M and Kietzmann M, 2012. Microneedle pretreatment enhances the percutaneous permeation of hydrophilic compounds with high melting points. BMC Pharmacology and Toxicology 2012, 13:5

Stark HJ, Baur M, Breitkreutz D, Mirancea N and Fusenig NE, 1999. Organotypic Keratinocyte Cocultures in Defined Medium with Regular Epidermal Morphogenesis and Differentiation. Journal of Investigative Dermatology (1999) 112, 681–691

Steinert PM and Marekov LN, 1997. Direct evidence that involucrin is a major early isopeptide cross-linked component of the keratinocyte cornified cell envelope. J Biol Chem 1997;272:2021-30.

Suhonen, Pasonen-Seppänen S, Kirjavainen M, Tammi M, Tammi R and Urtti A, 2003. Epidermal cell culture model derived from rat keratinocytes with permeability characteristics comparable to human cadaver skin. Eur J Pharm Sci. 2003 Sep;20(1):107-13.

Sun T, Norton D, Haycock JW, Ryan AJ and MacNeil S, 2005a. Development of a closed bioreactor system for culture of tissue-engineered skin at an air-liquid interface. Tissue Engineering Volume:11 Issue: 11-12 Pages: 1824-1831

Sun T, Mai S, Norton D, Haycock JW, Ryan AJ and MacNeil S, 2005b. Self-organization of skin cells in three-dimensional electrospun polystyrene scaffolds. Tissue Eng. 2005 Jul-Aug;11(7-8):1023-33

Sun T, Jackson S, Haycock JW and MacNeil S, 2006. Culture of skin cells in 3D rather than 2D improves their ability to survive exposure to cytotoxic agents. Journal of Biotechnology. Apr 10;122(3):372-81. (2006a)

Sun T, Norton D, McKean RJ, Haycock JW, Ryan AJ and MacNeil S. Development of a 3D cell culture system for investigating cell interactions with electrospun fibres. Biotechnology and Bioengineering 97(5):1318-1328. (2006b)

Supp DM and Boyce ST, 2005. Engineered skin substitutes: practices and potentials. Clin. Dermatol. 23, 403–412 (2005)

Swensson O, Langbein L, McMillan JR, Stevens HP, Leigh IM, McLean WH, Lane EB and Eady RA, 1998. Specialized keratin expression pattern in human ridged skin as an adaptation to high physical stress. Br. J. Dermatol. 139, 767–775.

Tachi and Iwamori, 2008. Mass spectrometric characterization of cholesterol esters and wax esters in epidermis of fetal, adult and keloidal human skin. Exp Dermatol. 2008 Apr;17(4):318-23.

Takada S, Naito S, Sonoda J and Miyauchi Y, 2012. Noninvasive In Vivo Measurement of Natural Moisturizing Factor Content in Stratum Corneum of Human Skin by Attenuated Total Reflection Infrared Spectroscopy. Applied Spectroscopy Volume: 66 Issue: 1 Pages: 26-32

Takayama S, Hsiao AY, Tung YC, Qu X, Patel LR, Pienta KJ, , 2011. 384 hanging drop arrays give excellent Z-factors and allow versatile formation of co-culture

spheroids. Biotechnology and Bioengineering. Volume 109, Issue 5, pages 1293–1304

Tarutani M, Nakajima K, Uchida Y, Takaishi M, Goto-Inoue, Ikawa M, Setou M; Elias PM, Kinoshita T, Maeda Y and Sano S, 2012. GPHR-dependent functions of the Golgi apparatus are essential for formation of lamellar granules and the skin barrier. Journal Of Investigative Dermatology Volume: 132 Issue: 8 Pages: 2019-2025

Takei T, Rivas-Gotz C, Delling CA, Koo JT, Mills I, McCarthy TL, Centrella M and Sumpio BE, 1997. Effect of strain on human keratinocytes in vitro. J. Cell. Physiol. 173, 64–72.

Thakoersing VS, Gooris GS, Mulder A, Rietveld M, El Ghalbzouri A and Bouwstra JA, 2012. Unraveling barrier properties of three different in-house human skin equivalents. Tissue Engineering. Part C, Methods 2012, 18(1):1-11

Torma and Berne, 2007. Sodium lauryl sulphate alters the mRNA expression of lipid-metabolizing enzymes and PPAR signalling in normal human skin in vivo. Exp Dermatol. 2009 Dec;18(12):1010-5.

Trappman B, Gautrot JE, Connelly JT, Strange DGT, Yuan L, Oyen ML, Stuart MAC, Boehm H, Li B, Vogel V, Spatz JP, Watt FM and Huck WTS, 2012. Extracellular-matrix tethering regulates stem-cell fate. Nature Materials Vol 11 July 2012, p642-649

Trovatti E, Freire CSR, Pinto PC, Almeida IF, Costa P, Silvestre AJD, Neto CP and Rosado C, 2012. Bacterial cellulose membranes applied in topical and transdermal delivery of lidocaine hydrochloride and ibuprofen: In vitro diffusion studies. International journal of pharmaceutics Volume: 435 Issue: 1 Pages: 83-7

Tu CL, Chang W and Bikle DD. 2001. The extracellular calcium-sensing receptor is required for calcium-induced differentiation in human keratinocytes. J Biol Chem 276:41079–41085.

Tu CL, Chang W and Bikle DD, 2011. The Calcium-Sensing Receptor-Dependent Regulation of Cell–Cell Adhesion and Keratinocyte Differentiation Requires Rho and Filamin A. Journal of Investigative Dermatology (2011) 131, 1119–1128

Turksen et al, 2005. Epidermal Cells. Methods and Protocols. Methods in Molecular Biology, Volume 289. Humana Press.

Uchida Y, Behne M, Quiec D, Elias PM, Holleran WM and 2001. Vitamin C Stimulates Sphingolipid Production and Markers of Barrier Formation in Submerged Human Keratinocyte Cultures. Journal of Investigative Dermatology (2001) 117, 1307–1313

Uchida Y and Holleran WM, 2008. Omega-O-acylceramide, a lipid essential for mammalian survival. Journal of Dermatological Science (2008) 51, 77—87

Uchida Y, Houben E, Park K, Douangpanya S, Lee YM, Wu BX, Hannun YA, Radin NS, Elias PM and Holleran WM, 2010. Hydrolytic Pathway Protects against Ceramide-Induced Apoptosis in Keratinocytes Exposed to UVB. Journal of Investigative Dermatology (2010), Volume 130, p2472-2480

Uitto J, Richard G and McGrath JA, 2007. Diseases Of Epidermal Keratins And Their Linker Proteins. Exp Cell Res. 2007 June 10; 313(10): 1995–2009.

Ujihara M, Nakajima K, Yamamoto M, Teraishi M, Uchida Y, Akiyama M, Shimizu H and Sano S, 2010. Epidermal triglyceride levels are correlated with severity of ichthyosis in Dorfman–Chanarin syndrome. Journal of Dermatological Science Volume 57, Issue 2, February 2010, Pages 102–107

Um SH; Lee JB; Park N, Kwon SY, Umbach CC and Luo D, 2006. Enzyme-catalysed assembly of DNA hydrogel. Nature Materials Volume: 5 Issue: 10 Pages: 797-801

Urs S, Roudabush A, O'Neill CF, Pinz I, Prudovsky I, Kacer D, Tang Y, Liaw L and Small D, 2008. Soluble forms of the Notch ligands Delta1 and Jagged1 promote in vivo tumorigenicity in NIH3T3 fibroblasts with distinct phenotypes. Am. J. Pathol. 173, 865-878.

Vaidya MM and Kanojia D, 2007. Keratins: Markers of cell differentiation or regulators of cell differentiation? Journal Of Biosciences Volume: 32 Issue: 4 Pages:629-634

van Smeden J, Hoppel L, van der Heijden R, Hankemeier T, Vreeken RJ and Bouwstra JA, 2011. LC/MS analysis of stratum corneum lipids: ceramide profiling and discovery. J. Lipid Res. 52, 1211–1221.

Vasioukhin V, Bowers E, Bauer C, Degenstein L and Fuchs E, 2001. Desmoplakin is essential in epidermal sheet formation. Nat. Cell Biol. 3, 1076-1085.

Vilgimigli L, Gabbanini S, Berlini E, Lucchi E, Beltramini C and Bertarelli YL, 2012. Lemon (Citrus limon, Burm.f.) essential oil enhances the trans-epidermal release of lipid- (A, E) and water- (B6, C) soluble vitamins from topical emulsions in reconstructed human epidermis. International Journal Of Cosmetic Science Volume: 34 Issue: 4 Pages: 347-356

Vavrova K, Zbytovska J, Hrabalek A. Amphiphilic transdermal permeation enhancers: Structure–activity relationships. Curr Med Chem 2005;12:2273–2291.

Vermeij W P and Backendorf C, 2010. Skin Cornification Proteins Provide Global Link between ROS Detoxification and Cell Migration during Wound Healing. PLoS ONE 2010: 5:e11957.

Vicanová J, Boyce ST, Harriger MD, Weerheim AM, Bouwstra JA, Ponec M, 1998. Stratum corneum lipid composition and structure in cultured skin substitutes is restored to normal after grafting onto athymic mice. J Investig Dermatol Symp Proc. 1998 Aug;3(2):114-20.

Vielhaber G, Pfeiffer S, Brade L, Lindner B, Goldmann T, Vollmer E, Hintze U, Wittern KP and Wepf R, 2001. Localization of Ceramide and Glucosylceramide in Human Epidermis by Immunogold Electron Microscopy. Journal of Investigative Dermatology. Vol. 117, No. 5 November 2001

Wagner K, Fach B and Kolar R, 2012. Inconsistencies in data requirements of EU legislation involving tests on animals. ALTEX. 2012;29(3):302-32.

Walker D, Sun T, MacNeil S, Smallwood R, 2006. Modeling the effect of exogenous calcium on keratinocyte and HaCat cell proliferation and differentiation using an agent-based computational paradigm. Tissue Eng. 2006 Aug;12(8):2301-9.

Wallace L, Roberts-Thompson L and Reichelt J, 2012. Deletion of K1/K10 does not impair epidermal stratification but affects desmosomal structure and nuclear integrity. Journal Of Cell Science Volume: 125 Issue: 7 Pages: 1750-1758

Warner, Stone and Boissy, 2003. Hydration Disrupts Human Stratum Corneum Ultrastructure. The Journal Of Investigative Dermatology. Vol. 120, No. 2.

Watkinson A, Harding C, Moore A and Coan P, 2011. Water modulation of stratum corneum chymotryptic enzyme activity and desquamation. Archives Of Dermatological Research Volume: 293 Issue: 9 Pages: 470-476

Watt FM, 2002. Role of integrins in regulating epidermal adhesion, growth and differentiation EMBO Journal. Volume: 21 Issue: 15 Pages: 3919-3926

Watt FM, Frye M, Benitah SA. MYC in mammalian epidermis:how can an oncogene stimulate differentiation? Nat Rev Cancer 2008;8(3):234–242.

Watt FM and Fujiwara H, 2011. Cell-Extracellular Matrix Interactions in Normal and Diseased Skin. Cold Spring Harbor Perspectives In Biology Volume: 3 Issue: 4

Weir L, Robertson D and Panteleyev A, 2009. Hypoxia affects differentiation patterns of epidermal keratinocytes in vitro. Journal of Investigative Dermatology (2009), Volume 129, S361.

Welss T, Basketter DA, Schröder KR, 2003. In vitro skin irritation: facts and future. State of the art review of mechanisms and models. Toxicology in Vitro Volume 18, Issue 3, June 2004, Pages 231–243

Wertz PW and Downing DT, 1990. Metabolism of linoleic acid in porcine epidermis. J. Lipid Res. 31 (1990) 1839–1844.

Werner S and Smola H, 2001. Paracrine regulation of keratinocyte proliferation and differentiation. Trends in Cell Biology Vol.11 No.4 April 2001

Weston CR, Wong A, Hall JP, Goad MEP, Flavell RA and David RJ, 2004. The c-Jun NH2-terminal kinase is essential for epidermal growth factor expression during epidermal morphogenesis. Proc Natl Acad Sci U S A. 2004 September 28; 101(39): 14114–14119.

Whang K, Thomas CH, Healy KE and Nuber Ga, 1995. A Novel Method to Fabricate Bioabsorbable Scaffolds. Polymer 36, 837.

Wickett RR and Visscher MO, 2006. Structure and function of the epidermal barrier. AJIC: American Journal of Infection Control Volume 34, Issue 10, Supplement , Pages S98-S110, December 2006

Wilhelm, K, Cua A.B, Wolff, H.H et al, 1993. Surfactant-induced stratum corneum hydration in vivo: prediction of the irritation potential of anionic surfactants. J Invest Dermatol, 101 (1993), pp. 310–315

Windoffer R, Beil M, Magin TM and Leube RE, 2011. Cytoskeleton in motion: the dynamics of keratin intermediate filaments in epithelia. Journal Of Cell Biology Volume: 194 Issue: 5 Pages: 669-678

Wood FM, Kolybaba ML and Allen P, 2005. The use of cultured epithelial autograft in the treatment of major burn wounds: eleven years of clinical experience. Burns. 2006 Aug;32(5):538-44

Wu XM, Todo H, Sugibayashi K, 2006. Enhancement of skin permeation of high molecular compounds by a combination of microneedle pretreatment and iontophoresis, J. Control. Release 118 (2006) 189–195.

Wu-Nan Wu, 2006. Atmospheric Pressure Ionization Tandem Mass Spectrometric Analysis of Steroids and Conjugated Metabolites. The Chinese Pharmaceutical Journal, 2006, 58, 1-9

Xu J, Ma M and Purcell WM, 2003. Characterisation of some cytotoxic endpoints using rat liver and HepG2 spheroids as *in vitro* models and their application in hepatotoxicity studies. Toxicol Appl Pharm 189, 112.

Yamada KM and Cukierman E, 2007. Modeling Tissue Morphogenesis and Cancer in 3D. Cell 130, August 24, 2007

Yan-Feng Xu et al, 2005. Percutaneous penetration of ketoprofen and ketoprofen isopropyl ester through a tissue engineering skin reconstructed with HaCaT cells. Source: Yaoxue Xuebao Volume: 40 Issue: 9 Pages: 782-786

Yano S, Komine M, Fujimoto M, Okochi H and Tamaki K, 2004. Mechanical stretching in vitro regulates signal transduction pathways and cellular proliferation in human epidermal keratinocytes. J. Invest. Dermatol. 122, 783–790.

Yoneda K, Nakagawa T, Lawrence OT, Huard J, Demitsu T, Kubota Y, Presland RB, 2012. Interaction of the Profilaggrin N-Terminal Domain with Loricrin in Human Cultured Keratinocytes and Epidermis. Journal of Investigative Dermatology 132, 1206-1214 (April 2012)

Yuki T, Yoshida H, Akazawa Y, Komiya A, Sugiyama Y and Inoue S, 2011. Activation of TLR2 Enhances Tight Junction Barrier in Epidermal Keratinocytes. Journal Of Immunology Volume: 187 Issue: 6 Pages: 3230-3237

Zahir N and Weaver VM, 2004. Death in the third dimension: apoptosis regulation and tissue architecture. Nat Rev Mol Cell Biol 4, 700, 2003.

Zenz R, Eferl R, Kenner L, Florin L, Hummerich L, Mehic D, Scheuch H, Angel P, Tschachler E, Wagner EF, 2005. Psoriasis-like skin disease and arthritis caused by inducible epidermal deletion of Jun proteins. Nature 437, 369-375

Zeyfert CM, Przyborski SA and Cameron NR, 2009. Surface functionalized emulsion-templated porous materials for in vitro cell culture in 3D. Abstracts Of Papers Of The American Chemical Society Volume: 238 Meeting Abstract: 307-PMSE Published: AUG 16 2009

Zhang JY, Green CL, Tao S and Khavari PA, 2003. NFkB RelA opposes epidermal proliferation driven by TNFR1 and JNK. Genes & Development 18:17–22

Zhang Z and Michniak-Kohn BB, 2012. Tissue Engineered Human Skin Equivalents. Pharmaceutics 2012, 4, 26-41

Zhu AJ and Watt FM, 1996. Expression of a dominant negative cadherin mutant inhibits proliferation and stimulates terminal differentiation of human epidermal keratinocytes. Journal of Cell Science 109, 3013-3023 (1996)

Zhu N, Warner RM, Simpson C, Glover M, Hernon CA, Brotherson TM, Ralston DR, Kelly J, Fraser S and MacNeil S, 2005. Treatment of Burns and Chronic Wounds Using a New Cell Transfer Dressing for Delivery of Autologous Keratinocytes. European Journal of Plastic Surgery 28:319 – 330.

Zinn M, Aumailley M, Krieg T, Smola H, 2006. Expression of laminin5 by parental and c-Ha-ras-transformed HaCaT keratinocytes in organotypic cultures. European Journal of Cell Biology Volume 85, Issue 5, 3 May 2006, Pages 333–343

Zuo Y, Zhuang DZ, Han R, Isaac G, Tobin JJ, McKee M, Welti R, Brissette JL, Fitzgerald ML and Freeman MW, 2008. ABCA12 maintains the epidermal lipid permeability barrier by facilitating formation of ceramide linoleic esters, J. Biol. Chem. 283 (2008) 36624–36635.

Zweifel CJ, Contaldo C, Köhler C, Jandali A, Künzi W and Giovanoli P, 2008. Initial experiences using non-cultured autologous keratinocyte suspension for burn wound closure. J Plast Reconstr Aesthet Surg. 2008 Nov;61(11):e1-4